

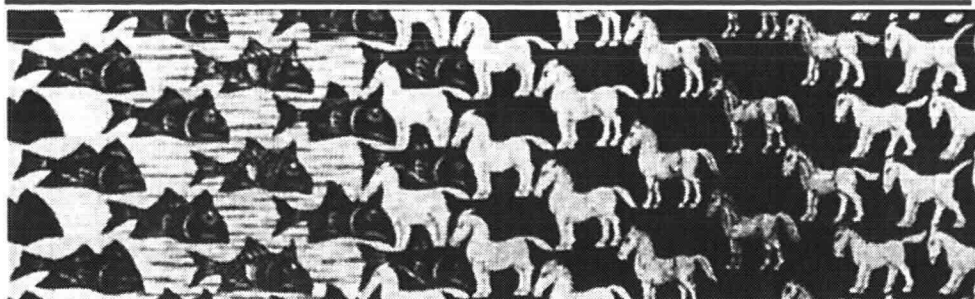
F4

Introduction to bed bank shore protection

Engineering the interface of soil and water

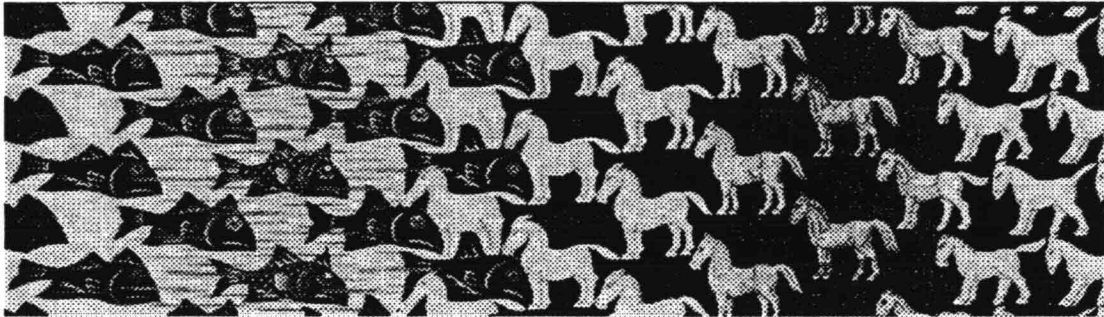
August 1993

G.J. Schiereck



f4

INTRODUCTION TO BED
BANK
SHORE PROTECTION



Engineering the interface of soil and water

September 1993

G.J.Schiereck

VOORWOORD

Ter herhaling van en in aanvulling op het op college gezegde het volgende:

De kern van het verhaal wordt gevormd door de hoofdstukken 6 t/m 12. Problemen die op het tentamen aan de orde gesteld worden gaan altijd over zaken uit die hoofdstukken. De hoofdstukken 2 tot en met 5 zijn nodig om zinnig te kunnen praten over de belastingen die uitgeoefend worden. Ze bevatten veel herhalingen van stof uit de eerdere jaren; nieuw zijn waarschijnlijk enkele dingen over turbulentie in hoofdstuk 2 en de turbulente stroming door poreuze media in hoofdstuk 5. Een paar zaken over onregelmatige golven worden aangesneden in hoofdstuk 3 omdat niet iedereen het vak windgolven doet en het dan zo vreemd is om in hoofdstuk 10 ineens over ξ_p of ξ_M te praten.

Hoewel de hoofdstukvolgorde op enige logika berust, wil dat niet zeggen dat die volgorde ook de meest plezierige is bij een eerste lezing. Daarvoor zou bijv. aangehouden kunnen worden:

Inleiding - 1, Stroming - 2,6,9, Golven - 3,4,7,10, Filters en grondmechanische aspecten - 5,7,8,11, Praktijktoeepassingen 12,13,14

Formules zijn nodig om ontwerpberekeningen te maken. Niemand kent die allemaal uit het hoofd en dat is maar goed ook, dus dat wordt ook niet op het tentamen gevraagd. Wel is het nodig om zo'n formule met verstand te kunnen hanteren en te weten wat er ongeveer in zo'n formule zit en waarom. In de veelheid van empirische relaties, geldt dat vooral voor paragrafen als 6.3, 9.1, 10.1, 10.2.1, 11.1, 11.3.2 en 11.3.3.

CONTENTS

CHAPTER/Paragraph	page
CONTENTS	i
REFERENCES	v
SYMBOLS	x
DICTIONARY	xiii
1. INTRODUCTION	
1.1 General	1.1
1.2 Relevant phenomena	1.4
2. LOADS part I - Flow	
2.1 Introduction	2.1
2.2 Basic equations	2.2
2.3 Boundary shear stress	2.6
2.4 Flow around bodies	2.8
2.5 Turbulent jets and wakes	2.10
2.5.1 General	2.10
2.5.2 Mixing layers	2.11
2.5.3 Free jets	2.12
2.5.4 Plane wall jets	2.14
2.5.5 3-Dimensional wall jets	2.15
2.6 Summary and examples	2.16
2.6.1 Vertical constriction and expansion	2.16
2.6.2 Horizontal constriction and expansion	2.18
3. LOADS part II - Waves	
3.1 General	3.1
3.2 Wind waves	3.4
3.2.1 Wave height distribution	3.5
3.2.2 Wave spectra	3.6
3.3 Boundary shear stress	3.8
3.4 Waves on slopes	3.9
3.4.1 Standing waves	3.9
3.4.2 Breaking waves	3.10
3.4.3 Run-up and run-down	3.14
3.4.4 Wave impacts	3.16
4. LOADS part III - Ships	
4.1 General	4.1
4.2 Primary waves	4.3
4.3 Secondary waves	4.7
4.4 Propeller races	4.10

5. LOADS part IV - Porous flow	
5.1 General	5.1
5.1.1 Steady flow	5.2
5.2 Laminar flow	5.4
5.2.1 Steady flow	5.4
5.2.2 Non-steady flow	5.7
5.3 Turbulent flow	5.8
5.3.1 Steady flow	5.8
5.3.2 Non-steady flow	5.9
6. EROSION part I - Flow	
6.1 General	6.1
6.2 Scour by jets	6.3
6.3 Time-dependent scour	6.5
6.3.1 Process description	6.5
6.3.2. The factor α	6.8
6.3.3 Influence of bottom protection	6.10
6.3.4 The slope β	6.11
6.3.5 Non-stationary flow	6.12
6.3.6 Non-stationary structure	6.12
6.3.7 Equilibrium depth	6.13
6.4 Scour around bodies	6.14
6.4.1 Scour around bridge piers	6.14
6.4.2 Scour around abutments	6.16
6.4.3 Scour behind groynes	6.17
6.4.4 Scour in constrictions	6.17
6.5 Discussion on scour	6.18
7. EROSION part II - Remainder	
7.1 Erosion by waves	7.1
7.1.1 Slopes	7.1
7.1.2 Bottom scour	7.2
7.2 Erosion by ships	7.3
7.3 Erosion by porous flow	7.4
7.3.1 Piping	7.4
7.4 Erosion by gravity	7.6
7.4.1 Slides	7.6
7.4.2 Flow-slides	7.7
8. LOAD REDUCTION	
8.1 Flow reduction	8.1
8.2 Wave reduction	8.2
8.2.1 Dams	8.2
8.2.2 Pile screens	8.3
8.2.3 Floating breakwaters	8.4
8.2.4 Reed	8.5
8.3 Ship's loads reduction	8.5
8.4 Porous flow reduction	8.6
8.4.1 Flow reduction	8.6
8.4.2 Pressure reduction	8.7

9. STABILITY part I - Flow	
9.1 Loose material	9.1
9.1.1 Uniform flow - horizontal bed	9.1
9.1.2 Strength reduction	9.6
9.1.3 Load increase	9.8
9.1.4 Reduced strength and increased load	9.12
9.2 Coherent material	9.14
9.2.1 Placed elements	9.14
9.2.2 Gabions	9.14
9.2.3 Cohesive soils	9.15
9.2.4 Vegetation	9.15
10. STABILITY part II - Waves	
10.1 Loose material	10.1
10.1.1 Horizontal bed	10.1
10.1.2 Slopes	10.2
10.1.3 Berms and toes	10.7
10.1.4 Low crests	10.7
10.1.5 Heads	10.8
10.1.6 Ship's waves	10.8
10.2 Coherent material	10.9
10.2.1 Placed blocks	10.9
10.2.2 Impervious layers	10.14
10.2.3 Vegetation	10.15
11. STABILITY part III - Porous flow	
11.1 Granular filters	11.1
11.1.1 Introduction	11.1
11.1.2 Geometric criteria	11.3
11.1.3 Hydraulic criteria	11.4
11.1.4 Application of results	11.7
11.2 Geotextiles	11.8
11.2.1 Introduction	11.8
11.2.2 Sandtightness	11.9
11.2.3 Permeability	11.10
11.3 Stability of slopes	11.12
11.3.1 Macro stability	11.12
11.3.2 Micro stability	11.15
11.3.3 Impervious layers	11.16

12. PROTECTIONS	
12.1 Shore protections	12.1
12.1.1 Shape of protections	12.2
12.1.2 Revetment choice	12.3
12.1.3 Transitions	12.4
12.1.4 Toes	12.6
12.1.5 Groynes	12.7
12.1.6 Breakwaters	12.8
12.2 Bank protections	12.9
12.2.1 Bank protection types	12.9
12.2.2 Limits of protection	12.10
12.2.3 Groynes	12.11
12.2.4 Falling aprons	12.12
12.3 Bed protections	12.13
12.3.1 Outlet structures	12.14
12.3.2 Bridge piers	12.16
12.3.3 Seawalls	12.16
13. CONSTRUCTION AND MAINTENANCE	
13.1 General	13.1
13.1.1 Quality assurance	13.2
13.2 Construction	13.3
13.2.1 Waterborne - Loose material	13.3
13.2.2 Waterborne - Coherent material	13.6
13.2.3 Land based - Loose material	13.7
13.2.4 Land based - Coherent material	13.8
13.2.5 Construction costs	13.9
13.3 Maintenance	13.10
13.3.1 General	13.10
13.3.2 Theory	13.11
13.3.3 Practice	13.13
14. DESIGN	
14.1 Design process	14.1
14.1.1 Introduction	14.1
14.1.2 Influencing factors	14.3
14.1.3 Design phases	14.5
14.2 Conceptual design	14.7
14.2.1 Generation of alternatives	14.7
14.2.2 Selection of alternatives	14.8
14.3 Structural design	14.9
14.3.1 Failure	14.9
14.3.2 Safety	14.13

Annex A: MATERIALS

Annex B: ENVIRONMENTAL ASPECTS

REFERENCES

- Akkerman
1985 Hydraulic design criteria for rockfill closure of tidal gaps - Vertical closure method, Delft Hydraulics Laboratory report M1741 part IV
- Akkerman
1986 Hydraulic design criteria for rockfill closure of tidal gaps - Horizontal closure method, Delft Hydraulics Laboratory report S 861
- Ariëns
1993 Relatie tussen ontgrondingen en steenstabiliteit van de toplaag (in Dutch), MSc thesis, Delft University of Technology
- Ashida/Bayazit
1973 Initiation of motion and roughness of flows in steep channels, Papers IAHR-congress Istanbul, page 475-484
- Battjes
1974 Computation of set-up, longshore currents, run-up and overtopping due to wind-generated waves, Dissertation Delft University of Technology
- Bear
1972 Dynamics of fluids in porous media, American Elsevier
- Bezuyen/Burger
/Klein Breteler
1990 Taludbekledingen van gezette steen, samenvatting van onderzoeksresultaten 1980-1988 M1795/H195 deel XXIV (in Dutch) RWS-Dienst Weg- en Waterbouwkunde
- Blom
1991 Turbulent flow over a sill, IAHR-congress Madrid
- Blom
1993 On the shallow water equations for turbulent flow over sills Delft University of Technology, 1993
- Booij
1986 Turbulentie in de waterloopkunde (in Dutch), lecture notes b82, Delft University of Technology
- Bouter
1991 Wave damping by reed- An investigation in environment friendly bank protections, PIANC bulletin, no 75
- Breusers/Raudkivi
1991 Scouring, Balkema
- Bruun/Gunbak
1977 Stability of sloping structures in relation to $\xi = \tan\alpha\sqrt{H/L}$ Coastal Engineering 1, page 287-322
- CIRIA
1990 Use of vegetation in civil engineering, Coppin/Richards editors CIRIA/Butterworths
- CUR/CIRIA
1991 Manual on the use of rock in coastal and shoreline engineering, CUR Report 154/CIRIA Special Publication 83, Balkema
- CUR/TAW
1992 Handboek voor dimensionering van gezette taludbekledingen (in Dutch), Rapport 155, Centrum Uitvoering research/Technische Adviescommissie voor de Waterkeringen

- Cohen de Lara 1955 Coefficient de perte de charge en milieu poreux basé sur l'équilibre hydrodynamique d'un massif (in French), La Houille Blanche No 2, page 167-176
- Delft Hydraulics 1960 Stroombestendigheid los materiaal in wervelstraat (in Dutch) report M 598 - VI
- Fredsøe/Deigaard 1992 Mechanics of coastal sediment transport, Advanced series in Ocean Engineering, Volume 3, World Scientific
- van Gent 1992 Formulae to describe porous flow, Report no 92-2, DUT Civil Engineering
- de Graauw/vdMeulen /vdDoes de Bye 1983 Design criteria for granular filters, Delft Hydraulics publication 287
- Groen/Dorrestein 1976 Zeegolven (in Dutch), Koninklijk Nederlands Meteorologisch Instituut
- Grune/Kohlhase 1974 Wave transmission through vertical slotted wall, Proceedings 14th International Conference on Coastal Engineering, Vol III, page 1906-1923
- Hedar 1986 Armor layer stability of rubble-mound breakwaters, ASCE Journal of Waterway, port, coastal and ocean engineering, Vol 112, No 3, page 343-350
- Hewlett 1985 Reinforcement of steep grassed waterways, CIRIA
- Hoffmans 1992 Two-dimensional mathematical modelling of local-scour holes, Dissertation Delft University of Technology
- Hoffmans 1993a A study concerning the influence of the relative turbulence intensity on local scour holes, Report W-DWW-93-251, Rijkswaterstaat, Road and Hydraulic Engineering Division
- Hoffmans 1993b A hydraulic and morphological criterion for upstream slopes in local scour holes, Report W-DWW-93-255, Rijkswaterstaat, Road and Hydraulic Engineering Division
- Hudson 1953 Wave forces on breakwaters, Proceedings-Separate ASCE, No 113, page 653-685
- Izbash/Khaldre 1970 Hydraulics of river channel closure, Butterworth
- Jansen 1979 Principles of river engineering, The non-tidal alluvial river, Pitman
- Jonsson 1966 Wave boundary layers and friction factors, Coastal Engineering Conference, Chapter 10, page 127-148

- Jorissen/Vrijling 1989 Local scour downstream hydraulic constructions, IAHR-congress Ottawa
- Jorissen/Konter 1991 Prediction of time development of local scour, New Orleans
- van der Knaap 1986 Design criteria for geotextiles beyond the sandtightness requirement, Delft Hydraulics, publication 358
- Kuijper 1992 Onderhoud in de waterbouw (in Dutch), Master thesis, Delft University of Technology, Civil Engineering
- LeMéhauté 1957/1958 Permeabilité des digues en enrochements aux ondes de gravité périodiques (in French), La Houille Blanche, dec. 1957 - june 1958
- LeMéhauté 1976 Hydrodynamics and waterwaves, Springer
- van Mierlo/de Ruijter 1988 Turbulence measurements above dunes, Report Q789, Volume 1 and 2, Delft Hydraulics Laboratory
- van der Linden 1985 Golfdependende constructies (in Dutch), Master thesis, Delft University of Technology, Civil Engineering
- van der Meer 1989 Rock slopes and gravel beaches under wave attack, Dissertation, Delft University of Technology
- van der Meer /d'Angremond 1991 Wave transmission at low-crested structures, Conference on Coastal Structures, Telford
- Oumeraci/Partensky 1990 Wave-induced pore pressure in rubble mound breakwaters, Int. Conf. on Coastal Engineering, Delft
- Paintal 1971 Concept of critical shear stress in loose boundary open channels, Journal of hydraulic research, 9-1, page 91-113
- Pilarczyk 1990 Coastal protection, Proceedings of short course on coastal protection, DUT, Balkema
- Pilarczyk/den Boer 1983 Stability and profile development of coarse materials and their application in coastal engineering, Delft Hydraulics, publication 293
- Rajaratnam 1976 Turbulent jets, Elsevier
- Rajaratnam/Berry 1977 Erosion by circular turbulent wall jets, Journal of Hydraulic Research 15(3)
- Rajaratnam 1981 Erosion by plane turbulent jets, Journal of Hydraulic Research 19(4), page 339-358

- Vellinga
1986 Beach and dune erosion during storm surges, Dissertation, Delft University of Technology
- Ven te Chow
1959 Open-Channel hydraulics, McGraw-Hill
- van Vledder
1990 Literature survey to wave impacts on dike slopes, Delft Hydraulics, Report H976
- de Vries
1992 River Engineering, Lecture notes f10, Delft University of Technology
- van der Weide
1989 General introduction and hydraulic aspects, Short course on design of coastal structures, AIT Bangkok
- Xie Shi-Leng
1981 Scouring patterns in front of vertical breakwaters and their influences on the stability of the foundations of the breakwaters, Delft University of Technology

SYMBOLS

Symbol	Meaning	Dimension
a	Wave amplitude ($=H/2$)	m
a_0	Amplitude of horizontal wave motion at bottom	m
A	Area of cross-section	m^2
A_C	Area of cross-section of navigation channel	m^2
A_S	Area of midship section of ship	m^2
b	Width of shear layer, plane jet or canal	m
b_0	Width of outflow nozzle in plane jet	m
B	Width of square nozzle of jet or ship	m
c	1. Wave celerity 2. Coefficient in piping formula	m/s
C	Coefficient of Chezy	$m^{0.5}/s$
C_D	Drag coefficient	-
C_F	Friction coefficient	-
C_L	Lift coefficient	-
C_R	Velocity decay coeff. in rough wall jets	-
d	Diameter of grain ($=d_{50}$, unless otherwise stated)	m
D	Diameter of cylinder or outflow nozzle or ship's propeller or height of dam or sill	m
g	Acceleration of gravity	m/s^2
h	Waterdepth	m
h_0	Original waterdepth before scouring	m
h_s	Scouring depth	m
h_{sm}	Maximum depth in scouring hole	m
$h_{sm\infty}$	Asymptotic or equilibrium max. scouring depth	m
H	Wave height	m
H_S	Significant wave height	m
H_I	Incident wave height	m
H_R	Reflected wave height	m
H_T	Transmitted wave height	m
I	Slope	-
k	1. in waves: Wave number ($=2\pi/L$) 2. in porous flow: Permeability	1/m m/s
k_s	Equivalent sand roughness	m
K_D	Coefficient in Hudson's formula	-
K_R	Wave reflection coefficient	-
K_T	Wave transmission coefficient	-
L	Wave length	m
L_0	Wave length in deep water	m
L_E	Entrance length of ship's bow	m
L_S	Ship's length	m
m_0	Area of wave spectrum	m
M	Momentum	kg/s^2
n	Porosity (volume of voids/total volume)	-
N	Number of waves in vdMeer's formula	-
p	1. Pressure	N/m^2

	2. Coefficient in parabolic beach profile	$m^{0.22}$
P	Power	W
Q	Discharge	m^3/s
r	1. Relative turbulence	-
	2. Radial distance from center of jet	m
R	Hydraulic radius	m
R_U	Wave run-up	m
R_D	Wave run-down	m
s	Distance from ship's sailing line	m
S	Sediment transport	m_3/s
S_d	Damage level in vdMeer's formula	-
t	Time	s
T	Wave period or averaging period in turbulence	s
T_M	Mean wave period	s
T_P	Wave period with maximum wave energy	s
T_s	Significant wave period	s
u	Velocity in x-direction	m/s
u_c	Critical velocity	m/s
u_f	Filter velocity	m/s
u_*	Shear velocity ($=\sqrt{\tau/\rho}$)	m/s
u_o	Outflow velocity in jets; vertically averaged velocity	m/s
u_m	Maximum velocity	m/s
\bar{u}	Average velocity (in time)	m/s
u'	Turbulent velocity fluctuation	m/s
\hat{u}_b	Amplitude of wave velocity at bottom	m/s
U_R	Return current along ship	m/s
v	Velocity in y-direction	m/s
V_L	Limit speed of ship	m/s
V_s	Ship's speed	m/s
w	Velocity in z-direction	m/s
W	Weight	$kg.m/s^2 = N$
x	Distance along horizontal axis parallel to main flow direction	m
y	Distance along horizontal axis perpendicular to main flow direction	m
z	Distance along vertical axis	m
z_R	Waterlevel depression in prim. ship wave	m
α	1. Slope angle	degrees
	2. Coefficient in scour formula	-
	3. Coefficient in piping formula	-
β	Slope of scour hole	degrees
γ_b	Breaker depth ratio (H/h)	-
δ	Boundary layer thickness	m
Δ	Relative density $(\rho_s - \rho_w)/\rho_w$	-
ϵ	Turbulent (eddy) viscosity	m^2/s
ϵ_s	Eddy diffusivity of sediment	m^2/s
η	Dimensionless distance in jets	-
η_t	Waterlevel in waves	m
ζ	Bow-geometry coefficient in ship's waves	-

κ	von Karman constant ≈ 0.4	-
λ	Leakage height	m
Λ	Leakage length	m
μ	1. Dynamic viscosity 2. Discharge coefficient	kg/m.s -
ν	Kinematic viscosity	m ² /s
ξ	Breaker parameter	-
ρ_s	Density of sediment	kg/m ³
ρ_w	Density of water	kg/m ³
σ	Standard deviation	
τ	Shear stress	N/m ² = Pa
τ_c	Critical shear stress	N/m ² = Pa
τ_0	Wall shear stress	N/m ² = Pa
ϕ	1. Angle of repose 2. Potential in porous flow	degrees m
ψ	Stream function	m ² /s
ω	Angular frequency in waves ($2\pi/T$)	1/s

THE GREEK ALPHABET

Lower case	Capital	Name	Lower case	Capital	Name
α	A	Alpha	ν	N	Nu
β	B	Beta	ξ	Ξ	Xi
γ	Γ	Gamma	\omicron	Ο	Omicron
δ	Δ	Delta	π	Π	Pi
ϵ	E	Epsilon	ρ	Ρ	Rho
ζ	Z	Zeta	σ	Σ	Sigma
η	H	Eta	τ	Τ	Tau
θ	Θ	Theta	υ	Υ	Upsilon
ι	I	Iota	ϕ	Φ	Phi
κ	K	Kappa	χ	Χ	Chi
λ	Λ	Lambda	ψ	Ψ	Psi
μ	M	Mu	ω	Ω	Omega

SPECIAL SIGNS

\propto Proportional to

DICTIONARY

abutment	landhoofd
antinode	buik (van trilling)
apron	stortebed, bodembescherming (lett. beschermlap, voorschoot)
armouring	beschermen, pantseren
backwash	terugstroming (in golfoploop)
bank	oever
bar	(zand)bank
bed	bodem
bow	boeg
clogging	dichtslibben
coherent	samenhangend
cohesive	cohesief
collapse	in elkaar storten
collide	botsen
concrete	beton
constriction	vernauwing
construction	bouw, uitvoering, constructie
core	kern
crest	kruin
culvert	duiker(sluis)
cuspl	interferentie piek
debris	rommel, afval
downrush	terugstromen (in golfoploop)
drag	slepen, trekken ,stromingsweerstand
eddy	neer, wervel
equilibrium	evenwicht
fascine mattress	zinkstuk
flow slide	zettingsvloeiing
gravel	grind
groyne	krib
hull	romp (van schip)
impermeable	niet poreus, ondoorlatend
impervious	ondoordringbaar, ondoorlatend
impinge	treffen, botsen
incipient motion	begin van beweging
inflection	buigen
interface	grensvlak, overgang
jet	straal
leach	uitloggen
leakage	lek
liquefaction	verweking
momentum	impuls
node	knoop (van trilling)
nozzle	tuit
orifice	(uitstroom)opening
pier	pijler, pier
pitch	plaveien, zetten

plunge	duiken
propeller race	schroefstraal
protrude	uitsteken
quicksand	drijfzand
quarry	steengroeve
rectifier	gelijkrichter
revetment	oeverbescherming, bekleding
riprap	breuksteen, stortsteen
rubble	puin, stortsteen
run-down	(golf)terugloop
run-up	(golf)oploop
saturated	verzadigd
scour	ontgroning, uitschuring
seepage	kwel
segregation	ontmenging
settlement	zetting
shallow	ondiep
shear stress	schuifspanning
sheet pile	damwand
sill	drempel
slags	slakken
slide	afschuiving
spill	morsen
split-barge	splijtbak
spur-dike	krib, scherm
stern	hek, achtersteven
surf	branding
surge	deinen
tailwater	benedenwater
threshold	drempel
tug	sleepboot
uprush	omhoog stromen in golfoploop
voids	porieën
vortex	wervel
wake	zog (van schip)
water-borne	vanaf het water (lett. door het water gedragen)

1	INTRODUCTION
----------	---------------------

1.1	GENERAL
------------	----------------

The interface of land and water has always played an important role in human development. Settlements and economic activities are often located at coasts, river-banks or deltas. Harbours, waterways, dikes, dunes and beaches, structures for water-control and water-resources management etc. are examples of hydraulic engineering on a macro-scale. In these lectures, the interface is studied on a micro-scale. The occurring phenomena are important in all branches of hydraulic engineering.

In a natural situation, the interface moves freely with the forces of erosion and sedimentation. Actually, there is nothing wrong with erosion, until some interest is threatened. Erosion is somewhat like weed: as long as it is in nobodies way, no action is needed or even wanted. There should always be a balance between the efforts of protection against erosion and the damage that would occur otherwise (see Figure 1.1).

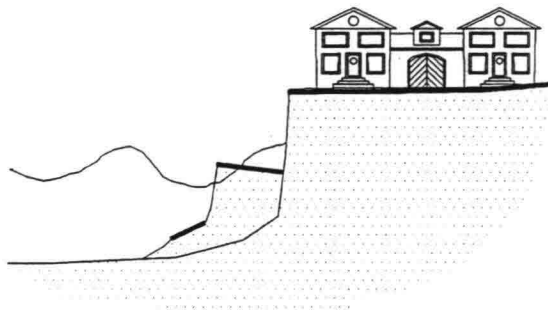


Figure 1.1 Erosion and threat

Moreover, it should be realised that once a location is protected along a coast or riverbank that is eroded on a large scale, the protected part can induce extra erosion and in the end the whole coast or bank has to be protected. So, look before you leap, should be the motto.

In many cases however, a protection is necessary: bottom protection behind outlet-structures or around objects, revetments in rivers and canals, dike protection, coastal defence works etc. Figure 1.2 gives some examples.

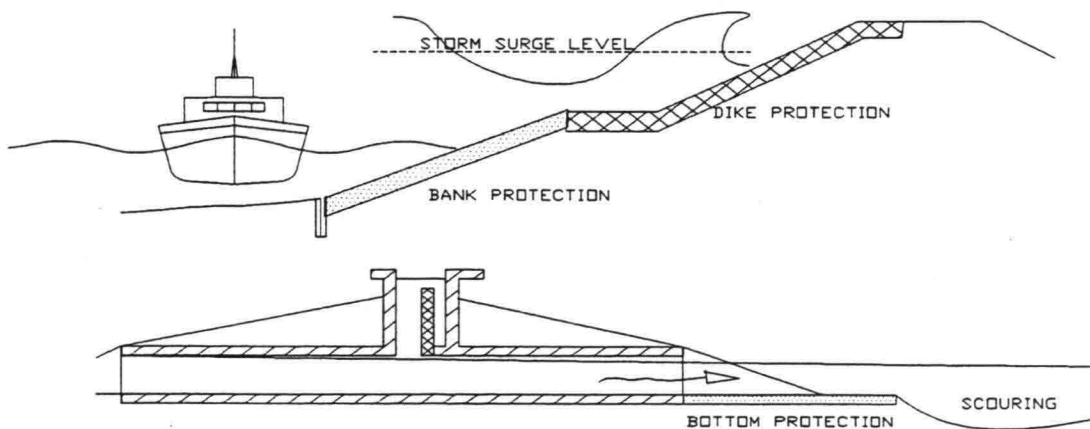


Figure 1.2 Examples of protection

A bare, erodable interface on one side and an interface that is protected with building materials like concrete, asphalt or rock on the other side, are two extremes. Nature itself offers a lot of possibilities in between, with vegetation as a major protection material. Mangrove trees along coasts and estuaries and reed along river banks are just two examples of a natural and low-cost protection. An important cause of erosion can be the removal of this vegetation, disturbing an equilibrium that has existed for many ages. So, a first measure in fighting erosion, will be the conservation of vegetation at the interface.

These lecture notes deal primarily with situations where the loads exceed the present strength and there is someone who wants to change that. In that case there are two possibilities to go from an unstable to a stable situation, see Figure 1.3:

A Reduce the load, e.g. build a wave reductor in front of the considered location

B Increase the strength, e.g. build a revetment at the location

For both strategies it is necessary to have a good understanding of the relevant phenomena and the interaction between load and strength. Therefore, there is ample attention for the background of the phenomena in the coming sections.

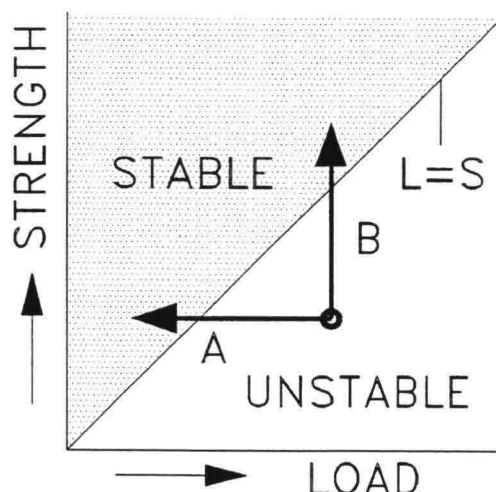


Figure 1.3 Load vs strength

At first, we will start to review some basic knowledge of hydraulic engineering in chapter 2 through 5 to get insight in the loads and forces acting on the interface. One can study these subjects on various scientific levels. Here the choice is made for a level that goes "one degree deeper" than the empirical design relations presented in the following chapters. This is considered necessary and appropriate to make a sensible use of the empirical relations. Although it can be boring to have to go through all this tough stuff before getting to the real thing, it is thought to be rewarding in the end.

Chapter 6 and 7 deal with the effect of the various loads on an unprotected interface, while chapter 8 gives some possible methods to reduce the loads. In chapter 9 through 11, the stability of protections is discussed. In chapter 12, possible construction types are presented, while the construction and maintenance aspects are reviewed in chapter 13. Finally, chapter 14 comes to the point of designing.

This division was chosen on purpose, with the idea in mind that a designer should have a thorough knowledge of the processes that occur at the interface of land and water in his head, before thinking of solutions. The same approach leads to chapters about erosion and load reduction before discussing stability; one should have an idea of possible erosion before one can have an idea of the necessary protection. The chapter on design is the last one: only after gaining knowledge about the phenomena, the possible protection types and the peculiarities of construction, talking about design is fruitful.

The story of protecting the interface of land and water is told three times in these notes: once in the text, once in the formulae and last, but certainly not least, in the figures. Although not really a comic-book, the reader is advised to study them carefully, because, often they tell the story in the most accessible and comprehensive way.

DEVELOPMENTS

Although protections of the interface of land and water are being made for more than 1000 years (at least in the Netherlands), that does not mean that there is nothing new. On the contrary, like in architecture there are always new materials, creating new possibilities and changing demands from society, creating new challenges.

Relatively new materials, like geo-textiles, give new opportunities to meet the contradicting demands in the design as showed in Figure 1.13. There is not yet one ideal material combining the right strength, flexibility and permeability but there are a lot more possibilities. The same goes for construction methods: new equipment makes application feasible of hitherto impossible structures. Major contributions to the design practice in the last decades, have been made possible by new research facilities, like (large scale) wind wave flumes, (turbulent) flow measurement devices etc. In general there is a tendency to use a more scientific approach in the research and design of hydraulic structures. Much knowledge is fragmented and it would be a step forward to get an overall picture. Moreover most knowledge is of an empirical nature, leading to sometimes dubious relations. Dimensional homogeneity is not always present while the use of the same variable in two dimensionless parameters can lead to spurious correlations, see de Vries,1992. One of the challenges of the coming years is the combination of the use of more scientific methods with experience which will always remain an important factor in hydraulic engineering.

An everlasting pressure on the designer is to create cheap solutions. "Cheap" has to be considered in a broad sense: low investment can mean high maintenance costs and vice versa. The optimal solution should be found. An important cost factor in western countries is the construction; mechanisation replaces more and more the old labour-intensive handwork, while in developing countries material and equipment is very expensive and labour relatively cheap. This can lead to a completely different design.

An important development in hydraulic engineering is the increasing relevance of environmental aspects. It was already mentioned that vegetation can act as protection in many cases and in situations where vegetation is present, it should be preserved as much as possible. There are several examples in the world where problems with erosion only started after the natural vegetation was removed (often to use plants or wood of trees or to make mooring facilities for ships). In the Netherlands, more and more use is made of vegetation as protection where possible. This has to do with the importance of the interface of soil and water in the ecosystem as a whole. It is of crucial importance for a lot of species of plants and animals. Not only the base of the food-chain, like worms and insects, lives there; river banks for example are vital for many kinds of fish, looking for quiet places with low velocity to lay eggs. Mammals, like deer, have difficulties in climbing out of the water at artificial river banks. Other mammals, like the readers of these notes have their demands when it comes to attractiveness of the landscape etc. In the design of a protection work, one should be aware of the fact that the interface of land and water is an essential part of the eco-system. More in general, especially in densely populated areas, there is a growing pressure on the use of the interface with many different interests. This leads to a growing awareness of the multi-functionality of a shore, a bank or a dike. These (usually conflicting) interests, have to be incorporated into the design.

Environmental aspects and new materials come together in the use of waste material in hydraulic engineering. Here again there are conflicting interests. On the one hand there is the need to get rid of a lot of waste material like slags from furnaces, which form a cheap building material. On the other hand there is the danger of leaching, causing contamination of the water-system. Annex B gives more information.

Water Type Phenomenon	(Units)	Rivers	Lakes	Estua- ries	Seas	Canals
Discharges						
waterlevel fluctuations	(m)	1-10	1-10	0,1-1	-	0-1
flow velocity	(m/s)	1-2	0,1	0,1-1	-	0,1-1
(velocity in in- and outlet sluices between waters: 1 - 5 m/s)						
Tides						
waterlevel fluctuation	(m)	-	-	1-10	1-4	-
flow velocity	(m/s)	-	-	1-4	1-2	-
Wind						
waterlevel fluctuation	(m)	0,1	0,1-1	1-5	1-5	0,1
wave height	(m)	0,1-0,5	0,1-1	0,5-1	1-5	0,1-0,5
Ships						
primary wave height	(m)	0,2-0,5	0,1-0,2	0,1-0,2	0-0,1	0,2-0,75
secondary wave height	(m)	0,2-0,75	0,1-0,75	0,1-1	0,1-1	0,2-1

Interfaces between land and water come in all sizes and circumstances. The table gives an idea of the loading phenomena and the order of magnitude of external loads that can be expected. The interface stability will be treated in these lecture notes for the phenomena on the vertical axis and the water systems on the horizontal axis. Not by treating them separately, but by treating them elementary, based on the physical processes. This is more exceptional than it seems, because most textbooks deal with either shore protection or river training works or shipping canals etc. This is mainly because much of the knowledge of these protection works is based on experience and experience is often gained in one of the mentioned fields and not in all of them. This is a pity because many of the phenomena involved are similar: ship waves and wind waves have different sources, but act very much the same. The same holds for flow in a river, through a tidal closure or in an outlet sluice, when it comes to protect the bed or bank. Therefore, an attempt is made to find the core of all these related problems. One thing all these protections have in common, is that their function is to **withstand the energy loss of moving water**.

Water in motion contains energy: currents, wind waves, ship movement, groundwater-flow etc., which can be available to transport material. The energy comes from external sources like wind, ships or the sun (evaporation, leading to precipitation in high areas, giving potential energy). Eventually it ends as heat by means of viscous friction. Just to get an idea of the amount of energy present in moving water, the following comparison is made.

To lift a mass of 1000 kg with a speed of 1 m/s, a power of $m \cdot g \cdot v$ (mass * acceleration of gravity * velocity) = 10 kW is needed (force x velocity). The equivalence of this power delivered by moving water can be calculated from the energy loss in various cases. The expression "energy loss" is actually not correct. It is an energy transfer, from kinetic energy via turbulence to heat. In the following examples, the equations from basic hydraulics are considered well known.

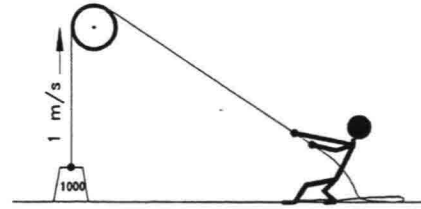


Figure 1.4 "Power lifting"

1. For an outflow of Q m³/s with a head difference of ΔH m, the loss is:

$$\Delta P = \rho g Q \Delta H \quad (1.1)$$

Q and ΔH are related via:

$$Q = u \cdot A = \mu \sqrt{2g \Delta H} \cdot A \quad (1.2)$$

For $A = 1$ m² and $\mu = 1$ we find $\Delta H = 0,37$ m. So, a hole of 1 m² and a modest head difference deliver 10 kW to lift 1000 kg with 1 m/s.

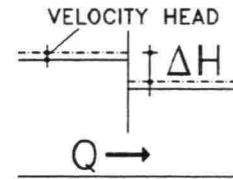


Figure 1.5 Energy loss in outflow

2. For a uniform flow in a river with Q m³/s and a slope I , the loss is:

$$\Delta P = \rho g Q I \quad (\text{per m in flow direction}) \quad (1.3)$$

where Q and I are related via:

$$Q = A \cdot C \sqrt{h I} \quad (1.4)$$

For a slope of 10^{-4} , $Q = 10000$ m³/s, $h = 5$ m, $C = 50$ m/s and a width of about 1800 m, give an energy loss 10 kW. These are high values but the loss is per m length, while the first example gave a total loss. This also shows that a local outflow gives a more concentrated attack than a flow with a gentle slope.

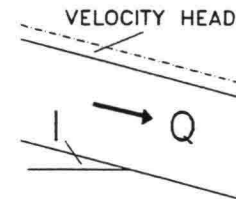


Figure 1.6 Energy loss in river

3. The energy loss caused by e.g. a bridge pier, is given by:

$$\Delta P = F_D \cdot u \quad (1.5)$$

(the water exerts a drag force F_D on the body and, reversely, the body exerts a same force on the water). The force and the flow velocity are related via:

$$F_D = \frac{1}{2} \rho u^2 \cdot C_D \cdot D \cdot h \quad (1.6)$$

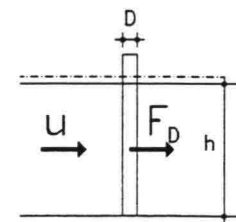


Figure 1.7 Energy loss in flow behind obstruction

For a pier with a diameter of 1 m in 10 m waterdepth and $C_D = 1$, this gives a velocity $u = 1.25$ m/s to get an energy loss of 10 kW.

4. For waves with height H and celerity c being dissipated at a slope without reflection, the energy loss per m width is given by:

$$\Delta P = \frac{1}{8} \rho \cdot g \cdot H^2 \cdot c \quad (1.7)$$

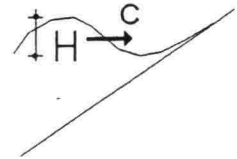


Figure 1.8 Energy loss in waves

With a waterdepth of 5 m and $c = (g \cdot h)^{1/2}$ we get $H = 0,94$ m.

5. A ship transfers energy to the water by waves and by the propeller induced flow. All this energy comes from the engine (sailing vessels usually cause little trouble). Assuming an engine efficiency of 70 % this leads, with $1 \text{ hp} = 736 \text{ W}$, to an engine of about 20 hp.

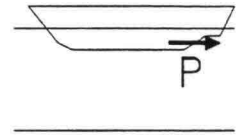


Figure 1.9 Energy loss in ship motion

It is clear that although, fortunately, this destructive power is not 100 % effective, moving water contains enough energy to cause much damage. The protection measures that will be discussed in the coming chapters, are meant to guide this energy loss and to prevent damage where necessary.

Turbulence plays an important role and will be discussed more in detail in the next chapter. Here it is sufficient to say that turbulence is related to the transfer of kinetic energy into heat. During this transfer, much of the energy is available for attacking an interface. Turbulence is coupled to the above mentioned energy loss and is often related with decelerating flow and friction. Geometry also plays a role. To illustrate this we look again at the given examples. For the outflow in Figure 1.5, equation (1.1) shows that for a given Q , a larger ΔH gives more energy loss. With equation (1.2) it is clear that this is the case when the same Q has to pass through a smaller A . This seems logic since the velocity in that case is higher and hence more deceleration. From the same equation follows that a smaller μ with the same A and Q , leads to a higher ΔH and hence to a higher energy loss. So, the configuration influences the energy loss and it can be expected that a lower coefficient μ will give more erosion and a heavier attack on a bottom protection.

Something similar can be seen in the example of Figure 1.7. A larger diameter D of the pier will give more energy loss and hence more erosion. The same holds for a blunt pier instead of a streamlined shape, leading to a higher C_D -value and, again more energy loss.

These tendencies are also found in experiments and it is an attractive idea to relate all these parameters to each other. A C_D -value for a certain bridge pier geometry would immediately give the depth of the scour hole that can be expected around that pier. Unfortunately however, these relations are at best qualitative. At first, the relations are much more complex. But most of all, much research in hydraulic engineering is empirical and fragmented. This leads to an avalanche of relations for each subject, while the connections often remain in the dark. This is a pity and there is still a lot of work to do to establish general applicable relations. For a better understanding of the phenomena it is advised to keep the general picture in mind as much as possible.

Neglectance of a relevant phenomenon can lead to a protection that causes more damage than it prevents or shifts the problem unconsciously to the neglected phenomenon, see Figure 1.10.

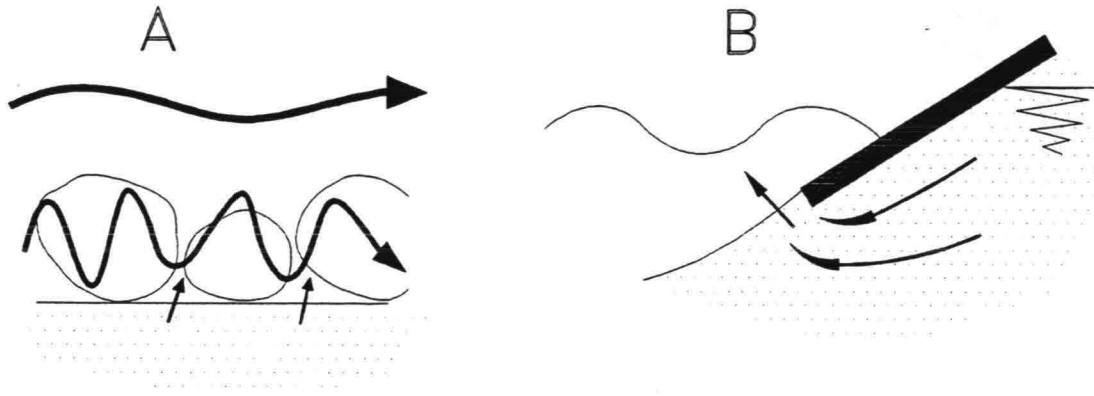


Figure 1.10 Ill-designed protections

In case A, large rocks are dumped on a sand bottom which erodes because of currents. The rocks lead to a somewhat lower velocity at the bottom, but to a considerable increase in turbulence and hence, an increase of erosion.

Case B shows an asphalt-protection on a slope. The difference between the water-tables inside and outside the slope during low water outside, cause the groundwater-flow to concentrate at the edge of the asphalt, leading to erosion at that spot.

In general there are hydraulic and soil-mechanical mechanisms involved in the stability of a structure. Cause and effect can lie in both fields: failure of a protection can cause settlements of a structure, but vice versa is also a possibility. Figure 1.11 gives some examples.

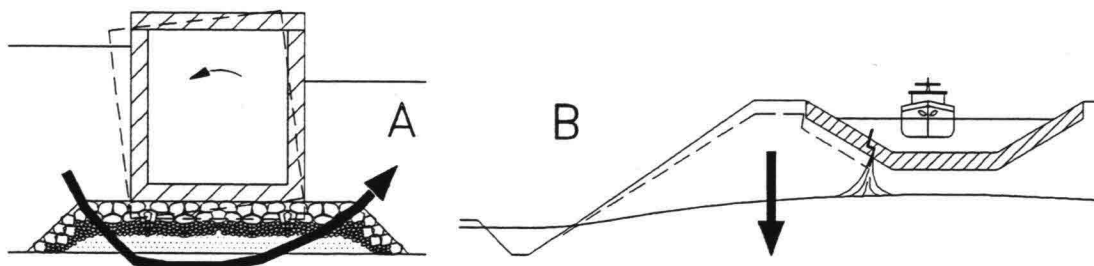


Figure 1.11 Cause and result

In case A there is a malfunctioning filter-protection under a water-retaining structure. Due to erosion, the structure will settle. Since the maximum gradient in the filter probably occurs at the entrance side of the flow, the settlement can be against the head difference.

In case B there is a canal situated above groundwater-level. To prevent waterlosses, the bottom of the canal is coated with an impermeable protection. When the dike along the canal settles, due to insufficient bearing capacity of the subsoil, a rupture in the protection can occur and the canal drains into the subsoil.

Figure 1.12 shows a general picture of the forces acting on a protected slope. A represents the loads from the water-side of the interface, the external load due to waves and currents. C is the load from inside due to a relatively high groundwater-potential in the soil-mass. B is the interaction between the external load and the inside of the construction. Although the external forces are usually rather violent and spectacular, many protections fail because of B or C.

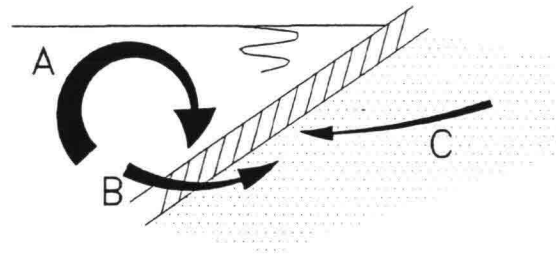


Figure 1.12 Loads

The external forces A ask for a strong protection. This strength can be reached e.g. by using large, heavy stones. But, from the example in Figure 1.10 we already saw that lack of sandtightness can be a problem then mainly caused by B. To make the protection sandtight, there should be something between the top-layer and the subsoil e.g. a cloth or a foil.

When that is too rigorous, it becomes impermeable and C becomes a threat. That means that there is also the demand of permeability (unless there are other reasons to make the protection impermeable, e.g. the canal in Figure 1.11 or a storage basin for contaminated dump material; in that case the protection has to be designed for the possible pressures).

Another way of increasing strength is establishing coherence in the top-layer e.g. by using placed blocks instead of dumped rocks or by injection of concrete or asphalt. Then again the protection can become impermeable or stiff which can cause problems when some settlement should be possible. So flexibility is another factor to reckon with. Figure 1.13 gives an idea of the contradicting factors in a protection design.

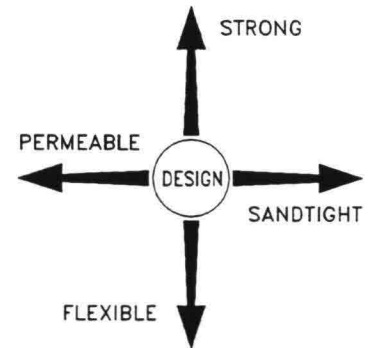


Figure 1.13 Contradicting influences

Although there has been done a lot of research in the field of hydraulics and soil-mechanics, the scientific basis of these designs is still rather weak. On one hand this is caused by the complexity of the interactions between water, the construction of the protection and the sub-soil. On the other hand there are many other factors influencing the functioning of the construction e.g. the weather (rain, frost, dust etc.) or pollution during its lifetime or the care with which it was executed. All this makes the hydraulic engineer more an artist than a scientist, to whom a sheet of white paper and a pencil are just as important as a computer and with creativity and experience playing a dominant role. A hand-made sketch of a stream or wave pattern on or around a structure is as valuable as the correct application of calculation rules. For both however, a good insight in the physics of the processes involved, is indispensable.

In the first chapter it was mentioned that energy of flowing water can dissipate into heat by means of friction. Turbulence plays a major role along the way from external energy to heat. What is turbulence? One of the most striking features in turbulent motion is the fact that the velocity and pressure at a fixed point perform very irregular fluctuations of high frequency. It resembles somewhat the movement of molecules, but here macroscopic fluid balls of various sizes live their own life in all directions. Turbulence is an irregular motion, but statistically distinct average values can be discerned and can be described by laws of probability.

It is obvious that turbulence plays a role in the protection against erosion, but most design formulas in hydraulic engineering are of an empiric nature, not bothering about what is going on inside the water. Is it really necessary then, to understand what exactly is going on. Furthermore, turbulence is difficult to understand or, in the words of an expert:

"The fluctuation which is superimposed on the principal motion is so hopelessly complex in its details that it seems to be inaccessible to mathematical treatment, ...". So why torment yourself with this trouble? The same expert however continues: *"... but it must be realized that the resulting mixing motion is very important for the equilibrium of forces. The effects caused by it are as if the viscosity were increased by factors of one hundred, ten thousand or even more."* (Schlichting, 1968).

An example may show why it is important to have at least an idea of the internal processes related with turbulence. Consider the stability of stones on the bottom of a channel with steady flow. In cross-section 1 in Figure 2.1 we can calculate the shear-stress as follows. From the equilibrium between the weight and the shear of a slice of water we can see: $\tau = \rho \cdot g \cdot h \cdot l$

With Chezy ($u = C \cdot (h \cdot I)^{1/2}$) this becomes: $\tau = \rho \cdot g \cdot (u/C)^2$ in which C can be calculated from:

$C = 18 \log 12h/k$ (hydraulically rough). With the well known Shields-formula (all this will be

discussed in detail in the coming chapters, here it serves just demonstration purposes) we can calculate the necessary diameter: $d = \tau / \psi \cdot (\rho_s - \rho_w) \cdot g$ What we have done in fact here, is using the external, total shear-stress resulting from the internal turbulent processes. So far so good.

In cross-section 2, the velocity is higher which can be calculated from the Bernoulli- and the continuity-equation. The friction-coefficient C is smaller because h/k is smaller. All this results in a larger shear-stress leading to larger stones. This goes in the right direction, but does it lead to the right result? The velocity-profile is no longer logarithmic due to the acceleration, leading to a much higher shear-stress, even when related to the velocity on the sill itself in cross-section 2 instead of 1.

In cross-section 3 it is even more obvious that the "Chezy"-approach leads to nonsense. The parameters in the above-mentioned formulae are the same as in cross-section 1, while the hydraulic situation is completely different. So, alas, in order to understand what is going on and to make a proper design, it is necessary to have at least a notion of what is going on in turbulent flow. Most design-rules are of an empirical nature; this will remain so in the foreseeable future. In these lecture-notes turbulent-flow features are discussed mainly to be able to judge empiric rules; for detailed knowledge of turbulence the reader is referred to the lectures concerned (e.g. Booij, 1986).

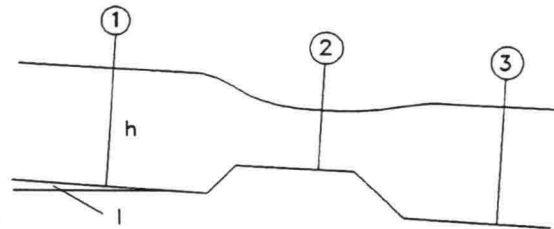


Figure 2.1 Steady flow over a sill

To be able to understand what is going on inside a turbulent flow, we turn to the source of all wisdom in hydraulics: the Navier-Stokes equations. These equations will be used here for demonstration purposes only. Mathematical and physical strictness is sacrificed for simplicity when this is considered appropriate. For a two dimensional flow this can be written for the x-direction (neglecting external forces):

$$\rho \left(\frac{\partial u}{\partial t} + u \frac{\partial u}{\partial x} + w \frac{\partial u}{\partial z} \right) = - \frac{\partial p}{\partial x} + \mu \frac{\partial^2 u}{\partial z^2} \tag{2.1}$$

local inertia convective inertia pressure gradient viscous shear

and the continuity-equation (conservation of mass):

$$\frac{\partial u}{\partial x} + \frac{\partial w}{\partial z} = 0 \tag{2.2}$$

The Navier-Stokes equations are in fact Newton's second law: $F = m \cdot a$ taking into account the viscous forces. The viscous shear is an internal stress caused by the transfer of molecular momentum. For a Newtonian fluid: $\tau = \mu \partial u / \partial z$, so, $\partial \tau / \partial z = \mu (\partial^2 u / \partial z^2)$, in which μ is the dynamic viscosity. So, the last term in equation (2.1) represents the rate of change in shear perpendicular to the flow, see also Figure 2.2 (In the z-direction there is a shear-stress equal in magnitude; in the x-direction there is also a viscous normal stress proportional with $\partial u / \partial x$. This is usually very small and is neglected here for simplicity). For an incompressible fluid with constant density the continuity-equation follows from Figure 2.3 (Check for yourself).

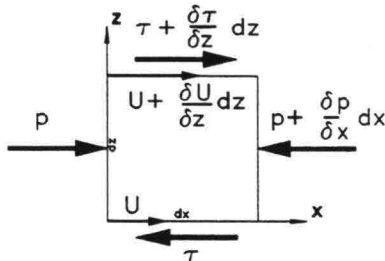


Figure 2.2 Forces on fluid-element

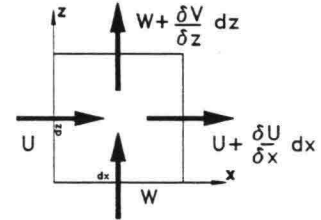


Figure 2.3 Mass conservation

The Navier-Stokes equations are valid for both laminar and turbulent flow. However in practical hydraulics the equations are averaged over a certain period of time, "smoothing" out the turbulent fluctuations. Due to this averaging, extra terms will appear in the equations. The values of velocity and pressure in equation (2.1) and (2.2) can be written as:

$$u = \bar{u} + u' \quad w = \bar{w} + w' \quad p = \bar{p} + p' \tag{2.3}$$

in which $\bar{\quad}$ indicates the average value and $'$ the fluctuation.

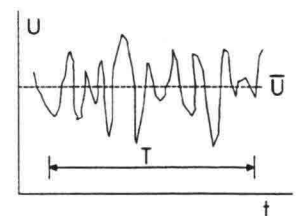


Figure 2.4 Averaging turbulence

The averaging period T is chosen such that it is long enough to smooth out turbulence and short compared to the principal motion (like the wave period).

The turbulence in a flow is often expressed by the root mean square (rms) value of the velocity fluctuations (which is equal to the standard deviation in a Gaussian distributed signal) and then again often made dimensionless with a turbulence averaged velocity:

$$r = \frac{\text{rms}(u')}{\bar{u}} = \frac{\sqrt{u'^2}}{\bar{u}} = \frac{\sigma}{\bar{u}} \quad (2.4)$$

In this case the rms-value is compared to its "own" average and then often called r in literature. The same can be done for the fluctuations of w (and v in the third dimension). One should always be aware of the parameter that is used to make the rms-value dimensionless, because it is also possible to use the average of u for w' or v' and even in another place.

Averaging equations (2.1) and (2.2) over T we get for the linear terms like $\partial u/\partial t$:

$$\frac{\partial \bar{u}}{\partial t} = \frac{1}{T} \int_0^T \frac{\partial u}{\partial t} dt = \frac{\partial}{\partial t} \frac{1}{T} \int_0^T (\bar{u} + u') dt = \frac{\partial}{\partial t} \frac{1}{T} \int_0^T \bar{u} dt + \frac{\partial}{\partial t} \frac{1}{T} \int_0^T u' dt = \frac{\partial \bar{u}}{\partial t} + 0 = \frac{\partial \bar{u}}{\partial t} \quad (2.5)$$

since, by definition:

$$\bar{u} = \frac{1}{T} \int_0^T u dt \quad \text{and} \quad \bar{u}' = \frac{1}{T} \int_0^T u' dt = 0 \quad (2.6)$$

The same holds for w and p . So, the linear terms for laminar and turbulent flow are expressed by the same type of function. This is not true however for the quadratic terms:

$$\begin{aligned} \overline{u^2} &= \frac{1}{T} \int_0^T u^2 dt = \frac{1}{T} \int_0^T (\bar{u}^2 + 2\bar{u} \cdot u' + u'^2) dt = \bar{u}^2 + \overline{u'^2} \\ \text{since: } \frac{1}{T} \int_0^T 2\bar{u} \cdot u' dt &= 2\bar{u} \frac{1}{T} \int_0^T u' dt = 2\bar{u} \cdot 0 = 0 \\ \text{and: } \frac{1}{T} \int_0^T u'^2 dt &= \overline{u'^2} \quad (\text{mean value of } u'^2 \neq 0!) \end{aligned} \quad (2.7)$$

Similarly:

$$uw = (\bar{u} + u') \cdot (\bar{w} + w') = \bar{u}\bar{w} + u'\bar{w} + w'\bar{u} + u'w' \quad \text{hence: } \overline{uw} = \bar{u}\bar{w} + \overline{u'w'} \quad (2.8)$$

and equation (2.1) becomes (note: the viscous term is of the second order but linear):

$$\rho \left(\frac{\partial \bar{u}}{\partial t} + \bar{u} \frac{\partial \bar{u}}{\partial x} + \bar{w} \frac{\partial \bar{u}}{\partial z} + \overline{u' \frac{\partial u'}{\partial x}} + \overline{w' \frac{\partial u'}{\partial z}} \right) = - \frac{\partial \bar{p}}{\partial x} + \mu \frac{\partial^2 \bar{u}}{\partial z^2} \quad (2.9)$$

local inertia *conv.inertia by mean vel.* *conv.inertia by fluct.vel.* *press. grad.* *visc. shear*

The continuity equation (2.2) becomes:

$$\frac{\partial \bar{u}}{\partial x} + \frac{\partial \bar{w}}{\partial z} = 0 \quad \text{and:} \quad \frac{\partial u'}{\partial x} + \frac{\partial w'}{\partial z} = 0 \quad (2.10)$$

From this we can add to the equation of motion the zero value:

$$\rho u' \left(\frac{\partial u'}{\partial x} + \frac{\partial w'}{\partial z} \right) \quad (2.11)$$

giving for the part of the convective inertia which is caused by the turbulent fluctuating velocities:

$$\rho \left(2 \cdot \overline{u' \frac{\partial u'}{\partial x}} + \overline{w' \frac{\partial u'}{\partial z}} + \overline{u' \frac{\partial w'}{\partial z}} \right) = \rho \left(\frac{\partial \overline{u'^2}}{\partial x} + \frac{\partial \overline{u'w'}}{\partial z} \right) \quad (2.12)$$

Equation (2.9) finally becomes:

$$\rho \left(\underbrace{\frac{\partial \bar{u}}{\partial t} + \bar{u} \frac{\partial \bar{u}}{\partial x} + \bar{w} \frac{\partial \bar{u}}{\partial z}}_{\substack{\text{inertia} \\ \text{by mean values}}} \right) = \underbrace{-\frac{\partial \bar{p}}{\partial x}}_{\text{press.}} + \underbrace{\mu \frac{\partial^2 \bar{u}}{\partial z^2}}_{\text{visc.}} - \underbrace{\rho \left(\frac{\partial \overline{u'^2}}{\partial x} + \frac{\partial \overline{u'w'}}{\partial z} \right)}_{\substack{\text{Reynolds-stresses} \\ \text{by turb. fluct.}}} \quad (2.13)$$

showing the turbulent normal and shear stress extra to the averaged values. For a more detailed (and better) derivation of the so-called Reynolds-equations (2.13) see e.g. Schlichting (1968) or Le Méhauté (1976).

PHYSICAL INTERPRETATION

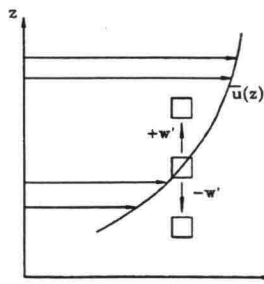


Figure 2.5 Transport of momentum

What is the meaning of all this? In Schlichting's quote it was already mentioned that the effects of the Reynolds-stresses are "as if the viscosity were increased". For the shear-stress this can be demonstrated as follows: consider a mean flow with $\bar{u} = \bar{u}(z)$, $w = 0$ and $d\bar{u}/dz > 0$, see Figure 2.5. The particles which travel upwards ($w' > 0$) arrive at a layer with a higher velocity \bar{u} . These particles or lumps preserve their original velocity causing a negative component u' , decelerating the flow in x -direction. Conversely, the particles arriving from above ($w' < 0$) give rise to a positive u' accelerating the flow. On the average a positive w' is associated with a negative u' and vice versa. So we may expect u' and w' to be correlated (the average of $u' \cdot w' \neq 0$ and negative). The vertical flux of turbulent momentum per unit surface area is equivalent to an

equal and opposite stress exerted on the area by the surroundings:

$$M_z = \rho \cdot \overline{u' \cdot w'} = -\tau'_{xz} \quad (2.14)$$

An important assumption in the mathematical treatment of turbulent shear is: $\tau :: \partial u / \partial z$ (gradient-type transport of momentum). This is in line with the analogy between turbulent and viscous shear. The proportionality is expressed as the turbulent viscosity or **eddy viscosity** ϵ .

The total shear stress then becomes:

$$\tau = \rho(\nu + \epsilon) \frac{\partial \bar{u}}{\partial z} \quad (\nu = \mu/\rho: \text{kinematic viscosity}) \quad (2.15)$$

There is however a great difference between the two viscosity coefficients: the (molecular) kinematic viscosity is a property of the fluid, while the eddy-viscosity is governed by the flow geometry. The purpose of many turbulence theories is to estimate ϵ and there is still a long way to go on that road before there are generally usable models. For a stationary flow with a parabolic distribution of ϵ in the vertical, this leads to the logarithmic velocity distribution. For more detail, the reader is referred to basic hydraulics.

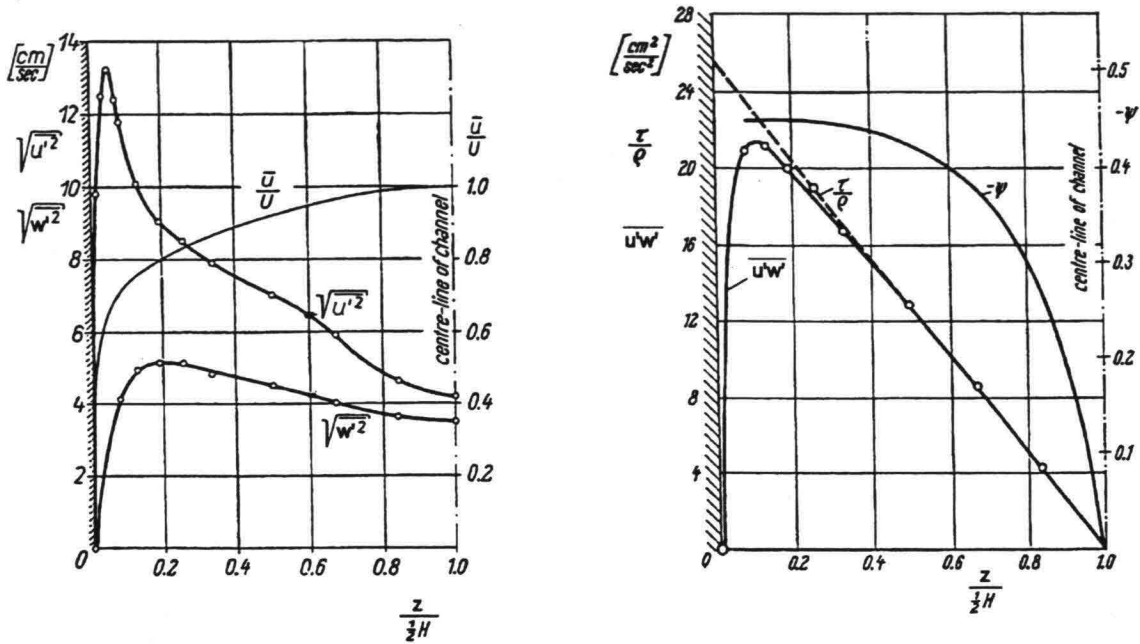


Figure 2.6 Measurements in a wind tunnel (Schlichting 1968)

Figure 2.6 shows the results of measurements in a wind tunnel. It can be seen that the turbulent fluctuations are 0 at the wall, but maximum very near the wall. In fact, the turbulence is generated by the wall, but very close to it, turbulent fluctuations cannot penetrate because of the laminar boundary layer, where molecular viscosity dominates. The same is visible for the relation between τ and $u'w'$. In the centre-line of the channel, the velocity-gradient, the shear-stress and also $u'w' = 0$, while the turbulent fluctuations in x- and z-direction are not 0. In that case u' and w' are not correlated like in Figure 2.5. The correlation can be expressed in a correlation-coefficient, ψ :

$$\psi = \frac{\overline{u'w'}}{\sqrt{\overline{u'^2}} \cdot \sqrt{\overline{w'^2}}} \quad (2.16)$$

When $\psi = 0$, the turbulence is called isotropic. The turbulent fluctuations are then equal in all directions, each living their own random life and not physically correlated. In isotropic turbulence there is no turbulent shear!

The shear-stress is an important factor in the stability of bottom-protections, revetments etc. Essentially in the approach of wall-shear is the assumption that there is no slip at the wall in a viscous fluid. This implies a velocity gradient between the wall and the flowing water. A practical approach is the concept of a boundary layer in which there is influence of the wall and the region outside where there is no influence. The transition is arbitrarily defined e.g. as the place where $u = .99u_\infty$.

The boundary layer grows when water suddenly flows along a wall, see Figure 2.7 where an infinitely thin plate is placed in a flow with $u = u_\infty$. At the start, $\delta(x) = 0$, leading to a theoretically infinite shear stress. The boundary layer grows because of the exchange of momentum, smoothing the velocity differences.

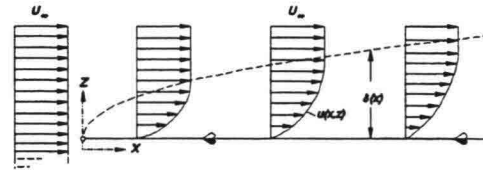


Figure 2.7 Growth of boundary layer

The limit at the downstream end is reached when the whole geometry e.g. waterdepth is boundary layer. This is usually the case in river-flow, approximately in tidal-flow and certainly not in wind waves which we will discuss later. It is usual to relate the shear stress at the wall, τ_0 , to the square of the velocity in the main stream by a friction-coefficient, C_f :

$$C_f = \frac{\tau_0}{\frac{1}{2} \rho u_\infty^2} \quad (2.17)$$

Note: The use of $1/2$ in the denominator is not self-evident. It comes from the relation between pressure and velocity in the Bernoulli-equation where $p + 1/2\rho u^2 = \text{constant}$. Expressed in waterlevels ($h = p/\rho g$), $1/2\rho u^2$ represents the velocity head: $u^2/2g$. In the determination of drag forces, see paragraph 2.4 and equation (2.24), this is a logical measure to use, since it represents the increase in pressure in front of a body. It is customary to use $1/2\rho u^2$ in all flow forces.

It is not easy to determine C_f for the situation given in Figure 2.7. Under the assumption that $\partial p/\partial x = 0$ and that the boundary layer is turbulent from the beginning, Schlichting found for rough plates (see Figure 2.8):

$$C_f = (2.87 + 1.58 \log \frac{x}{k})^{-2.5} \quad (2.18)$$

in which k is the equivalent sand roughness (see later in this paragraph). The assumption $\partial p/\partial x = 0$ means that u_∞ is constant along the wall. When this is not the case, the approximation is reasonable as long as there is no separation of the flow. For a smooth plate the boundary layer will be laminar in the beginning, but for application in hydraulic engineering it is reasonable to assume that the boundary layer is always turbulent.

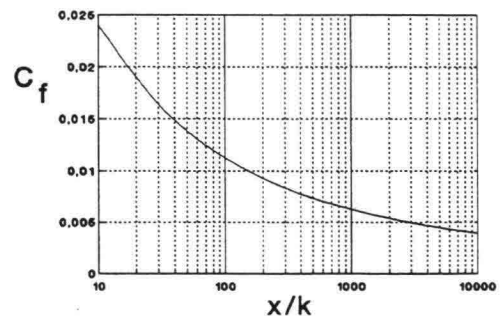


Figure 2.8 C_f in a growing boundary layer

At the downstream end, C_f is limited by the situation that the whole waterdepth is a fully developed boundary layer (**uniform flow**) and C_f becomes:

$$\left. \begin{aligned} \tau_0 &= \rho g h I \\ u_0 &= C \sqrt{h I} \end{aligned} \right\} \rightarrow \tau_0 = \rho g \frac{u_0^2}{C^2} \rightarrow C_f = \frac{2g}{C^2} \quad (2.19)$$

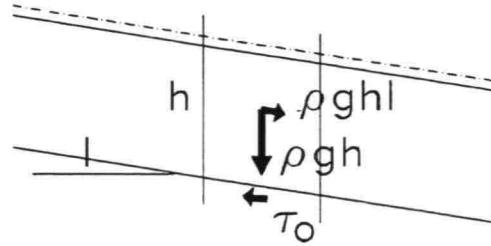


Figure 2.9 Bottom shear in uniform flow

from the Chezy formula, the equilibrium between the shear stress at the bottom and the slope gradient of the weight of a "slice" of water (see Figure 2.9) and equation (2.17). u_0 is the velocity averaged over the turbulence period and the vertical. The factor 2 comes from the use of 1/2 in the denominator of equation (2.17).

Figure 2.10 shows for uniform flow in a flume, a measured velocity profile with the turbulent fluctuations in the flow direction. A value of r , see equation (2.4), of about 10% is normal in uniform flow (where the energy transfer due to bed friction is the only cause of turbulence). Note that r is defined with the vertical averaged velocity in the denominator.

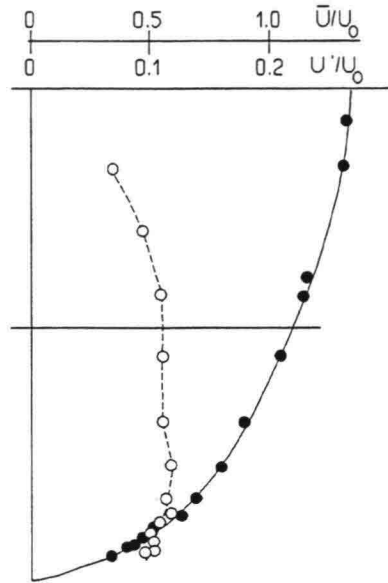


Figure 2.10 Velocity profile and fluctuations in uniform flow

Other useful relations for uniform flow are:

$$u_* = \sqrt{\frac{\tau_0}{\rho}} = \frac{\sqrt{g}}{C} u_0 \quad (2.20)$$

where u_* is the so-called shear velocity. u_* has no physical meaning, but is used in many relations dealing with stability.

$$C = \frac{\sqrt{g}}{\kappa} \ln \frac{12h}{k} \approx 18 \log \frac{12h}{k} \quad (2.21)$$

in which k is the so-called equivalent sand-roughness. This roughness has to be related to the grain-sizes of the bed. For a stable bed without transport, a value of $k \approx 3d_{50}$ is often used, while for a well-leveled bed $k \approx 2d_{50}$ is applied. It must be stated that the choice of k is not well-defined and also depends on the accuracy of the construction method!

Instead of h in equations (2.19) and (2.21), which is only correct for an infinitely wide channel, the hydraulic radius R is used for cases where also wall friction plays a role. Finally, In Anglo-saxon textbooks the formula by Manning is often used instead of the Chezy formula. The relation between the two (in metric units) reads:

$$u_0 = \frac{R^{1/6}}{n} \sqrt{RI} \quad \text{and} \quad C = \frac{R^{1/6}}{n} \quad (2.22)$$

In flow around a body, the water in the vicinity of that body decelerates in front of it, accelerates at the sides and decelerates again at the back. The pressure that goes with it, rises, falls and rises again (see D-E-F in Figure 2.11). The conversion of potential energy into kinetic energy on its path from D to E can be considered as a "ride downhill", from E to F is then "uphill" into an area with increasing pressure. In a perfect fluid there is no friction and the pressures in D and F are equal, hence the net force on the body is zero. The viscosity in a real fluid however changes the picture completely. The friction in the boundary layer makes the uphill motion stop between E and F and the flow separates from the body.

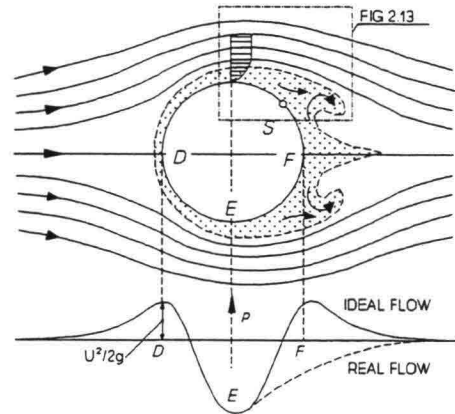


Figure 2.11 Flow around a body

The combination of (viscous) friction and a negative pressure-gradient is essential for flow-separation. Figure 2.12 shows streamlines for three situations:

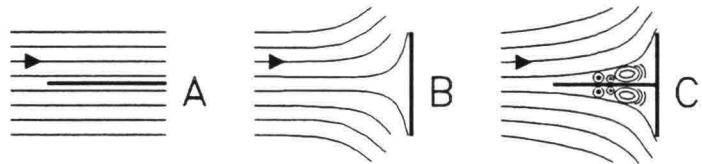


Figure 2.12 Conditions for flow separation

- A: Flow parallel to a plate, friction but no pressure gradient. No flow separation (see also Figure 2.7)
 - B: Flow perpendicular to a plate, pressure gradient but no friction. No flow separation.
 - C: Both, friction and pressure gradient. Flow separation.
- This can be verified by experiments, see Schlichting, 1968.

For stationary flow in that case only the right-hand-side of equation (2.1) remains (no slip at the boundary, hence u and $\partial u/\partial x = 0$) when the x - z coordinates are transferred to natural coordinates (s and n , hence $w = 0$). The equation then becomes:

$$\frac{\partial p}{\partial s} = \mu \frac{\partial^2 u}{\partial n^2} \tag{2.23}$$

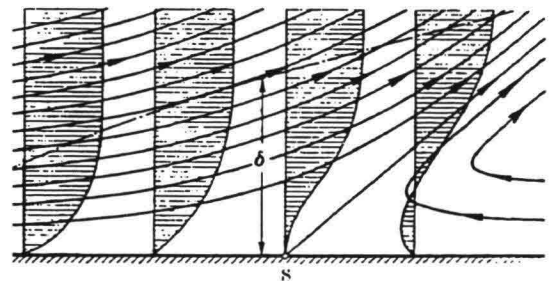


Figure 2.13 Flow separation

from which can be seen that a change in the sign of $\partial p/\partial s$ leads to a point of inflection in the $u(n)$ curve leading to separation (see Figure 2.13 which is an enlargement of the upper part of Figure 2.11).

In the case of a sharp edge it is easy to see that the flow has to separate, since no separation would mean that a streamline would make a right angle with a radius = 0, leading to an infinite centripetal force ($F = u^2/r$). So, the water cannot follow such a sharp curve and goes straight on.

The result of flow separation is a wake behind the body and a shear layer between the main flow and the wake, which plays an important role in the attack on the bottom as we shall see later. The flow-separation and wake also cause an extra resulting drag force on the body (extra to the friction along the body). This drag force is usually related to the velocity field by:

$$C_D = \frac{F_D/A}{\frac{1}{2} \rho u_\infty^2} \quad (2.24)$$

in which C_D is the drag-coefficient, D the drag force, A the area perpendicular to the flow and u_∞ the undisturbed velocity. $\frac{1}{2} \rho u^2$ represents the velocity head and is the rise in pressure in front of the body (point D in Figure 2.11), see also the note with equation (2.17). C_D depends on the Reynolds-number (defined as $u.L/\nu$) and the geometry of the body.

Figure 2.14 gives C_D for various bodies. For small Re there is hardly any influence of the geometry (Stokes-region). For higher Re there are interesting differences. A flat plate shows a constant C_D ; the sharp edge gives a fixed separation point ($\partial p/\partial x \ll 0$). For a cylinder and a sphere, the separation point depends on Re . At $Re \approx 3 \cdot 10^5$ there is a sudden drop in the drag; this is related to the transition of the boundary layer from laminar to turbulent. Due to turbulent mixing, the main flow takes fluid-particles from the boundary layer "uphill", see Figure 2.11, so the wake behind the body and the flow resistance are less than at lower Re -numbers. For a streamlined body, C_D is much lower because there is no flow separation. In fact, the drag consists completely of shear stress which is much lower than form resistance. This demonstrates that viscous stress itself is not dominating, but the influence of viscosity on the flow pattern.

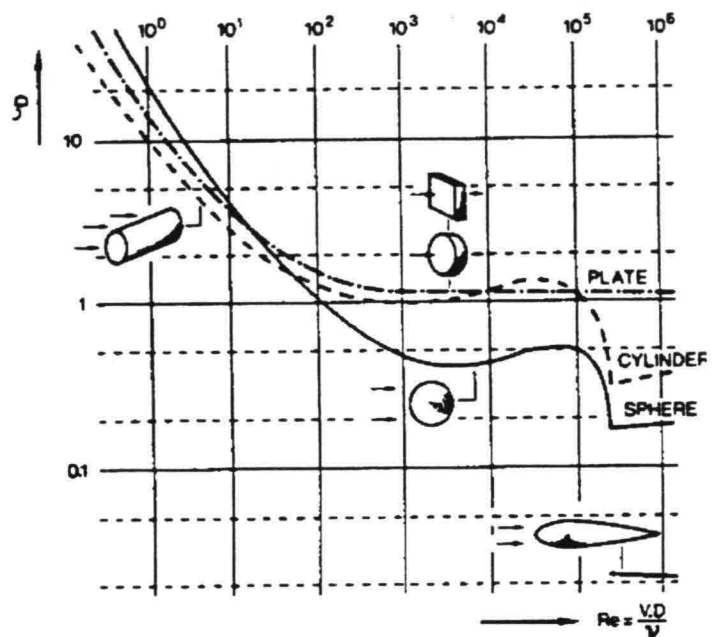


Figure 2.14 C_D as a function of Re

In the case of an asymmetric pressure distribution a force transverse to the flow occurs, the so-called lift-force. This force plays a role in the stability of stones where water flows over a bottom, due to the curved streamlines, see figure 9.1. When there is a lift-force it is expressed in the same way as drag and shear:

$$C_L = \frac{F_L/A}{\frac{1}{2} \rho u_\infty^2} \quad (2.25)$$

2.5.1

GENERAL

A jet is a flow into a large body of water with an excess velocity compared to the surrounding fluid. A wake is the opposite: behind a solid body with a velocity relative to the surrounding fluid, an area is formed with a lower velocity. Both in jets and wakes the velocity tends to become equal to that of the surrounding fluid. Many flow situations in hydraulic engineering show similarity to jets or wakes. Flow from a culvert or behind a ship's propeller can be described as a jet. The flow behind a ship or a bridge pier can be seen as a wake. When there is no influence of walls, there is a so-called free turbulent flow. In that case the transition between turbulent and viscous friction in a thin layer near the wall plays no role, which makes these phenomena better accessible for computation. They will be described here shortly, for more details the reader is referred to e.g. Rajaratnam, 1976, Schlichting, 1968 or the 82 lectures.

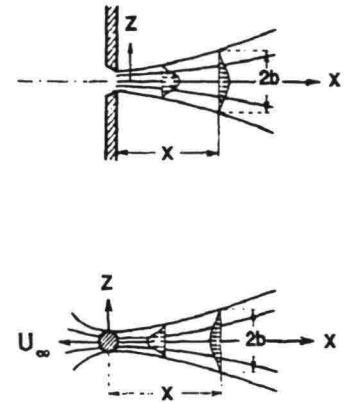


Figure 2.15 Jet and wake

Starting-point for the mathematical description are again the Navier-Stokes equations (in the form of equation (2.13)). The following simplifications can be made: $\partial u/\partial t = 0$ (steady flow), $\partial p/\partial x = 0$ (no external force downstream of the outflow, hence no pressure gradient in the flow direction) and the viscous shear stress and the turbulent normal stress are small compared with the turbulent shear stress. The remaining equations then become:

$$u \frac{\partial u}{\partial x} + w \frac{\partial u}{\partial z} = \frac{-\partial \overline{u'w'}}{\partial z} = \frac{1}{\rho} \frac{\partial \tau}{\partial z} \quad (2.26)$$

$$\frac{\partial u}{\partial x} + \frac{\partial w}{\partial z} = 0$$

Note: the bars have been left out; u and w now represent the turbulent mean. τ is the turbulent shear stress.

With these equations and assumptions for the relation between τ and $\partial u/\partial z$ (and additional experiments to find the necessary constants), solutions for the velocity distribution can be found. A very important assumption in the derivation of these relations is the similarity of velocity distributions in different locations. Here only some results will be given.

At the outflow of a jet or at the separation of the flow in a wake behind a body, there is a difference between the velocity in the jet or mainflow and the surrounding fluid or wake respectively. This leads to an intense shear at the velocity discontinuity, inducing turbulence. The stagnant fluid is accelerated, whereas the flowing mass loses momentum. The layer affected by this exchange of momentum is known as a mixing layer or shear layer, see Figure 2.16.

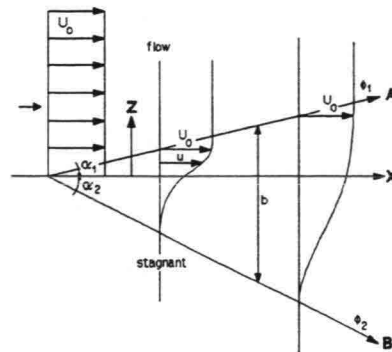


Figure 2.16 Definitions for a plane shear layer

The width of the mixing layer, between \$\phi_1\$ and \$\phi_2\$ in Figure 2.16 is \$b\$. Assuming \$u/u_0\$ is a function of \$z/b\$ (similarity!), from equation (2.26) can be found: \$b \propto x\$ and from experiments it is found (Rajaratnam, 1976):

$$b \approx 0.26 x \quad \alpha_1 \approx 5^\circ \quad \alpha_2 \approx 10^\circ \tag{2.27}$$

The flow in a mixing layer diverges along a line with a slope of \$1 : \cot\alpha_2 \approx 1 : 6\$. When the turbulence that comes with a mixing layer has to be avoided or postponed till a point where the velocity is lower, wing walls are often applied with slopes of \$1 : 8\$ or even less.

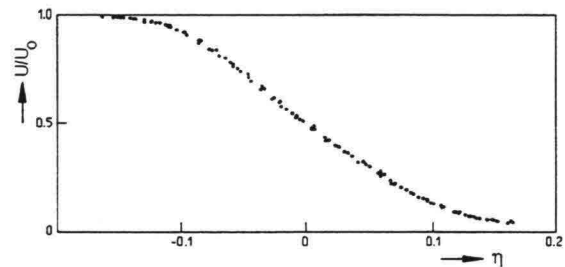


Figure 2.17 Velocity similarity in shear layer

The assumption of similarity is confirmed by experiments, see Figure 2.17 where \$u/u_0\$ is plotted against \$\eta = z/x\$ (which is with \$b \propto x\$ equivalent to \$z/b\$)

Since we are interested in turbulent fluctuations, because they possibly influence protections, some measurements of fluctuations are presented in Figure 2.18. Note that the fluctuations in all directions have been made dimensionless with the driving velocity of the shear layer: \$u_0\$. In the flow direction the relative fluctuations have an order of magnitude of about 20%, while the fluctuations perpendicular to the main flow are about 15%. The maximum of \$u'\$ occurs where the velocity gradient is maximum and where \$u = 0.5u_0\$. So, compared with the local velocity, the fluctuations are twice as high.

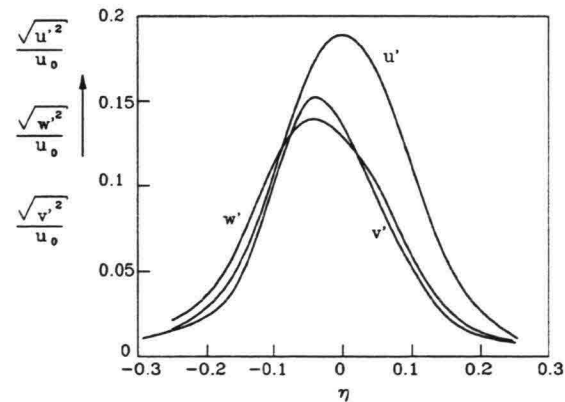


Figure 2.18 Turbulent fluctuations in shear layer

A plane jet is a two-dimensional outflow from an orifice (see Figure 2.19, the orifice is infinitely long perpendicular to the paper). A circular jet is 3-dimensional with axial symmetry. Free means: no wall influence. Close to the orifice (the flow development region) turbulence penetrates into the core of the jet. This is the mixing layer as described in the previous paragraph. Here the velocity in the centerline is equal to u_0 .

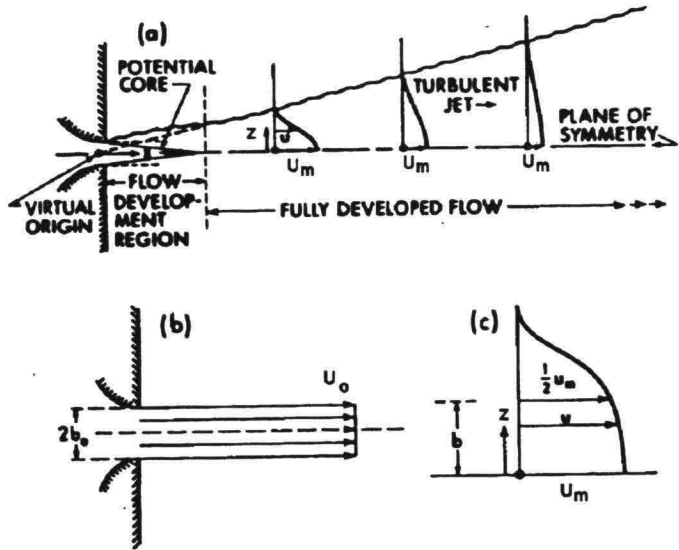


Figure 2.19 Definition sketch of plane free jet

After the flow is fully developed, the velocity decreases and the jet spreads with a velocity profile that is very similar in all locations, see Figure 2.20.

Particles from the surrounding fluid are dragged into the jet, increasing the mass flow (Figure 2.21).

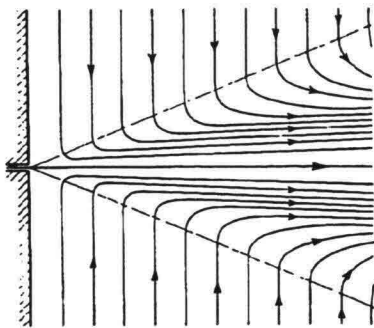


Figure 2.21 Streamlines in jet

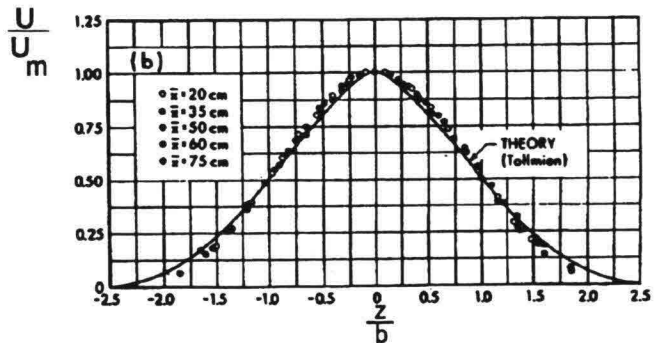
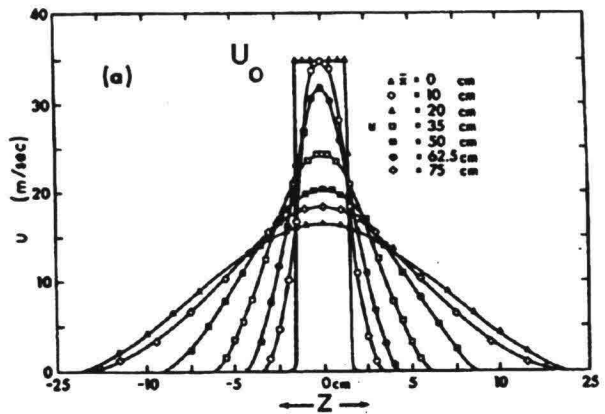


Figure 2.20 Velocity distribution in plane jets

The total momentum however, remains constant, which is essential for a jet. In the extremes we have at one end an infinitely small orifice with an infinitely high velocity (but with a finite momentum, $M_0 = 2\rho b_0 u^2$), called the virtual origin of the jet (usually very near the orifice). The other extreme is an infinitely large flow area with an infinitely small velocity, but with the same momentum, M_0 . Important results for hydraulic engineering will be presented. For a detailed description the reader is referred to Rajaratnam, 1976. The velocity distribution can be described as a Gaussian curve with only two parameters, u_m (u in the center of the jet) and b (a typical width, usually taken as the value where $u = u_m/2$). Plots of u/u_m against z/b (for plane jets; for circular jets r/b , r being the radial distance from the center) are similar for all x (in the developed flow region!, see Figure 2.20). For plane jets can be derived that: $u_m \propto 1/\sqrt{x}$ and $b \propto \sqrt{x}$ and for circular jets: $u_m \propto 1/x$ and $b \propto x$. These proportionalities are only valid in the region of fully developed flow, which starts at about $x=12b_0$ for plane jets and $x=6D$ for circular jets (D being the radius of the orifice). In the flow development region the velocity can be approximated by u_0 . Numerical values for these proportionalities must be derived from experiments. It was found for free jets, see Figure 2.22 (for definitions, see Figure 2.19):

<i>Plane jets</i>	<i>Circular jets</i>	
$u_m = \frac{3.5 u_0}{\sqrt{x/b_0}}$	$u_m = \frac{6.3 u_0}{x/D}$	(2.28)
$b = 0.1x$	$b = 0.1x$	
$u = u_m e^{-0.69(z/b)^2}$	$u = u_m e^{-0.69(r/b)^2}$	

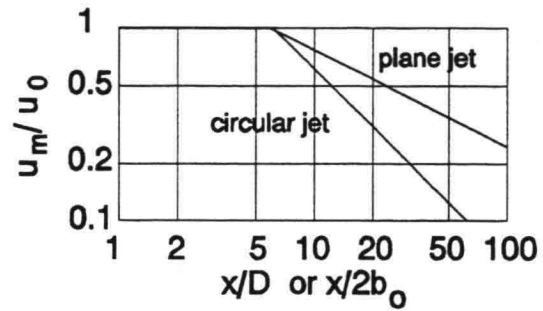


Figure 2.22 Velocity decay in centerline of jets

Since we are again interested in turbulent fluctuations, Figure 2.23 shows some measurements for a circular jet. At the left hand side of the figure in the centerline as a function of x and at the right hand side from the center to the edges of the jet. Note that again all fluctuations are compared with the velocity in x -direction, but now with u_m which is the maximum velocity in the centerline, which decreases linearly with x . The relative fluctuations in the centerline become constant with increasing x with a value of about 30% in the center-line for the flow direction. For $b \approx 0.1x$ the velocity is, by definition, $u_m/2$. The fluctuation there ($z/x = 0.1x/x = 0.1$) is about 25% compared to u_m . So, compared to the local velocity it is about 50%

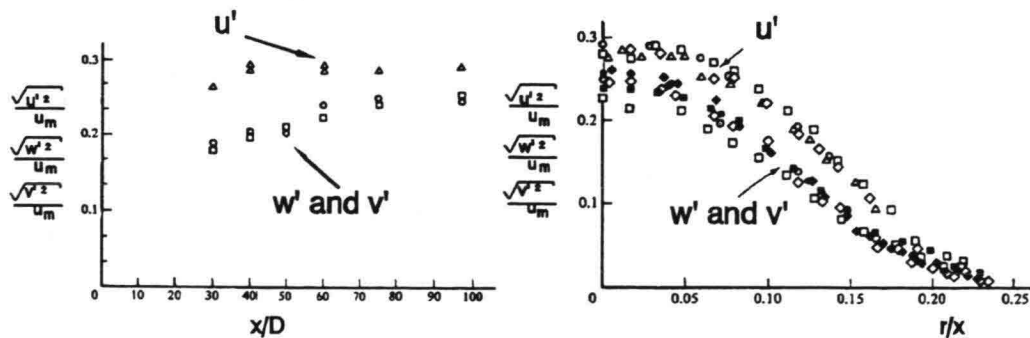


Figure 2.23 Turbulent fluctuations in circular jet

Figure 2.24 shows the configuration for this case.

Most work has been done for the situation with a smooth wall, but Rajaratnam, 1976 discusses the influence of roughness. The same proportionalities as for the free plane jet were found. The experimental results give:

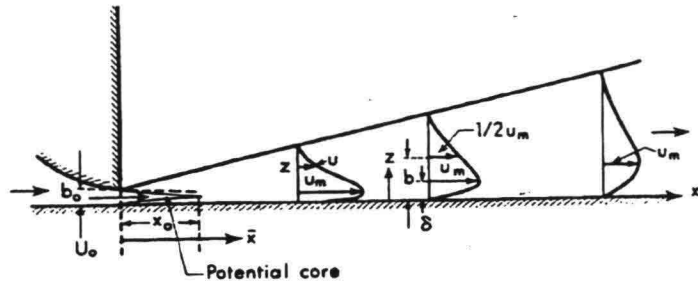


Figure 2.24 Plane wall jet

$$\begin{aligned}
 u_m &= \frac{3.5 u_0}{\sqrt{x/b_0}} \\
 b &= 0.068 x \\
 u &= 1.48 u_m \left(\frac{z}{b}\right)^{\frac{1}{7}} \left[1 - \operatorname{erf}\left(0.68 \frac{z}{b}\right)\right]
 \end{aligned}
 \tag{2.29}$$

The differences with the plane free jet are the growth of the jet, which is 30 % smaller and the shape of the velocity distribution which is asymmetric. The lower part (the boundary layer, under u_m , see Figure 2.24) can be described by a power law, while the upper part (the free mixing region) has again a Gaussian shape. Both parts are reasonably described by an error function.

Wall-roughness does influence the boundary layer but not the free mixing region. The error-function does not describe correctly the velocity distribution anymore, see Figure 2.25.

Another difference is the velocity decay, which is given for a rough wall by:

$$\frac{u_m}{u_0} = C_R - 0.54 \log(x/k) \tag{2.30}$$

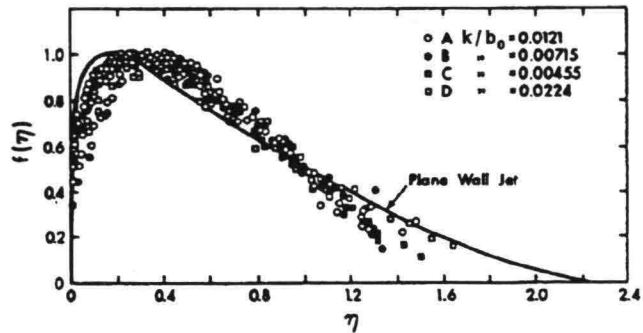


Figure 2.25 Velocity distribution on rough walls, $\eta = z/b$

in which k is the roughness and C_R is a constant depending on the roughness, see Figure 2.26. Figure 2.27 shows the difference between the velocity decay according to equation (2.30) and (2.29). Compared with a smooth boundary, the velocity u_m decreases faster with a rough boundary.

Note: the experimental results are valid for $k/b_0 < 0.13$, see Figure 2.26. For larger roughness values, C_R seems to be constant. Using equation (2.30), this leads to higher velocities for higher roughness which is unlogic. This again means that using such an empirical relation outside the investigated range is dangerous. Instead, it is recommended to use the lower curve in Figure 2.27 as a lower boundary for the velocity decay.

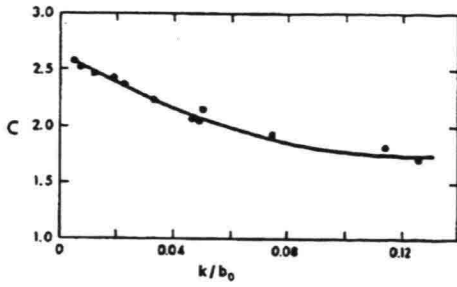


Figure 2.26 Velocity-decay coefficient for rough walls

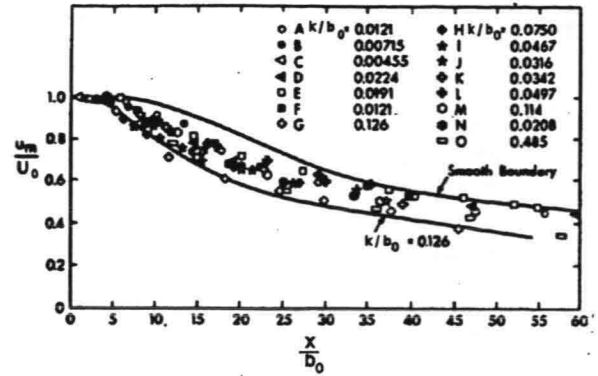


Figure 2.27 Decay of u_m for smooth and rough walls

2.5.5

3-DIMENSIONAL WALL JETS

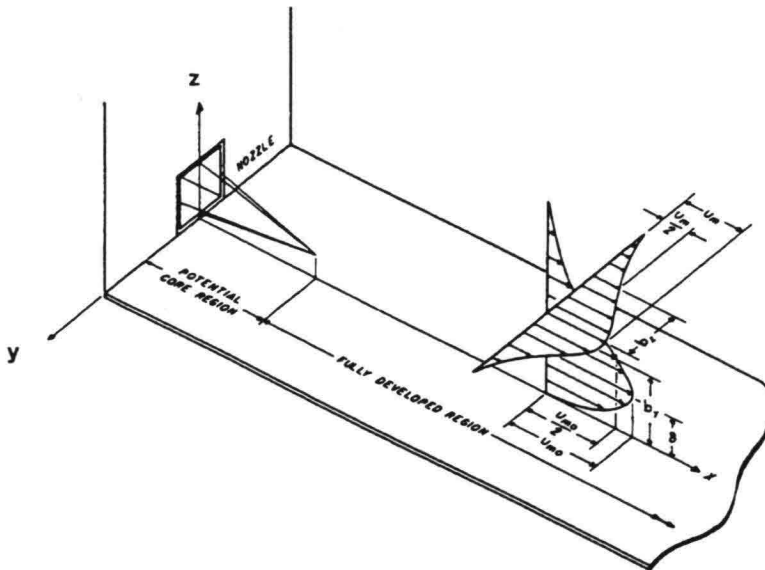


Figure 2.28 3-dimensional wall jet

A situation that occurs often in practice is given in Figure 2.28. The orifice has a height h , a width B and an area A . It can be derived that $u_{m0} \propto 1/x$, b_y and $b_z \propto x$. Again, experiments have been done to establish numerical values for the various parameters. It was found:

$$u_{m0} = \frac{8u_0}{x\sqrt{A}} \quad (\text{approximately}) \quad (2.31)$$

$$\frac{b_z}{h} = 0.9 + 0.045 \frac{x}{h} \quad \text{and} \quad \frac{b_y}{B} = 0.2 \frac{x}{B} - 1.25$$

Note that the virtual origin of the jet is no longer in the orifice; for b_y it lies behind and for b_z in front of it. \sqrt{A} is used for all kinds of orifice-shapes: circular, rectangular, square and triangular.

In the preceding sections, some flow phenomena were derived from the basic equations. That knowledge will be used in this section to illustrate some important flow factors in the stability of grains on an interface. Acceleration, deceleration and turbulence will be demonstrated with measurements in and behind vertical and horizontal constrictions. These constrictions can be regarded as archetypes of geometrical variations in many flow situations.

2.6.1

VERTICAL CONSTRICTION AND EXPANSION

A sill is a good example of a vertical constriction in hydraulic engineering, but also dunes on a river bed, while a scour hole can be seen as a vertical expansion. The flow accelerates in the constriction, while it decelerates in the expansion where turbulence plays a major role. In the expansion the following areas can be discerned, see Figure 2.29 and Hoffmans,1992 and Hoffmans,1993a.

Downstream from the obstacle, a mixing layer originates from the friction between the main flow and the initially stagnant water behind the obstacle. Due to this friction, the stagnant water turns into a wake or eddie, where the water flows opposite the main flow direction. Downstream from the wake, a new boundary layer grows and the flow tends to become uniform again. At first the turbulence in the mixing layer grows, while after reattachment it diminishes again. This can be seen from measurements above an artificial dune, see Figure 2.30 and van Mierlo,1988 or Hoffmans,1992. The turbulence is here expressed as k , the kinetic turbulent energy, defined as:

$$k = 1/2 (\overline{u'^2} + \overline{v'^2} + \overline{w'^2}) \quad (2.32)$$

made dimensionless with the vertically averaged velocity on the top of the dune. The values on the vertical axis in Figure 2.30 are roughly equal to the square of the relative turbulence, r , as defined in equation (2.4). The turbulence in the mixing layer grows rapidly to a maximum, which is much larger than the turbulence caused by the bed-roughness. Downstream of the reattachment point, the turbulent energy of the mixing layer dissipates until the total turbulence is again governed by the bed-roughness, which is the only source of turbulence in uniform flow.

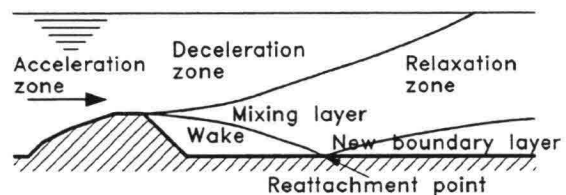


Figure 2.29 Flow regions in expansion

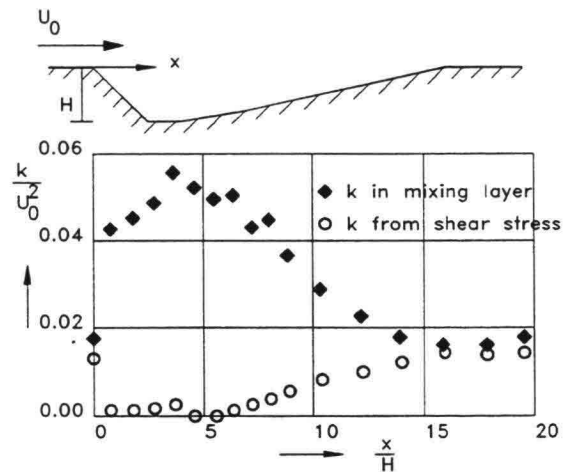


Figure 2.30 Measured turbulent energy above an artificial dune (van Mierlo & de Ruiter,1988)

At Delft University of Technology another study was performed to the flow over a sill. Calculations were made with a turbulence model (Blom,1991) and measurements were done in a flume (Blom,1993).

Figure 2.31 shows a summary of the results. In the calculations (top of the figure) we see the changes in the velocity profile: logarithmic before the sill, accelerating and more rectangular on top, decelerating and almost separating behind the sill, slowly recovering to a logarithmic profile in uniform flow again. The computed shear stress is made dimensionless with the Chezy-friction, see equation (2.19) and can therefore be seen as an enlargement factor. On top of the sill the pattern of Figure 2.8 can be recognized: at first high values due to the acceleration, later on lower values due to the growing boundary layer, although the friction stays on a level, higher than in the stationary situation. Behind the sill the shear drops to zero in the reattachment point.

The measurements show the same pattern, although measurements very near the bottom could not be executed, leaving uncertainties on what is going on. In the acceleration zone, the increase in shear stress is clearly visible. The turbulent fluctuations (u'^2 and w'^2) remain more or less the same, leading to a much lower relative turbulence (the average velocity doubles). In the deceleration zone, the energy loss, due to the head difference over the sill, leads to high turbulent velocity fluctuations behind the sill where the energy is transmitted to turbulence (this is the internal process of the so-called Carnot energy-loss in basic hydraulics).

From all this it can be seen that, from the point of view of stability of grains on the interface, there are two aggravating factors: increase in shear in the acceleration zone and high velocity fluctuations in the decelerating zone. In chapter 6 and 9, we will study the consequences for scour behind a sill and stability of stones on and behind a sill.

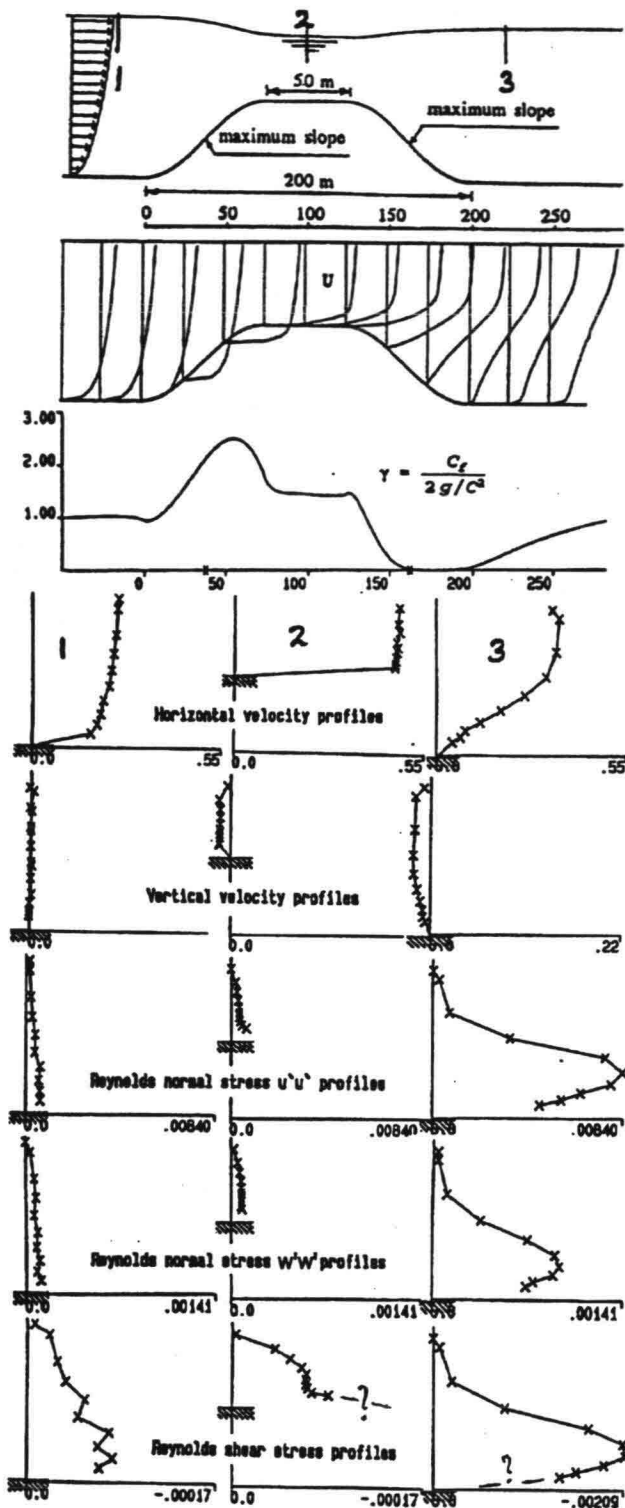


Figure 2.31 Flow over sill

Horizontal constrictions and expansions come in many shapes. Abutments and groynes are clear examples, as well as the inflow and outflow of a discharge sluice. But also natural variations in the width and protruding points in a river show the same phenomena. A horizontal constriction causes the flow to accelerate. After the obstacle, the flow usually separates and a mixing layer with a vortex street grows in the deceleration zone. In the framework of a study on scour and grain stability at Delft University of Technology, the flow pattern was measured for a situation with 1/6 of the width of a flume blocked, see Ariëns, 1993. Figure 2.32 shows (vertically averaged) measured values of the velocity (averaged over the turbulence period): \bar{u} , the relative turbulence (related to the local value of u): r and the (absolute) value of the "maximum" velocity: $u+3\sigma$. The acceleration and deceleration are clearly visible in the average velocity. (Note that the mixing layer is now curved because of the flow concentration around the constriction.) Acceleration acts as a "rectifier" and hence, the relative turbulence decreases in the acceleration zone from 8% to less than 5%, increasing again in the deceleration zone. In the mixing layer, the relative turbulence reaches high values. The "maximum" velocity ($u+3\sigma$) shows a large zone with high values. It is in this area where maximum damage to bottom protections and maximum scour, occurs. The first scour (when the bed is unprotected) and the first moving stone is found very near the tip of the obstruction, not near the maximum value of $u+3\sigma$. For scour this can be explained by the rapidly increasing sediment transport capacity and the lack of sediment supply from upstream. See chapter 6, Scour. For the top layer of a bottom protection this can be explained by the increase of the velocity near the bottom due to the acceleration. For more detail, see chapter 10, Stability in flow

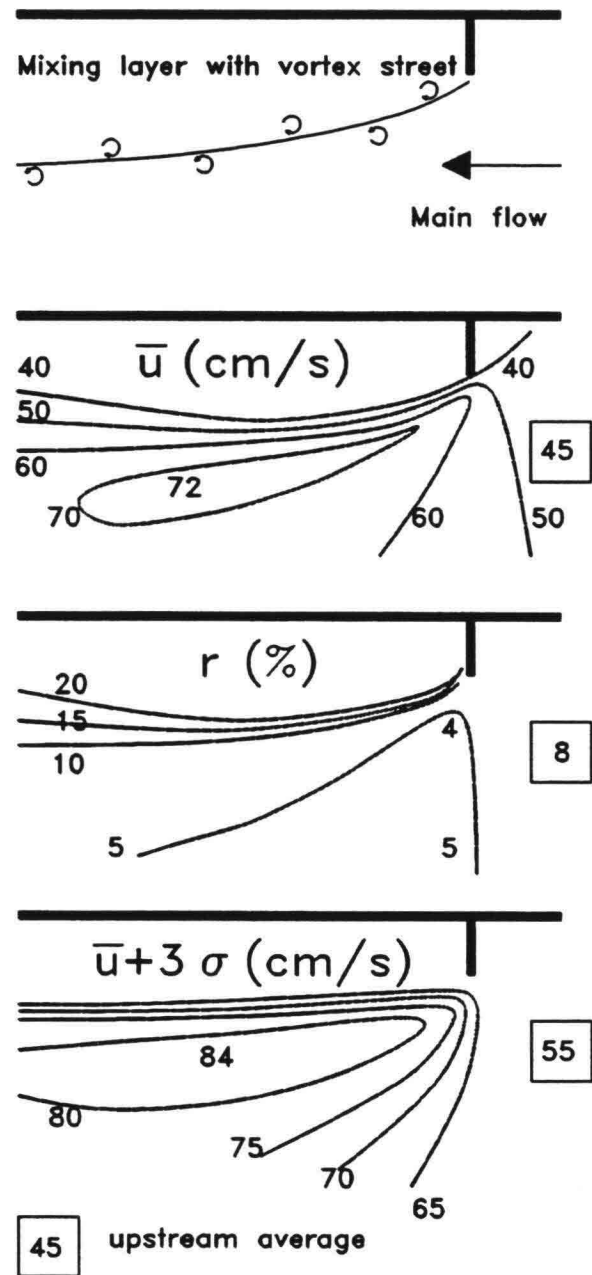


Figure 2.32 Vertically averaged flow values for a horizontal constriction

Waves, either caused by wind or ships, play an important role in the stability of soil-water interfaces. The same holds for tidal waves, but for our purpose these can be considered as a succession of stationary flow conditions. Tidal waves are so-called long waves (see b73-lectures) in contrast with the short waves dealt with in this paragraph. "Long" and "short" are relative hydrodynamic notions; "long" means that the vertical accelerations are neglected, so the pressure distribution is hydrostatic. We start with the description of velocities and pressures in waves; for more details, see the b76 lectures or LeMehaute, 1976. The description is limited to the so-called linear or small amplitude wave theory. This is a simplification of what is really happening and is valid only for waves with small amplitudes, see Figure 3.1. For an adequate understanding however, the linear theory is very useful and the calculated values outside the range of validity can serve as an indication.

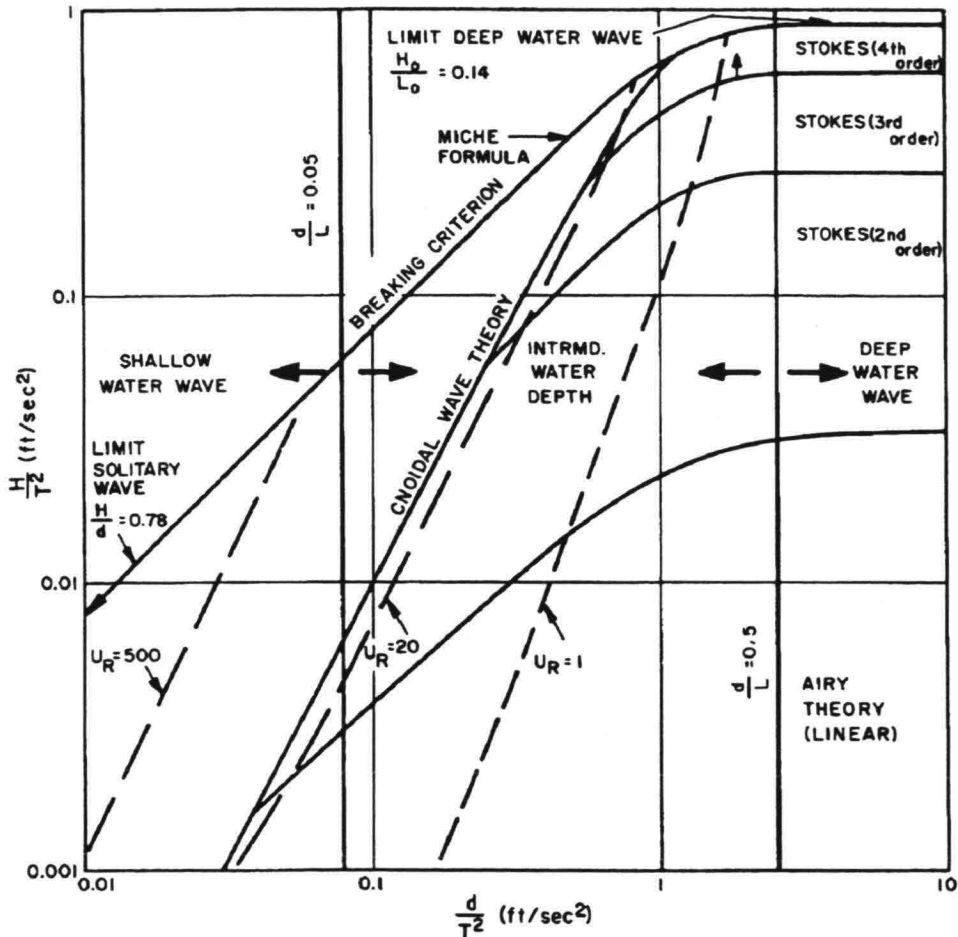


Figure 3.1 Validity of wave theories (LeMehaute, 1976)

Starting point is again the Navier-Stokes equation, neglecting boundary effects. Inside the boundary layer this equation reduces to:

$$\rho \frac{\partial u}{\partial t} = \mu \frac{\partial^2 u}{\partial z^2} \quad (3.1)$$

When \hat{u} is the maximum velocity in the oscillating flow with period T and the boundary layer thickness is δ , the order of magnitude of the terms in equation (3.1) are $\rho \cdot \hat{u}/T$ and $\mu \cdot \hat{u}/\delta^2$, from which follows $\delta \approx \sqrt{(\mu \cdot T/\rho)}$. With $\mu/\rho = \nu \approx 10^{-6} \text{ m}^2/\text{s}$ and $T=10 \text{ s}$ we find a boundary layer thickness of less than a centimeter (in an oscillating flow, the boundary layer gets no time to grow). This means that the neglect of viscous shear is valid for almost the complete waterdepth; in the boundary layer itself another approach has to be applied. Where in the coming paragraphs the bottom velocity is mentioned, this means the velocity at the boundary layer. Outside the boundary layer viscous shear can be neglected and the flow can be considered irrotational. In that case there are no Reynolds-stresses and the basic equations can be solved when a surface-profile is assumed (see also Figure 3.3):

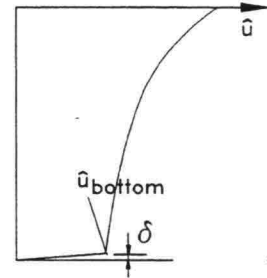


Figure 3.2 Velocities in short waves

$$\eta = \frac{H}{2} \sin\left(\frac{2\pi t}{T} - \frac{2\pi x}{L}\right) = a \sin(\omega t - kx) = a \sin\theta \quad (3.2)$$

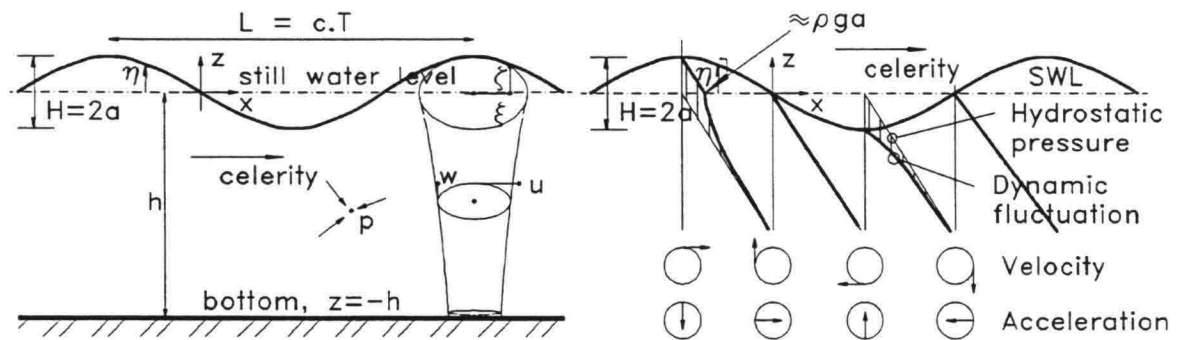


Figure 3.3 Definition and processes in sinusoidal, progressive wave

Note: $z = 0$ represents the still water level and z is positive upwards.

Figure 3.3 shows the relations between waterlevel fluctuations, velocities, accelerations and pressures, from which can be seen how the pressures under a wave are influenced by the vertical accelerations demonstrating the fact that the pressure is not hydrostatic.

In the following table (Table III.1), a summary of the various parameters is presented. The extremes for deep and shallow water in the table follow from the values for transitional water, since for deep water: $kh \rightarrow \infty$, so: $\tanh = 1$, $\sinh = \infty$ and $\cosh = \infty$ and for shallow water: $kh \rightarrow 0$, so: $\tanh = kh$, $\sinh = kh$ and $\cosh = 1$.

Relative depth Characteristics	Shallow Water $\frac{h}{L} < \frac{1}{20}$	Transitional water $\frac{1}{20} < \frac{h}{L} < \frac{1}{2}$	Deep Water $\frac{h}{L} > \frac{1}{2}$
Wave Celerity	$c = \frac{L}{T} = \sqrt{gh}$	$c = \frac{L}{T} = \frac{gT}{2\pi} \tanh kh$	$c = c_0 = \frac{L}{T} = \frac{gT}{2\pi}$
Wave Length	$L = T\sqrt{gh}$	$L = \frac{gT^2}{2\pi} \tanh kh$	$L = L_0 = \frac{gT^2}{2\pi}$
Group Velocity	$c_g = c = \sqrt{gh}$	$c_g = nc = \frac{1}{2} \left[1 + \frac{2kh}{\sinh 2kh} \right] * c$	$c_g = \frac{1}{2} c_0 = \frac{gT}{4\pi}$
Energy Flux (per m width)	$F = Ec_g = \frac{1}{2} \rho g a^2 \sqrt{gh}$	$F = Ec_g = \frac{1}{2} \rho g a^2 nc$	$F = \frac{T}{8\pi} \rho g^2 a^2$
Particle velocity horizontal	$u = a \sqrt{\frac{g}{h}} \sin\theta$	$u = \omega a \frac{\cosh k(h+z)}{\sinh kh} \sin\theta$	$u = \omega a e^{kz} \sin\theta$
vertical	$w = \omega a \left(1 + \frac{z}{h} \right) \cos\theta$	$w = \omega a \frac{\sinh k(h+z)}{\sinh kh} \cos\theta$	$w = \omega a e^{kz} \sin\theta$
Particle displacement horizontal	$\xi = -\frac{a}{\omega} \sqrt{\frac{g}{h}} \cos\theta$	$\xi = -a \frac{\cosh k(h+z)}{\sinh kh} \cos\theta$	$\xi = -a e^{kz} \cos\theta$
vertical	$\zeta = a \left(1 + \frac{z}{h} \right) \sin\theta$	$\zeta = a \frac{\sinh k(z+h)}{\sinh kh} \sin\theta$	$\zeta = a e^{kz} \sin\theta$
Subsurface pressure	$p = -\rho g z + \rho g a \sin\theta$	$p = -\rho g z + \rho g a \frac{\cosh k(h+z)}{\cosh kh} \sin\theta$	$p = -\rho g z + \rho g a e^{kz} \sin\theta$

Table III.1 Summary of Wave Characteristics

$$a = \frac{H}{2} \quad \omega = \frac{2\pi}{T} \quad k = \frac{2\pi}{L} \quad \theta = \omega t - kx$$

For a detailed description of wind waves, the reader is referred to the b78 lectures. Wind itself is a turbulent flow with velocity variations. So, when wind blows over a water surface, the waves that are the result, cannot be expected to be identical in shape and indeed, they are not (see Figure 3.4). The question is how to characterize this irregularity; can these waves be represented by a characteristic wave height and period?

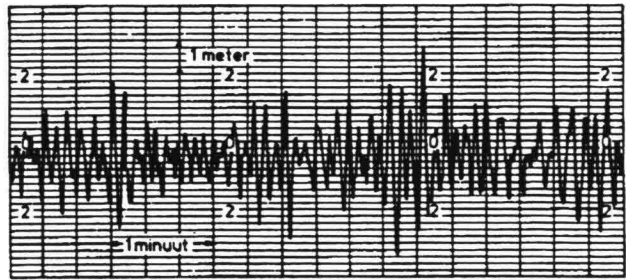


Figure 3.4 Wave registration North Sea

The first difficulty encountered is even more basic: what is actually a wave in this registration? Figure 3.5 shows the answer: the period of an individual wave is defined as the time between two "zero-crossings" (upward or downward), T_z and the wave height H is the highest crest minus the lowest trough between these zero-crossings. There are many values of H and T to characterize waves. Widely used are the so-called significant wave height and period, H_s or $H_{1/3}$ and T_s or $T_{1/3}$, defined as the mean values of the highest third part of the waves. The reasons for this are twofold. The higher waves are less sensitive for errors in measuring and visual estimates appear to be approximately equal to H_s . The latter reason is a historical one, since most wave observations until 25 years ago were done visually. It must be stressed however, that from a physical or statistical point of view, there is nothing "significant" in these values.

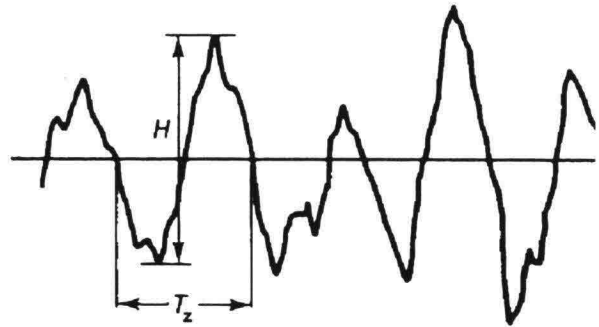


Figure 3.5 Definition of H and T

Many attempts have been made to relate wind wave heights and periods. The relation between individual height and period is however rather weak, see Figure 3.6. Instead, a distribution function for the wave heights is used, the Rayleigh-distribution, see next paragraph, while the distribution of the periods is presented in the form of an energy-spectrum. This is a measure of the distribution of the wave energy over the various wave periods in a registration.



Figure 3.6 Wave heights and periods in a registration

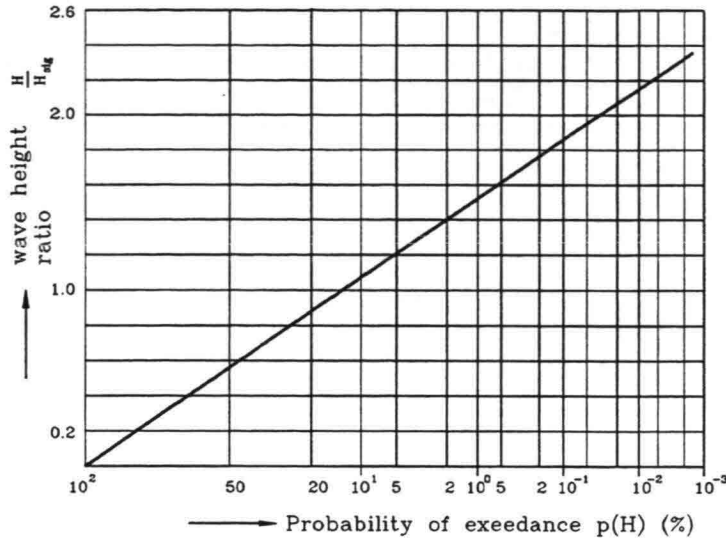


Figure 3.7 Rayleigh distribution

The population of wave heights can be described by a Rayleigh-distribution:

$$P\{H > H_s\} = e^{-2\left(\frac{H}{H_s}\right)^2} \tag{3.4}$$

This distribution is valid in water deeper than 3-4.H_s, in shallow water the highest waves break and the distribution deviates. According to the Rayleigh-distribution, H_s is exceeded by 13,5 % of the waves; H_s ≈ 1.6H_{av}. Extreme values are e.g. H_{1%} ≈ 1,5H_s.

A significant wave height with a Rayleigh-distribution is used to characterize waves in a record of about half an hour. For long-term wave height distributions, many observations of these values for H_s are used. The long-term distribution of H_s is often described with a Weibull-distribution:

$$P\{H_s \leq H\} = 1 - e^{-\left(\frac{H-A}{B}\right)^c} \tag{3.5}$$

Figure 3.8 gives an example of curve fitting of H_s-values on paper with a Weibull-scale.

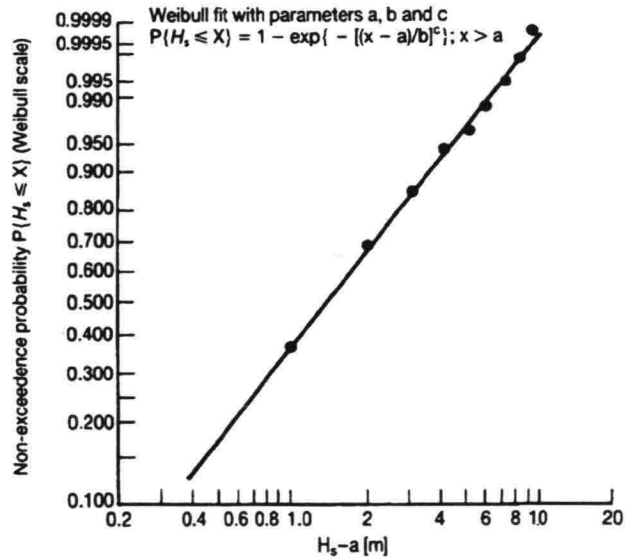


Figure 3.8 Long-term wave height distribution

A widely used description of irregular wind waves is given by an energy-density spectrum. The mathematical basis of this method can be used for the statistical description of any fluctuating signal, e.g. the deviation of a sailing ship from its course, the turbulent velocity fluctuation etc. Mathematically spoken it is the Fourier transform of the auto-covariance of the waterlevel fluctuation. The waterlevel is assumed to be the sum of an infinite number of simple sine waves:

$$\eta(t) = \sum a_i \cos(2\pi f_i t + \phi_i) \quad (3.6)$$

Every component i has a distinct value for a and f , ϕ_i is the only random variable. η is considered to be only a function of t , hence equation (3.6) is usually indicated as the one-dimensional random phase model. When the process is assumed to be stationary (the characteristics of the process do not change within a registration period) and Gaussian, it can be characterized by a mean value (still water level = 0) and the autocovariance-function:

$$C(\tau) = \text{covariance}(\eta_t, \eta_{t+\tau}) = \frac{1}{2} \sum a_i^2 \cos(2\pi f_i \tau) \quad (3.7)$$

The autocovariance (**co**, because it is the variance between two values and **auto** because it is within the same process) is a measure for the correlation between two values in a record, it is a kind of memory. For $\tau = 0$ it is the correlation of a value with itself, so $C(\tau)$ can nowhere become higher. and equation (3.7) reduces to:

$$C(0) = \text{variance}(\eta_t) = \frac{1}{2} \sum a_i^2 = \sigma^2 \quad (3.8)$$

in which σ is the standard deviation of the wave record.

The variance-spectrum is now the Fourier transform of the autocovariance function:

$$E(f) = \int_{-\infty}^{\infty} C(\tau) e^{-i2\pi f\tau} d\tau \quad (3.9)$$

The physical meaning of all this becomes clear when it is realised that the variance of a signal is highly identical to the energy in waves. The specific energy, see table III.1, is, with $H = 2a$, identical to the standard deviation in equation (3.8) apart from a factor ρg . The physical interpretation of a wave spectrum is then the distribution of energy over the various wave frequencies, hence the name energy-density spectrum. From the same identity it becomes clear that there must be a relation between the wave height and the area of the spectrum. For a Rayleigh distribution, this is theoretically given by:

$$H_s = 4\sqrt{m_0} \quad \text{with} \quad m_0 = \int_0^{\infty} E(f) df \quad (3.10)$$

In practice H_s is found to be about 5 % smaller. Relations between wave periods are less simple and depend on the shape of the spectrum. For a very narrow spectrum, T_s will be equal to T_p which is the peak period, equal to $1/f_p$, the frequency where the energy density is maximum. As a first approach for most spectra $T_s \approx 0,9 T_p$ can be used, and for the mean period: $T_M \approx 0,8 \sim 0,9 T_s$.

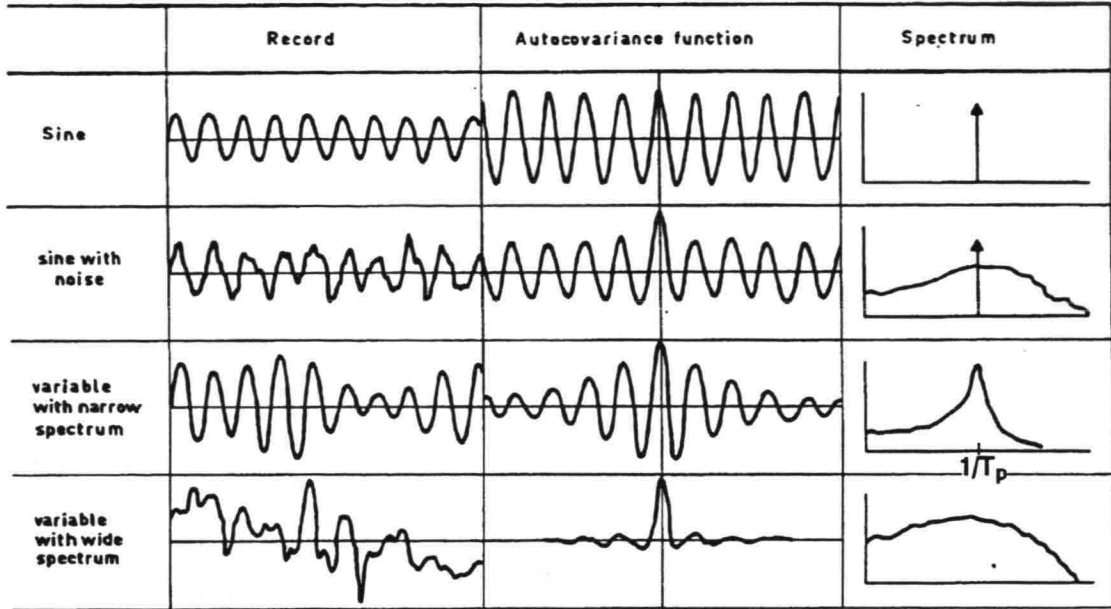


Figure 3.9 Relation between registration, autocovariance and energy spectrum

Wave spectra are widely used in hydraulic engineering. Therefore some examples are given for a better understanding. At first, some examples are given for a combination of registration, autocovariance and spectrum. Finally two "real" spectra are presented. The first belongs to the registration of Figure 3.4 ($H_s = 4\text{m}$, $T_s = 6.5\text{ s}$). The second is double peaked: "fresh" wind waves with $f \approx 0.4\text{ Hz}$ and "old" wind waves from another area, swell, with $f \approx 0.1\text{ Hz}$.

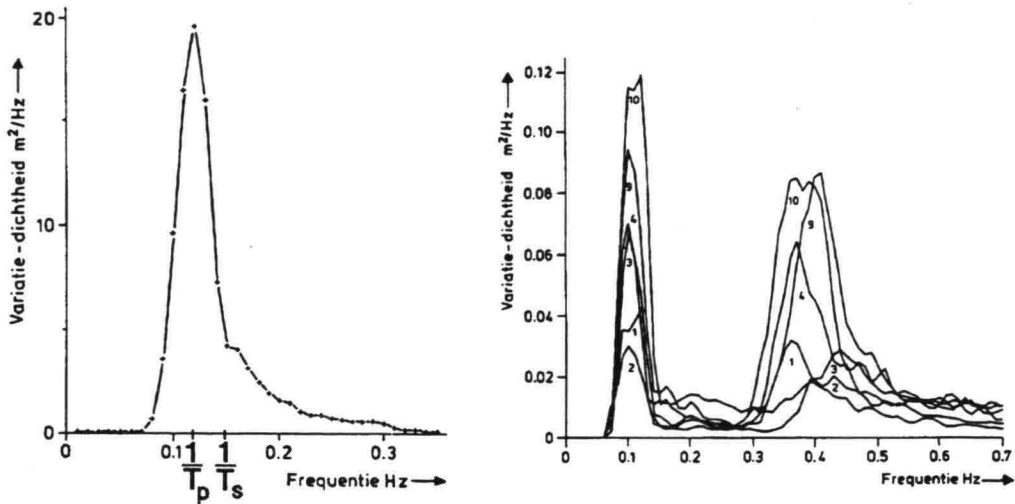


Figure 3.10 Spectra of North Sea registrations

In section 3.1 it was already mentioned that the boundary layer in short waves is relatively very thin. Every wave period the growth has to start again and the situation is similar to that of the start of a flow along a flat plate (see sect. 2.3). In short waves the boundary layer never gets the order of magnitude of the waterdepth, hence high friction factors can be expected. The friction factor is defined in a way analogous to that in a flow:

$$\hat{\tau}_w = \frac{1}{2} \rho C_f \hat{u}_b^2 \quad \text{with: } \hat{u}_b = \omega a_b = \frac{\omega a}{\sinh kh} \quad \text{and: } u = \hat{u}_b \sin \omega t \quad (3.11)$$

where the index w stands for wave and b for bottom. The average value over a wave period is half the value of the maximum (the average of $\sin^2 \omega t$ is 1/2).

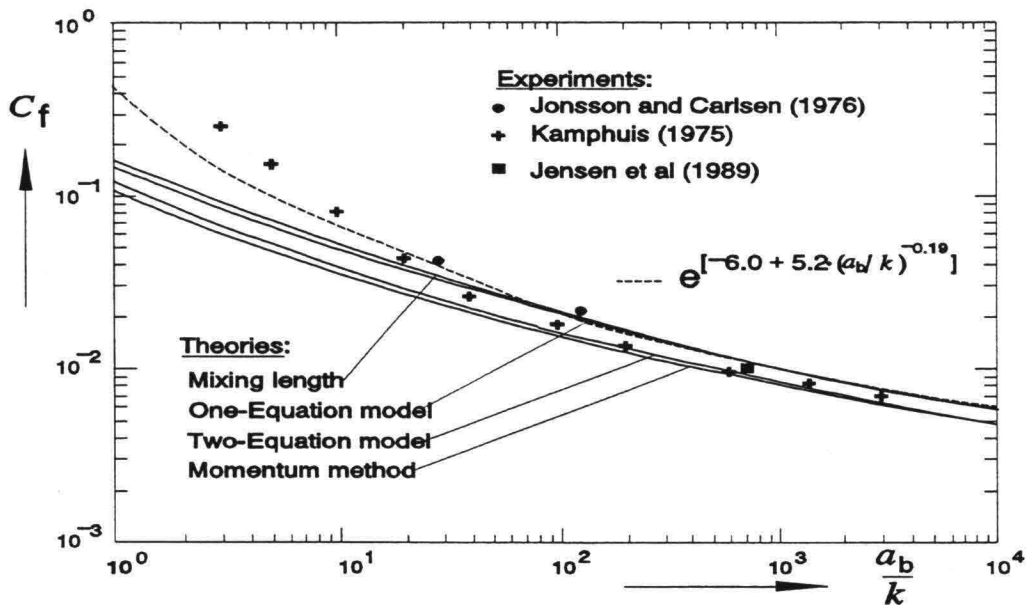


Figure 3.11 Friction factor under waves

In non broken waves, values for C_f can be calculated, using some assumption on the eddy viscosity in the oscillating flow, see Figure 3.11 from Fredsøe, 1992. For small values of a_b/k (short waves over a rough bottom) the value of C_f derived from measurements is much higher. This is possibly due to the fact that all these models use overall values of shear stress on the bed, while probably the flow around the individual grains also play a role when the water movement has the same order of magnitude as the grain size. Jonsson, 1966 found an expression for turbulent flow over a rough bed based on experiments, rewritten in a more practical form in e.g. CUR/CIRIA, 1991:

$$C_f = \exp \left[-6.0 + 5.2 (a_b/k)^{-0.19} \right] \quad (3.12)$$

Comparing the values in this figure with those for flow, it can be seen that shear stress under short waves can be much higher than in flow. C_f in uniform flow is: $2g/C^2$ (see section 2.3) which results in values of 0.005 - 0.01, while figure 2.8 for a growing boundary layer gives 2-3 times higher values. In very short waves, where the amplitude at the bottom has the same order of magnitude as the roughness, values of 0.1-0.5 seem possible.

In section 3.1 a characterization for progressive waves was given; progressive meaning: travelling on without being halted. Walls, dikes and beaches do stop the waves, either by reflecting or absorbing them. We start with the simple case of a vertical wall. This acts as a mirror: the incoming waves are sent back and the result is superposition of two progressive waves with celerity $+c$ and $-c$. This leads to a stand-still of the resulting wave, hence the name standing wave. The height is twice of that of the incoming wave.

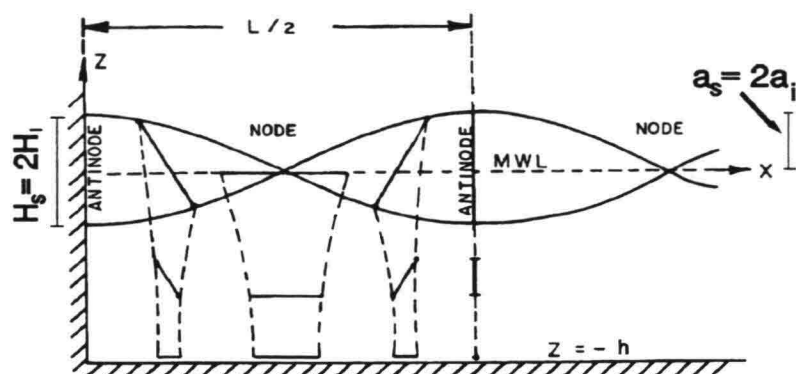


Figure 3.12 Standing wave

Figure 3.12 gives the pattern of a standing wave (or "clapotis"). Note that the orbits of the particle movement have degenerated into straight lines. At the antinodes there is only a vertical and at the nodes a horizontal movement. The wave profile for a standing wave in first approximation according to linear theory is given by:

$$\eta = a_s \cos kx \sin \omega t = 2a_i \cos kx \sin \omega t \quad (3.13)$$

in which H_i is the height of the incoming wave.

Other characteristic expressions for standing waves are:

$$\begin{aligned} u &= \omega a_s \frac{\cosh k(h+z)}{\sinh kh} \sin kx \cos \omega t \\ w &= \omega a_s \frac{\sinh k(h+z)}{\cosh kh} \cos kx \sin \omega t \\ p &= -\rho gz + \rho g a_s \frac{\cosh k(h+z)}{\cosh kh} \cos kx \sin \omega t \end{aligned} \quad (3.14)$$

When the vertical wall tilts backwards, the vertical motion of the water at the interface increases: the maximum waterlevel becomes higher than H_s as is the case in Figure 3.12. But the standing wave pattern remains till the waves break (depending on the slope and the wave steepness).

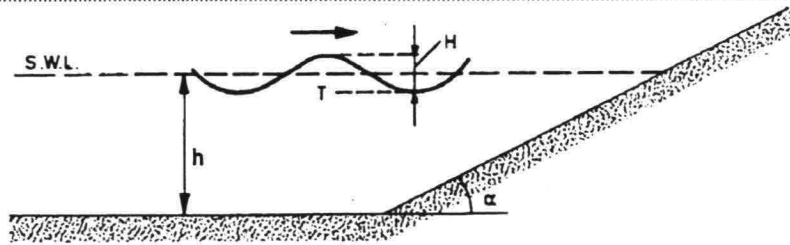


Figure 3.13 Definitions

Further decrease of the slope α of the shoreline (see Figure 3.13) leads to breaking of the waves. Breaking is instability and means in fact that the wave cannot longer exist; the particle velocity u becomes greater than the celerity c . The particles "come out of the wave profile". This instability makes the flow highly complex and lends itself hardly to computation. Breaking is also energy-dissipation where motion is transformed into heat, with a high degree of turbulence. When α becomes very small there is hardly any breaking and the wave energy is dissipated mainly by bottom shear. For $\alpha = 0$ we have arrived again at a progressive wave.

A dimensionless parameter which is of crucial importance to all kinds of problems in shore protection is the so-called Iribarren number, given by:

$$\xi = \frac{\tan \alpha}{\sqrt{H/L_0}} \quad (3.15)$$

This parameter indicates that the notions "steep" and "gentle" for a slope are relative ones. A slope of 1:100 is very "gentle", but for a tidal wave it can be just as steep as a vertical wall for a wave with a period of a few seconds. This is illustrated by the fact that a tidal wave on a beach does not break and is completely reflected (the phenomena described in this paragraph are completely different from those in tidal waves; the example only shows the relativity of all notions in hydrodynamics).

$\sqrt{H/L_0}$ can roughly be seen as the wave steepness (roughly, because H is the local wave height and L_0 is the deep-water wavelength). This indicates that an incoming wave that is already very steep will easily break, even at a very steep slope. Another way to look at L_0 is that it represents the influence of the wave period, since $L_0 = gT^2/2\pi$.

BREAKER TYPES

For different values of ξ , waves break in a completely different way; Figure 3.14 shows the various types. The transition between breaking and non-breaking lies around $\xi \approx 2.5 - 3$. For higher values the wave surges up and down the slope with minor air entrainment. The behaviour of the waves from $\xi \approx 3$ to 5, is therefore often called surging breaker although it can be questioned whether this is a breaking or a standing wave. A collapsing breakers could be seen as the transition between breaking and non-breaking. The most photogenic breaker is the plunging type ($\xi \approx 0.5$ to 3). In plunging breakers the crest becomes strongly asymmetric; it curls over, enclosing an air pocket, after which it impinges on the slope like a water jet. With decreasing slope angle, the crest of a plunging breaker becomes less asymmetric and the forward projected jet of water from the crest becomes less and less pronounced. This leads to the spilling breaker type ($\xi < 0.5$). The transition between the various breaker types is gradual and these values for ξ are just an indication. For more detail, see Battjes, 1974.

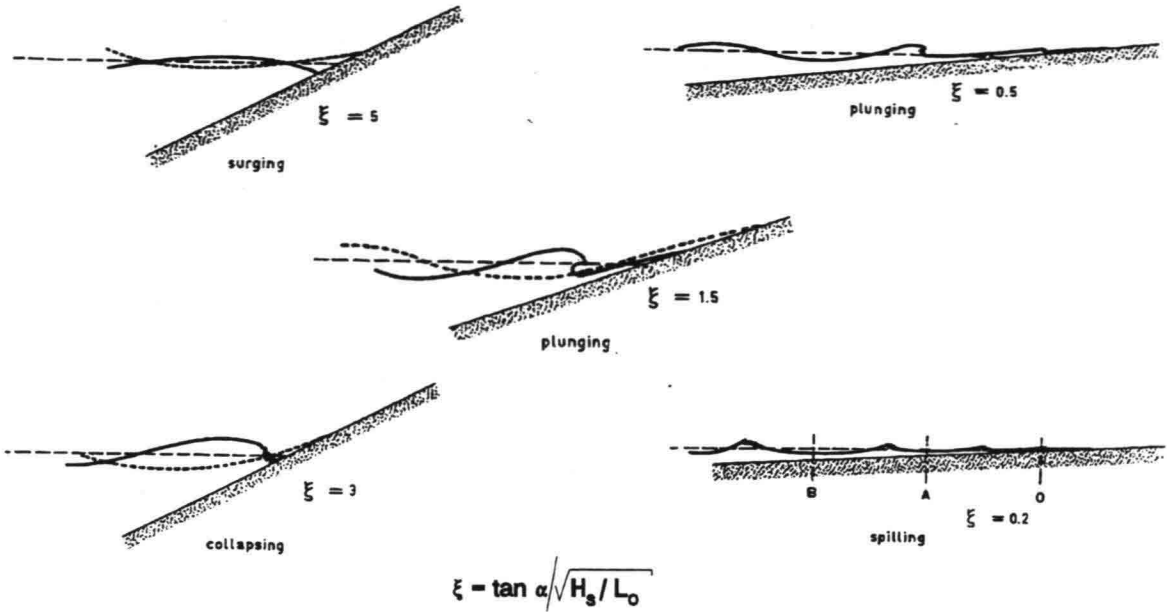


Figure 3.14 Breaker types

After breaking, the wave travels on with a celerity about equal to \sqrt{gh} and the wave behaviour can be described by a bore or a moving hydraulic jump, see for more detail Fredsøe, 1992.

BREAKER DEPTH

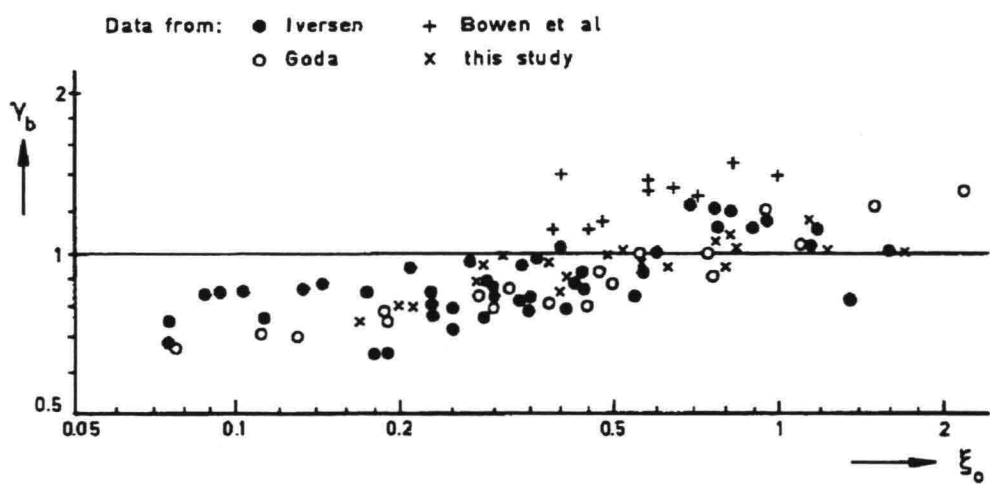


Figure 3.15 Breaker height-to-depth ratio (Battjes, 1974)

For a horizontal bottom, the solitary wave theory gives a relation for breaking between the wave height and the waterdepth: $\gamma_b = H/h \approx 0.78$ (see Figure 3.1). For slopes, γ_b depends on ξ . Figure 3.15 shows some experimental results (using ξ_0 with the deep water wave height H_0 , since H is hard to define at the point of breaking). For low ξ these are in reasonable agreement with the solitary wave theory; for steeper slopes, the waves break at a smaller depth. Apparently, the waves need time to break, in which they can travel to a smaller depth. These values are valid for individual waves; for irregular waves $\gamma_b = H_s/h \approx 0.5$

Since the highest waves are broken in this situation, the wave heights are no longer Rayleigh distributed, see Figure 3.16. $H_{1\%}$ e.g. is $1/(1 + H_s/h)^{1/3}$ times smaller than would follow from the Rayleigh-distribution, see also CUR/CIRIA,1991.

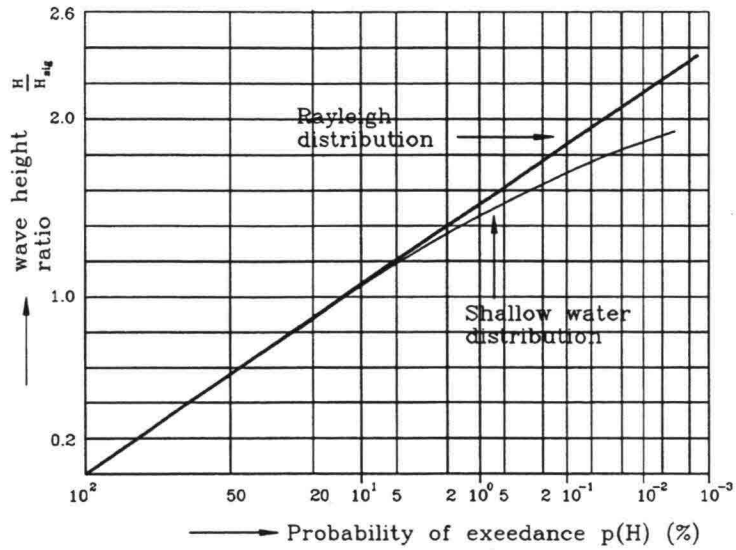


Figure 3.16 Wave-height distribution in shallow water

REFLECTION

Vertical walls fully reflect the incoming waves. The reflection is defined as the height of the reflected wave in relation to the incoming wave height: K_R (reflection-coefficient) = H_R/H_I . It can be reasoned

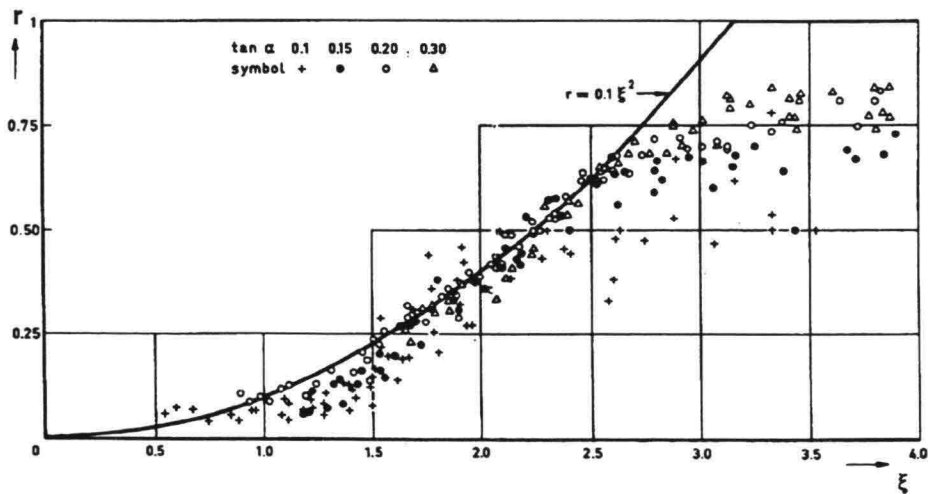


Figure 3.17 Reflection as a function of ξ (Battjes,1974)

that K_R is proportional to ξ^2 . Experimentally was found $K_R \approx 0.1 \xi^2$, see Figure 3.17, for values of ξ below the breaking limit. The wave energy that is not reflected, is absorbed on the slope, see next section.

TURBULENCE

All wave energy that is not reflected on a slope has to be absorbed. This means dissipation of energy via turbulence and friction into heat. This dissipation takes place on a distance along the slope which depends on the breaker type (Figure 3.18). It is obvious that the plunging type, which is common for dikes and seawalls, forms a heavier load for a protection than the spilling type.

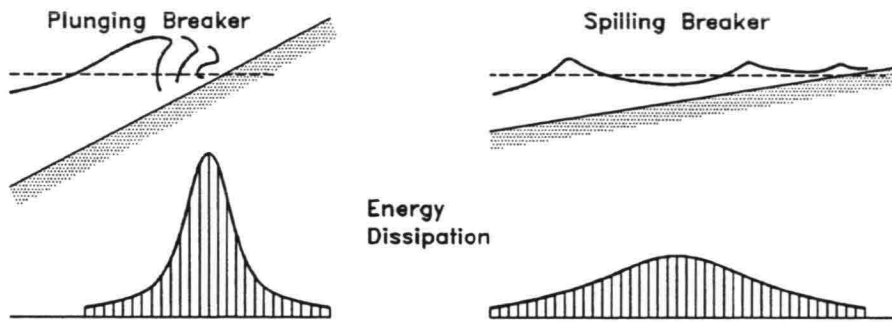


Figure 3.18 Energy dissipation for two breaker types

Turbulence in wind waves has been studied only recently and much is yet unknown. A qualitative description will be given here to get some idea. For more detail and some quantitative analysis, the reader is referred to Fredsøe, 1992. In flow we made a distinction between wall turbulence, e.g. induced by friction along the bed, and free turbulence, e.g. in mixing layers. The same can be done in waves. In non broken waves, the only source of turbulence is bed friction. In breaking and broken waves much turbulent kinetic energy is produced by the friction between the surface roller and the body of water moving with the wave. This kinetic energy (which is much more than produced by the bed friction) is diffused to the bed and dissipated along the way, see Figure 3.19 from Fredsøe, 1992.

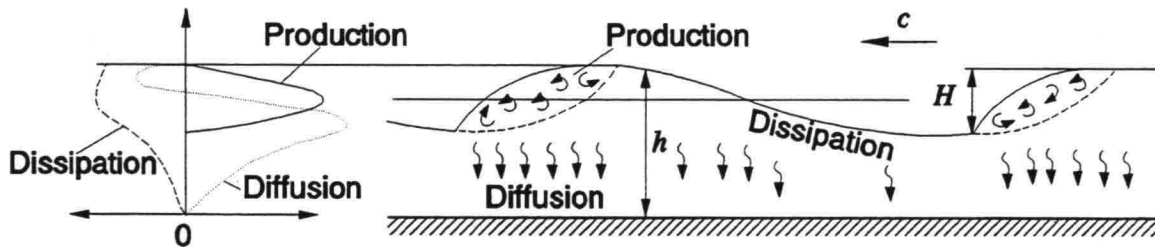


Figure 3.19 Turbulence in a broken wave

Another aspect of the heavy loading by plunging breakers is due to the jet-like behaviour of the plunging water, see Figure 3.20. This jet can act directly on the bed, doing much more harm than diffusing turbulence from a surface roller.

In stability relations it is often found that collapsing breakers cause the most damage, see chapter 10. This can possibly be explained by the fact that both surface roller turbulence and a (beginning) jet act directly on the slope (no body of water between roller or impinging jet and the bed to act as a buffer)



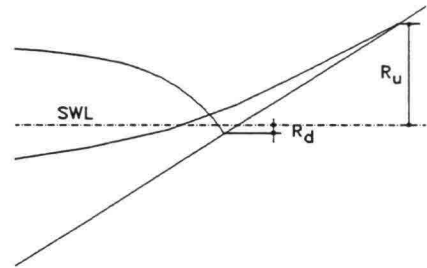
Figure 3.20 Jetflow in plunging breaker

REGULAR WAVES

The run-up of a wave is defined as the maximum waterheight during a wave period with regard to the still water level and the run-down as the minimum waterheight (Figure 3.21). For smooth slopes the experimental formula of Hunt gives for breaking waves ($\xi < 2.5$ -3):

$$\frac{R_u}{H} = \xi$$

(3.16) Figure 3.21 Run-up and run-down



Rough slopes give values which are about 50% lower, see Figure 3.22. Run-up appears to be maximum around $\xi = 2.5$ -3, which means just at the transition between breaking and non-breaking. For $\xi \rightarrow \infty$ the theoretical value would be $R_u = H$ (standing wave).

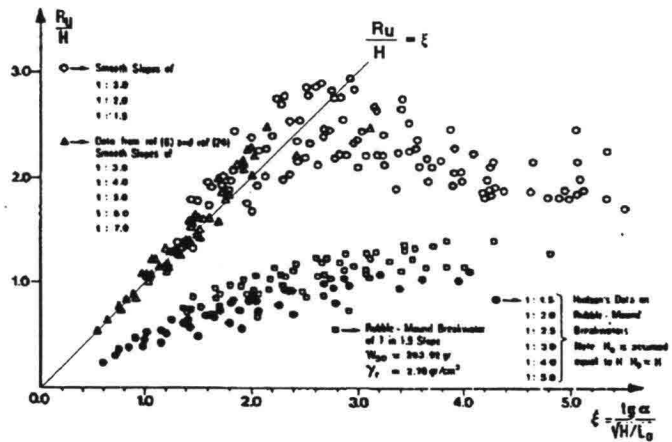


Figure 3.22 Run-up for smooth and rough slopes

In Battjes, 1974 the run-down is given by:

$$R_d = R_u (1 - 0.4 \xi) \tag{3.16}$$

This would implicate that for "real" breaking waves, the waterlevel does not come under the still waterlevel because the water in a wave that flows down on a slope, meets the water running up from the next wave (for gentle slopes like beaches this phenomenon is dominating and is named set-up). Figure 3.23 shows experimental results for smooth slopes, with a coefficient 0.45 instead of 0.4 in the curve fit.

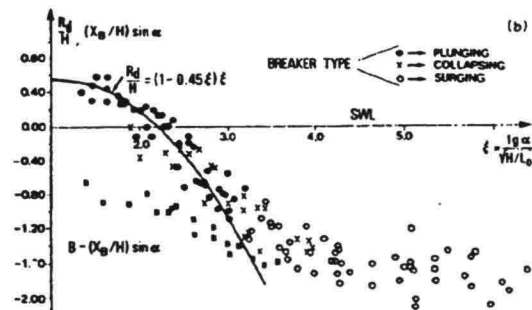


Figure 3.23 Run-down on smooth slopes

IRREGULAR WAVES

Most wave run-up formulae for irregular waves use a value in the distribution that is exceeded by only a small number of the waves, because usually the considered slope is meant to protect something and not too much water should pass the slope. Here $R_{u2\%}$, will be used.

A formula based on experiments, widely used in the Netherlands for the last 20 years is:

$$R_{u2\%} = 0.74 T_m \sqrt{g H_s} \tan \alpha \quad (3.18)$$

Recent investigation and combination of many data from other research have led to, see CUR/TAW,1992 and Figure 3.24:

$$R_{u2\%} = 1.5 H_s \xi_P \quad (R_{u2\% \max} = 3 H_s) \quad (3.19)$$

This is slightly lower than equation (3.18), but the most important difference is the maximum when $\xi > 2$. This is the same as we have seen for regular waves, see Figure 3.22

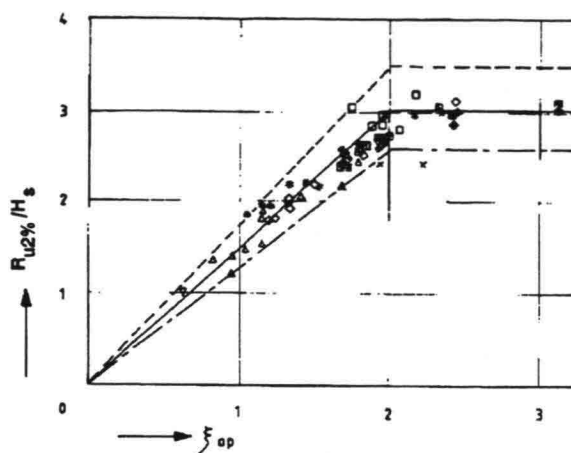


Figure 3.24 Wave run-up irregular waves

The run-down in irregular waves is given by (see CUR/CIRIA,1991):

$$R_{d2\%} = 0.33 H_s \xi_P \quad (R_{d2\% \max} = 1.5 H_s) \quad (3.20)$$

Note: here the run-down is always below SWL, indicated as a positive value in the expression.

CORRECTION FACTORS

The run-up formulae are for smooth slopes like asphalt or smooth concrete blocks. For a rubble slope a reduction factor of 0.5-0.6 is usually applied and for concrete blocks with some profile: 0.7-0.9. For run-down no roughness reduction is applied.

When the wave attack is not perpendicular to the slope ($\beta \neq 0$), a reduction factor γ_β is applied: $\sqrt{\cos \beta}$ (from the energy flux, which is $\propto H^2 \cos \beta$) for long crested waves like swell or ship's waves.

A berm on a slope has a favourable influence on the wave run-up. Instead of a berm-reduction factor (usually $1 - B/L$), it is easier to work with an equivalent slope (which is also useful for determining α in ξ for slopes with a berm). Figure 3.25 gives the procedure to establish the equivalent slope.

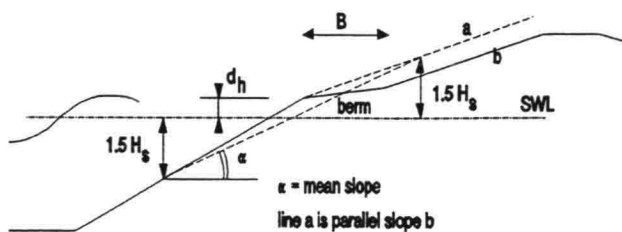


Figure 3.25 Definition equivalent slope with berm

For more information, see CUR/TAW,1992

The pressure under a wave goes up and down with the wave cycle as long as the water keeps in touch with the point where the pressure is registered. This is often called the quasi-static wave load. When the water from the wave can collide with the surface, a very short, very high, very nasty impact pressure can occur, the dynamic wave load, wave impact or wave shock, see Figure 3.26.

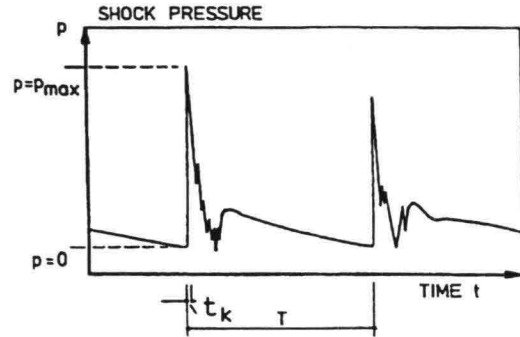


Figure 3.26 Registration wave impact

There are some possible mechanisms, leading to a wave shock, see Figure 3.27:

- a - ventilated shock: a very fast rise of the pressure due to a steep wave front
- b - compression shock: the air cushion in a breaking wave is compressed (leading to spectacular spouts when it can escape)
- c - hammer shock: a real collision between the water mass and the surface with the character of a karate-beat.

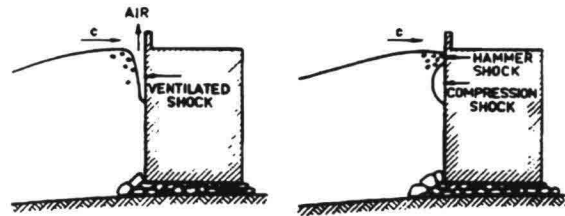


Figure 3.27 Wave impact mechanisms

On slopes, the hammer shock is probably the most important. This type of shock was studied for hydroplanes landing on water; the maximum pressure could be:

$$p = \rho u c \tag{3.21}$$

where u is the collision speed and c the celerity of sound-waves in water ($= \sqrt{K/\rho}$, K is compression modulus). With $u \approx 2$ m/s and $c \approx 1500$ m/s this leads to a pressure which is equivalent to 300 m waterdepth! (If you have difficulties to imagine the difference between quasi-static wave pressures and wave impacts you can easily measure it in a swimming pool. Going up and down to the bottom, you register the quasi-static pressures on your ears. Next, you fall flatly from the high diving board and you will never forget the difference again).

In practice these values have never been measured. This is mainly due to the air in the water. The sound velocity decreases a factor 10 - 50 with a few percent of air bubbles, see Figure 3.28.

For wave impacts on slopes ($2 < \cot \alpha < 8$) a first approximation is given in vVledder, 1990:

$$p = 12 \rho_w g H_s \tan \alpha \tag{3.22}$$

which is much lower than (3.21) indicates, but still several times higher than follows from the possible pressures in the wave itself.

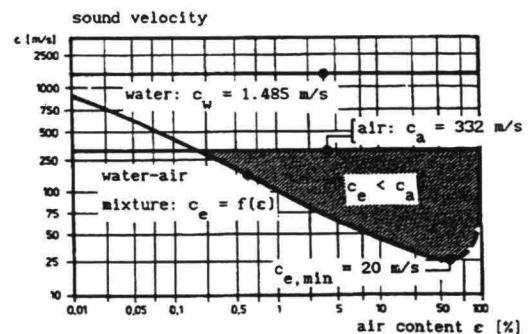


Figure 3.28 Sound velocity in water and air

A moving ship causes an interesting pattern of waves and currents. This will be briefly discussed in these lecture notes, in as far as they influence the bank or bed stability. Other aspects of these hydraulic phenomena, like manoeuvrability and dimensioning of waterways are beyond the scope of these lectures. Figure 4.1 shows the pattern of waves and currents caused by a moving ship.

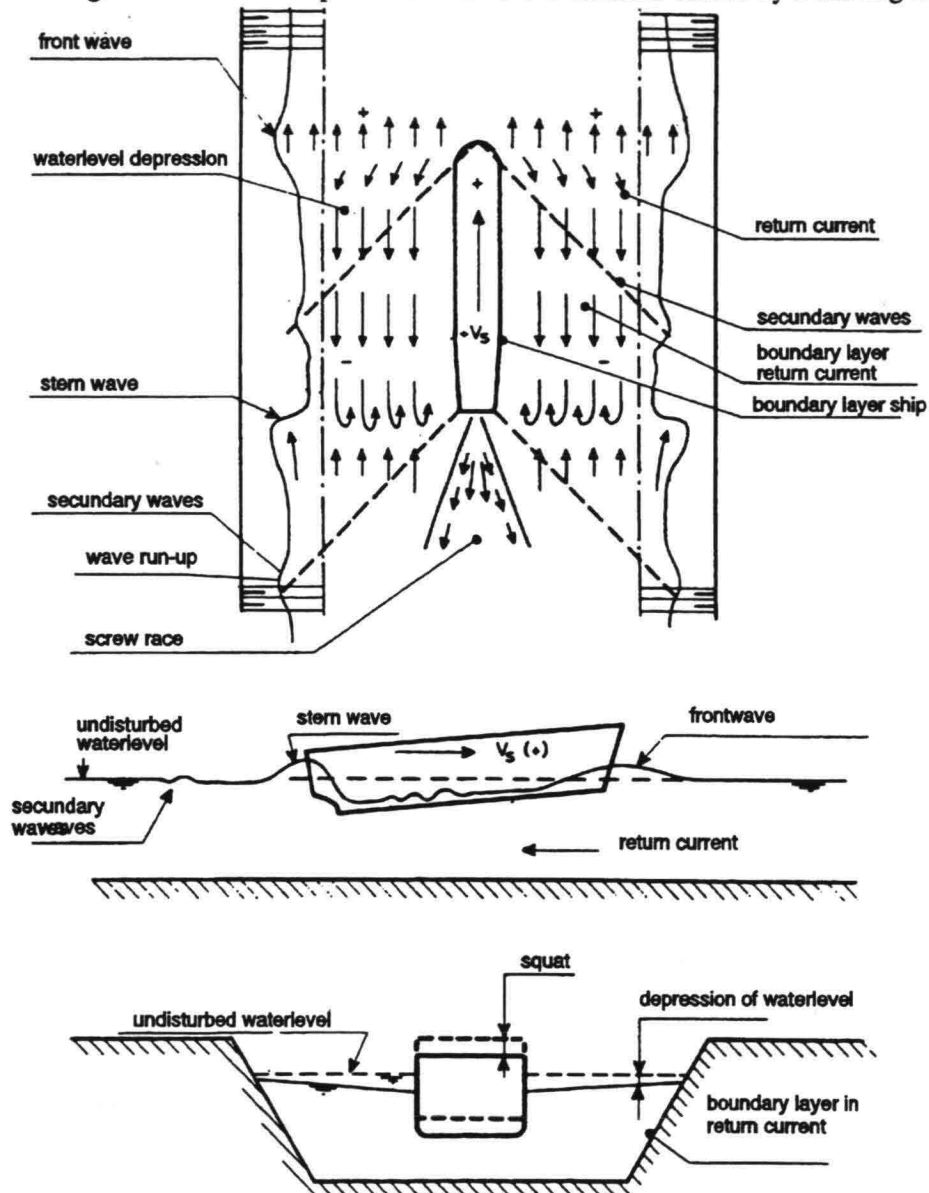


Figure 4.1 Ships waves and currents

A moving ship is, from a hydrodynamical point of view, similar to flow around a body. The waterlevel depression along the ship's hull and the so-called return flow, which are well known from ships in canals, are also present when water flows around a body (see figure 2.11). This waterlevel depression is the primary wave with a length of about the ship's length. The much shorter waves that come from the hull and which are e.g. visible on aerial photographs, are the so-called secondary waves. Both types of waves behave like "normal" water waves, which means that the relations for wave length, celerity etc. from chapter 3 are valid. In practice, the primary wave can be long or short, dependent on the same depth-length relations as were mentioned in chapter 3; the secondary waves are practically always short. In relative narrow navigation channels the primary waves are important, otherwise only the secondary waves play a role. The currents caused by the ship's propeller have the character of a free jet.

Many investigations on ship motion have been done in the past, but most of them were aimed at shipbuilders practice. An important source of information is formed by the investigations done by the Delft Hydraulics Laboratory for the Dutch Rijkswaterstaat in the 70's. Although this research was set up primarily for inland water transport canals, the results and especially the literature survey, have a wider range of application. For more details, see RWS/WL,1988.

All hydraulic aspects depend on the ship's speed, which can be determined in several ways. When speed data of the relevant type of ships are available, it is preferable to use these. If not, the speed can be calculated from the engine power and the ship's resistance (which consists of both friction and form drag, see par. 2.4). This will not be done here; the reader is referred to the f12 lectures or RWS/WL,1988. For a first approach, use can be made of the physical properties of the primary wave, which is limited regardless of engine power. For deep water the speed is limited by the ship's length according to:

$$\left. \begin{aligned} c &= \frac{gT}{2\pi} \\ L &= \frac{gT^2}{2\pi} \end{aligned} \right\} c = \sqrt{\frac{gL}{2\pi}} = V_L \quad (4.1)$$

in which V_L is the limit speed for a ship. For shallow water the speed is limited by the depth:

$$c = \sqrt{gh} = V_L \quad (4.2)$$

This limit speed is analogous to the sound barrier for planes. Self propelled ships can pass this barrier when they are able to plane on the water (e.g. speed-boats). The speed of displacement-type ships usually does not exceed $Fr (= V_s/\sqrt{gh}, V_s$ is ship speed) ≈ 0.75 when they are self propelled. Being towed, they can exceed $Fr = 1$. The width of the canal can further limit the maximum speed of a ship; this will be shown in the next paragraph. When the speed is also limited by the width, a practical approach is: $V_s = 0.9V_L$.

It is good to notice that most damage on revetments is not caused by the largest ships, which often sail relatively slow and as far as possible from the banks. Small service crafts, tugs etc, sailing full power near the banks, can do most harm. Figure 4.2 gives a measure for the minimum distance to the bank (for full speed sailing ships)

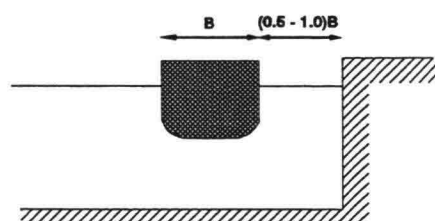


Figure 4.2 Extreme position

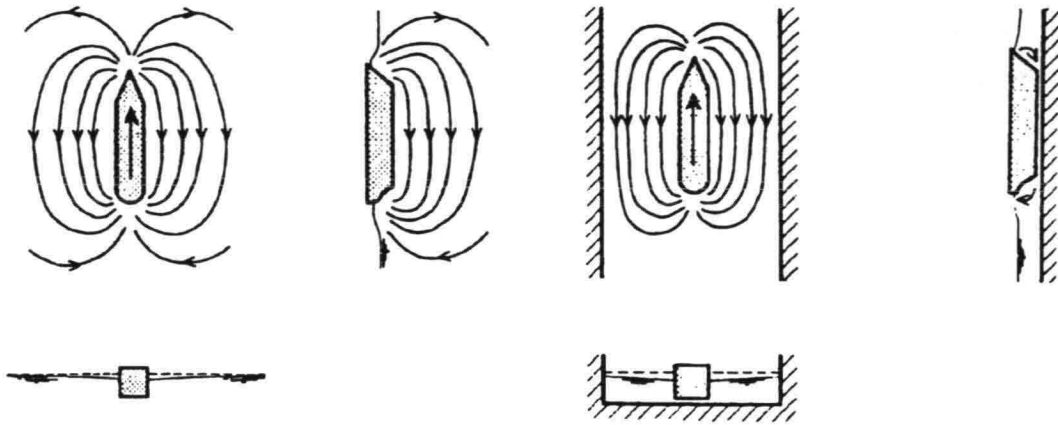


Figure 4.3 Flow around a ship in unrestricted and restricted water

The flow around a ship is of a 3-dimensional nature. In a relative narrow and shallow canal, this can be schematized as a 1-dimensional flow (Figure 4.3).

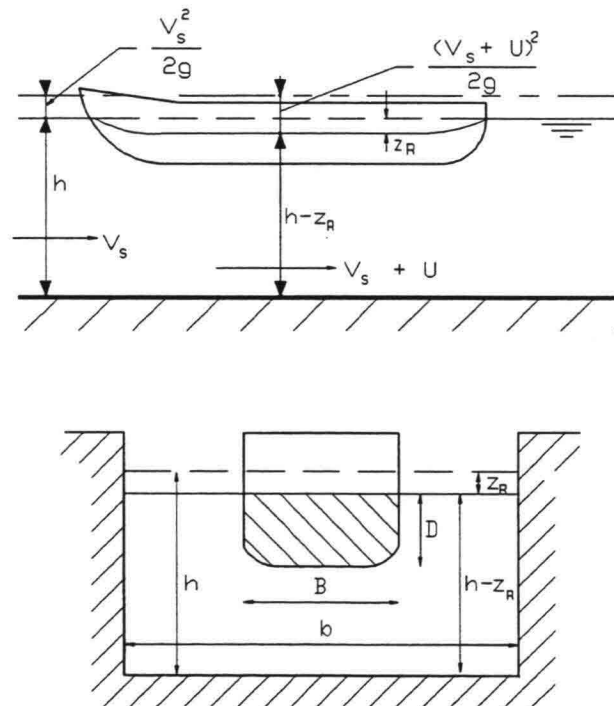


Figure 4.4 Definitions for primary wave calculation

In that case, the phenomenon can be approached with a simple equation of motion (Bernoulli, neglecting energy losses) and the continuity equation. Other assumptions in this method are: the ship sails in the axis of the canal, prismatic cross-section of ship's hull, ship is horizontal, channel cross-

section is prismatic, return flow and waterlevel depression are constant over the channel's cross-section and the squat of the ship is equal to the waterlevel depression. The equation of motion then becomes (see Figure 4.4, definitions for coordinates moving with the ship or a ship lying still with a current velocity V_s):

$$z_R = \frac{(V_s + U_R)^2}{2g} - \frac{V_s^2}{2g} \tag{4.3}$$

And the equation of continuity:

$$Q = A_C \cdot V_s = (V_s + U_R)(A_C - A_s - b z_R) \tag{4.4}$$

The ship's limit speed is reached when the return flow becomes critical, or in other words, is maximum as a function of the waterlevel depression:

$$\frac{dQ}{dz_R} = \frac{d(V_s + U_R)(A_C - A_s - b z_R)}{dz_R} = 0 \tag{4.5}$$

Together with the equation of motion, for that case is found (Figure 4.5):

$$1 - \frac{A_s}{A_C} + \frac{1}{2} Fr_L^2 - \frac{3}{2} Fr_L^{2/3} = 0 \tag{4.6}$$

with: $(Fr_L = \frac{V_L}{\sqrt{gh}})$

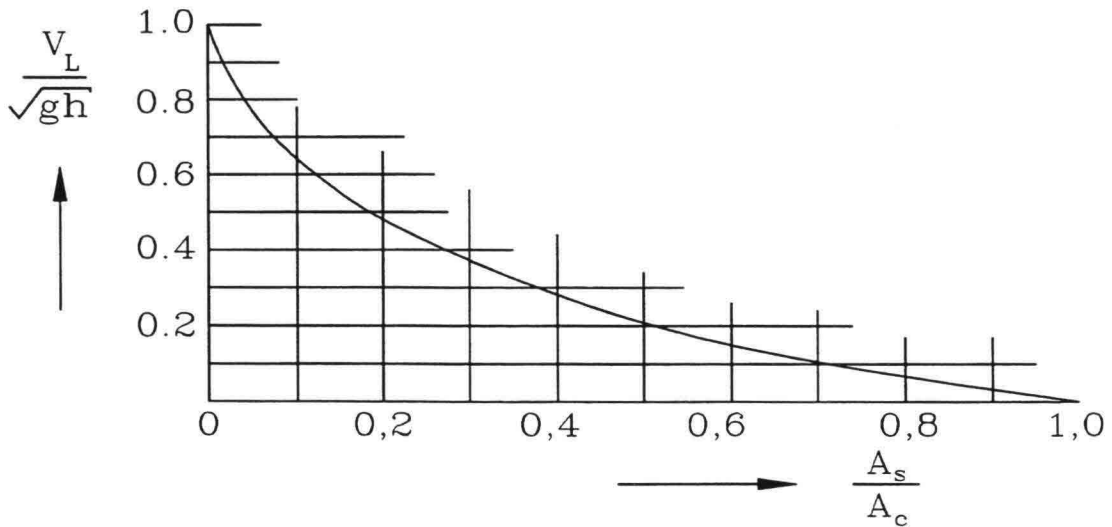


Figure 4.5 Limit speed as function of blockage and depth

The extremes in this equation are: $A_s/A_C = 0 \rightarrow V_L = \sqrt{gh}$ and $A_s/A_C = 1 \rightarrow V_L = 0$.

This means that a ship that blocks the complete canal cannot move at all which seems reasonable and that at unrestricted width the ship can sail with a maximum speed equal to the speed of a wave in shallow water.

Note 1: As stated in paragraph 4.1, a practical limit is $0.9V_L$. Even for small values of A_s/A_C this leads to $Fr < 0.7$ (see Figure 4.4, Figure 4.5). This is important for the behaviour of the secondary waves which can be considered deep water waves in that case (see par 4.3).

Note 2: Equation (4.6) would lead to limit speeds for a ship on the ocean of $\sqrt{(10.5000)} \approx 800$ km/hr which in turn leads to the question how airplanes ever could compete with ships. In reality, the limit speed in that case is given by the celerity of a deep water wave (equation (4.1)): $c = \sqrt{(gL/2\pi)}$, For an ocean-going ship of 100 m long this leads to $V_L \approx 45$ km/hr. Because these computations assumed a shallow water situation right from the start, a deep water relation could never be found. So, this whole approach is limited to shallow water.

The waterlevel depression and the return flow can be calculated iterating the same equations, written in the dimensionless form:

$$\frac{V_s}{\sqrt{gh}} = \left[\frac{2z_R/h}{\alpha(1 - A_s/A_C - z/h)^2 - 1} \right]^{\frac{1}{2}} \quad (4.7)$$

$$\frac{U_R}{\sqrt{gh}} = \left[\frac{1}{1 - A_s/A_C - z_R/h} - 1 \right] \frac{V_s}{\sqrt{gh}}$$

α is a correction factor for the non-uniform distribution of U_R and is given by $\alpha = 1.4 - 0.4 V_s/V_L$ which gives $\alpha = 1$ for $V_s = V_L$ and to $\alpha = 1.1$ for $V_s = 0.75 V_L$.

Figure 4.6 gives a diagram ($\alpha = 1.1$) from which the values of U_R and z can be found directly from the known values of A_s/A_C and V_s (either from speed measurements or related to the limit speed).

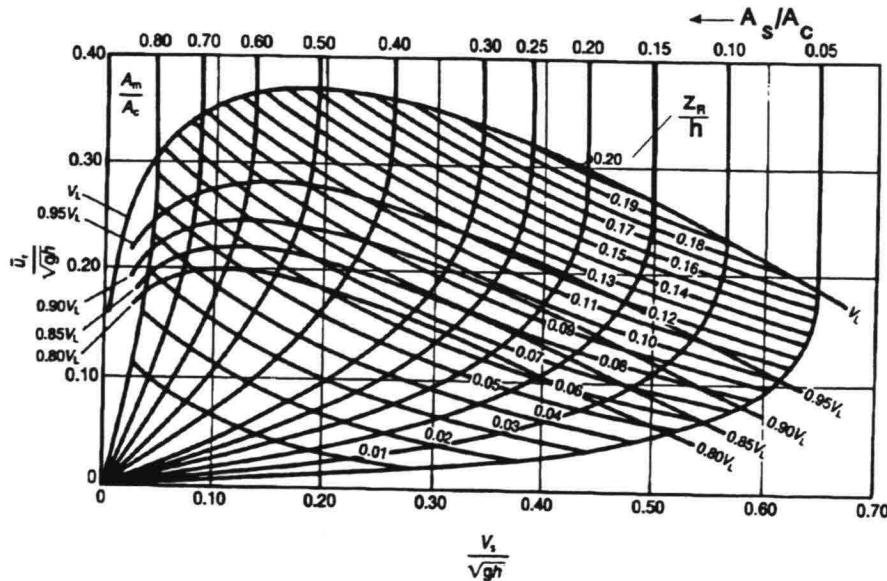


Figure 4.6 Schijf's diagram for estimating return current and waterlevel depression ($\alpha=1.1$)

When there is a flow in the channel, V_s has to be taken relative to the flow velocity. From that directly follows the waterlevel depression; the flow velocity (positive or negative) has to be added to the return current.

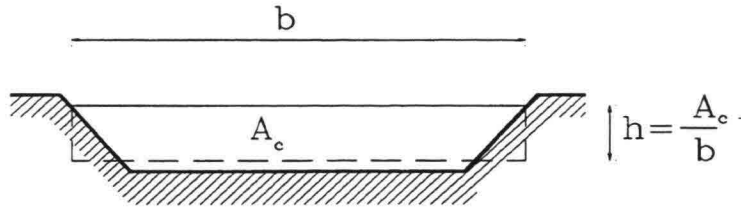


Figure 4.7 Trapezoidal canal

When the canal is not rectangular but trapezoidal, the same diagram is used with h defined as $h = A_c/b$ (Figure 4.7).

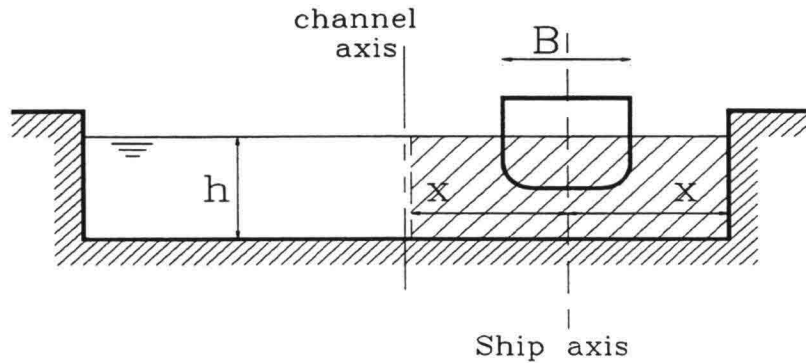


Figure 4.8 Excentric position of ship in canal

In Figure 4.6 it is assumed that the ship is sailing in the centre of the canal. When this is not the case the values can be found as follows (Figure 4.8), which is a crude approximation: take $A_c = 2X \cdot h$ and follow the same procedure. In this case, the flow through the ship-axis is neglected, giving conservative values.

There are frequently situations where there is more than one ship in a cross-section of a channel, e.g. when two ships encounter or when a ship overtakes another. Only the last situation causes greater loads than for the case with a single ship. A first approximation is then to add the two ships cross-section and to calculate the waterlevel depression and return flow as if it was one ship.

The return flow causes a boundary shear stress on the bank of the channel. This is not a stationary flow, but it is a case of a growing boundary layer. We will use the formula given by Schlichting:

$$C_f = (2.87 + 1.58 \log \frac{x}{k})^{-2.5} \quad (x = \frac{u_R}{v_S + u_R} L_E) \quad (4.8)$$

in which L_E is the "entrance-length", the distance from the bow to where the cross-section of the ship is equal to the midship section. When L_E is unknown, it can be estimated with $L_E \approx 0.1L_s$. In the primary wave, usually the stern wave is dominating. This can be approximated by:

$$H_{STERN} = z_{MAX} = 1.5 z_R \quad (4.9)$$

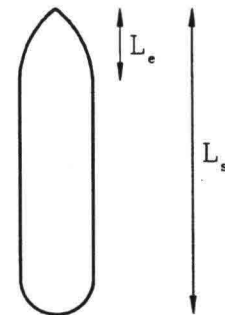


Figure 4.9 Entrance length

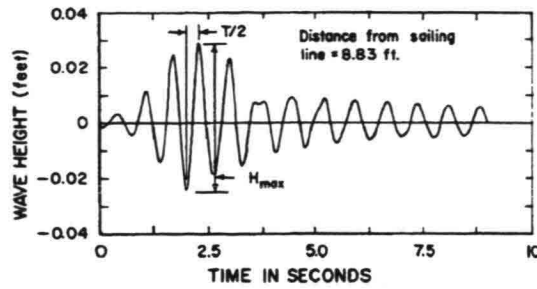


Figure 4.10 Train of secondary waves

The primary wave has more or less the character of a negative solitary wave; the secondary waves are formed by a number of periodic waves, a wave train (Figure 4.10). Secondary waves are caused by the pressure pattern along the ship's hull. Discontinuities in the hull-profile are the primary causes. These discontinuities are found at the bow and the stern which both emit waves. Usually the bow is dominant.

These ship waves have been studied for a long time; already in 1887, Kelvin made a study of the wave pattern behind a ship. He considered a "pressure point", moving through the water. He found a pattern that is very much like the one observed in reality. Unfortunately, much less is known when it comes to values for the wave heights; these still rely very much on experiments. More detail is given in RWS/WL, 1988 and Sorensen, 1973.

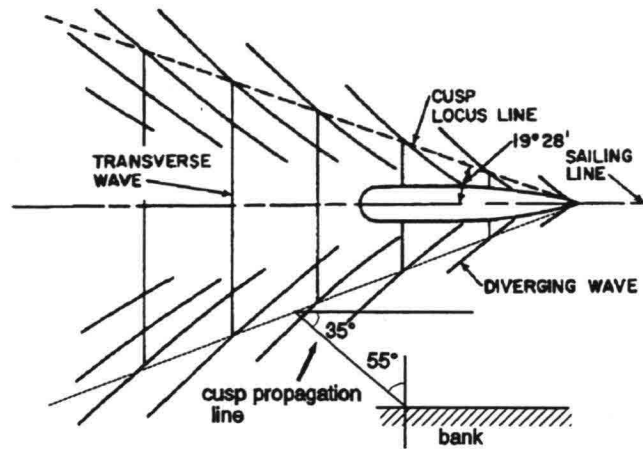


Figure 4.11 Pattern of secondary waves

Figure 4.11 shows the secondary waves behind a ship. There are two systems of waves: diverging and transverse waves. The first type diminishes with the square root of the distance perpendicular to the sailing line and the second with the square of this distance. The diverging waves are dominant in this pattern (for $Fr < 0.75$). Where transverse and diverging waves meet, there is interference and they form cusps, which are important for the stability of revetments. For moderate speed ($Fr < 0.75$), the cusp locus line forms an angle of about 20° with the sailing line and the direction of propagation of the cusps an angle of about 35° with the sailing line, hence the angle of approach for a bank parallel to the sailing line is 55° .

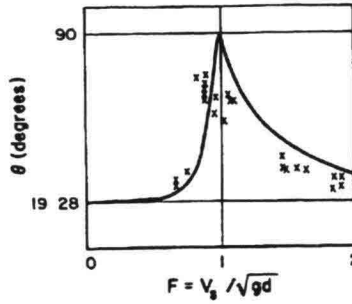


Figure 4.12 Angle of cusp locus line

For higher speeds the cusps propagate more in the direction of the sailing line (see Figure 4.12). For $Fr = 1$, transverse and diverging waves coincide and for $Fr > 1$ transverse waves can no longer exist. This is all very interesting from a scientific point of view, but in practice, as stated before, for self-propelled ships, $Fr = 0.75$ can be regarded as a maximum.

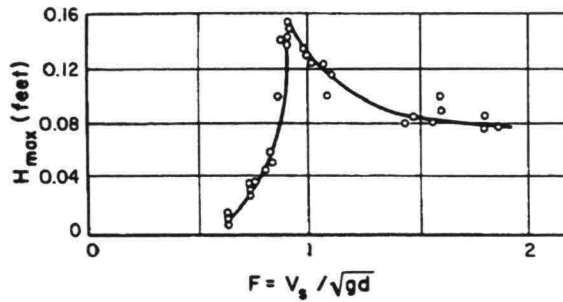


Figure 4.13 Cusp height vs. Fr (model test)

The wave height strongly increases with the speed, reaching a theoretical maximum at $Fr = 1$. In experiments however, this maximum is reached before this value (Figure 4.13). The sharp increase of the wave height with the speed can be explained as follows: the limit speed is similar to the sound barrier for airplanes. The energy from the engine cannot be transformed into speed, but it must remain somewhere. Hence, many fuel is used to make waves. This explains why ships usually sail well under their limit speed.

The wave height of the cusps moreover depends on the type of ship and the degree of loading. For practical use the following formulae are available:

$$H = \zeta \cdot h \cdot Fr^4 \quad (4.10)$$

ζ represents the ship's geometry. It was found that the ship's length and the block coefficient hardly influence the secondary waves. The draught D and the entrance length L_E dominate ζ . This is in line with the fact that the discontinuities in the ship's hull are responsible for the emission of pressure waves. In the already mentioned investigations (RWS/WL, 1988-V) for ζ was found:

$$\zeta = \zeta^1 \frac{D}{L_E} \quad (4.11)$$

where ζ^1 has been found to vary between 1.5 and 4.0. Although this is a large range, it covers all types of ships, from ocean-going carriers to barges and small crafts. When no data are available, $\zeta^1 = 4$ is recommended. When L_E is not known, $\zeta = 1.2$ is recommended.

The wave height of the cusps diminishes with the cubic root of the distance to the sailing line, for relatively deep water. For moderate Fr-numbers (< 0.75) this is a good approximation. The relation for the wave height at any distance from the sailing line then becomes:

$$H = \zeta \cdot h \cdot \left(\frac{s}{h}\right)^{-0.33} \cdot Fr^4 \tag{4.12}$$

in which s = distance from the ship's hull. This relation is not valid directly besides the ship's hull ($H \rightarrow \infty$). With a minimal distance of $0.5 B$ to the banks, this will give no difficulties.

The relation of equation (4.12) is shown in Figure 4.14 with data from hundreds of measurements (derived from RWS/WL, 1988-V), which shows that equation (4.12) with $\zeta = 1.2$ gives a reasonable upper limit for the wave heights to be expected. When more accurate values are wanted, model tests have to be performed.

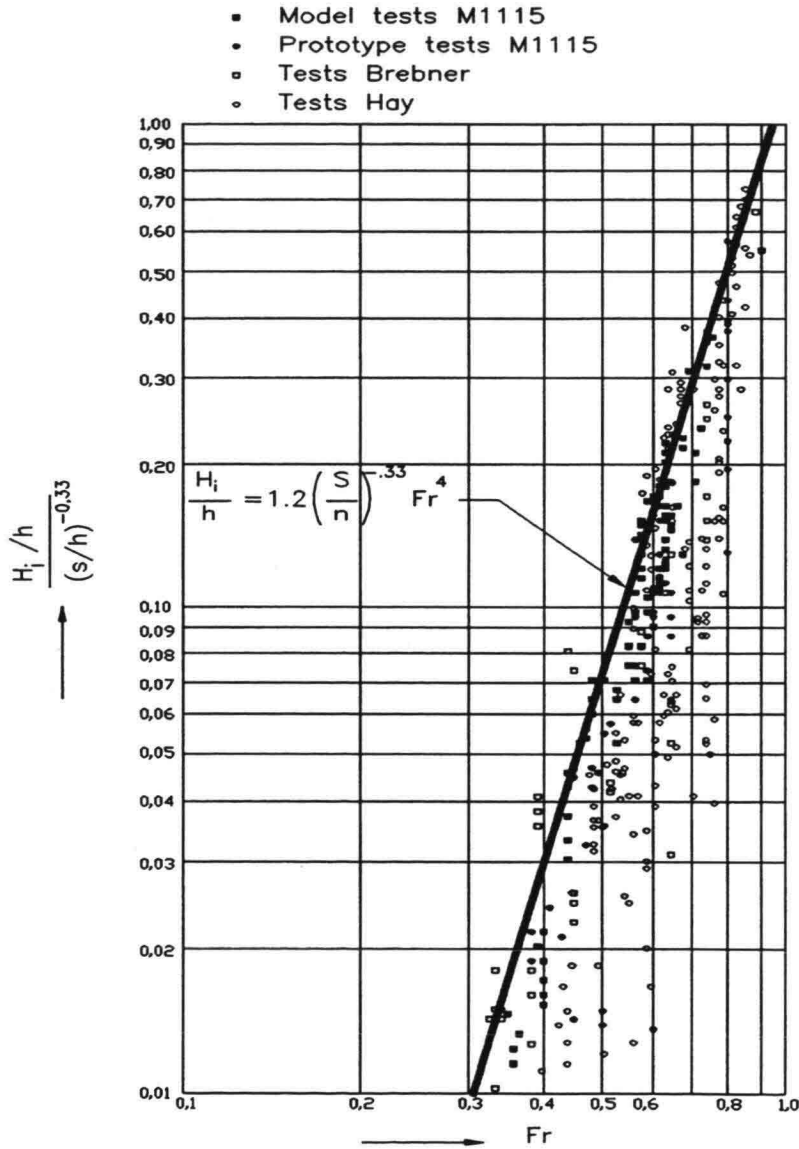


Figure 4.14 Wave height measurements from many sources in relation to recommended formula

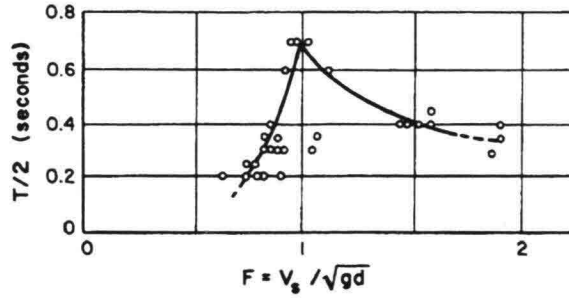


Figure 4.15 Half period vs Fr (model test)

The wave period also reaches its maximum at $Fr = 1$ (Figure 4.15). The wave period and wave length can be derived as follows. As reasoned before, for $Fr < 0.75$ the secondary waves are deep water waves. In that case (with $c = V_s \cos \phi$ and $\phi = 35^\circ$):

$$L = \frac{c^2}{g} 2\pi = 0.67 \frac{V_s^2 2\pi}{g} \quad (4.13)$$

$$T = \frac{L}{c} = 0.82 \frac{V_s 2\pi}{g}$$

In model and prototype-measurements, the agreement with these formulae was good.

4.4 PROPELLER RACES

The flow behind a ship's propeller is very similar to that in a free circular jet. So, it can be expected that the same proportionalities are valid. This is not necessarily so for the numerical values, since there are also differences. For example, the water in the jet is already turbulent because of the propeller blades; this will make the flow establishment region shorter than in a free jet. Another difference is the water surface which will also influence the divergence of the jet.

Figure 4.16 shows the turbulent velocity fluctuations in a free circular jet, compared to those in a screw race. The values in the fully developed jet lie both around 30%, but in the propeller race this value is reached much earlier.

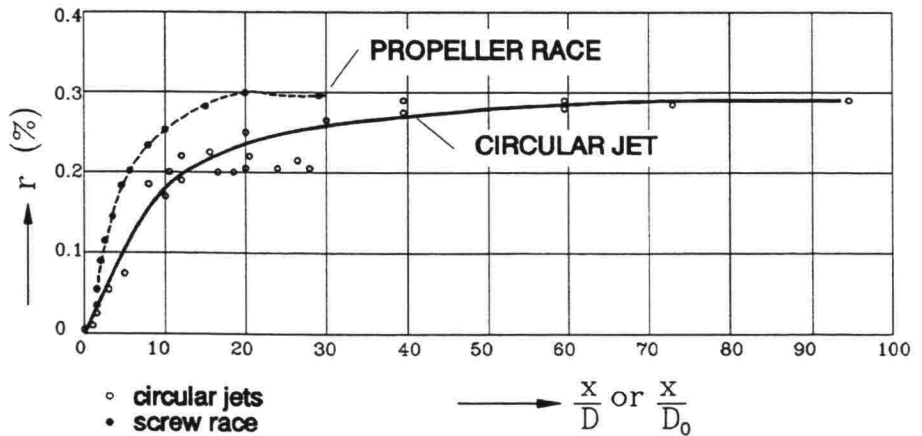


Figure 4.16 Turbulent fluctuations in free jet and screw race

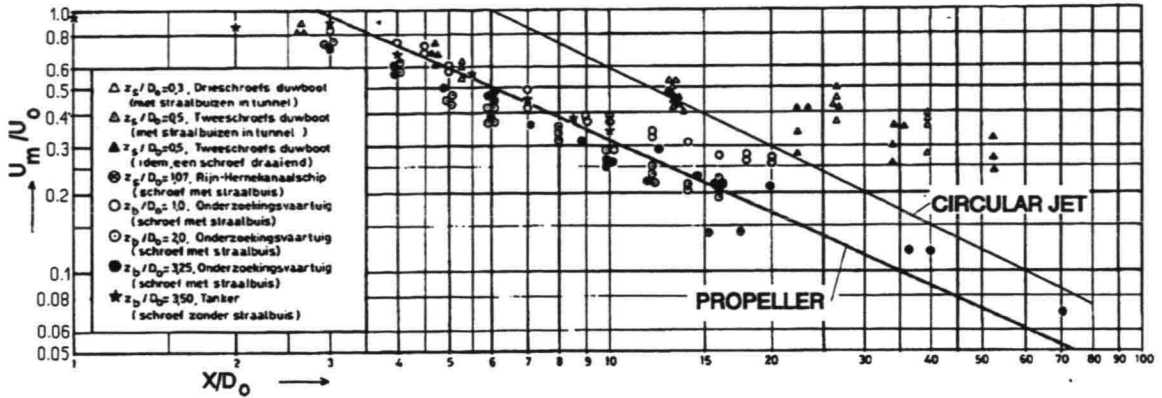


Figure 4.17 Velocity decay in the propeller axis

Figure 4.17 shows the decay of the velocity in a jet behind ship's propellers. The jet properties can be described in an analogous form as for the jets in paragraph 2.5 with:

$$\begin{aligned}
 u_m &= \frac{2.8 u_0}{x/D_0} \\
 b &= 0.21 x \\
 u &= u_m e^{-0.69 \left(\frac{x}{b}\right)^2}
 \end{aligned}
 \tag{4.14}$$

From this and Figure 4.17 can be seen that, compared to a free circular jet, a propeller jet diverges faster.

The values in these formulae can be estimated with:

$D_0 = 0.7$ diameter for a normal propeller and $D_0 =$ diameter for a propeller in a jet tube. When the diameter of the propeller is not known, it can be estimated as about 70% of the ship's draught. The outflow velocity u_0 can be estimated with $u_0 = 1.15(P/\rho D_0^2)^{.33}$, with $P =$ power of engine. For a first approximation of the velocity on the bottom, use can be made of:

$$u_b = 0.3 u_0 \frac{D_0}{z_b}
 \tag{4.15}$$

where z_b is the vertical distance between propeller axis and bottom.

The velocities behind a ship's propeller are important in case the revetment or the bottom can be attacked by this flow when the ship lies still or is manoeuvring near the bank. Once the ship is sailing this load becomes less important. An indication of the velocity at the bottom in that case can be found by diminishing the value for u_b found with equation (4.15) with half the speed of the ship.

Starting point is again the Navier Stokes equation for the x-direction, written in the Reynolds-form (like equation 2.13):

$$\frac{\partial u}{\partial t} + u \frac{\partial u}{\partial x} + w \frac{\partial u}{\partial z} = -\frac{1}{\rho} \frac{\partial p}{\partial x} + \nu \frac{\partial^2 u}{\partial z^2} - \frac{\partial \overline{u'^2}}{\partial x} - \frac{\partial \overline{u'w'}}{\partial z} \quad (5.1)$$

in which ν is the kinematic viscosity.

With this equation the flow in a porous medium can be calculated, provided that every stone and every pore is taken into account individually. From a practical point of view this is impossible and not necessary. An averaging procedure will be followed to reach practical solutions.

The first step in this procedure is to define an average velocity, the so-called filter-velocity:

$$u_f = \frac{1}{A} \iint_A u dA = n \cdot u \quad (n = \frac{V_p}{V_T}) \quad (5.2)$$

in which n is the porosity and u the real velocity in the pores. The porosity is usually defined as the pore-volume divided by the total volume, although this is not necessarily a measure for the permeability (compare Emmenthal cheese: many pores but no permeability). For a normal grain-structure this is however no objection.

Note: The averaging has to cover enough pores to be able to speak of an average flow in a process which is of a random nature in detail. On the other hand the area dA must be small compared to the mean motion (LeMehaute,1976). This may be physically translated as: a large flow pattern through relatively small grains. Wave action (with a characteristic length order of 1m) in the cover layer of a breakwater with elements of the same order of magnitude, cannot be described by porous flow formulae.

The next step is to combine terms in equation (5.1). $\partial u/\partial z$ has a physical meaning in a particular pore, where there is a velocity-gradient from the centre of the pore to the grain (no slip at the boundary), but with an average of many pores it loses its meaning. Common practice is to combine all square inertia and turbulence terms to one quadratic friction term and to replace the (linear) viscous gradient with a linear friction term. The result is (see also van Gent,1992):

$$\frac{1}{\rho g} \frac{\partial p}{\partial x} = i = c_1 u_f + c_2 u_f |u_f| + c_3 \frac{\partial u_f}{\partial t} \quad (5.3)$$

For a stationary flow $\partial u_f/\partial t = 0$, this is the classical Forchheimer equation.

For stationary flow equation (5.3) reads:

$$i = c_1 u_f + c_2 u_f^2 \quad (5.4)$$

which, in many practical formulae, is written as:

$$u_f = k(i)^{\frac{1}{a}} \quad (5.5)$$

in which k is the permeability (m/s) of the porous material.

For laminar flow, $a = 1$ (linear relation between u_f and i , Darcy-flow); for turbulent flow, $a = 2$ and there is a transition zone in which $1 < a < 2$. Figure 5.1 shows this power relation between u_f and i for various materials, ranging from sand to rock.

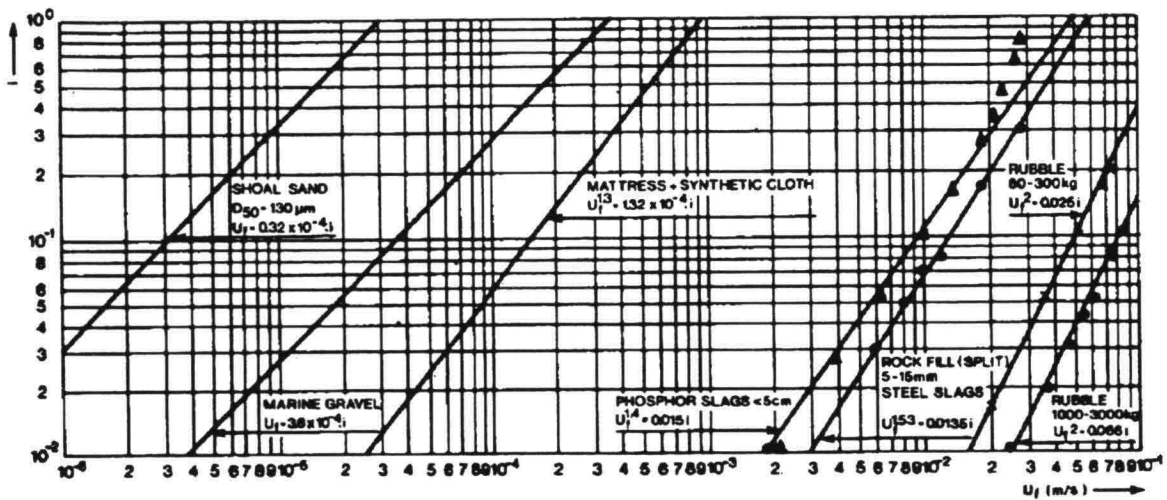


Figure 5.1 Relation between filter velocity and gradient for various materials as measured by DHL

The following table and Figure 5.2 give an indication of the permeability of some often used materials:

MATERIAL	DIAMETER (m)	PERMEABILITY (m/s)	CHARACTER OF FLOW
Clay	$10^{-7} - 5 \cdot 10^{-5}$	$10^{-12} - 10^{-8}$	laminar
Fine sand	$5 \cdot 10^{-5} - 5 \cdot 10^{-4}$	$10^{-8} - 10^{-5}$	laminar
Coarse sand	$5 \cdot 10^{-4} - 2 \cdot 10^{-3}$	$10^{-5} - 10^{-2}$	laminar
Fine gravel	$2 \cdot 10^{-3} - 5 \cdot 10^{-2}$	$10^{-2} - 10^{-1}$	transition
Coarse gravel	$5 \cdot 10^{-2} - 10^{-1}$	$10^{-1} - 2 \cdot 10^{-1}$	turbulent
Small rock	$2 \cdot 10^{-1} - 4 \cdot 10^{-1}$	$3 \cdot 10^{-1} - 4 \cdot 10^{-1}$	turbulent
Large rock	$5 \cdot 10^{-1} - 2$	$5 \cdot 10^{-1} - 1$	turbulent

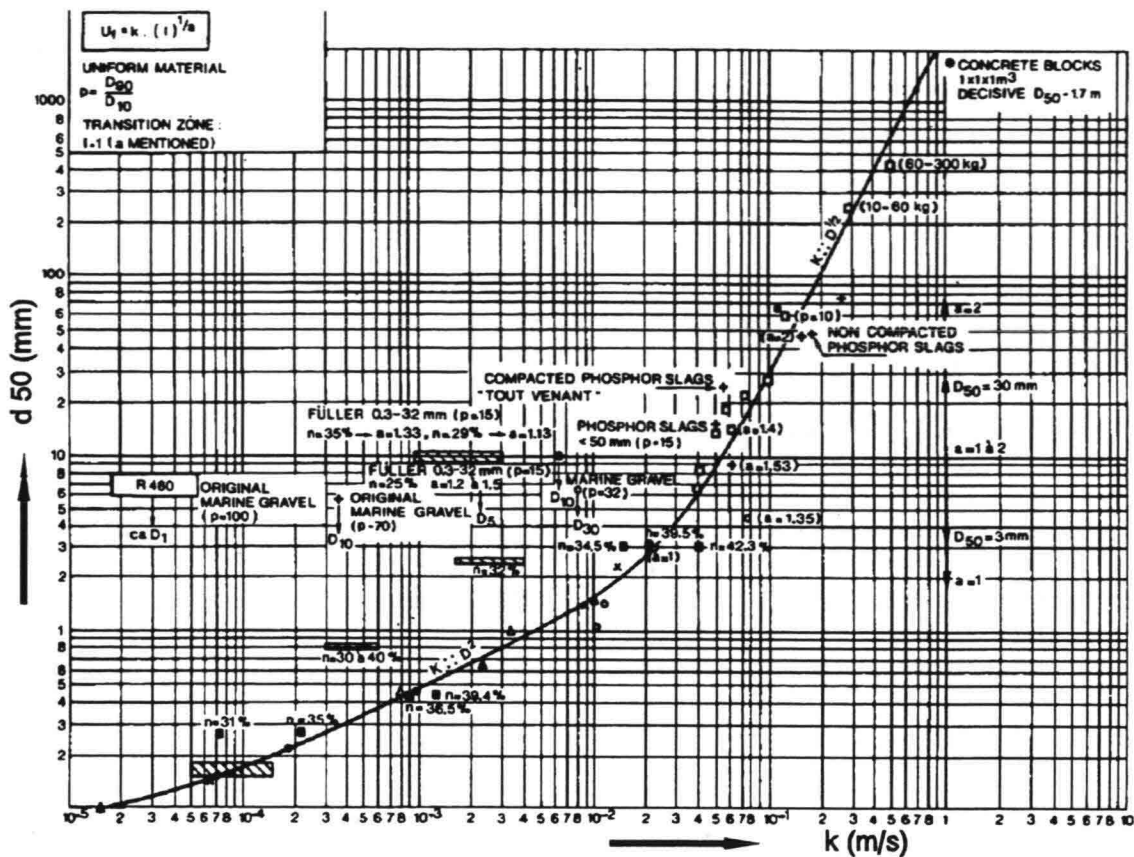


Figure 5.2 Permeability of porous media

An empirical form of eq. (5.5) is:

$$u_f^2 = 2g \frac{D_n}{C_D} n^5 i \quad (5.6)$$

(Cohen de Lara, 1955).

n , the porosity, has a tremendous influence! Equation (5.6) is valid for the whole range from laminar to turbulent via the factor C_D , which is the same as the drag-coefficient for a single sphere, see Figure 5.3. For laminar flow, $C_D = 24/Re$, which again leads to $u_f \propto i$, while for turbulent flow $C_D = 0.5$, giving $u_f \propto i^{1/2}$.

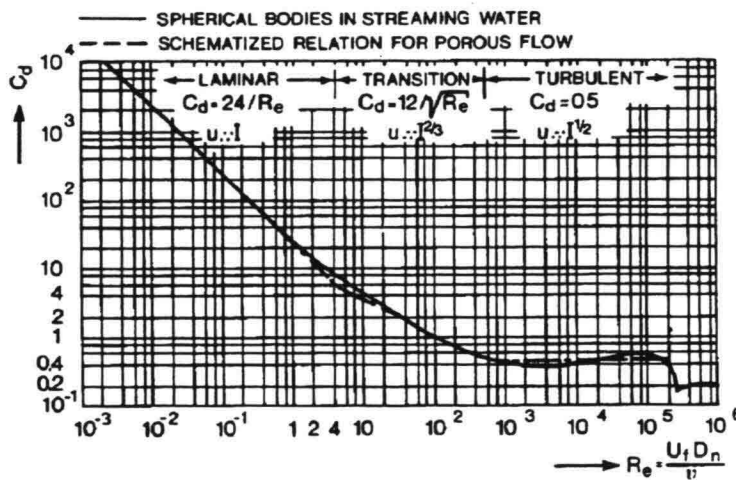


Figure 5.3 C_D as function of Re

Note: The transition between laminar and turbulent flow is more gradual than in open channel flow, because beside turbulence, convective terms also play a role in the averaged formula. Despite this difference, the flow types will be named laminar and turbulent in the following paragraphs.

The equation of motion (5.4) reduces for laminar, stationary flow to the well known law of Darcy:

$$u_f = k \cdot i = \frac{-k}{\rho_w g} \frac{\partial p}{\partial x} \quad (5.7)$$

The permeability can be expressed by the relation of Kozeny:

$$k \approx \frac{\rho_w g}{180 \mu} d^2 \frac{n^3}{(1-n)^2} \quad (5.8)$$

In practice however, it is easy and much more accurate to measure k in a laboratory test.

For a homogeneous fluid, the waterlevel can be used instead of the pressure, since:

$$h = z + \frac{p}{\rho_w g} \quad (5.9)$$

For homogeneous soil (isotropic permeability), the Darcy relations are identical for all three dimensions:

$$u_f = -k \frac{\partial h}{\partial x} \quad v_f = -k \frac{\partial h}{\partial y} \quad w_f = -k \frac{\partial h}{\partial z} \quad (5.10)$$

The structure of grains and pores cause friction for the flowing water. Reversely the water exerts a force on the grains (action = reaction). This is the flow force (sometimes called the flow pressure, but it has the dimension of force per volume), which is important in the stability of the grains at the outer boundaries of the soil. It is given by:

$$p_f = \rho_w \cdot g \cdot i = \rho_w \cdot g \cdot \frac{\partial h}{\partial x} \quad (5.11)$$

for the x-direction; for the other directions, the expression is similar.

Darcys law is the equation of motion for laminar groundwaterflow. To compute a velocity- and pressure distribution in a soil-mass we also need to take into account the continuity equation:

$$\frac{\partial u_f}{\partial x} + \frac{\partial w_f}{\partial z} = 0 \quad (5.12)$$

These equations can be solved, but only for simple geometries there exist analytical solutions. For more complex situations the equations can be solved numerically (either by finite elements or finite differences), graphically (with a rectangular flow net pattern) or with an electric analogon (based on the analogy between Darcys law and Ohm's law for conductivity).

ANALYTICAL SOLUTIONS

For some simple cases, analytical solutions are available. For detailed derivations the reader is referred to the mentioned sources.

At first the phreatic level in a dike is presented, see also Bear, 1972. The dike is schematized to a rectangular soil-mass, see Figure 5.4, Figure 5.8. At each cross-section the flow is given by:

$$q = -k h(x) \frac{dh(x)}{dx} \quad (5.13)$$

Integration to x gives:

$$h^2 = h_0^2 - (h_0^2 - h_L^2) \frac{x}{L} \quad \text{and} \quad q = \frac{k(h_0^2 - h_L^2)}{2L} \quad (5.14)$$

Note 1: The position of the phreatic surface is independent of k ! Of course, q is not.

Note 2: In the calculation, the phreatic level at the downstream end coincides with the downstream waterlevel. In reality, also on less steep slopes, there is always a seepage surface where water flows out of the slope. That means that there is always a part of the downstream slope where there is a groundwater flow parallel to the slope. This is important in determining the stability of the slope, see paragraph 11.1.1.

A second example is given for the pressure under a closed protection.

For $h/H_0 < 0.8$, the maximum pressure under the protection, with regard to the waterlevel on the slope, is given in first approximation by:

$$P_{\max} = \left(1 - \frac{h}{H_0}\right) \cdot \rho_w g h \quad (5.15)$$

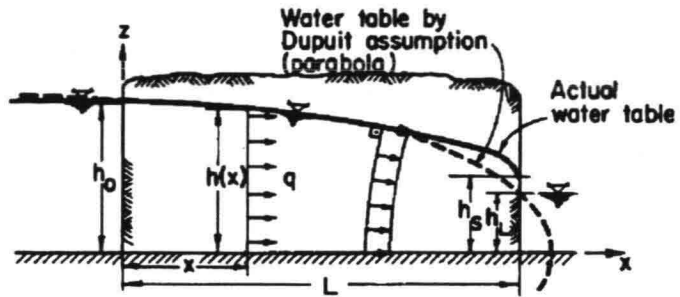


Figure 5.4 Unconfined flow through a dike

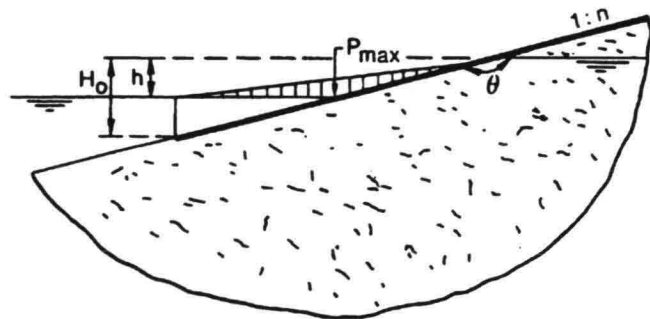


Figure 5.5 Pressure under impervious revetment

See also van der Veer, 1979 or RWS, 1987 where also more accurate expressions are given.

GRAPHICAL APPROACH

Approximate solutions can be obtained by using a graphical method, known as rectangular flow net. In that case Darcys law is written in a slightly different form again, defining a potential $\phi = k.h$:

$$u_f = -\frac{\partial\phi}{\partial x} \quad \text{and} \quad w_f = -\frac{\partial\phi}{\partial z} \quad (5.16)$$

From this can be seen that no change in potential means no flow, hence all streamlines are perpendicular to equipotentials. We can now define a streamfunction ψ such that:

$$u_f = -\frac{\partial\psi}{\partial z} \quad \text{and} \quad w_f = +\frac{\partial\psi}{\partial x} \quad (5.17)$$

Combining equations (5.16) and (5.17) and the continuity equation (5.12) we find:

$$\frac{\partial^2\phi}{\partial x^2} + \frac{\partial^2\phi}{\partial z^2} = -\frac{\partial^2\psi}{\partial x\partial z} + \frac{\partial^2\psi}{\partial x\partial z} = 0 \quad (5.18)$$

There is now a rectangular pattern of streamlines, along which ψ is constant and equipotentials, along which ϕ is constant, see Figure 5.6. The distance between two equipotentials, $\Delta\phi = k.\Delta h$ and the distance between two streamlines $\Delta\psi = -u_f.\Delta z$. This means that $\Delta\psi$ is equal to the discharge between two streamlines. When $\Delta\psi = \Delta\phi$, $\Delta x = \Delta z$ leading to a flow net of squares. In any case there should be a constant relation between $\Delta\psi$ and $\Delta\phi$.

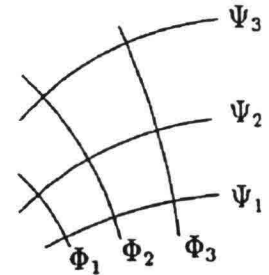


Figure 5.6 Rectangular flow net

It is, with some effort and skill, possible to draw a flow net by hand leading to a rough insight in the flow pattern and the pressures in the subsoil which are important for the stability of protections. Boundary conditions are for example a given ϕ from hydrostatic pressures in the water above the soil or an impermeable boundary perpendicular to which the velocity is 0, hence the boundary is a streamline. Figure 5.7 shows an example of a flow net under a caisson with a head loss.

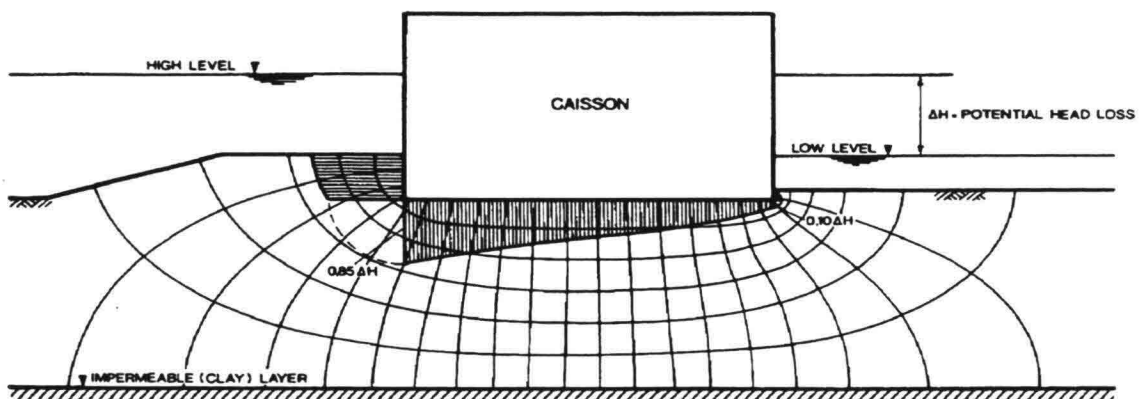


Figure 5.7 Groundwaterflow under a caisson

For non-stationary groundwaterflow, hardly any analytical solutions exist. In most cases a numerical model is needed. Here only a few words will be said about these phenomena.

For rapid fluctuations, like those induced by wind waves, the equation of motion should include the inertia term (see equation (5.3)). No analytical solutions are described in literature.

For slower fluctuations, like in tidal waves, inertia does not play an important role and the Darcy equation of motion can be used. The continuity equation is extended with a time-dependent term, expressing the storage of water in the soil. There are two possibilities for storage in groundwaterflow: phreatic and elastic storage. The first appears when the water level can rise and fall freely. The second phenomenon occurs in confined aquifers, where there is no free surface. An increase in pore pressure leads to a decrease of grain stresses and, hence to a greater porosity in which (a little) water can be stored. This is the same process as consolidation. For more information see the lectures on groundwater flow.

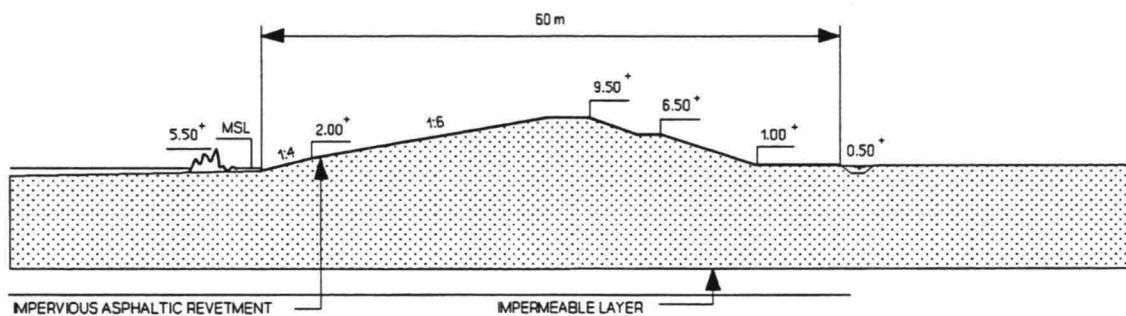


Figure 5.8 Cross-section of dike with asphalt revetment

Figure 5.8 shows a dike for which the internal waterpressures during a storm surge were determined with an electric analogon. Figure 5.9 shows the results. (Note that the low waterlevel in front of the dike is limited by the high level of the foreshore).

Especially when after a long storm, when much water is stored inside the dike, the waterlevel drops suddenly, large excess pressures from inside are possible when the water cannot easily flow out. The permeability of the soil now plays an important role, just as the geometry of the dike, like the toe construction (permeable or sheet-piles).

- 1 = Raise of sea level during storm outside of the dike; max. level is 5.50 m + M.S.L.
- 2 = Constant waterlevel at the landside of the dam.
- 3 = Waterpressure inside of the dike below an impervious revetment

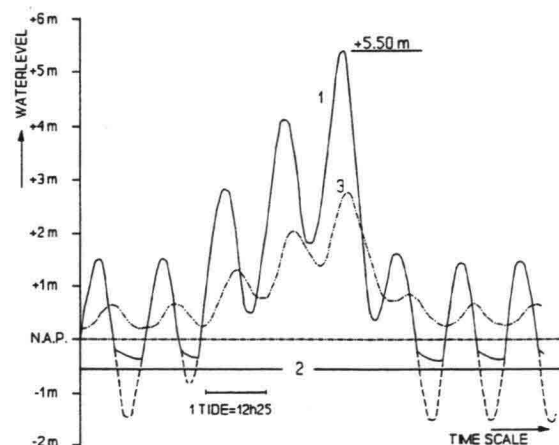


Figure 5.9 Results of measurements in analogon

For this case, use can be made of the already mentioned relation of Cohen de Lara (equation (5.6)). With this equation it is for example possible to compute the flow through a sill under a caisson, where Darcy's law fails. In fact in Figure 5.7, when there is a rock-sill present, at first the flow through this sill should be computed to establish the boundary conditions for the (laminar, Darcy) flow net.

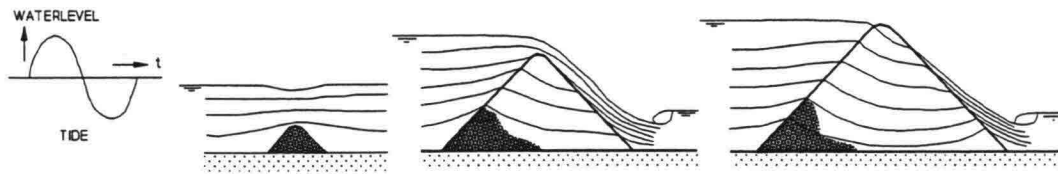


Figure 5.10 Various stages of a closure dam

Another application is the flow through a rockfill dam. Figure 5.10 shows the gradual build-up of a rockfill dam in a river or tidal estuary. When the dam gets higher, the porous flow increases with the head difference. Moreover, it becomes more important compared with the overflow of the dam.

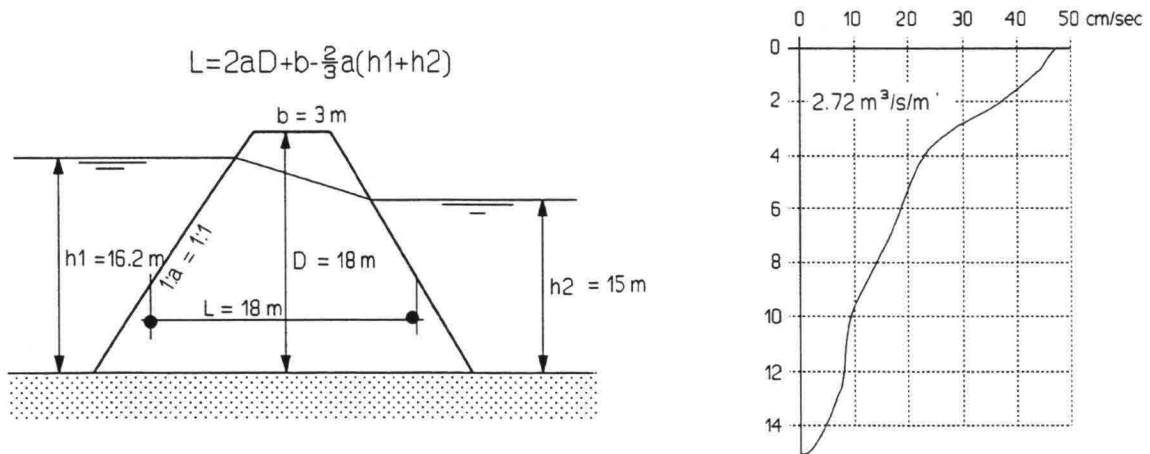


Figure 5.11 Flow through closure dam Brouwershavensche Gat

Figure 5.11 shows a measurement of the flow through a closure dam of concrete blocks of 1 m. The velocity in the upper layer is about 1/2 m/s, which means 1-1.5 m/s for the pores in the dam. Such a velocity through blocks of 1 m makes it clear that Darcy's law does not describe the phenomenon. Note the shape of the velocity vertical which is governed by the shape of the dam (high pressure gradient in the upper area and low at the bottom). The length of the dam, ($L = 18\text{ m}$ in the example), has to be schematised for a 1-dimensional computation as indicated in the figure. With a porosity of 42-43% (from volumetric measurements) equation (5.6) gives: $q = h \times u_t \approx 15 \times \sqrt{[(19.6 \times 1 / 0.5) \times 0.014 \times (1.2 / 18)]} \approx 2.9 \text{ m}^3/\text{s}/\text{m}$ which is in reasonable agreement with the measurements.

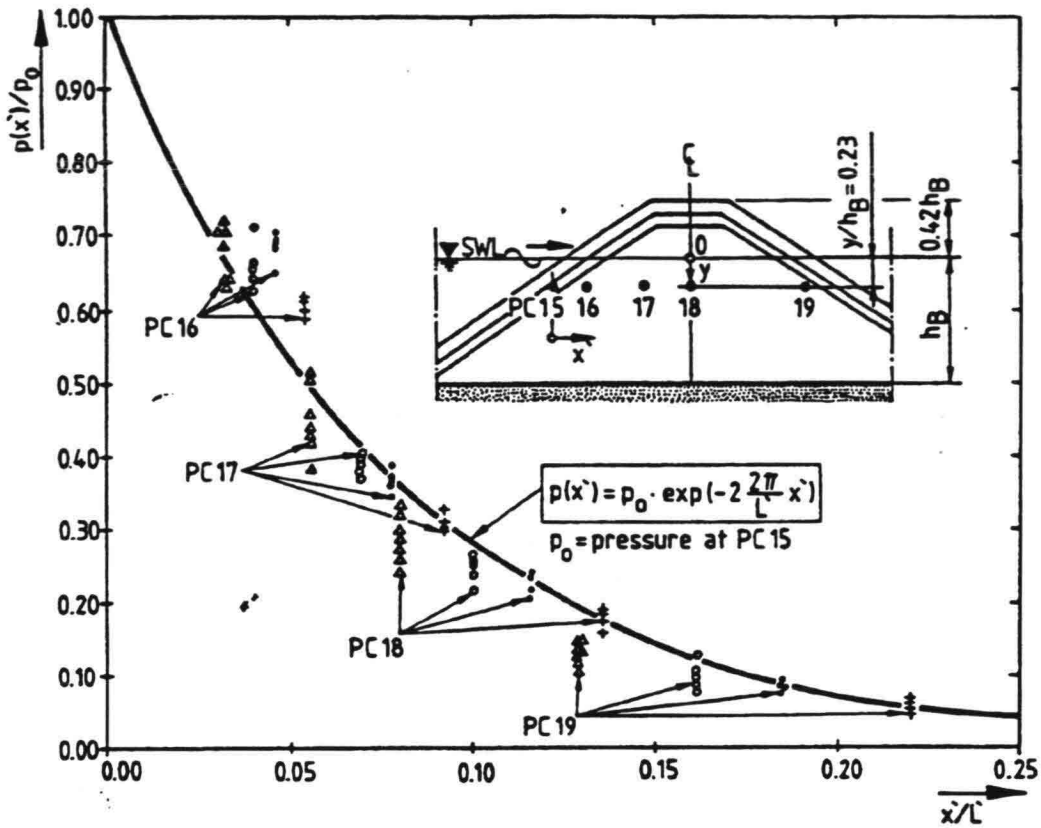


Figure 5.12 Pore pressure dissipation in breakwater

This phenomenon causes even more trouble than non-stationary (laminar) groundwaterflow. In fact, many attempts are made at this moment to solve these problems numerically. In the past some simplified solutions have been presented, mainly based on linearized equations, see e.g. Le Mehaute, 1957. He found a solution for the damping of a short wave in a porous structure:

$$p(x) = p_0 e^{-\beta \frac{2\pi}{L} x} \quad (5.19)$$

The shape of this curve is confirmed in measurements, see Figure 5.12 (from Oumeraci, 1990)

For the stability of elements on slopes, turbulent porous flow plays an important role. At the moment there are not yet reliable computation methods available for non-stationary turbulent porous flow. Scale models are still necessary when detailed information is wanted about this flow.

Before even thinking of protection works, one should have an idea of the measure and extension of possible erosion. Erosion occurs in many forms and is present everywhere in natural flow systems. A summary is given in Breusers/Raudkivi, 1991 from which many examples in this chapter have been taken. These lecture notes do not cover morphological processes; they are limited to local scour in the vicinity of structures. This scour may be caused by the structure, like a bridge pier in a river or it comes from a natural process and the structure is meant to prevent or limit it, like a protected bank in a meandering river. It must be stressed that awareness and knowledge of morphological processes is very important for engineering in natural systems. Bridges have been build across rivers where no water flows anymore because the river has chosen another path, leaving the bridge as a monument of lousy engineering.

In fact, scour is a special case of sediment transport and occurs when the local transport is more than the supply from upstream. The difference in transport can be due to either a difference in velocity or in turbulence or both. The general expression for mass conservation of the sediment reads:

$$\frac{\partial z_b}{\partial t} + \frac{\partial S}{\partial x} = 0 \quad (6.1)$$

in which z_b is the position of the bed and S the total sediment transport (bed load and suspended load) per unit width.

Possible situations for local scour are, see Figure 6.1:

1. $S_2 > S_1 = 0$. This is e.g. the case when cross-section 1 is in a lake, upstream of a dam, and cross-section 2 is downstream of an outlet structure. From section 1 there is no sediment supply to counterbalance the eroding capacity in section 2, because the flow in 1 is too weak to transport material. From equation (6.1) then follows that there will be erosion in 2. This case is the so-called clean-water scour. It stops when the scour reaches a depth such that the velocity becomes lower than the critical value. (This critical velocity will be discussed in detail in chapter 9. Here it is enough to be aware that there is such a velocity above which sediment can be transported. Another parameter often used is the critical shear-velocity ($u_{*c} = \sqrt{\tau_c/\rho}$) with the same meaning)
2. $S_2 > S_1 > 0$. This is e.g. the case when section 1 is in a river upstream of a bridge pier, a groyne or a sill and section 2 is directly downstream of it. The structure causes accelerations and decelerations with turbulence, leading to an increase of transport capacity. The flow upstream is strong enough to transport sediment, this case is therefore named live-bed scour. The scour stops when the eroding capacity in 2 equals the supply from 1.
3. $S_2 = S_1 > 0$. This is a dynamic equilibrium situation. It is possible that between cross-section 1 and 2, there is a situation with a larger transport capacity, e.g a bridge pier in the flow. In that case there is erosion followed by sedimentation, where the eroded sediment is again deposited. This shows

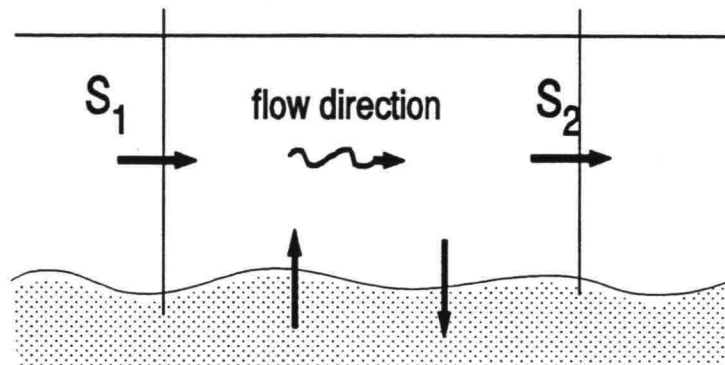


Figure 6.1 General picture local scour

that local scour is a process which is superimposed on the morphological processes.

4. $S_2 > S_1 = 0$. The bottom at section 1 is protected and at section 2 it is not. The flow in 1 has a distinct transport capacity, equal to section 2, but in section 1 there is no sediment. This leads to erosion in section 2. This situation is equivalent to situation 1 in practice, but the circumstances are different. It shows that a bottom protection of infinite length cannot prevent scour completely (unless the velocity at the edge is below the critical value).

Suspended sediment load plays an important role in most scouring processes. In uniform, stationary conditions, there is a dynamic equilibrium in the vertical direction (for more detail, see the lectures on sediment transport):

$$w_s \bar{c} + \epsilon_{sz} \frac{\partial \bar{c}}{\partial z} = 0 \quad (6.2)$$

where w_s is the fall velocity of the sediment, \bar{c} the time-averaged concentration and ϵ_{sz} the eddy diffusivity. The first term in equation (6.2) is the settling of the sediment and the second term represents the stirring up; they can also be interpreted as "rest" and "unrest". w_s depends almost completely on the sediment material; ϵ_{sz} depends on the flow situation and is related to the turbulence in the flow. It is similar to the eddy viscosity but it is not the same. Due to inertia of the grains, the exchange of mass in the flow is not necessarily equal to the exchange of momentum. A usual assumption is that they are proportional, so they can be related to the flow geometry in the same way. Another often used parameter in sediment transport is the quotient w_s/u_* , which again can be seen as the relation between settling and upstirring. A high value of w_s/u_* means bottom transport, a low value suspension transport.

In the case of scour there is no equilibrium between rest and unrest and the second term in equation (6.2) exceeds the first. It can be expected that scouring and a high turbulence intensity are correlated somehow. This is indeed the case. Figure 6.2 shows a scour hole downstream of a horizontal and vertical constriction. The turbulence in the mixing layer (vortex street) acts like a whirlwind and is manifested in a relatively deep scour hole. When there is no horizontal constriction and hence no vertical mixing layer, the scour process is slower and the depth of the scour hole is less. The relation between ϵ_{sz} and the flow geometry is not yet fully understood. A first attempt to approach the scouring phenomenon along this line is given by Hoffmans, 1992. For engineering practice, this approach does not yet give useful results and empirical relations have to be used. In the coming paragraphs some of those will be presented for different cases. In paragraph 6.5, the differences and correspondences will be discussed.

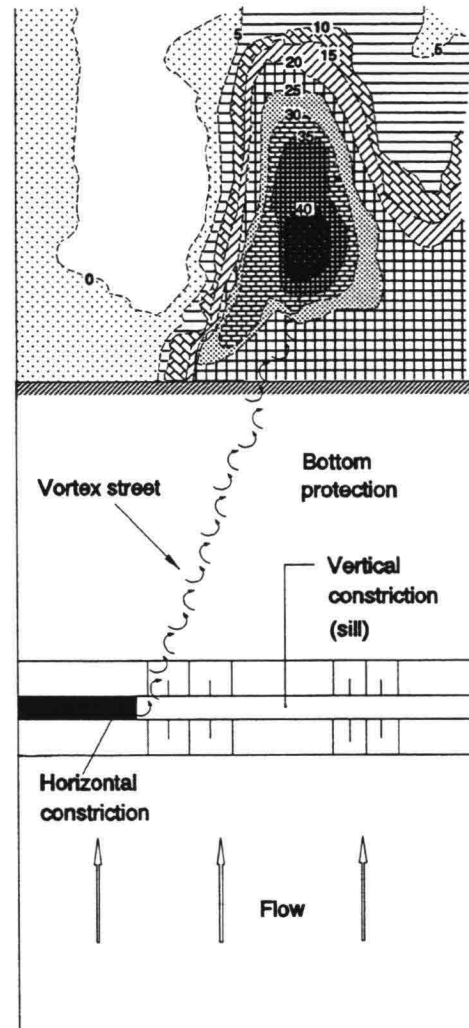


Figure 6.2 Scour in 3-dimensional flow

A high head outflow can cause severe erosion. The type of scour described in this paragraph develops very rapidly and there is usually no time to accompany the scouring-process with maintenance measures. Hence, it is not the relation between scouring and time which is of interest, but the final dimensions of the scour, the equilibrium depth or better: the asymptotic depth, since there is always still some scouring at the end, due to the stochastic nature of the load.

An important name in this field is again Rajaratnam, summarized and elaborated by Breusers. Only horizontal jets will be presented here, see Figure 6.3; for vertical jets and more information in general the reader is referred to Breusers/Raudkivi,1991.

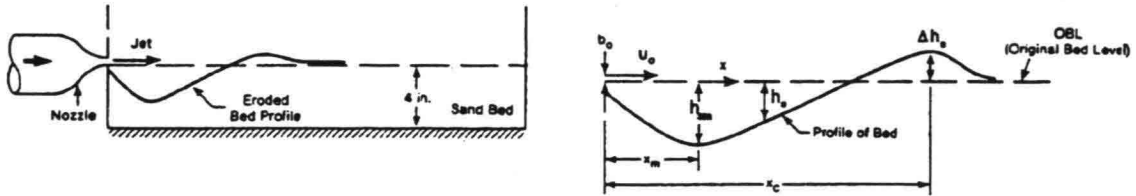


Figure 6.3 Definitions of scour dimensions

First the development of scour by a plane jet (from Rajaratnam,1981) is presented in Figure 6.4.

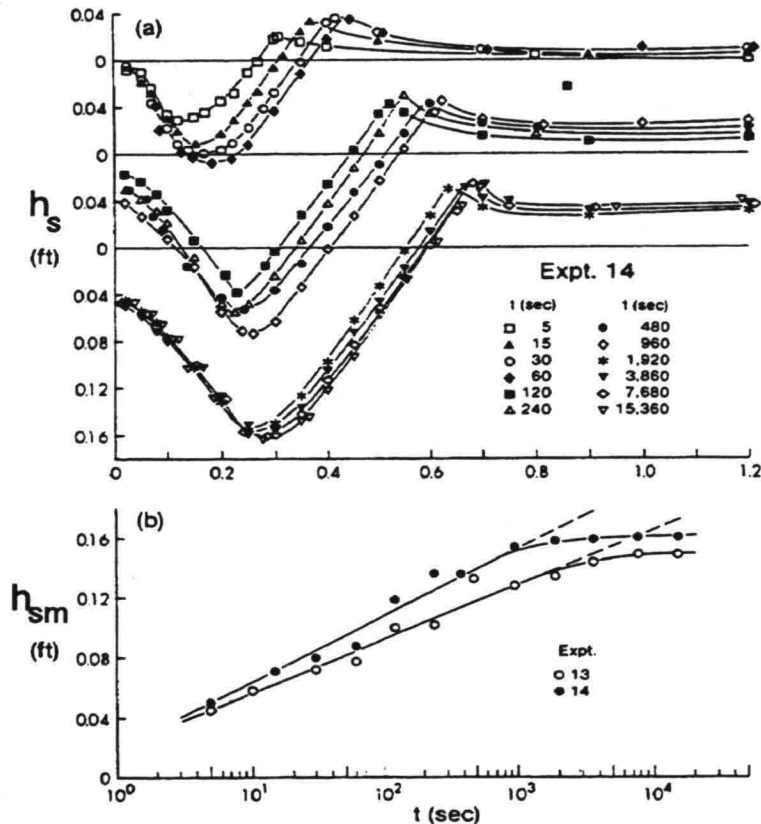


Figure 6.4 Development of scour by plane jet

The scouring process develops rapidly and the scour hole reaches an equilibrium shape.

Rajaratnam found that for high **Re**-numbers and outflow opening (B_u for plane jets and D for circular jets) large compared with the particle size (d), the asymptotic relative scour depth was found to be a function of F_0 only (F_0 defined as $u_0\sqrt{(g\Delta d)}$). Breusers replotted the results of Rajaratnam and others, using U_0/u_{*c} , which is very similar to F_0 (see chapter 9). He finally gives, see also Figure 6.5:

$$\text{plane jet: } \frac{h_{sm\infty}}{2B_u} = 0.008 \left(\frac{U_0}{u_{*c}} \right)^2 \quad \text{circular jet: } \frac{h_{sm\infty}}{D} = 0.08 \frac{U_0}{u_{*c}} \quad (6.3)$$

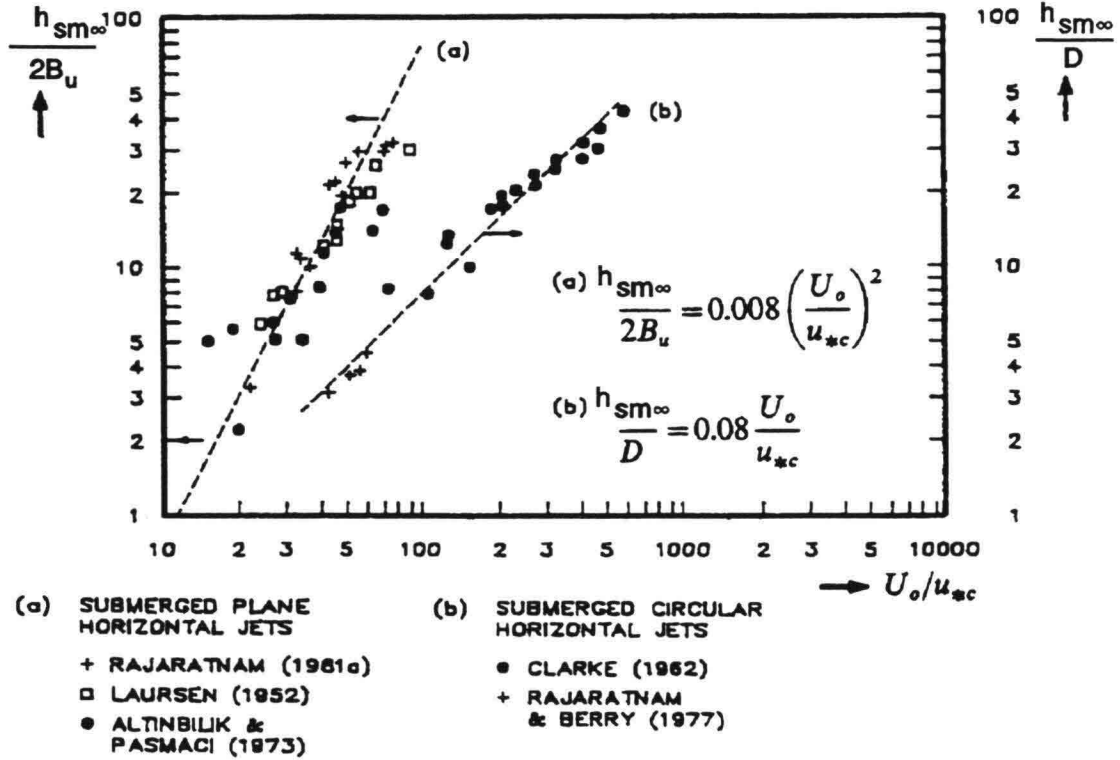


Figure 6.5 Asymptotic scouring depth related to velocities

The length of the scouring hole is about 5-7 times the depth and the width (only relevant for circular jets) is about 3-4 times the depth.

A jet is usually supposed to flow into a space with an infinite waterdepth. Rajaratnam performed some tests with little tailwater (order of magnitude the same as the outlet dimensions). In that case the depth of the scour holes was much smaller (about 50 %) and the length much longer. Culvert outlets with diameters of twice the waterdepth gave even less deep scour holes, see Breusers/Raudkivi, 1991. For a first conservative estimate, equation (6.3) can be used, bearing in mind that the scour can be much less in shallow water.

Further downstream in a jet or behind a culvert when there is a protection apron present, the flow is more quiet and the scour develops more moderately. This will be often the case behind hydraulic structures. Many investigations on this subject were done in the framework of the Deltaproject. Time was an important factor there, since the closure dams had only a temporary function and equilibrium depths for every building stage were never reached. But also in other situations it is good to know the scour as a function of time. It can play an important role in maintenance policy, since relatively little is known up to now about the slopes of scouring holes and the soil-mechanical stability. Then it is important not to be surprised by unknown rapid developments.

The research for the Deltaproject aimed mainly at establishing reliable scale relations for interpreting model results. Large parts of it however can be used for prediction purposes in a preliminary design. Several hundreds of tests have been performed and the experimental relations have gained some general validity.

6.3.1

PROCESS-DESCRIPTION

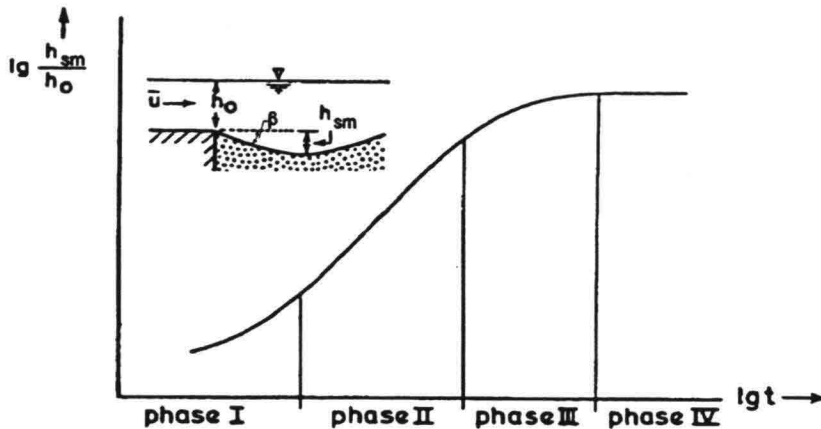


Figure 6.6 Phases of scouring process

The development of a scour hole can be described in 4 phases (see Figure 6.6):

Phase I: the initiation of the process; the bottom is still flat and the velocity-profile is not yet influenced by the scour hole.

Phase II: flow separation occurs in the hole and the flow in the eddy is against the main flow direction.

Phase III: the velocity in the scour hole reaches values which are near the critical value and the process slows down.

Phase IV: equilibrium is reached; this phase is equivalent to the asymptotic profile as described for jets.

For practical purposes only phase II and phase IV are important. About phase IV, some remarks will be made in paragraph 6.3.4. The focus will be on phase II for which the formulae in this chapter are valid.

Figure 6.7 shows the velocity, averaged over the turbulence period, the root mean square of the velocity-fluctuation and the Reynolds shear-stress at various locations in a scour hole between the upstream crest and the deepest point. From this it can be seen that a scour hole itself is also a disturbance of the flow: a relatively "normal" velocity profile at the crest, turns into a deceleration profile with intense turbulence. Like behind a sill (see chapter 2), the shear stress is relatively small (even smaller than the critical value for transport) and the turbulent fluctuations are dominant.

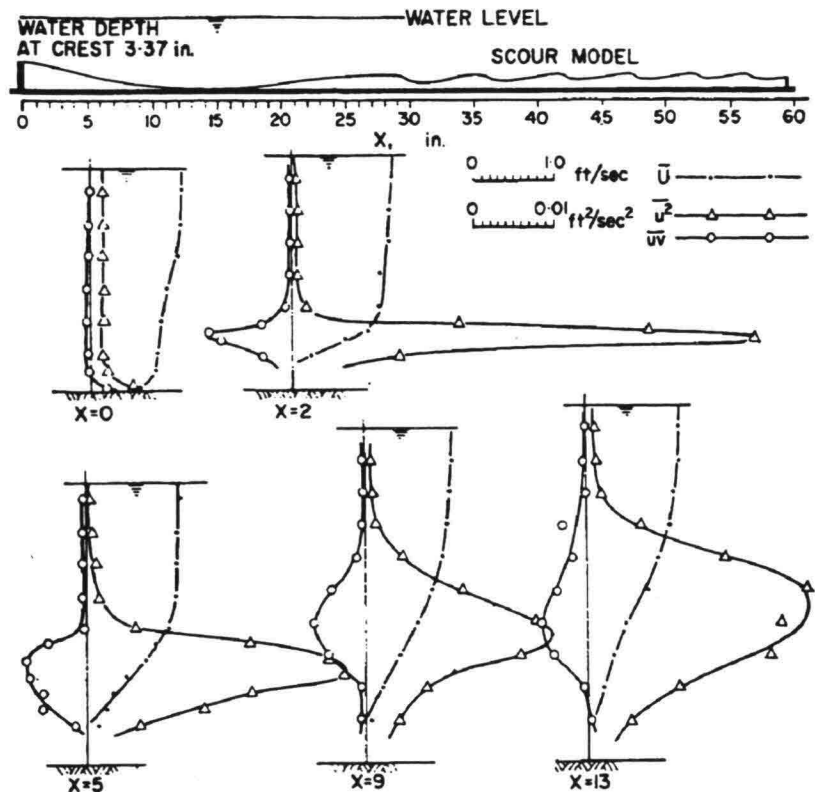


Figure 6.7 Velocity characteristics in scour hole (Breusers/Raudkivi, 1991)

From a dimensional analysis and many experiments, finally the following expression was developed:

$$h_{sm}(t) = \frac{(\alpha u_0 - u_c)^{1.7} h_0^{0.2}}{10 \Delta^{0.7}} t^{0.4} \quad (6.4)$$

in which h_{sm} is the maximum depth in the scour hole as a function of time, while h_0 is the original waterdepth; u_0 is the vertically averaged velocity at the end of the protection (see also section 6.3.2). t is the time in hours in this empirical relation; the constant 10 is not dimensionless. α represents, among other things, turbulence and acts as an increase in the effective velocity. This is the "dust-bin" of the scouring formula; in the next paragraph special attention will be paid to this important parameter. α is related to the geometry of the flow and is usually derived from a scale model where h_0 , u_0 , u_c and Δ are known and where h_{sm} as a function of time is measured. Then, α can be calculated from equation (6.4). With this α , equation (6.4) is then again used to calculate the scour for prototype circumstances. For schematized situations that have been investigated earlier, it is possible to estimate α .

From equation (6.4) we can see:

- the scour depth grows with a power 0.4 in time
- there is some influence of the specific weight of the sediment and very little of the waterdepth
- the difference between the actual velocity with α and the critical velocity is dominant

Note 1 Equation (6.4) is derived for phase II of the scouring process; $\alpha u - u_c$ should therefore be not too small ($> \approx 0.1$ m/s). Otherwise the process is in fact in phase III.

Note 2 The power 0.4 in the relation with time in equation (6.4) is strictly speaking derived for 2-dimensional flow situations. For 3-dimensional flow (horizontal contraction, outflow from discharge sluice etc.) the power is in the beginning higher and later on somewhat smaller. As a first approximation 0.4 will be used for all time dependent scour processes.

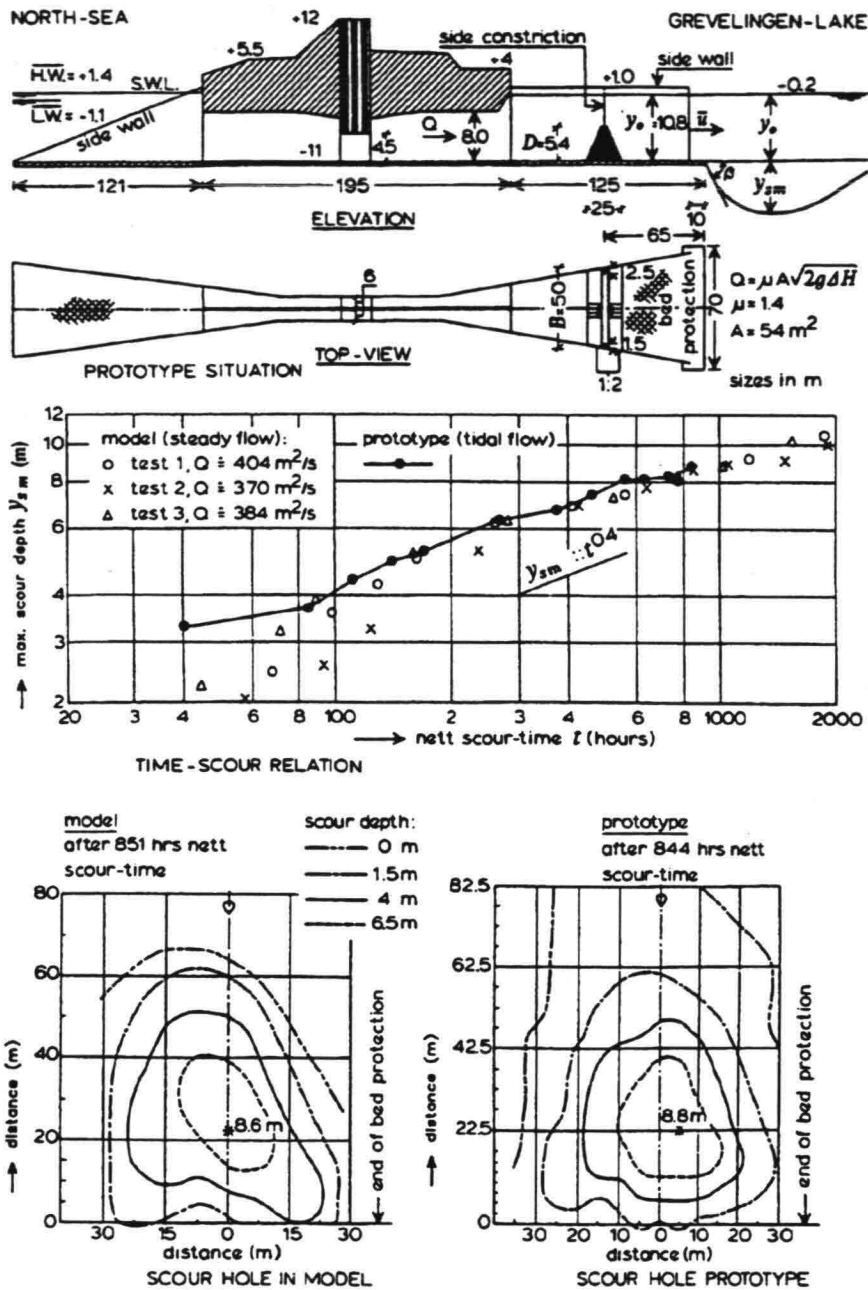


Figure 6.8 Comparison model-prototype scour development (de Grauw/Pilarczyk, 1981)

The presented relation is based on many modeltests. Accurate comparison with prototype measurements in the Deltaproject was very difficult because of the ever-changing situation during the construction of the dams. In order to get more confidence in the relations, a special test was performed with the outlet sluice in the Brouwersdam (part of the Deltaworks) and a scale model of the same sluice. Figure 6.8 shows the result; the conformity in development and shape is good.

α is a very important parameter in the computation of time-dependent scour. As already said, it is a dust-bin, following from model-investigations for a given geometry. For predictive preliminary design purpose it is necessary to have some insight in the relation between geometry and α . Therefore we look into how α is defined and its consequences, see also Jorissen/Vrijling, 1989.

Figure 6.9 shows two ways to define α depending on the definition of u_0 in equation (6.4). When u_0 is defined as Q/A , the influence of a locally increased velocity disappears into α , thus "polluting" this coefficient with the velocity distribution. When u_0 is defined locally, α only represents the magnifying factor due to turbulence. The product $\alpha \cdot u_0$ is the same of course in both cases.

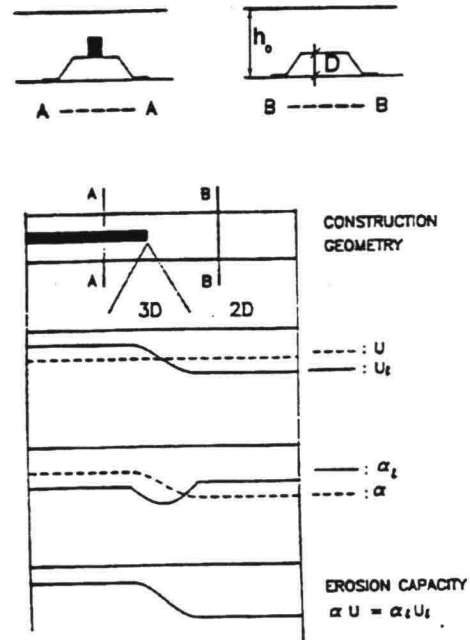


Figure 6.9 Possible definitions of α

For $u_0 = Q/A$, Figure 6.10 gives α as a function of the vertical constriction for 2-dimensional and 3-dimensional scouring (without and with horizontal constriction respectively). These data come from the systematic scour investigations in the framework of the Deltaproject. There is a big difference in α , a large part of which is due to the velocity distribution.

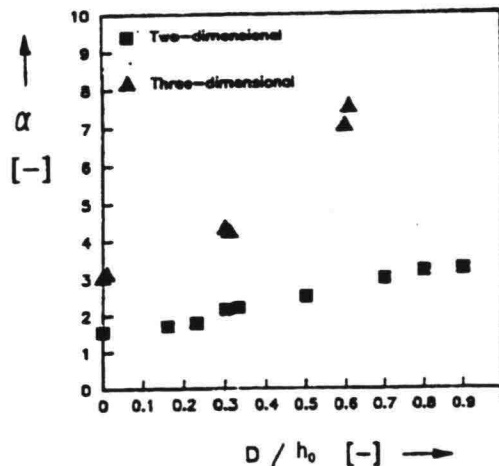


Figure 6.10 α with $u_0 = Q/A$ vs. vertical constriction

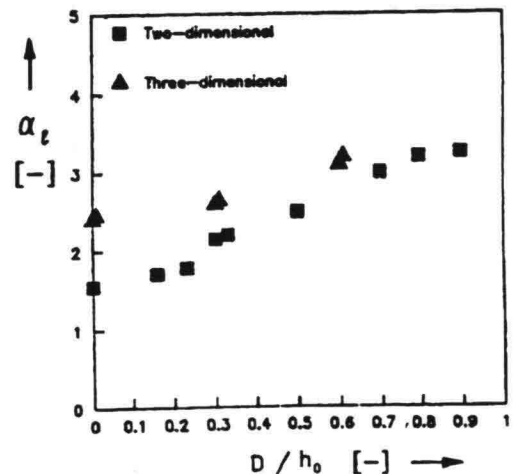


Figure 6.11 α with local u_0 vs. vertical constriction

When α is a magnifying factor for the velocity, expressing the disturbance in the flow, it can be expected to have a relation with the turbulent fluctuations in the flow. Figure 6.12 shows the relation between α_1 (defined with the local u_0) and the turbulent fluctuations, expressed as r , here defined as the root mean square depth averaged local velocity divided by the depth and time averaged local velocity:

$$r = \frac{\sqrt{\overline{u_l'^2}}}{\overline{u_l}} \quad (\%) \quad (6.5)$$

There is indeed a relation between α_1 and r :

$$\alpha = 1.5 + 5r \quad \text{for } \alpha > 1.8 \quad (6.6)$$

indicating that turbulence together with a locally known velocity, can be used to explain and compute time-dependent scour.

Note: In equation (6.2), a relation between ϵ_{α} and the turbulent fluctuations was mentioned. At this moment there is still a gap between the approach with a sediment transport model as used by Hoffmans, 1992 and the empirical relation of Breusers. Figure 6.12 is a sign however that this gap possibly can be closed in the future.

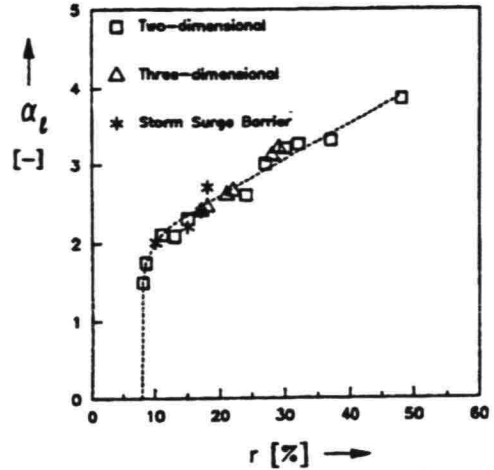


Figure 6.12 α_1 vs r

For a preliminary design, Figure 6.14 gives values for α based on local velocities with the geometry defined according to Figure 6.13

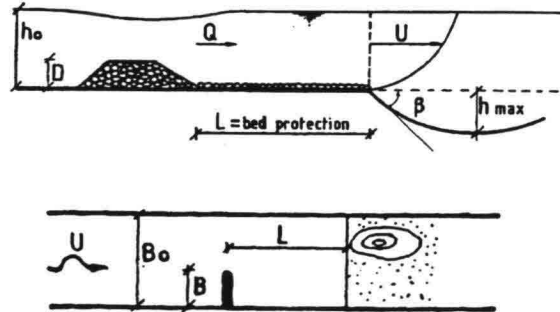


Figure 6.13 Definition of geometry parameters

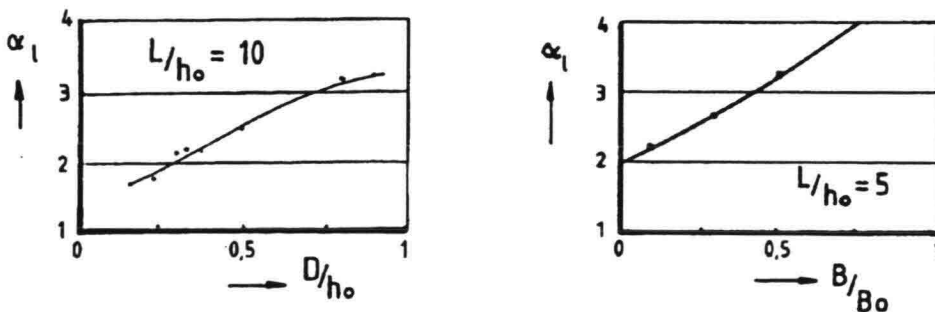


Figure 6.14 First estimate of α_1

When the local velocities are not known, Figure 6.15 can serve as a first approximation for vertical and horizontal constrictions, based on $u_0 = Q/A$ and $L_p/h_0 = 10$.

In the case of an outlet structure discharging into a large body of water, there is not clearly a vertical and/or horizontal constriction. In that case the scour can be approximated with the α -value for a vertical vortex-street which lies between 3.5 and 5 for a bottom protection length of $10h_0$ and u_0 defined as Q/A at the place where the outlet flows freely into the large body of water e.g. at the end of wing walls or the edge of the bottom protection.

It will be clear that for a first design only rough estimates can be made. For a project of some importance, investigations in a scale model will be necessary

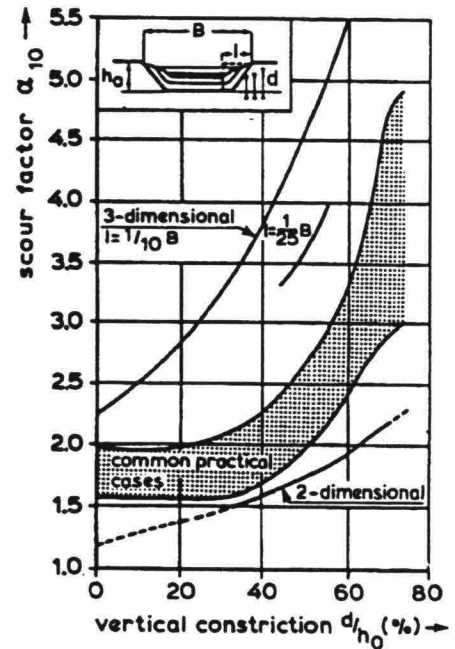


Figure 6.15 α with $u_0 = Q/A$

6.3.3

INFLUENCE OF BOTTOM PROTECTION

At first, the roughness of the bottom protection is of influence. With a smooth protection, the velocities near the bed are high and cause more scour. The influence of the roughness on α is given by Hoffmans, 1993a in a slightly adapted form of equation (6.6):

$$\alpha = 1.5 + 4.4 r_0 f_c \quad \text{with } f_c = \frac{C}{40} \quad (f_c = 1 \text{ for } C \leq 40)$$

Smooth (e.g. asphalt) bottom-protections lead to 20-30% higher α -values than rough protections. The equation also shows that it has no use to make the protection very rough. In that case the roughness elements induce extra turbulence, compensating the effect of a lower bottom velocity.

A longer bottom protection leads to lower values for α , but the influence of the length is not spectacular; turbulence in a flow dissipates slowly, see section 2.6 and Hoffmans 1993a. Moreover, even with an infinitely long protection, there will be scour, see section 6.1. For $L/h_0 > 5$ the influence of the length on α is given by:

$$\alpha(L/h_0) = 1.5 + (1.57 \alpha_{10} - 2.35) e^{(-0.045 L/h_0)} \quad (6.8)$$

where α_{10} is the α -value for $L_p/h_0 = 10$, see also Figure 6.16. Note that for an infinitely long bottom protection α_{\min} is 1.5!

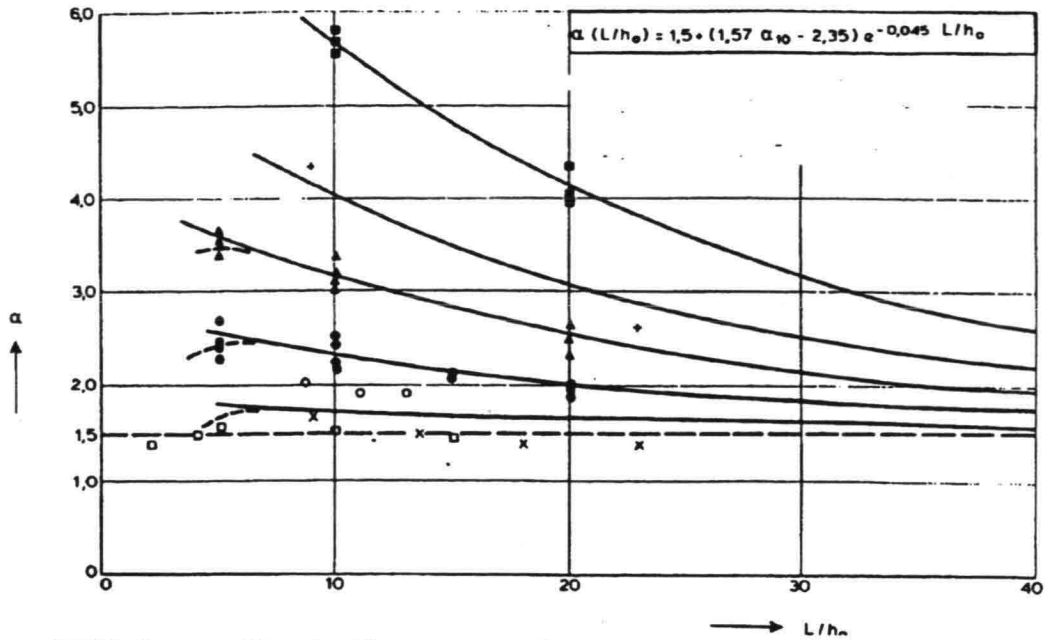


Figure 6.16 Influence of length of bottom protection on α

6.3.4 THE SLOPE β

Scour as such is not a problem as long as it does not undermine the considered structure. To be able to judge the stability of slopes in scour holes it is necessary to know β (see Figure 6.13). From the systematic scour research, Hoffmans, 1993b derived the relation:

$$\beta = \arcsin \left[3 \cdot 10^{-4} \frac{u_0^2}{\Delta g d_{50}} + (0.11 + 0.75 r_0) f_c \right] \quad \text{with } f_c = \frac{C}{40} \quad (f_c = 1 \text{ for } C \leq 40) \quad (6.9)$$

indicating that a high velocity, high turbulence, a smooth protection and fine sand, cause steep slopes.

Figure 6.17 shows the results of equation (6.9) for some possible values of the relative turbulence, the velocity and the roughness of the protection (all for a grain diameter of $200\mu\text{m}$). Sometimes, even a slope β steeper than 25° ($\sim 1:2$) can cause problems, depending on the depth, see also the geotechnical aspects in chapter 7. Again, it is clear that a long (low r !) and rough(ened) bottom protection helps in preventing steep slopes. It must be stressed however, that there is much uncertainty about these slopes. Therefore it is also important to know the scour as a function of time to be able to deal with maintenance, like dumping protective material on the slope.

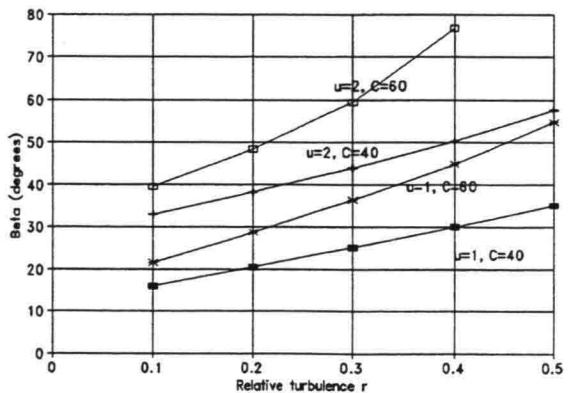


Figure 6.17 Slope β as function of hydraulic parameters

For scour in a tidal flow, equation (6.4) can be used with the tide taken into account as a succession of stationary flow situations, replacing $(\alpha u_0 - u_c)^{1.7}$ for each flow direction of the structure, by (see also Figure 6.18):

$$\frac{1}{T} \int_0^T (\alpha u_0 - u_c)^{1.7} dt \quad (6.10)$$

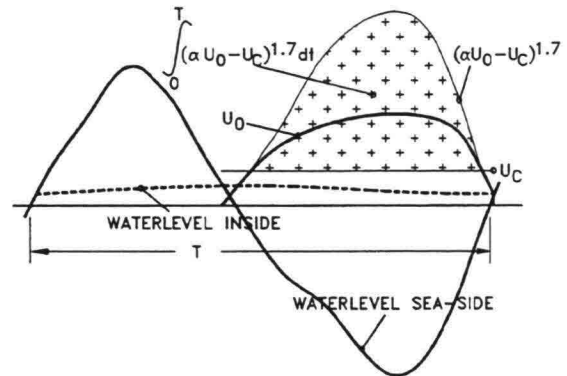
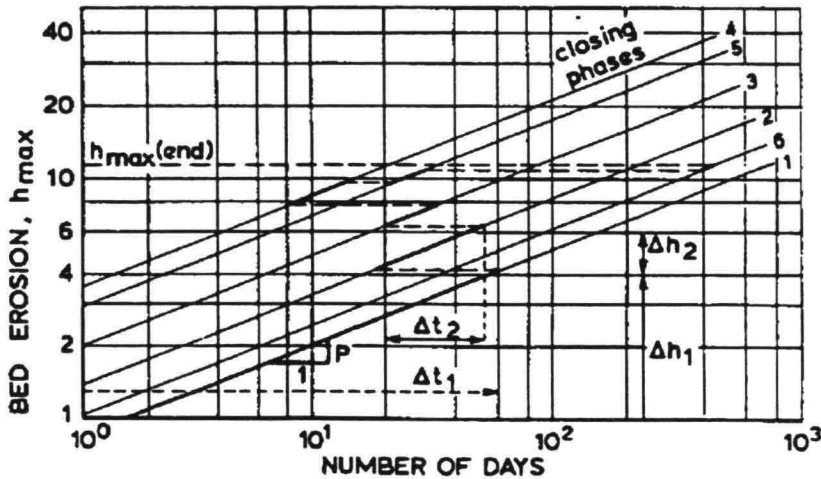


Figure 6.18 Use of scour formula in non-stationary flow

In the case of e.g. an outlet sluice discharging into the sea during low water, u_0 in equation (6.10) exists only part of the tidal period, while T always represents the whole period, indicating that scouring at the sea side of the structure is only effective during some hours.



$$\frac{h_{max}}{h_0} = \left(\frac{t}{t_1}\right)^p$$

Figure 6.19 Scour-time curve for successive building stages

When scour has to be determined for the construction period of some structure, Figure 6.19 shows the procedure. For various representative building stages, the various scour-time curves are determined. The first curve is followed during Δt_1 . At the end of this period is horizontally switched to the second curve (the scour hole according to the second curve starts with the end value of the first period) and so on till the end. (This can be done since similarity of the shape of the scour hole is an important finding of the systematic scour research).

A simple approach to equilibrium depth would be to say that it is reached when αu_0 in the hole becomes equal to u_c . With the continuity-equation this leads to:

$$\frac{h_{sm\infty}}{h_0} = \frac{\alpha u_0 - u_c}{u_c} \quad (6.11)$$

There are reasons to say that equation (6.11) overestimates the equilibrium depth e.g. because it is based upon equation (6.4) which is derived for phase II of the scouring process and not for phase III or IV, see section 6.3.1. Therefore αu_0 in (6.11) has to be reduced with a factor of about 0.5.

When there is a sediment supply from upstream, equilibrium will be reached when the outflow from the hole becomes equal to the inflow (see par 6.1.1). In that case the scouring formula represents the clean-water scour and the sediment supply turns it into a live-bed scour. When the hole is schematized to a triangle, see Figure 6.20, the volume of the hole per m width is:

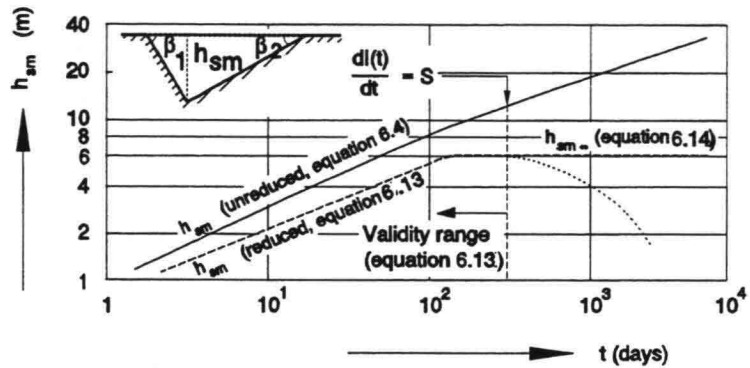


Figure 6.20 Scour reduction by sediment supply

$$I = \frac{1}{2} (\cot \beta_1 + \cot \beta_2) h_{sm}^2 = .005 (\cot \beta_1 + \cot \beta_2) \Delta^{-1.4} h_0^{0.4} (\alpha u - u_c)^{3.4} t^{0.8} = K t^{0.8} \quad (6.12)$$

With sediment supply this becomes:

$$I_{red} = K \cdot t^{0.8} - S \cdot t \rightarrow h_{sm\ red} = \sqrt{\frac{I_{red}}{\frac{1}{2} (\cot \beta_1 + \cot \beta_2)}} \quad (6.13)$$

Equilibrium is reached when, see Figure 6.20:

$$\frac{dI}{dt} = 0 \rightarrow 0.8 K t^{-0.2} = S \rightarrow t_{eq} = \left(\frac{0.8 K}{S} \right)^5 \rightarrow h_{sm\infty} = \sqrt{\frac{K \cdot t_{eq}^{0.8} - S \cdot t_{eq}}{\frac{1}{2} (\cot \beta_1 + \cot \beta_2)}} \quad (6.14)$$

There are however many uncertainties in this procedure: $\cot \beta_{1,2}$ have to be estimated (e.g. 4 and 40), S must be calculated and t_{eq} is very sensitive for K and S . Therefore in closures it is preferable to use a measured value of t_{eq} from an early building stage, see Figure 6.19. Better results might be expected when the scouring is treated as sedimenttransport, like in Hoffmans, 1992 approach.

It is easy to imagine that the flow phenomena around bodies like acceleration, flow separation and wake, stand for an increase of the sediment transport capacity, causing local scour. Bodies in a flow can stand alone, like bridge piers, or be attached to the banks, like abutments or groynes. Development in time is usually not very important for this type of structures; only the equilibrium situation will be discussed. Most information in this paragraph has been derived from Breusers/Raudkivi, 1991; for more details the reader is referred to that book.

6.4.1

SCOUR AROUND BRIDGE PIERS

At first we look somewhat more in detail to the flow around a (cylindrical) pier because there is more between surface and bottom than acceleration and wake, see Figure 6.21.

At the face of the pier the water is stopped. Since the velocity at the surface is higher than at the bottom, there is a pressure gradient ($\rho u^2/2$ varies along the height) leading to a downflow. This downflow can reach a value of 80% of the undisturbed flow velocity and acts as a vertical jet. This jet together with the accelerated flow at the sides of the pier, start the erosion. Once there is an erosion hole, the same circulating current as in the scour holes of par. 6.3 appears. This eddy is taken away by the flow, leading to a horseshoe-shaped vortex. This vortex, together with the accelerated flow and wake vortices transport the sediment further downstream. A few diameters behind the pier, the transport capacity decreases again and a bar is formed.

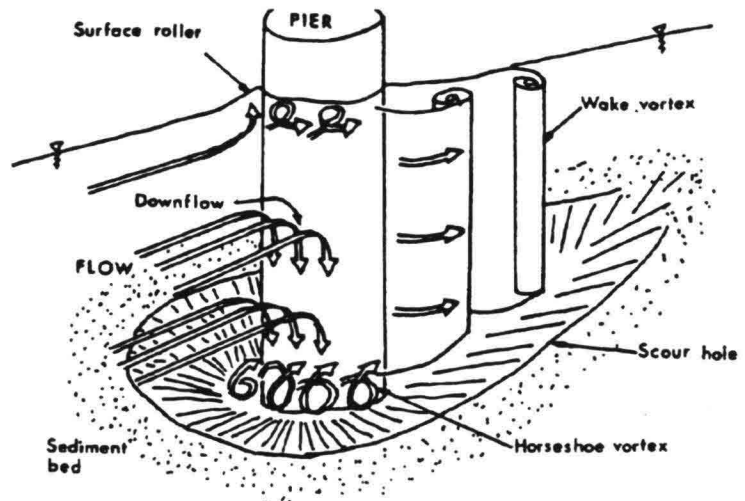


Figure 6.21 Flow pattern around pier

Figure 6.22 shows the equilibrium depth (dimensionless with the pier diameter) with increasing velocity. When $u < u_c$, there is already a distinctive scour due to the described flow factors (compare α in the time dependent scour formula). The scour reaches a maximum when $u = u_c$; when $u > u_c$ it decreases again because then the whole bed is moving and the scour is reduced.

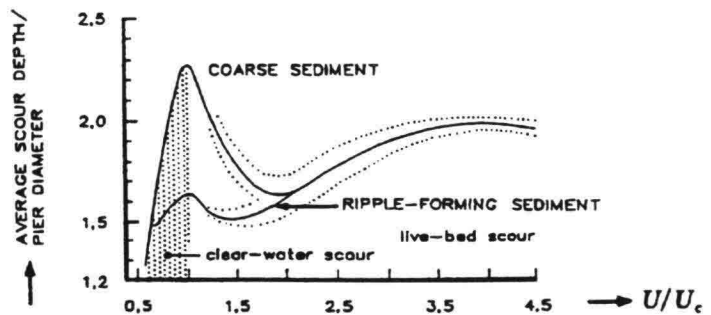


Figure 6.22 Scour depth for cylindrical piers in uniform sediment

This is the transition between clear-water and live-bed scour; the process is similar as described in par 6.3.6 where the scour was reduced by sediment supply. A second peak occurs at the transition between ripples/dunes and anti-dunes where the bed is flat. Then, the flow does not need to spend energy in form drag and can devote itself completely to sediment transport. The second peak is lower than the first; for a preliminary design the first peak is recommended. Figure 6.23 shows the difference in scour development between clear-water and live-bed scour.

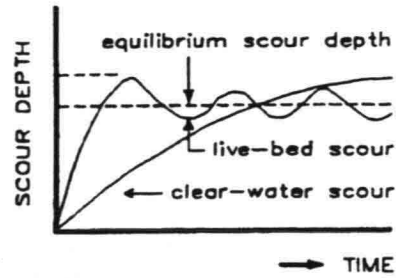


Figure 6.23 Scour as function of time

Other shapes of piers lead to other coefficients than for cylindrical piers. For a square cross-section for example, the scour depth is about 20% higher; with a streamlined shape 20-30% lower values are possible, see table.

This is however dangerous in design practice, since one has to be sure that the flow is exactly in the direction of the streamlined body. An angle (in river bends or with moving channels) leads to another flow separation pattern and considerably more scour, see Figure 6.24.

Pier shape	l/b	K_s
cylinder	-	1.0
rectangular	1	1.2
	3	1.1
	5	1.0
elliptic	2	0.85
	3	0.8
	5	0.6

For a first design the next formula is proposed:

$$\frac{h_{sm}}{D} = 2.3 K_s K_\alpha \quad (6.15)$$

Note:

- for a bridge with many piers extra scour may occur due to the flow constriction, see par. 6.4.3.

- floating debris or ice can enlarge considerably the effective width of the pier

- wave action around the pier does not enlarge the scour compared with only flow

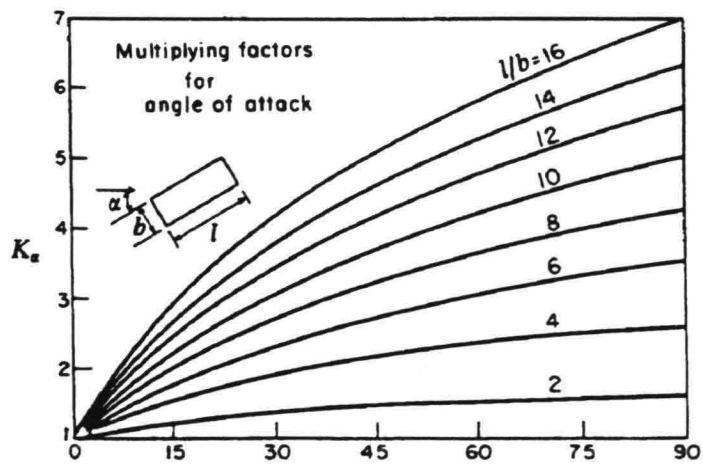


Figure 6.24 Multiplying factor for piers not aligned with flow

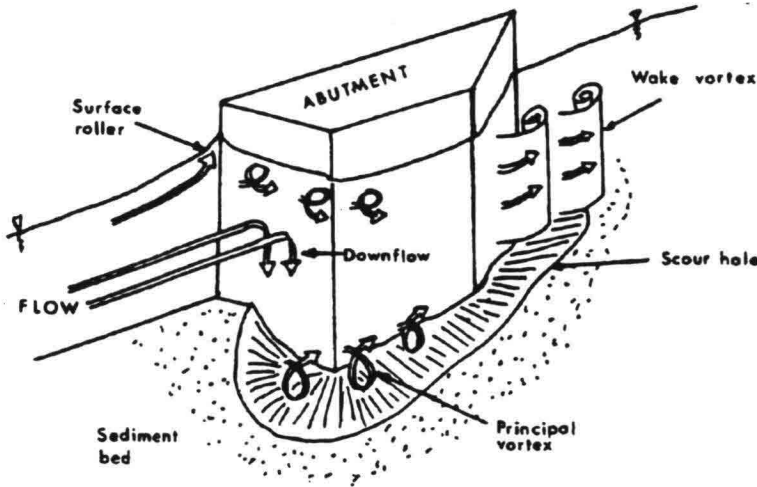


Figure 6.25 Flow pattern around abutment

The first approach to abutment-scour is simply to consider it to be a half pier. Indeed, the processes are very similar, but the numerical values are somewhat lower since the wall hinders the downflow and the vortices. Streamlining is now relevant, because the angle of attack is less important.

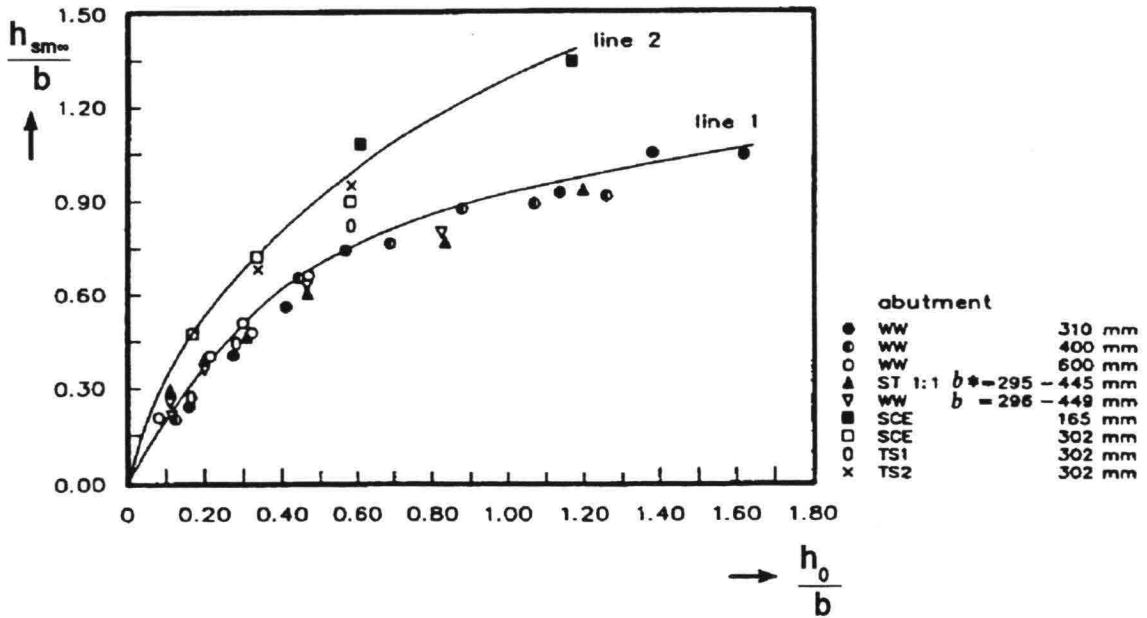


Figure 6.26 Relative scour depth for various abutments

Figure 6.26 shows the relation between scour depth, abutment width (b , the protrusion from the bank into the water) and waterdepth. Line 1 is for streamlined abutment shapes like wing walls as in Figure 6.25. Line 2 is for more blunt forms. In both cases the values for the scour depth in relation to the abutment width is less than for piers. In relation to the waterdepth the values are still considerable.

6.4.3

SCOUR BEHIND GROYNES

Groynes can be seen as (very blunt) abutments, but also the narrowing of the river bed is going to play a role. The constricted river width therefore appears in the relation for scour depth. Breusers recommends for a first approach, see Figure 6.27:

$$h_0 + h_{smax} = 2.2 \left(\frac{Q}{B-b} \right)^{2/3} \quad (6.16)$$

for a vertical groyne perpendicular in a straight channel. Corrections of (6.16) for other angles are:

α (°)	Factor
30	0.8
45	0.9
60	0.95
90	1.0
120	1.05
150	1.1

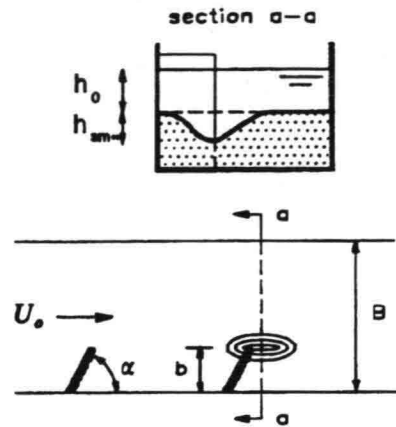


Figure 6.27 Groynes-definition sketch

When the head of the groyne is not vertical, but has a slope of 45° , the depth is about 15% lower. With very gentle sloping heads, reductions of 50% seem possible. When the groynes are situated at the concave side in a river bend, the depth can increase 10 - 50%, depending on the bend radius.

6.4.4

SCOUR IN CONSTRICTIONS

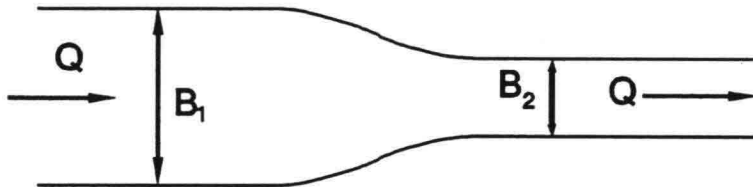


Figure 6.28 Definition sketch for constriction scour

Equation (6.16) gives the depth of a scour hole behind an individual groyne. Narrowing a river stretch, either by a row of groynes or by embankments, leads to a general deepening of the river bed. The depth in the constriction can be calculated with (see Figure 6.28):

$$\frac{h_2}{h_1} = \left(\frac{B_1}{B_2} \right)^{\frac{m-1}{m}} \quad (6.17)$$

in which m comes from the relation between velocity and sediment transport in the form: $S \propto u^m$. m lies usually between 3 and 5, so the power in equation (6.17) lies between 0.67 and 0.8. For more knowledge on this subject, the reader is referred to the domain of the river morphology.

In the previous paragraphs, various kinds of scour were discussed. They all form a kind of local erosion, caused by a local increase of velocity and/or turbulence, leading to a local increase of sediment transport capacity. With so much in common it is all the more amazing and frustrating that the various types of scour have been examined in so different ways and that the results cannot be combined into one overall picture. The following table presents some characteristics of the various scour investigations:

Par.	Type of scour	Live-bed	Protection	Dev.in time	Eq. depth
6.2	Jets and culverts	no	no	some	yes
6.3	Time dependent	no (indirect via calcul.)	yes	yes	roughly
6.4	around bodies	yes	no	some	yes

A logical relation would be e.g. the scour by a jet on an unprotected bottom of paragraph 6.2, via a protected bottom to the time dependent scour of paragraph 6.3, where one would like to have an idea of the equilibrium depth. The latter situation is literally the extension of the first. Another link would be to try to describe the scouring around a body from paragraph 6.4 with the time-dependent relations of paragraph 6.3.

The explanation of the different approaches is of course the fact that every investigation had its own limited goals for which the research program gave more or less satisfactory results. It is about time however, to try to make an overview of this jig-saw puzzle in which all these pieces get their proper place. Such a general approach would have to include the relations between the turbulent flow characteristics, the sediment transport and the local scour process as a function of time.

Hoffmans, 1992 has started this for a two-dimensional situation without sediment supply from upstream, which could be extended with the supply of sediment. A major problem that remains is the translation from geometry to turbulent flow. Future research is necessary to make further steps forward. Figure 6.29 shows a result of Hoffmans work, applied to the same outlet-structure as in Figure 6.8 which gives some confidence that we are getting nearer. When applying an empirical formula like (6.4), at least the use of Q/A should be avoided and the local velocity should be used. Relating α with the turbulent flow situation for various geometries, already would be a step forward, see also Ariëns, 1993.

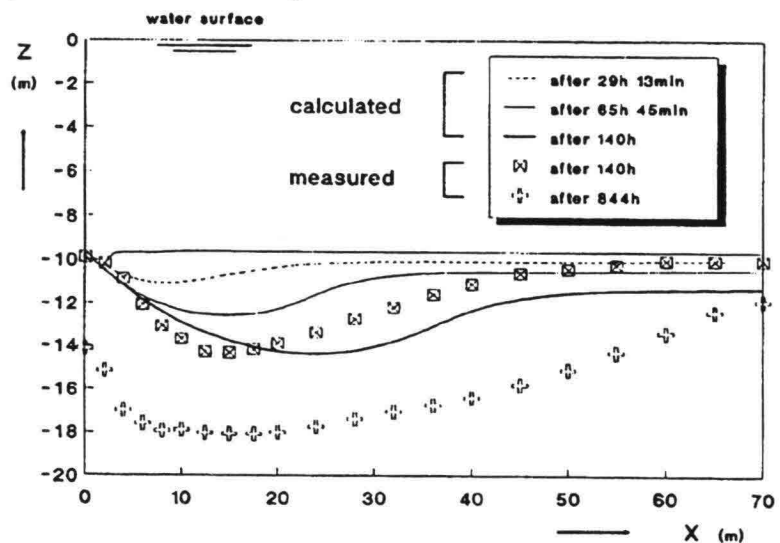


Figure 6.29 Calculated and measured scour profile at Brouwersdam

Again, before considering the necessity of protecting a bank, a shore or a bottom against waves, one should have an idea of the possible erosion. For banks and shores this will be done on the basis of beach and dune erosion research; for bottom erosion, breakwater investigations will be used.

7.1.1

SLOPES

Waves acting on an unprotected slope, cause a step-profile or S-profile. This is the natural equilibrium profile for all slopes composed of loose material (see e.g. Vellinga, 1986). From theoretical considerations for beaches a parabolic profile is found with $z \propto x^{2/3}$. This theory however is valid for monochromatic, linear waves. Vellinga proposes:

$$z = 0.39 w^{0.44} x^{0.78} = p x^{0.78} \quad (7.1)$$

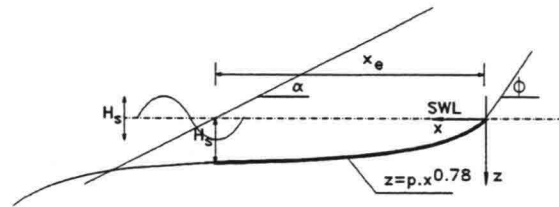


Figure 7.1 Erosion profile by waves

in which w is the fall velocity of the particles; for the definition of z and x , see Figure 7.1. This is an equilibrium profile; development in time is not considered. The erosion depth below SWL is about H_s . From equation (7.1) the intrusion depth of the waves in the profile is then found by:

$$x_e = p^{-1.28} H_s^{1.28} \quad (7.2)$$

Above the still water level the slope is assumed to be equal to the angle of repose. Figure 7.2 gives a relation for the value of p in the profile-formula. The given relations can serve only as a first indication and should be applied for wave attack well beyond the limit of stability, see chapter 10.

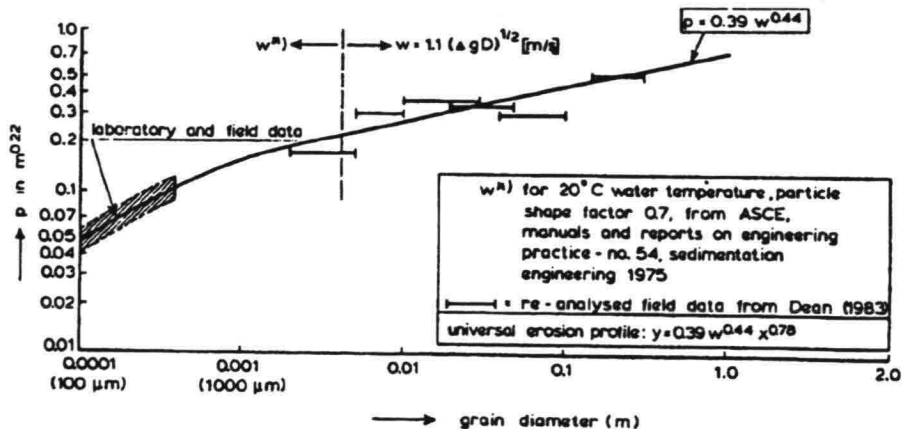


Figure 7.2 Relation between grain diameter and p in erosion profile

Bottom scour due to waves can be important in front of vertical walls where a standing wave pattern is possible. From chapter 3 we know that the highest velocities occur in the nodes of such a wave and indeed, for fine sediments, the maximum scour is found there. For coarse sediments however, the maximum scour is found between the node and antinode, probably due to another eddy and ripple pattern. The equilibrium depth of the scour hole can roughly be estimated with (see Xie Shi-Leng, 1981):

$$\frac{h_{smax}}{H} = \frac{0.4}{\left(\sinh 2\pi \frac{h}{L}\right)^{1.35}} \tag{7.3}$$

This formula indicates that the scour depth depends on the wave height and the waterdepth related to the wavelength. Equation (7.3) is experimentally determined for fine sediment; for coarser sediment it can be seen as an upper boundary, see Figure 7.3.

When the wall is not vertical but inclining, the maximum scour will occur at the foot of the wall, due to the backflow from the sloping wall, see Figure 7.4. The depth as predicted by equation (7.3) will usually not be exceeded. The erosion is roughly proportional to the reflection coefficient, so a vertical wall gives maximum values.

The standing wave pattern for irregular waves is less distinct than for regular waves. This is also found in the scouring pattern, which decreases strongly with the distance from the wall, see Figure 7.5. Using H_s in equation (7.3) (based on regular waves), overestimates somewhat the scour depth, but as a first guess for all cases, $h_{smax} = H_s$ can be used.

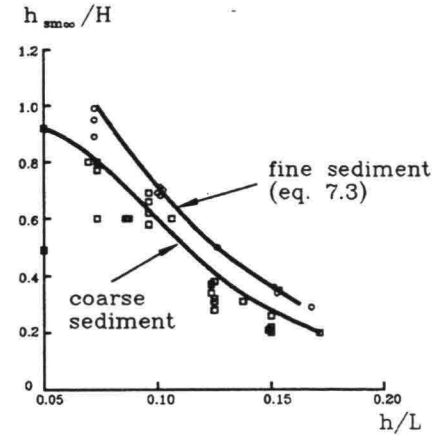


Figure 7.3 Relative scour depth for fine and coarse sediments

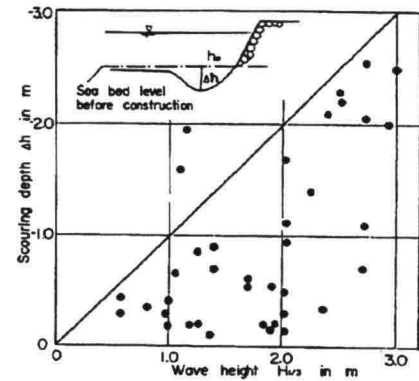


Figure 7.4 Scouring at inclining slope

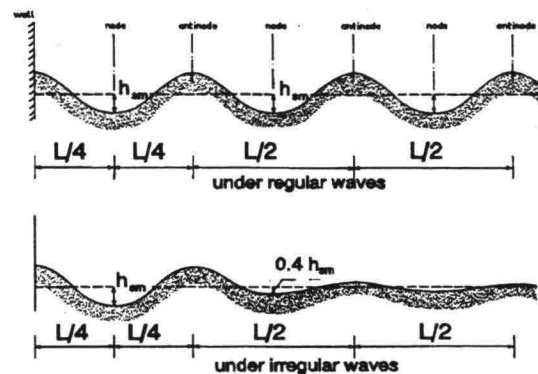


Figure 7.5 Profiles for regular and irregular waves (fine sediment)

Loads induced by ships were divided into primary waves, secondary waves and propeller jets, each with a different character. Their effect on unprotected soil is equally different; they will be treated here separately. It must be stated that the information presented here is not more than an idea of the effect when nothing is done to protect the soil against ship's waves.

The return current in the primary waves, can erode an originally trapezoidal bank-profile when it exceeds the critical velocity. In that case the profile will get a cosine-shape (a.o. based on experiences in the Suez-canal, see DellaLuna/Agostini,1981). Ven te Chow,1959 used the same approach for irrigation canals and got the same shape, assuming an equal distribution of the shear stress along the sloping bank. This results in:

$$z = z_0 \cos\left(\frac{\tan \phi}{z_0} y\right) \quad (\text{in radians}) \quad (7.4)$$

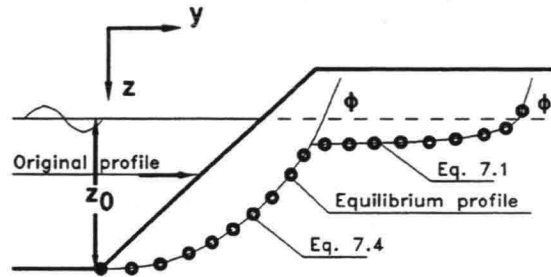


Figure 7.6 Erosion profile in unprotected navigation canal

At the still waterlevel the slope would be the angle of repose.

Erosion due to secondary ship's waves is comparable to what has been said about erosion profiles due to wind waves. There is one difference however. In equilibrium beach- and dune profiles it is implicitly assumed that these are formed under storm conditions and that during more quiet circumstances, the shore can restore. With ship's waves there is not much restauration and the erosion can go on "infinitely". This has also to do with the situation of the foreshore; when there is enough deep water, it is difficult to transport sediment from the foreshore to the shallow water. In fact, in several lakes in the Netherlands this "perpetual" erosion has been observed. For a first idea, the approach of paragraph 7.1.1 can be used, see Figure 7.6.

For scour by propellers we cannot use the same formulae as for jet scour as presented in chapter 6, because there, the scouring occurred directly behind the orifice. Instead, we use the formulae as given in paragraph 4.4, describing the velocity field behind a propeller. By equating $u = u_c$, we find from equation 4.15:

$$u_c = \frac{2.8 u_0}{x/D_0} e^{-15.6 \left(\frac{r}{x}\right)^2} \quad (7.5)$$

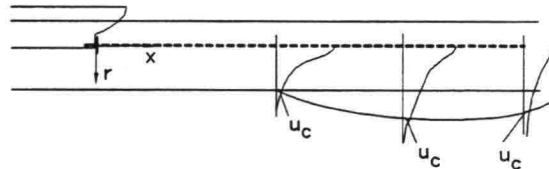


Figure 7.7 Scour by propeller

For various x behind the propeller, r can be calculated, giving the shape of the scour hole, see Figure 7.7. This type of scour will occur only near mooring places. The designer will have to consider nautical practice near the considered mooring place. Will tugs be used? Do the ships have bow-propellers? The latter can cause more damage than the propellers of the main engine.

7.3.1

PIPING

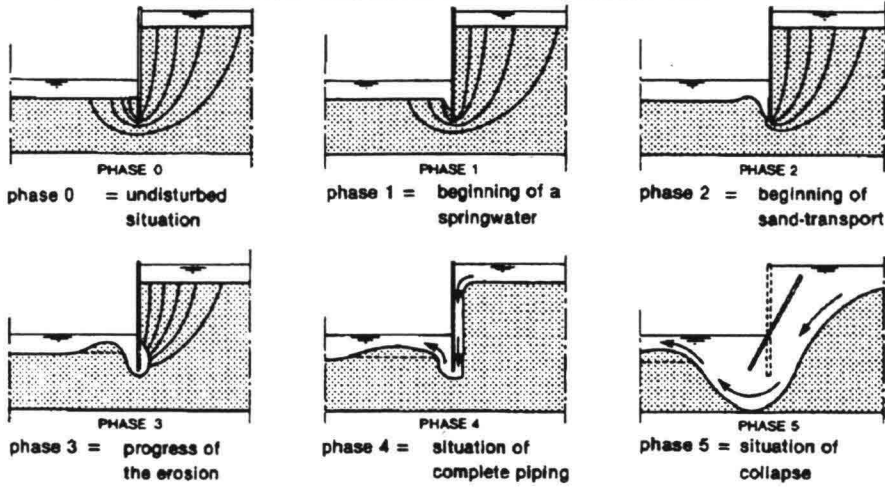


Figure 7.8 Piping under sheet pile

When the flow-pressure in a porous flow becomes higher than the weight of the grains, these grains will float and, when a channel can develop, will be transported, see Figure 7.8. Once this process has started it will lead to progressive failure when the load remains because the seepage length becomes shorter all the time. Theoretically the piping starts at the downstream end when the upward flow force is equal to the weight of the soil:

$$\rho_w g i \approx (1-n)(\rho_s - \rho_w)g \tag{7.6}$$

which, with $\rho_s \approx 2650$ and $n \approx 40\%$ leads to $i_c \approx 1$. In practice however, much lower values for the critical gradient are found, due to irregularities in the porous medium which lead to a concentration of the flow. The classical approach to these phenomena is by (see e.g. RWS,1987) Bligh, Griffith and Lane dating back to the first decades of this century.

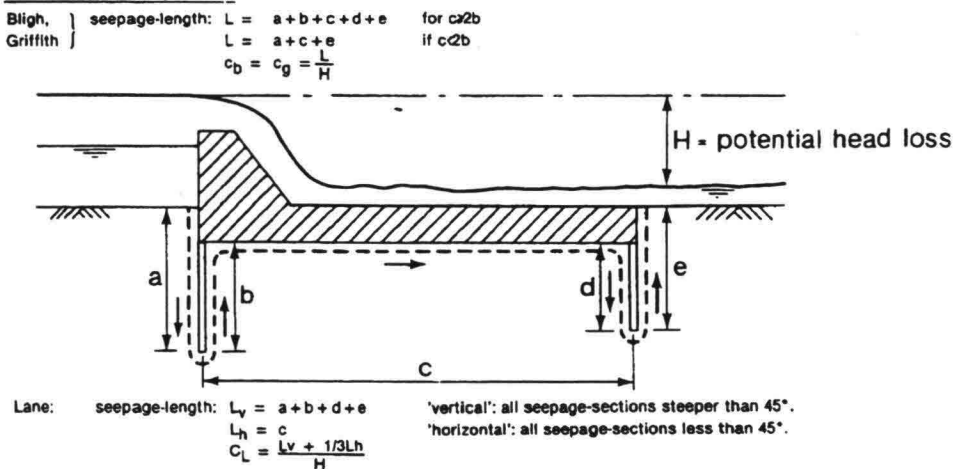


Figure 7.9 Definitions of seepage-length in the classical approach

The coefficients C_B resp. C_L are:

Material	Lane's creep ratio C_L	Bligh's creep ratio C_B
Silt	8.5	18
Fine sand	7.0	15
Coarse sand	5.0	12
Gravel	3.5	9

When, in these formulae, $L/H < C$, piping begins.

In the framework of the raising of the dikes in the Netherlands, many research has been done on piping. The generally accepted analysis is by Sellmeyer. He designed a mathematical model, describing the phenomenon of piping. Not only the threshold of piping as given in equation (7.6) was taken into account, but also the transportation of grains through an already formed channel. His model consists of a numerical solution of the relevant differential equations. By curve-fitting the results of this model the following formula was obtained, see (Calle/Weijers,1992).

$$H_c = \alpha c \Delta \tan \theta (0.68 - 0.10 \ln c) L$$

$$\text{with: } \alpha = \left(\frac{D}{L} \right) \left[\frac{0.28}{\left(\frac{D}{L} \right)^{2.8} - 1} \right] \quad (7.7)$$

$$\text{and: } c = \eta d_{70} \left[\frac{1}{\kappa L} \right]^{1/3}$$

The parameters θ and η are the angle of repose and a resistance-coefficient for the material to be washed away respectively, for which values of 41° and 0.25 are recommended (for all kinds of sand where piping can play a role). The other parameters have to be measured.

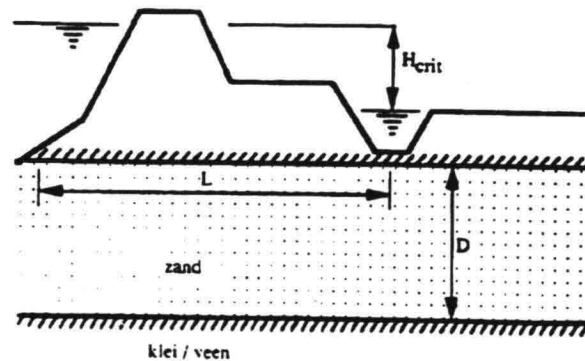


Figure 7.10 Definition piping new method

In equation (7.7) the quotient D/L plays an important role, see Figure 7.10. When the thickness of the permeable layer D becomes small, the necessary L can be reduced. Based on equation (7.7), new rules for the safety against piping in dike stability in the Netherlands have been established. For situations where D is relatively small (say less than 10m), a reduction of about 20-30% of L is possible. For a dike to be raised, with many houses in the vicinity, this can mean the difference between demolition of the houses or not.

Although gravity is usually not seen as a load, slopes become unstable and erode when they have become too steep by other influences like waves or scouring. The slope is then no longer able to withstand the gravitational forces and slides. Soil moves side- and downwards and the result is a flatter slope. In chapter 11 we will discuss stability of slopes in detail; here the focus is on the process after stability is lost. When a part of a construction fails, it can threaten another part, so this possible type of erosion determines the extensiveness of a protection. For this reason it is important to have some idea of slopes after failure, especially when scouring occurs at the end or foot of a protection.

7.4.1

SLIDES

Sliding occurs after a slope loses its stability, see Figure 7.11. The grains roll over each other till the friction is again sufficient to stop the sliding. Due to the inertia of the moving soil mass, the final slope will be gentler than the angle of repose ϕ , as an average $\cot\alpha' \approx 6$.

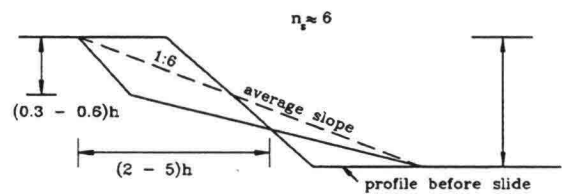


Figure 7.11 Average slope after slide

When the external forces remain active after the slide, the process will go on like in the case of dune erosion. In the case of sliding in a scour hole at the end of a bottom protection, the process can go on when the protection itself is damaged, leading eventually to the failure of the structure for which the protection was meant, see Figure 7.12

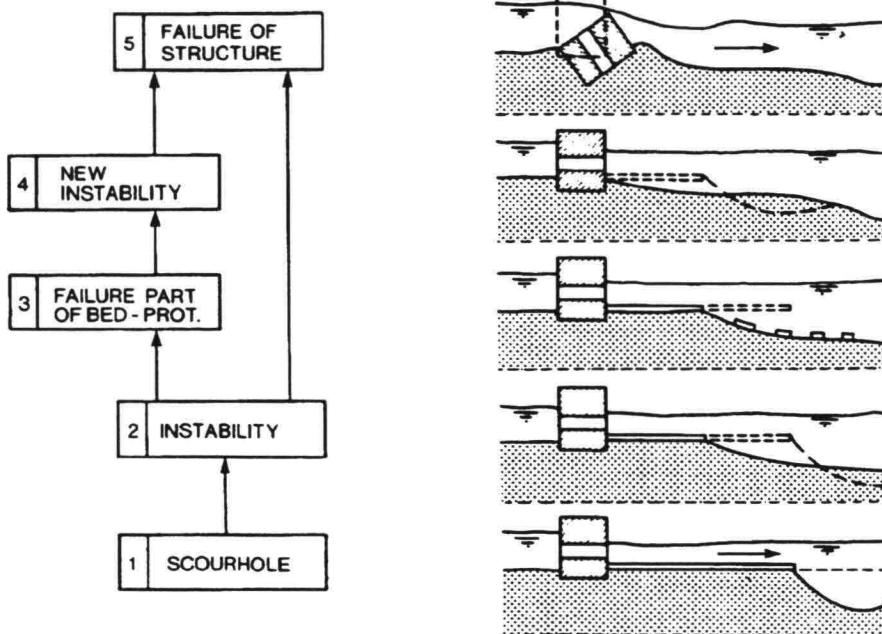


Figure 7.12 Progressive failure of bottom protection

When the soil consists of loosely packed sand, the situation is worse. Figure 7.13 shows the difference between loosely and densely packed. When a shear stress is exerted on loose sand, the grains tend to a denser packing, giving an excess pressure on the pore water (with dense sand the reverse happens; there is a density in between, the critical density, for which the effect of a shear stress is neutral). This excess pore pressure decreases the contact forces between the grains (the grain stress) and hence, to a complete shear strength reduction. The soil becomes, temporarily, a thick fluid. This phenomenon is called liquefaction. (Note: in porous flow we had fluidization which turns sand into a fluid by a porous flow, while liquefaction is induced by pore pressures. The result in both cases is a fluid: quicksand.)

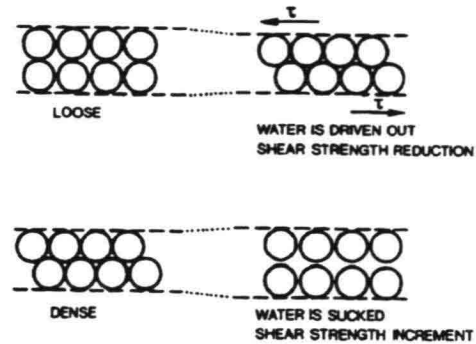


Figure 7.13 Effect of shear on loose and dense sand

The excess pore pressure can propagate as an elastic shock wave through the sand, turning a large area into quicksand. The result is a much flatter slope after failure than with a normal slide. Slopes of 1:25 have been reported; an average value of 1:15 is usually recommended, see Figure 7.14.

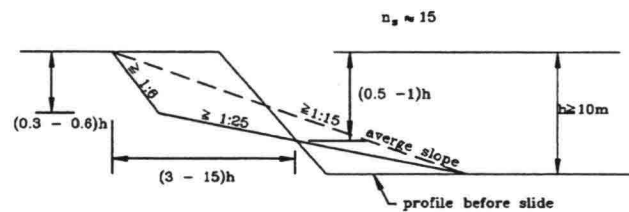


Figure 7.14 Flow slide

Note:

A similar phenomenon occurs when an embankment or any sand mass is constructed with a dredger and hydraulic transport through pipes. The sand-water mixture coming out of the pipe acts as a thick fluid until the grains can settle. This also results in slopes of about 1:20 or even gentler. When a steeper slope is wanted, measures have to be taken, like supporting dikes during construction, see Figure 7.15

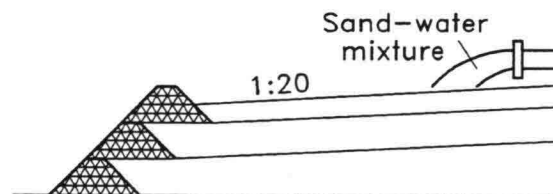


Figure 7.15 Construction method with sand-fill

When the expected degree of erosion is too high, the strength of the interface water-soil can be increased. Another way is to reduce the loads. This can be advantageous in some situations e.g. when the original character of a river-bank has to be preserved or as a temporary measure during construction. The various possibilities to reduce loads will be discussed in this chapter.

It is assumed that the total discharge of a river or canal is given; only measures to reduce the margins of the flow along banks will be discussed.

Groynes keep the main flow at a distance from the banks. In rivers, this is usually not just done to reduce the velocity, but as part of a complete river training scheme, to get a stable channel with sufficient depth for navigation. Here the focus is on flow reduction. At the tip of a groyne, the flow separates and an eddy is formed (see Figure 8.1). To keep the flow from the bank, the distance between two groynes should be less than 5 times the length. A more strict demand is the eddie pattern. For a proper guidance of the main flow, there should be one eddy between two groynes with a length about twice the width of the eddy. This leads to a distance between groynes of about twice the groyne length.

The velocity in the eddy is about 1/3 of the velocity in the main current, so the reduction is about 2/3. See for more information Jansen, 1979. Groynes however, are very costly and cause their own problems, e.g. scouring holes at the tip. The cost-benefit relation should be considered in all cases.

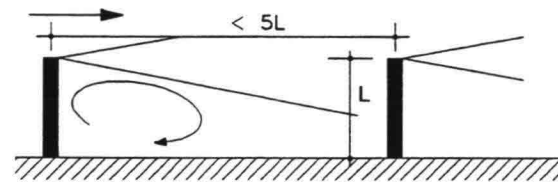


Figure 8.1 Flow behind groyne

Instead of groynes, the resistance to flow near the bank can be enlarged in a diffuse way by increasing the roughness. This can be done by making the bottom more rough or by placing resistance elements in the flow. The latter is the case when vegetation, e.g. reed or trees, is planted along the bank. It is possible to express the resistance of a roughened bed in a Chezy-coefficient.

A first approach of the C-value can be obtained by considering trees or reed stalks as piles, according to Kosorin, see Ruff/Verhey, 1991:

$$C = \sqrt{\frac{4g}{\pi m h D}} \quad (8.1)$$

in which m is the number of "piles" per m^2 and D the diameter. C-values less than $10\sqrt{m/s}$ (see Bouter, 1992) have been measured.

A first approximation of the velocity reduction is found by assuming that the waterlevel-slope is equal for main flow and bank, see Figure 8.2:

$$u = C\sqrt{hI} \rightarrow \frac{u_2}{u_1} = \frac{C_2\sqrt{h_2}}{C_1\sqrt{h_1}} \quad (8.2)$$

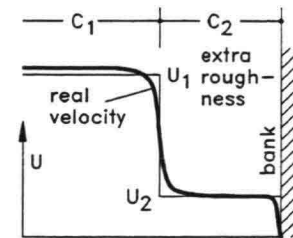


Figure 8.2 Flow reduction

There are many ways to reduce waves. The best wave reductor is probably a shallow foreshore where waves break and loose energy due to bottom friction. The maximum possible wave height on a shallow bottom was given in chapter 3: $H_s \approx 0.5h$. In this chapter, the starting point is the wave in front of the considered structure. The two principal mechanisms are **reflection** and **absorption**. Reflection is complete when an incoming wave is sent back and a standing waves occurs, see paragraph 3.4.1. In that case, the wave **transmission** is zero. Absorption can be achieved in many ways. The first main group occurs when the water in the waves has to flow through and around many construction-parts: stones, piles, bars, trunks and roots etc. The wave energy is dissipated via turbulence into heat. The same occurs at the edges of dams or plates which are meant as wave reductors. The second main group of absorption is the internal work in structures: floating mattresses, bending reed etc.

For the general case the relation between incoming, transmitted, reflected and absorbed energy is:

$$\frac{1}{8} \rho g H_I^2 = \frac{1}{8} \rho g H_T^2 + \frac{1}{8} \rho g H_R^2 + \text{absorption} \quad (8.3)$$

The effectiveness of a wave reducing device, is often expressed by means of the transmission-coefficient:

$$K_T = \sqrt{F_T / F_I} = H_T / H_I \approx (H_T)_{1/3} / (H_I)_{1/3} \quad (8.4)$$

in which F_T and F_I are the energy flux of the transmitted and the incoming wave respectively; for irregular waves, the expression with wave heights is a first approximation.

For the case when absorption can be neglected, we can see:

$$K_T^2 + K_R^2 = 1 \quad (8.5)$$

In the following a short review of wave reductors will be given.

8.2.1

DAMS

A very common type of wave reductor is a dam or reef with its crest around SWL. It is possible to compute transmission and reflection coefficients with the linear wave theory, neglecting absorption, see e.g. van der Linden, 1985. These results are not presented here, since they have little practical importance. A vertical wall from bottom to still water level gives a $K_T = 0$, because the linear wave theory assumes infinitely small wave amplitudes and overtopping is not taken into account. In practice for that case $K_T \approx 0.5$ is found, indicating that about 25% of the wave energy is transmitted.

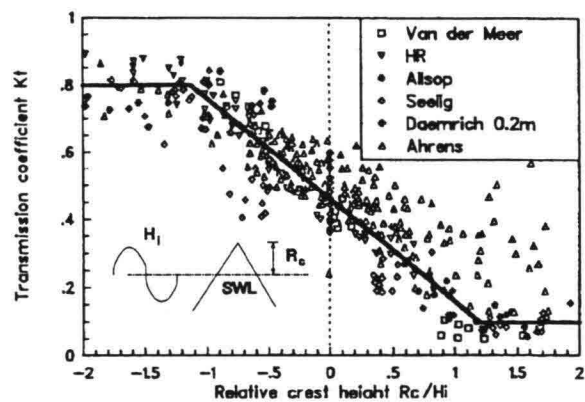
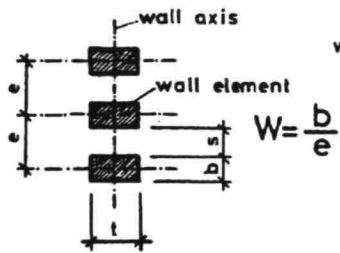


Figure 8.3 Wave transmission vs. crest height (vd Meer/dAngremond, 1992)

Figure 8.3 shows the results for a great number of measurements, relating the wave transmission to the relative crest height: R_c/H_{si} with regard to the still water level. When $R_c/H_{si} \approx 1$ there is still considerable transmission possible. These points in the figure represent small amplitude waves which transmit easily through the large elements on the top of a porous dam. For realistic waves in design conditions, $K_T \approx 0.1$ for R_c/H_i as indicated in the figure.

There is a lot of scatter in this figure; it is possible to improve the results by relating the transmission to the crest height, made dimensionless with the diameter of the elements: R_c/D_{50} . For more information, see vd Meer/dAngremond,1992. Figure 8.3 can serve as a first indication.

8.2.2 PILE SCREENS



A wall that consists of vertical piles can act as a wave reductor when there is little spacing between the piles. Now the linear wave theory can be used, assuming that the transmitted energy is equal to the relative spacing between the piles, see Figure 8.4. In that case it is found, with $E = 1/8\rho gH^2$:

$$H_T = \sqrt{(1-W)H_I^2} \quad - \quad K_T = \sqrt{(1-W)} \tag{8.6}$$

Figure 8.4 Notation for screen

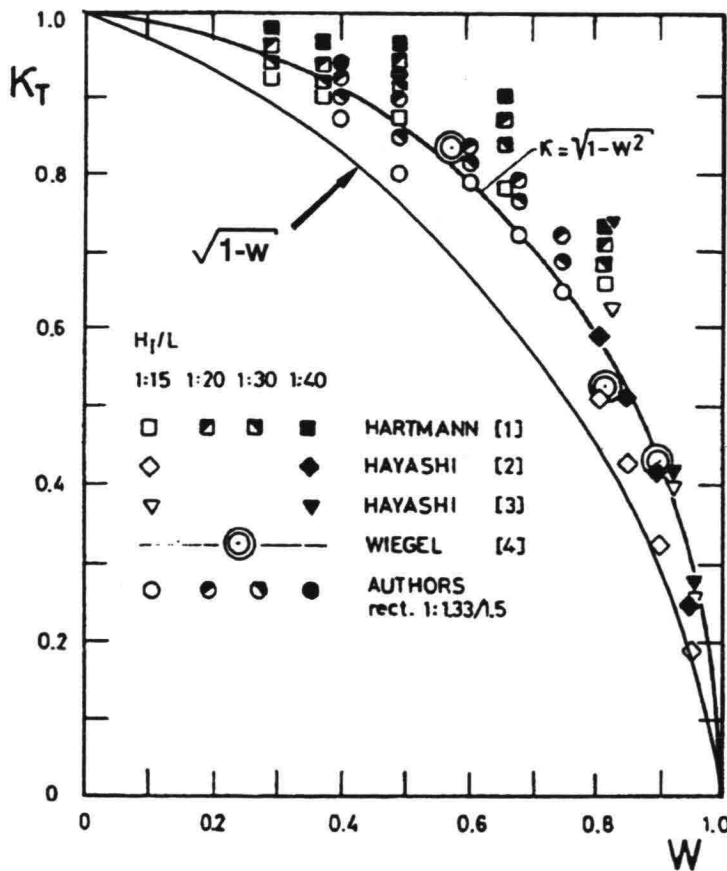


Figure 8.5 Wave transmission through pile screen (Grune/Kohlhase,1974)

Figure 8.5 shows experimental results (Grune/Kohlhase,1974). Equation (8.6) underestimates the transmission, probably because of diffraction of the reflected energy which is higher than the energy losses in the wakes around the piles (both being neglected in (8.6)). An equal simple and satisfying expression appeared to be:

$$K_T = \sqrt{1 - W^2} \tag{8.7}$$

8.2.3 FLOATING BREAKWATERS

There are many types of floating breakwaters: rigid, flexible, porous etc. They have in common that they are only effective when the length in the wave direction becomes of the same order of magnitude as the wave length. A practical problem is formed by the mooring forces on the anchors; they can become prohibitive, see vd Linden,1985. Floating breakwaters are probably only of practical importance for small scale applications, but in those situations one can wonder if wave reduction is necessary. Figure 8.6 gives a theoretical curve compared with measurements for a floating plate. λ is the length of the protection, L the wave length.

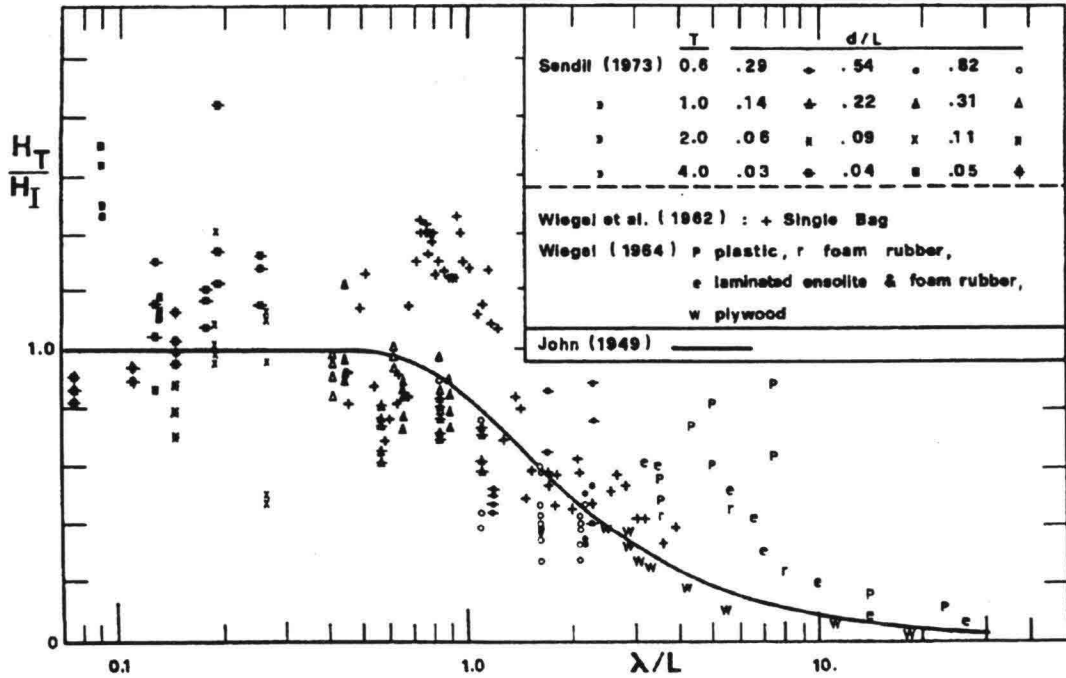


Figure 8.6 Transmission vs. relative wave length

Reed is a natural wave reductor, applied in many rivers and canals. There is little known about the effectivity of reed in wave damping; measurements in a natural situation deal with the problem of ill-defined boundary conditions. At the TUD, measurements were done in a wave flume, see Bouter, 1992. This investigation was a first start, so no general conclusions can be drawn.

It was found that most energy dissipation was due to the flow around the reed stalks; the bending of the stalks was relatively unimportant. On the contrary, extensive bending because of resonance with the wave period, made wave damping less effective. Stiff rods appear to be more effective than flexible stalks. An important parameter is the waterdepth, which is also related to the bending of the stalks, since the resistance of an elastic beam is proportional to the 4th power of the length. Bouter found damping of about 20% of the incoming waves with a reed bed of 1 m long in the wave direction. In tests done in a natural situation, the damping appeared about half of the value found by Bouter, see annex B. Further investigations will be necessary in order to find out the possibilities and shortcomings of reed as wave damper.

8.3

REDUCTION OF SHIP'S LOADS

In chapter 4 we have seen that the velocity of a ship is the dominating factor in loads induced by moving ships. So, when these loads become too high for an (un)protected bank, it seems logic to limit the speed of the passing ships. Another measure would be to order more distance from the banks. It is possible to do so, and in European waterways there exist even traffic signs for these purposes, see Figure 8.7.

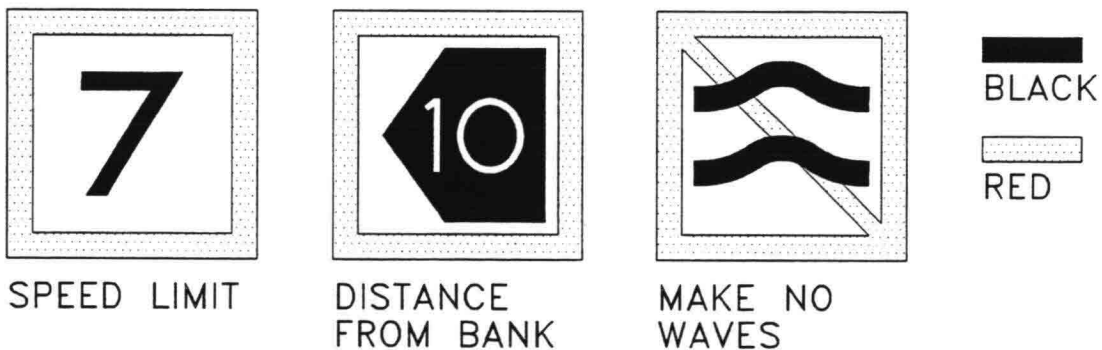


Figure 8.7 Traffic signs to reduce loads

But these are usually meant for situations where other ships are moored or where there is an obstruction in the waterway etc. Speed limits to reduce loads on the banks are very hard to control. It seems to be good engineering practice, to design the banks of a waterway such that all possible situations are taken into account (which does not mean that damage may never occur).

For temporary situations, like during construction works in the waterway, it is reasonable to ask for a minimum of hindrance. When a definite situation ask for limitations, it is better to do so by means of a maximum size or engine power, which is easier to control.

Porous flow can be reduced in two completely different ways, with opposite results. The choice depends on the problem that occurs when no reduction is applied. When the porous flow velocities are too high and piping forms a threat, the seepage length should be lengthened. This however, leads to higher pressures in the underground. When the pressures are too high, a drain can be made. In that case provisions will be necessary to prevent washing away of grains from the subsoil. Both ways will be illustrated here.

8.4.1

FLOW REDUCTION

From paragraph 7.3.1 we know that the seepage length should have a minimum value to prevent erosion from piping. When these values are not met, lengthening can be achieved by a wider body of soil or by sheet piles, both creating a larger seepage length. Another example can be the flow under a gate, like in this case the Eastern Scheldt storm surge barrier. With a head difference of more than 5 m and a width of the same order of magnitude, the flow through the sill becomes very high, see Figure 8.8:

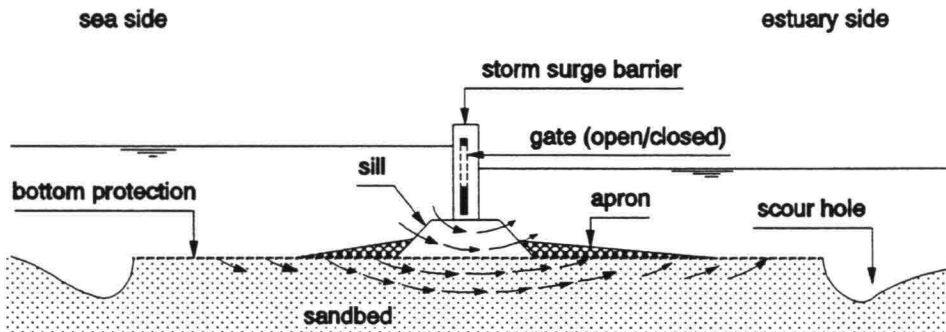


Figure 8.8 Flow under gate

In that case, the head difference has to be spread over a longer distance in order to reduce the gradient, see Figure 8.9:

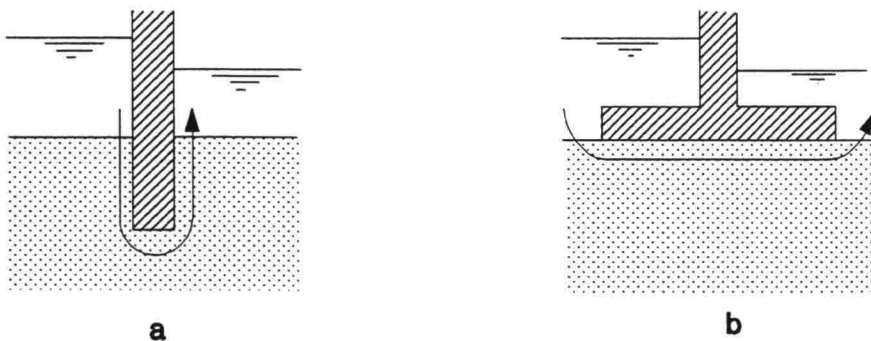


Figure 8.9 Two ways of enlarging the seepage length

When the pressure in the subsoil becomes high, this can lead to a heavy and expensive bottom protection when this is composed of a material like asphalt, see Figure 8.10:

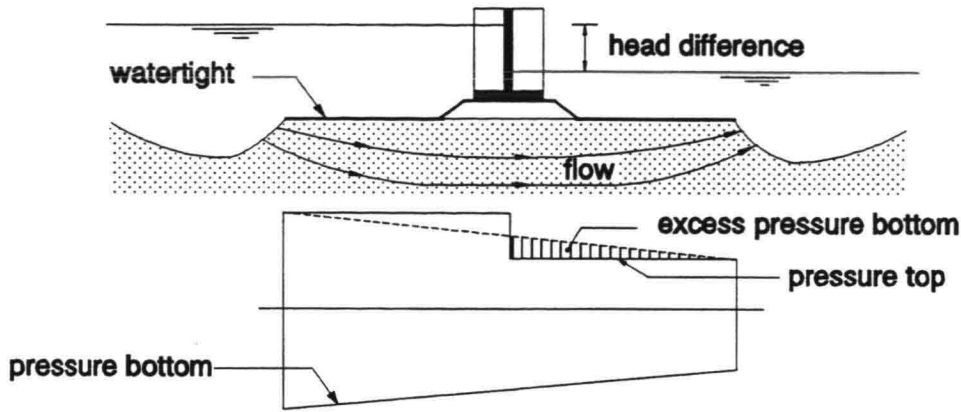


Figure 8.10 Pressures with watertight bottom protection

(Why choose asphalt when this problem can occur? The reason for that can be the demand for high flow resistance against the water that flows over the bottom protection). In that case a drain can be constructed, giving relief to the pressures. Figure 8.11 shows another design for the Easterscheldt storm surge barrier. Without the drain the pressures under the bottom protection would have been twice as high.

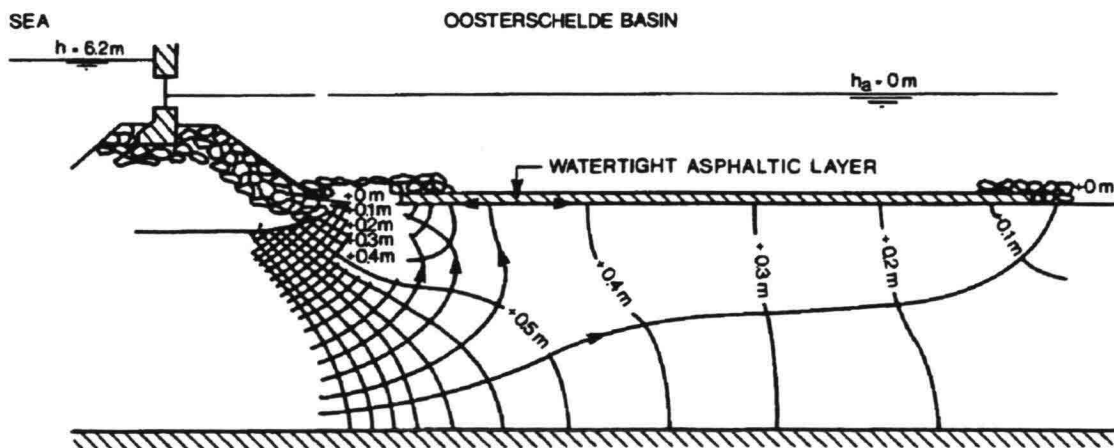


Figure 8.11 Location of drain in bottom protection

The drain itself should be designed in such a way that the outflowing water cannot wash out grains, see paragraph 11.1 for filter design. One should be sure that the filter is not blocked by dirt or by the growth of plants and/or shells.

9	<i>STABILITY part I - FLOW</i>
----------	---------------------------------------

9.1	<i>LOOSE MATERIAL</i>
------------	------------------------------

Rock, gravel and other stony material consisting of loose non-cohesive grains, form a very important building material for protections. It is almost omnipresent in the world and relatively easily to obtain. The specific mass of natural rock lies around 2650 kg/m³ with maximum values of about 3000 kg/m³. This is favourable for the stability and is difficult to match by artificial material like concrete. It comes in all sizes and weights, varying from millimeters to several meters (weighing more than 10 tons). So, as a building material for hydraulic engineering, it is almost indispensable. For this reason, relatively much attention is paid to the stability of stony protections. Unfortunately, despite many research activities and an avalanche of reports, the knowledge about the behaviour of rock exposed to currents and/or waves, is still very empirical. For the design of a stable top-layer which is meant to protect the underlying soil, it is necessary to know what forces make a stone move or not. This is the main subject of this chapter. Unless otherwise stated, *d* means *d*₅₀, which is the size of the cube with equivalent volume to the stone with median weight, see annex A.

9.1.1	<i>UNIFORM FLOW - HORIZONTAL BED</i>
--------------	---

This is the simplest possible situation. The flow is turbulent and the grains protrude the laminar boundary-layer if present. It is easy to imagine that there is a critical value for the flow velocity at which a grain is no longer in equilibrium and starts to move. It is not so easy to indicate exactly how the flow induces movement and how the grains resist it. Figure 9.1 shows the forces acting on a grain. Many investigators have dealt with this problem; some use the shear stress as principal acting force, others the drag force; some do take lift forces into account, others don't. A drag force by the flow on a stone is easy to imagine. The concept of a shear stress for a single stone is somewhat more troublesome; it seems more appropriate for a certain area of the bed. A lift force can be caused by the curvature of the flow around a grain or the turbulent vertical velocity fluctuations. The various forces on the grain can be expressed as follows:

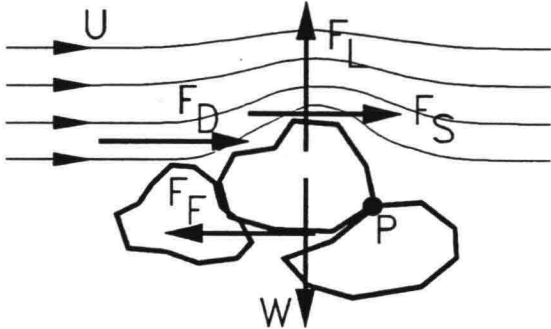


Figure 9.1 Flow-forces acting on a grain

<p><i>Drag force:</i> $F_D = \frac{1}{2} C_D \rho_w u^2 A_D$</p> <p><i>Shear force:</i> $F_S = \frac{1}{2} C_F \rho_w u^2 A_S$</p> <p><i>Lift force:</i> $F_L = \frac{1}{2} C_L \rho_w u^2 A_L$</p>	$\left. \vphantom{\begin{matrix} F_D \\ F_S \\ F_L \end{matrix}} \right\}$	$F \propto \rho_w u^2 d^2$	(9.1)
--	--	----------------------------	--------------

So, all forces are proportional to the square of the velocity and since the grain-areas are proportional to the square of some representative length dimension d , the resultant force can be expressed in one term where a constant of proportionality remains unknown.

The same can be done for the equilibrium. Here again, several resisting forces and mechanisms can be present: a lift force is balanced directly by the (submerged!) weight; shear and drag, either by the moment around P or by the friction force (which is like the shear a somewhat peculiar notion for a single grain). It does not matter however, whether the horizontal, vertical or moment equilibrium is considered, only one proportionality follows:

$$\left. \begin{array}{l} \Sigma H = 0: \quad F_{D,S} = fW \\ \Sigma V = 0: \quad F_L = W \\ \Sigma M = 0: \quad F_{D,S} d_1 = W d_2 \end{array} \right\} \rho_w u_c^2 d^2 \propto (\rho_s - \rho_w) g d^3 \quad (9.2)$$

This leads to a simple relation between the critical velocity and the effective weight of a grain:

$$u_c^2 \propto \left(\frac{\rho_s - \rho_w}{\rho_w} \right) g d = \Delta g d \quad (9.3)$$

All formulae on grain stability come down to this proportionality. The constant in this relation has to be found experimentally and that is where the problem starts. There are numerous formulae based on (9.3), but there are two names you can not avoid when dealing with stability of stones in flowing water: Izbash and Shields.

IZBASH

Izbash, 1970 (a translation from a Russian book dated 1930, also widely used in the USA) expressed relation (9.3) in the following form (with equivalent forms, used in other sources):

$$u_c = 1.2 \sqrt{2 \Delta g d} \quad \text{or} \quad \frac{u_c}{\sqrt{\Delta g d}} = 1.7 \quad \text{or} \quad \Delta d = 0.7 \frac{u_c^2}{2g} \quad (9.4)$$

There is no influence of depth in this formula; in fact Izbash did not define the place of the velocity. It is presented as a tool for first approximation in cases when a velocity is known but no shear stress can be determined. In other cases the following approach is recommended.

SHIELDS

Probably the most well known formula for uniform flow is the one by Shields from 1936. Shields plotted a dimensionless shear-stress against a grain related Reynolds-number:

$$\Psi = \frac{\tau_c}{(\rho_s - \rho_w) g d} = \frac{u_*^2}{\Delta g d} = f \left(\frac{u_* d}{\nu} \right) \quad (9.5)$$

Note that the grain diameter and the shear stress appear on both sides of the formula. For high Re-numbers however, Ψ becomes constant with a value of about 0.06, see Figure 9.2. In practice this

is already the case for stones with a diameter of about one centimeter.

Relations (9.5) and (9.4) look different, but are very similar: u_* (the so-called shear velocity) = $u_0\sqrt{g/C}$, where u_0 is the velocity averaged over the vertical or the cross-section, see section 2.3. This leads to another form of (9.5) in the shape of (9.4) (with $u_c = u_{0c}$):

$$\frac{u_c}{\sqrt{g\Delta d}} = \frac{C\sqrt{\psi}}{\sqrt{g}} \quad (9.6)$$

or: $\Delta d = \frac{u_c^2}{\psi C^2}$

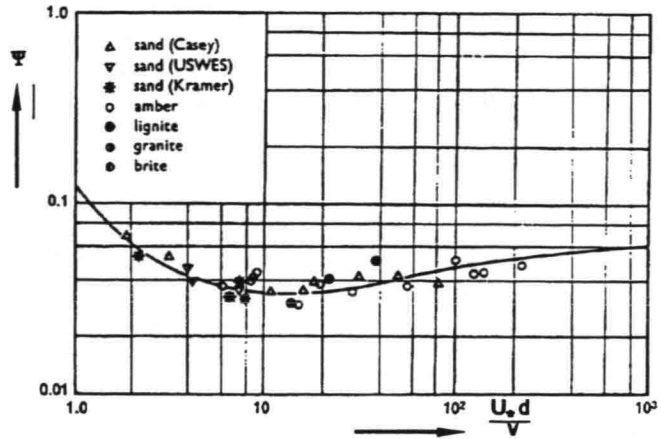


Figure 9.2 Shields diagram

DISCUSSION ON CRITICAL VALUES

Shields found his values by extrapolating a measured transport of material to zero. The value 0.06 for ψ does not mean that no single grain is moved; a value at least twice as low should be taken. In fact there does not exist such a thing as a critical velocity ! The idea of a single critical velocity cannot be true because of the following:

- The threshold of movement is a subjective matter when judged in an experiment; is it the first loosely lying stone that moves 1 cm and then stops again or should grains be moving all over the bed.
- The protrusion, even on a flat bed, is different for every stone. The influence on the threshold of movement is tremendous, see Figure 9.3. $P/d = 0$ means that the top of the grain is equal to the bed level and $P/d = 1$ means that the bottom of the grain is equal to the bed level. In that case the critical shear is 0, which indeed can be seen when a grain is lying on a smooth, flat bottom. (For this reason, a protection should consist of at least two layers of grains).

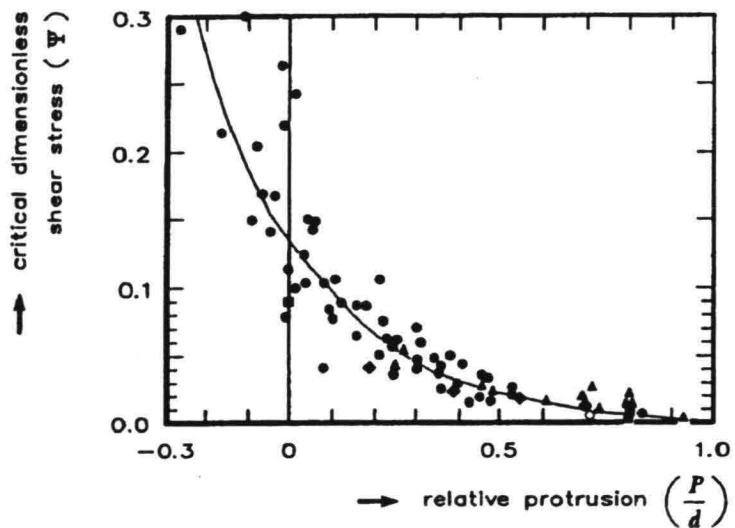


Figure 9.3 Critical shear and protrusion

When $P/d < 0$ it is very hard to make a stone move.

- When the material is graded, the small particles can be taken away with the current, while the large ones remain, armouring the rest of the bed.

- The flow itself is turbulent, which means that peak pressures and velocities can be much higher than the average value. In theory there is no limit.

Figure 9.4 shows the situation in which the average shear in the flow is lower than the critical shear. Due to the deviations from the mean value of the load and the strength, movement of stones can still occur. It can be seen that indeed, there is no critical value below which movement is impossible. This is important to bear in mind when designing a safe bottom protection; maintenance will be necessary after some time. The following might be a useful tool for estimating the transport over a period of time.

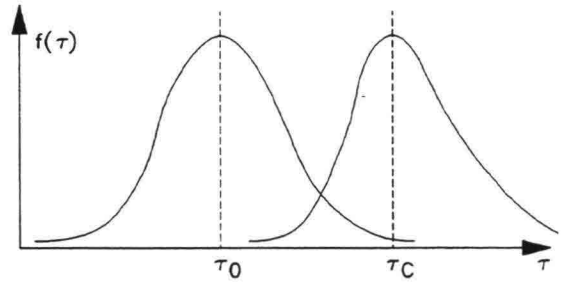


Figure 9.4 Load and strength distribution

Paintal, 1971 performed similar tests as Shields, but he did not extrapolate his transport measurements to 0. Instead, he gave a transport relation, see also Figure 9.5:

$$q_s^* = 6.56 \cdot 10^{18} [\tau_0^*]^{16}$$

with : $q_s^* = \frac{q_s}{\rho_s g d \sqrt{\Delta g d}}$ (9.7)

and : $\tau_0^* = \frac{\tau_0}{(\rho_s - \rho_w) g d}$

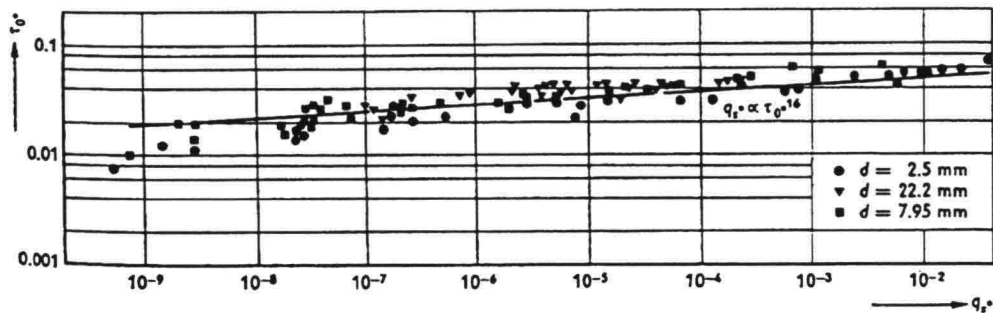


Figure 9.5 Transport around "critical" shear stress (Paintal, 1971)

Indeed, this relation gives a transport for every shear stress differing from zero. But it decreases with the 16th power of the shear stress, which means with the 32nd power of the velocity. Most sedimenttransport-formulae have a power relation of 3 to 5 with the velocity. The Paintal relation is valid only in the region of the threshold of motion (whatever that may be after this discussion). When τ_0^* becomes greater than 0.05-0.06 Paintal found q_s proportional with the 5th power of the velocity, so relation (9.7) should not be used beyond $\tau_0^* = 0.06$.

Now back to Shields. For a first design it is still useful to work with a critical velocity or shear stress. It was mentioned that Shields found $\psi = 0.06$ for high **Re**-numbers. Since ψ is the same parameter as Paintal's τ_0^* , the link is easily made. 0.06 is the upper limit of Paintal's formula and when "no" movement is allowed, a lower value should be taken. When using the Shields formula for no movement, $\psi = 0.03$ is often recommended. From Figure 9.5 it can be seen that even then there is still some transport. Figure 9.5 should be the basis when choosing a value for ψ in the case that a design is made.

DISCUSSION ON WATERDEPTH

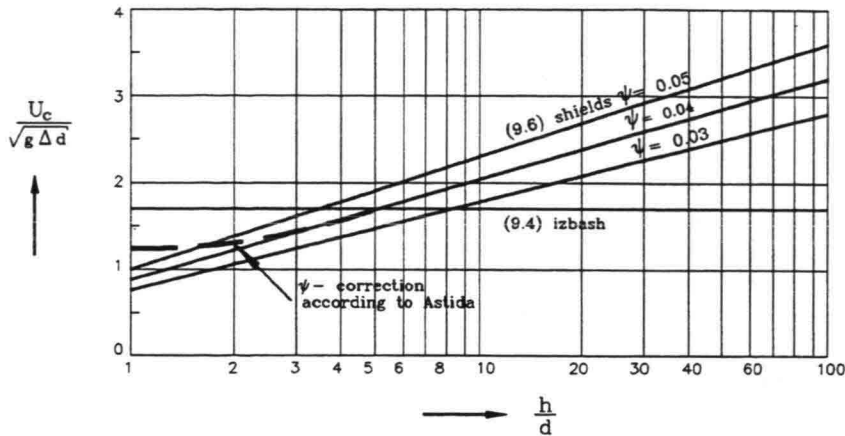


Figure 9.6 Critical velocity vs waterdepth

Equation (9.6) shows a dependence of the critical velocity on the waterdepth since C increases, given a bottom material, with the waterdepth: $C = 18 \log 12h/k$, with the roughness $k \approx 2d$ often written as $C = 18 \log 6h/d$. Equation (9.6) then becomes: $u_c \sqrt{(\Delta g d)} = 5.75 \sqrt{\psi} \log 6h/d$. In Figure 9.6 this relation is drawn for several values of ψ and compared with Izbash, equation (9.4). Shields gives a greater permissible velocity at greater depths. This has been found also in many experiments, making Shields "superior" to Izbash. This can be stated in another way by saying that Shields uses a critical shear stress which is a constant for a given material, while Izbash's velocity is not well defined. Some remarks, however, have to be made.

The favourable influence of the waterdepth on the critical velocity cannot go on infinitely, since the logarithmic velocity profile in natural streams with large depths is only found in the lower half of the depth. $h/d = 100$ should be seen as an upper limit in Figure 9.6.

At small waterdepths, somewhere around $h/d = 5$, Izbash gives higher permissible velocities than Shields. For $h/d < 5$, Ashida, 1973 found a considerable increase in ψ , see Figure 9.7. This can possibly be contributed to the velocity profile where there is another relation between the drag on the grains and the shear stress on the bed as in deep water. As we have seen earlier in this paragraph, drag and shear are not separated in the empirical relations. Another possible explanation are the turbulent eddies: at waterdepths in the order of magnitude of the grain diameter, these eddies have maximum dimensions of the same order of magnitude. At larger waterdepths, the eddy dimensions can and will grow, leading to a heavier attack on the bottom. Even then, Izbash seems to overestimate the permissible velocity for small waterdepths, see Figure 9.6.

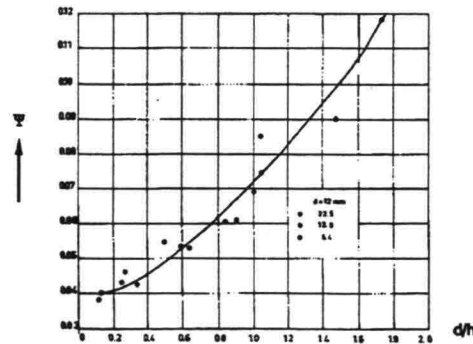


Figure 9.7 Increase of ψ at small waterdepths

The relations in paragraph 9.1.1 are valid for stones on a horizontal bed. We already discussed a strength influencing factor for that case, i.e. the protrusion of a stone into the flow. Another factor that influences the stability is the slope of the bed. When the slope is equal to the angle of repose, a stone is already on the threshold of motion and any load will induce movement. Figure 9.8 gives an idea of the value of ϕ for various materials.

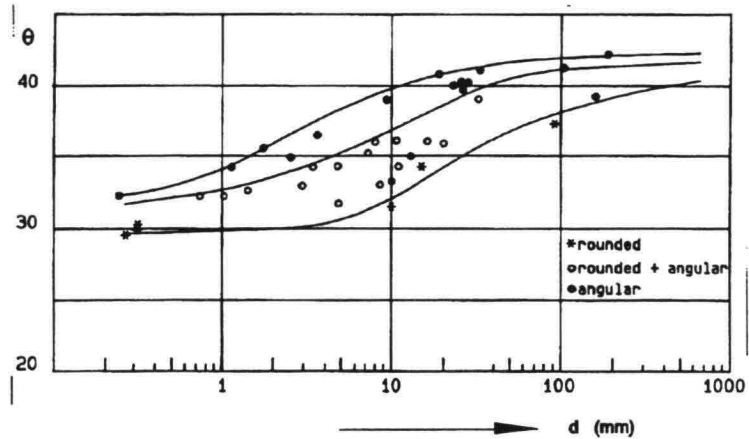


Figure 9.8 Angle of repose for non-cohesive materials (Pilarczyk, 1990)

To determine the influence of a slope on the stability, it is assumed that for a flat bed the friction factor is given by $f = \tan\phi = F(0)/G$, see Figure 9.9, meaning that the friction factor of a stone on a horizontal bed is equal to the tangent of the angle of repose. That will depend strongly on the protrusion of the grains; when $P/d = 0$, see paragraph 9.1.1, the resistance will be greater than $\tan\phi$. This is not necessarily a problem; the slope correction factor is only used relatively.

SLOPE IN FLOW DIRECTION

When the flow is in the downstream direction of a slope, the component of the weight of a grain along the slope works with the flow, while the effective resistance perpendicular to the slope becomes less: $F(\alpha) + G\sin\alpha = G\cos\alpha \tan\phi$ (When the flow is reverse, the resulting force is $F(\alpha) - G\sin\alpha$ and the grain gets more stable). The relation between $F(\alpha)$ and $F(0)$ gives the reduction to be applied on the shear stress:

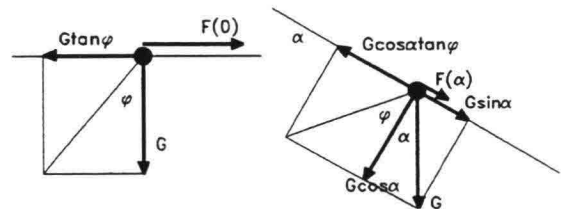


Figure 9.9 Slope in flow direction

$$K(\alpha) = \frac{F(\alpha)}{F(0)} = \frac{G\cos\alpha \tan\phi - G\sin\alpha}{G\tan\phi} = \frac{\sin(\phi - \alpha)}{\sin\phi} \tag{9.8}$$

Note 1: When $\alpha = \phi$, $K(\alpha) = 0$, indicating that the critical shear stress in that case is 0.

Note 2: $K(\alpha)$ is a reduction factor for forces; when using velocities $\sqrt{K(\alpha)}$ has to be used.

SLOPE PERPENDICULAR TO FLOW

For a side slope with angle β , the same procedure can be followed, see Figure 9.10.

$F(R)^2 = F(\beta)^2 + G^2 \sin^2 \beta = G^2 \cos^2 \beta \tan^2 \phi$, leading to:

$$K(\beta) = \frac{F(\beta)}{F(0)} = \sqrt{\frac{\cos^2 \beta \tan^2 \phi - \sin^2 \beta}{\tan^2 \phi}}$$

$$= \cos \beta \sqrt{1 - \frac{\tan^2 \beta}{\tan^2 \phi}} = \sqrt{1 - \frac{\sin^2 \beta}{\sin^2 \phi}} \quad (9.9)$$

Again, $K(\beta)$ is a factor for forces; for velocities $\sqrt{K(\beta)}$ has to be applied.

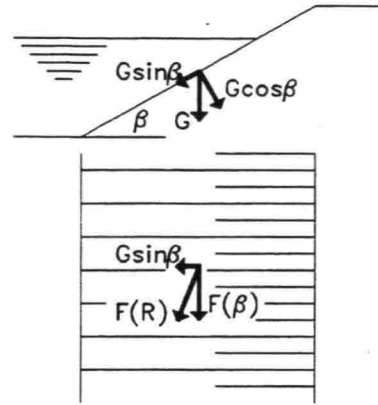


Figure 9.10 Stability on side slope

COMPARISON OF SLOPES

In Figure 9.11, both the reduction factors $K(\alpha)$, equation (9.8), for a slope in flow direction and $K(\beta)$, equation (9.9), for a slope perpendicular to the flow, are drawn for the case that $\phi = 35^\circ$. It is clear that a slope in the flow direction is much more unfavourable.

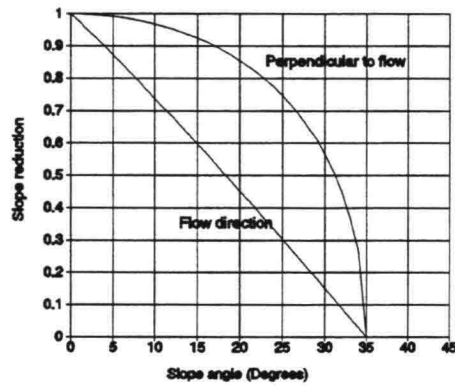


Figure 9.11 Comparison of slope reduction

SEEPAGE

When water flows out of a bed of grains, this reduces the stability (the question can raise, whether this is an extra load or a reduction of strength; the choice is arbitrary). The effective weight becomes: $G(1-i)$, (when $i \approx 1$, for $\Delta = 1.65$, the grains float and the bed is fluidized).

Note 1: A difficult point is to determine the porous flow-gradient over the last grain. It has to be approximated with the gradient over the outer layer.

Note 2: In case of a slope, $G \cos \alpha$ or $G \cos \beta$ has to be used instead of G and the gradient perpendicular to the slope. See paragraph 11.1.1

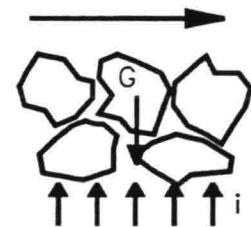


Figure 9.12 Seepage and stability

Relations like the one given by Shields is valid for stationary, uniform flow. This is the most "gentle" load by flowing water. When the flow is stationary but not uniform, the load will be locally higher. This could be expressed in a factor for the velocity in stability relations:

$$K = \frac{u_c \text{ uniform flow}}{u_c \text{ with load increase}} \tag{9.10}$$

Note: The use of the critical velocity in the denominator comes from experiments where with some obstacle a lower velocity is measured at which stones start to move. This does not mean that the critical velocity of the bed is lower: the strength of the bed does not change, but the load increases. K is a magnifying factor in stability relations like Shields, so a higher velocity leads to a larger stone.

In accelerating flow we have seen an increase in shear stress and a decrease of (relative) turbulence and in decelerating flow the other way around (chapter 2). For these phenomena in vertical and horizontal constrictions, only results of empirical research are available. These results will be discussed here, with the knowledge of fluid motion from chapter 2 as background.

VERTICAL CONSTRICTION

Figure 9.13 shows the various regions when a flow passes a vertical constriction. In the uniform flow zone, relations like the one by Shields are valid. For stones on top of a sill, one might expect a more unfavourable relation, because of the increased shear stress due to the acceleration. This, however, does not appear from experiments.

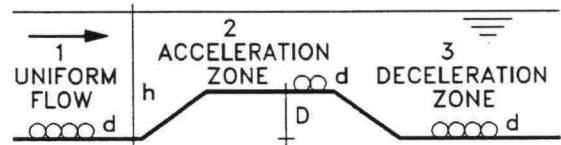


Figure 9.13 Flow regions around vertical constriction

Figure 9.14 gives experimental results, compared with the Shields formula for several values of ψ , using the velocity on top of the sill. It is essentially the same figure as Figure 9.6, the squares now representing the results of flume experiments in the framework of the Deltaworks, see Akkerman, 1985. All measured critical velocities lie above the line for $\psi = 0.04$ indicating that the relation between critical velocity and stone diameter is certainly not more unfavourable than for uniform flow.

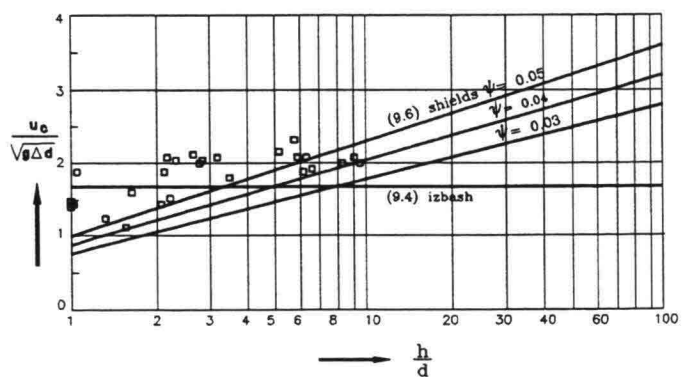


Figure 9.14 Stability on sill

An explanation can be found in the fact that the "maximum" velocity is lower than in uniform flow since $u+3\sigma = (1+3r)u$ and r is lower in the acceleration zone. (Note: the velocity is defined in region 2 of Figure 9.13 on top of the sill. Compared with the velocity in region 1, the maximum always increases) Another explanation could be that in an accelerated flow over a (very) rough boundary, the same phenomenon occurs as in very small waterdepths, see section 9.1.1, Discussion on waterdepths. The velocity gradient is concentrated in the upperlayer of the protection and the turbulent eddies have the same dimensions as the stone diameter. See also Figure 9.7

Behind the sill, the situation is completely different. The overall energy loss results in high turbulence intensities. Related to the average velocity in the downstream part (zone 3 in Figure 9.13) it can be reasoned from the energy loss that the influence of a sill on the velocity load downstream can be expressed by $K = h/(h-D)$, see Figure 9.15 and box below. The experimental results in this figure again come from research for the Deltaworks, see Akkermans,1985. Behind relatively high sills amplification factors in the Shields formula of 3 are possible! This result is only valid for the heaviest attacked point behind the sill (near the reattachment point. Further downstream, the situation tends again to uniform flow.

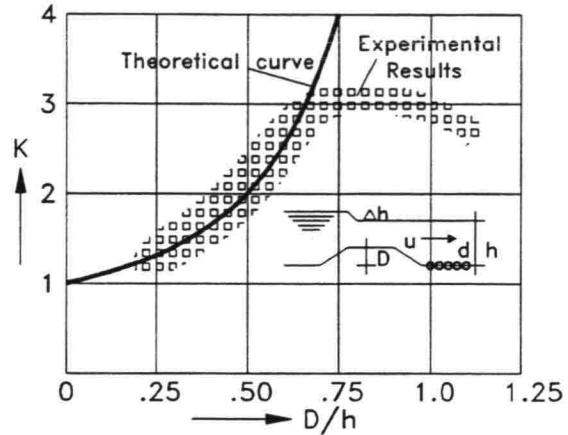


Figure 9.15 Load increase behind a sill

The energy loss over a sill is assumed to be used for attacking the bottom and is presented in a force F' per m width. F' is proportional to u^2 ; we do not bother about lift, drag or shear, in the same way as discussed in paragraph 9.1.1. We only compare the situation with and without sill. The work done by F' per unit time is $F' \cdot u$ (u and h defined downstream of the sill). Equating this with the energy loss, we get:

$$F' \cdot u = \rho g q \Delta h = \rho g u h \Delta h \quad (9.11)$$

u and Δh are related by $uh \approx \sqrt{(2g\Delta h) \cdot (h-D)}$ (continuity), leading to:

$$F' = \frac{\rho}{2} \frac{u^2 h^3}{(h-D)^2} \quad (9.12)$$

Comparing the situation with and without sill ($D = 0$), we get:

$$\frac{F_{SILL}}{F_0} = \frac{h^2}{(h-D)^2} \rightarrow K = \frac{h}{h-D} \quad (9.13)$$

The load increase goes on till the situation of critical flow over the sill is reached, which is the case when: $h - D = 2/3\Delta h$ from which we find (again with $uh = \sqrt{(2g\Delta h) \cdot (h-D)}$):

$$\frac{(h-D)^3}{h^2} = \frac{u^2}{3g} \rightarrow \left(1 - \frac{D}{h}\right)^3 = \frac{u^2}{3gh} \quad (9.14)$$

With h normally in the range 5-10 m and u 1-2 m/s we find $D/h \approx 0.7 - 0.8$ which is in agreement with Figure 9.15. When D/h increases further, the total energy loss also increases, but the "extra" loss, compared to subcritical flow, is absorbed at the downstream slope of the sill. Recent investigations indicate that this already can happen at lower values of D/h than 0.70

HORIZONTAL CONSTRICTION

Horizontal constrictions occur in many situations. The influence of the relevant flow phenomena (see section 2.6) on stone stability will again be expressed by means of the amplification factor K . In traditional hydraulic engineering it is often said that the critical velocity in a vortex street with vertical axis, is half the value of that in uniform flow. As already said above (vertical constriction), this a wrong way of thinking, because the strength does not change in a vortex street, only the load is different. Translated to the terminology applied here, it means: $K = 2$. In the following we will try to affirm or disaffirm this statement. Unfortunately, there are not many systematic tests, because most research was done for the specific geometry of some hydraulic structure. In the work of Ariëns, 1993 some attention was paid to the magnitude of K for various geometries, see Figure 9.16.

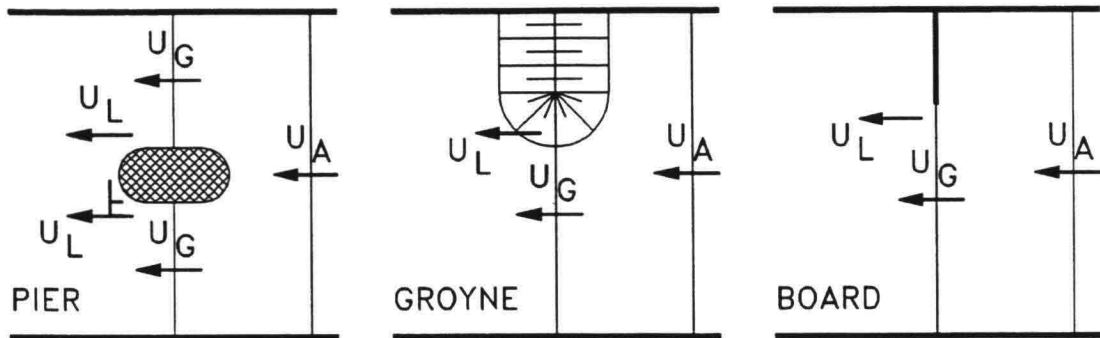


Figure 9.16 Various geometries of horizontal constrictions

Like with α in the scour relation (see chapter 6), the magnitude of K depends on the definition of u . Figure 9.16 shows some possibilities: the average velocity upstream $u_A = Q/A_{Flume}$, the average velocity in the narrowest cross-section of the gap: $u_G = Q/A_{Gap}$ or the local maximum velocity: u_L . In the following table the various K -factors, in accordance with the various definitions of u , are presented:

Type of constriction	Constriction (% of width)	$K-u_A$	$K-u_G$	$K-u_L$
Board	16.5	1.91	1.59	1.23
	30	2.58	1.81	1.37
	50	4.08	2.04	1.37
Groyne	10	1.55	1.40	1.17
	50	2.87	1.43	-
	69	4.49	1.39	1.01
	75	5.49	1.37	-
	85	9.38	1.41	-
Pier	16	2.5-2.7	2.0-2.2	-
	20	2.3-2.9	1.9-2.5	-

Note: Some of these figures come from a literature survey where u_L was not measured.

From these figures we can draw the following conclusions:

- 1 When the average upstream value of the velocity is used (which is often done), K is "polluted" with the variation in velocity due to the different degree of constriction.
- 2 Using the velocity in the narrowest cross-section gives already much better results. For groynes, K becomes practically constant.
- 3 Although only very few measurements were done, it can be expected that K related to the maximum velocity will give the best results, because then K only contains the influence of turbulence and the shape of the velocity vertical and not the velocity distribution over the width.
- 4 A groyne with a round head is more favourable for stability than a vertical board or a pier. The disturbance of the flow is much less abruptly (compare $K_G = 1.4$ for a 50% groyne versus 2.0 for a 50% board or 2 for a pier)
- 5 The statement that "the critical velocity is half the value for uniform flow" (or $K = 2$) is reasonably correct for boards that constrict the cross-section for not more than 10-20% and when the upstream velocity is used. This classical statement was not better specified, and it appears to be dangerous to use without thinking, which can be seen from the K-values for higher constriction percentages.
- 6 There is still a lot of research to do. Comparison of the "maximum" velocity ($u+3\sigma$) for uniform flow and for a constriction with a board, show about the same values, see Ariëns,1993. So it is clear that the explanation should be searched in the combination of velocity and turbulence.

JETS

Another example of load increase is formed by turbulent jets. r in a free circular jet or a propeller race can reach values of about 30% compared to the velocity in the axis, see chapter 2 and 3. Investigations in the framework of RWS/WL,1988 resulted in Figure 9.17. This leads to a condition of no movement:

$$\frac{u_c}{\sqrt{g\Delta d}} = 0.55 \quad (9.15)$$

This formula has the same shape as the Izbash formula for uniform flow, but the constant is three times smaller or better: $K = 3$. It is not yet possible to explain this difference from the magnitude of the turbulent fluctuations, so here too, the need for research to understand and design is not yet over.

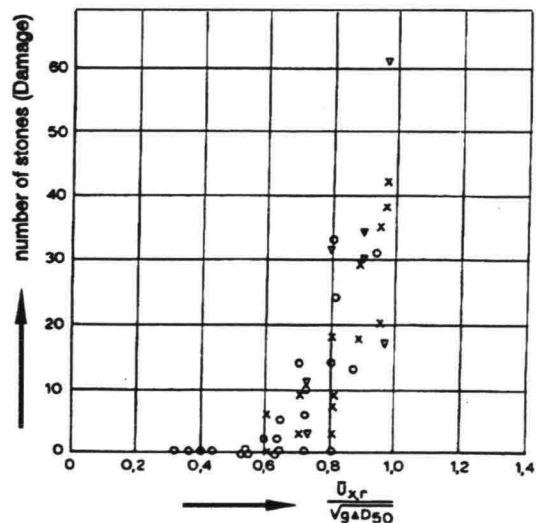


Figure 9.17 Damage by propeller

VERTICAL CONSTRICTION

In the previous section we saw that stones on a sill are not heavier loaded than in a uniform flow with the same velocity as on top of the sill. At the downstream end the strength of the stones is less because of the downward slope in flow direction. In all experiments it is found that the first damage on a sill occurs at the downstream crest. There the velocity is maximum and the waterdepth minimum. When a single stone on that crest has a protruding position, it will move at almost any velocity, reshaping somewhat the crest. This is usually not considered as damage. In fact, for a preliminary design for sills and dams, $\psi = 0.04$ is often recommended instead of 0.03 for bottom protections. Some loose-lying stones will move, leaving a stronger sill without any further movement under the same velocity load.

When a sill becomes relatively high, especially when critical flow can occur, the whole flow-pattern becomes completely different. The flow lines over the sill get strongly curved and at the downstream crest the waterflow through the stones becomes important. In that case it has no use to work with velocities anymore. In Akkerman, 1985 many experimental results have been reanalysed and for higher dams the relation between waterdepths upstream and downstream appeared to be satisfactory.

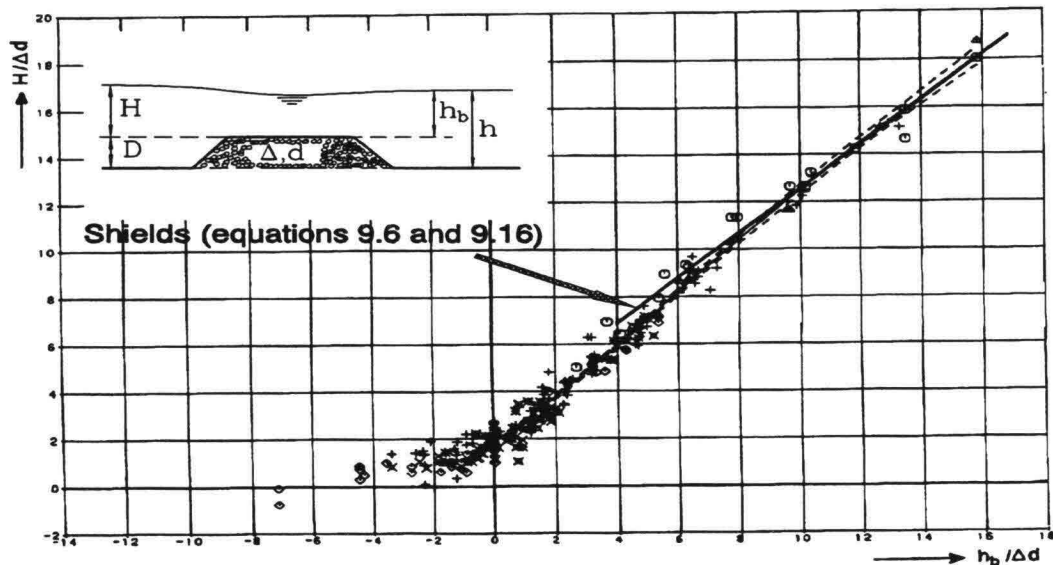


Figure 9.18 Overall results rockfill dams (DHL, 1985)

For comparison, Shields (equation (9.6)), is reworked in the format of Figure 9.18, using:

$$u_0^2 = \mu^2 2g(H - h_b) = (0.5 + 0.065 \frac{h_b}{\Delta d}) 2g(H - h_b) \quad (9.16)$$

the relation for μ coming from the same experiments. With $\psi = 0.04$ this relation is drawn in Figure 9.18. For low dams, Shields is satisfactory, which is also convenient because the velocity on the sill can easily be measured while the head difference is very small. For high dams, Figure 9.18 should be used, where now the head is the parameter which can easily be defined and measured. $h_b/\Delta d \approx 4$ can be seen as a transition point, also between critical and sub-critical flow.

HORIZONTAL CONSTRICTION

For a stone on a slope perpendicular to the flow, we found a correction factor in paragraph 9.1.2 The head of a groyne gives such a situation, plus the fact that the flow accelerates around this obstruction. Akkerman, 1986 analysed the stability in that situation based on experiments on horizontal closure of a river with stones.

The stability is approached with Shields and a slope correction (equation (9.6) and (9.9)):

$$\frac{\overline{u_{gap}}}{\sqrt{\Delta g d}} = C \sqrt{\frac{\psi}{g}} \sqrt[4]{1 - \frac{\sin^2 \beta}{\sin^2 \phi}} \tag{9.17}$$

in which $C = 18 \log(12h/k)$. Since the damage appears to occur at half depth, $12h/k$ becomes $(12 \times 1/2h)/2d = 3h/d$. For closure works in a river and with $\beta = 30^\circ$ and $\phi = 40^\circ$ (normal values for a rockfill dam), (9.17) appears to reduce to:

$$\frac{\overline{u_{gap}}}{\sqrt{\Delta g d}} = \log\left(\frac{3h}{d}\right) \tag{9.18}$$

The comparison between (9.18) and some model and prototype measurements are presented in Figure 9.19

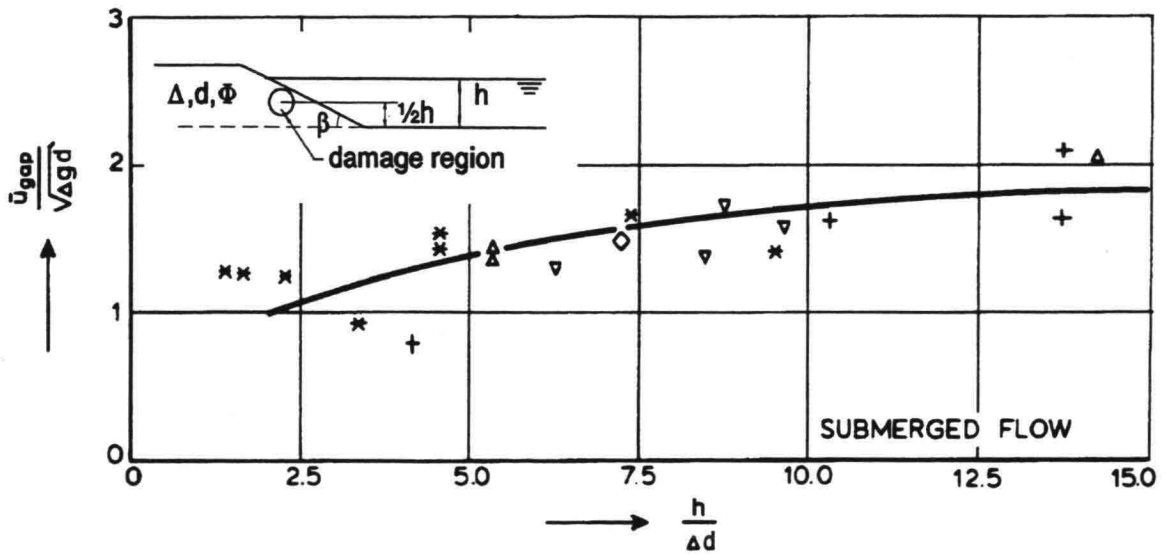


Figure 9.19 Stability of stones on head of dam or groyne

For permanent structures like groynes, it is recommended to use equation (9.17) with $\psi = 0.03$

The word coherent is used here on purpose for all materials that show some coherence in contrast with paragraph 9.1. Coherent materials are e.g. placed concrete blocks which are stronger than loose grains since they work together, cohesive soils like clay or loam and soils with vegetation. The contrast between loose and coherent material is not so black and white as it looks. A placed block that is not connected with cables or geotextile with its neighbours or a stone with a negative protrusion, see paragraph 9.1.1, form the transition between the two categories.

In contrast with the many investigations that have been done with rock and gravel, there are only few data on the flow-stability of coherent materials. For various types of material, some data will be given here.

9.2.1

PLACED ELEMENTS

Square or rectangular blocks can be piled as a vertical wall, so the angle of repose is 90° leading to an infinite resistance with $\tan 90^\circ = \infty$. Theoretically this is correct; blocks that are well-placed and interlocked cannot turn and are jammed. The only way to lift a block is by groundwater pressure from below, or by suction from above. In practice blocks will not interlock ideally and flow resistance will be less. In Izbash-form, critical values of $u/\Delta g d$ of 1.5 to 2 times higher than for loose grains were found (RWS, 1990). It must be stressed however that these values are based on few data.

For situations with a heavy attack of turbulent flow behind hydraulic structures, there seem to be interesting possibilities for this material, so more research on this subject should be done.

9.2.2

GABIONS

Gabions consist of loose stones, packed together with some thread into larger elements, see annex A. This can be useful when available elements are not large enough for the flow. Ease of placing can also be the reason to apply gabions. Using the same relations for stability as for individual stones, like Shields or Izbash, the following should be taken into account:

The relative density is less than for a solid rock, because of the pores between the stones in the gabion:

$$\Delta = \frac{(1-n)(\rho_s - \rho_w)}{\rho_w} \quad (9.19)$$

The porosity, n , lies usually around 40%

The stability is better than for a single stone, since the porosity also makes the load of the flow less effective. For the stability only few data are available, see RWS, 1990. The critical velocity in $u/\Delta g d$ is about 2 times higher than for stones or the Shields-parameter ψ is about 4 times higher.

9.2.3

COHESIVE SOILS

Somewhat more data on cohesive soils are available. Figure 9.20 gives the permissible velocity for various soil-types. The void ratio in this figure is the volume of pores divided by the volume of material!

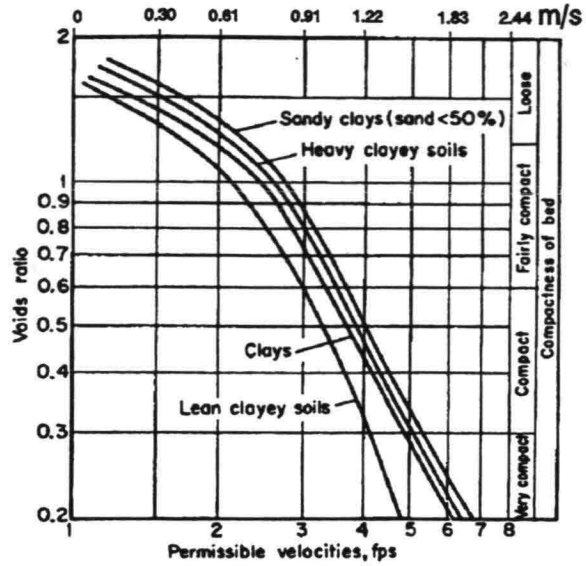


Figure 9.20 Permissible velocities for cohesive soils (Ven te Chow, 1959)

9.2.4

VEGETATION

Vegetation can resist flow to a certain extent, but the resistance diminishes in time. Figure 9.21 gives some values for plain and reinforced grass (see CIRIA, 1990). Based on this figure it is recommended that a good grass cover can withstand in permanent flow:

- 5 m/s less than 2 hours
- 3-4 m/s for several hours
- 2 m/s more than 10 hours
- 1 m/s for days

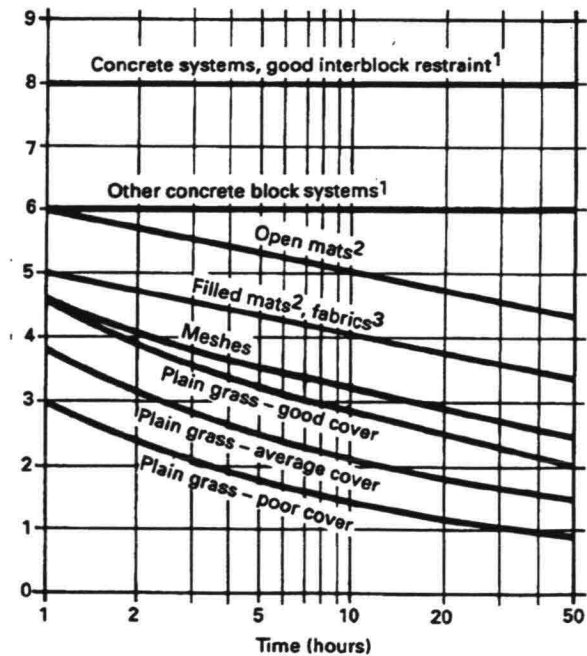


Figure 9.21 Permissible velocities (in m/s) for grass with and without reinforcing mats

Much research has been done on stability of rocks etc. in wave attack and again, most of the work is empirical. As a logical continuation of the previous chapter, we will start with the stability of loose grains on a flat bottom.

For long waves, the stability of stones on a bed can be treated as in a succession of uniform flow situations. In short waves however, the shear stress can be considerably higher as we have seen with the results of Jonsson, 1966 in paragraph 3.3. Using Jonsson's relation for shear stress under a wave, the "normal" Shields formula (9.5) can be applied and experiments show a satisfactory result.

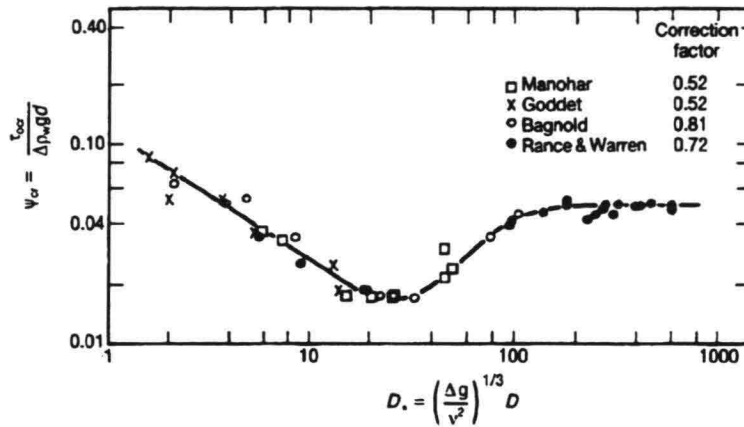


Figure 10.1 Modified Shields curve for oscillating flow

Figure 10.1 shows the measurements of various authors, summarized by Sleath, 1978 and presented in CUR/CIRIA, 1991. Instead of the grain-related Re -number, a dimensionless grain diameter is used in the horizontal axis ($d_* = [\Delta g/v^2]^{1/3}d$, thus avoiding the shear velocity u_* in the horizontal axis).

For large d_* (turbulent boundary layer), the value for ψ is found to be 0.056. This is almost the same value as Shields himself used for the threshold of movement and as we have seen in paragraph 9.1.1, this value is rather high and means a relatively large amount of stones in motion in steady flow. How logic is it that the same value is found in oscillating flow?

Two factors can play a role. The criterion for the threshold of movement in oscillating flow is not quite clear, but a potentially unstable stone in oscillating flow does not move a long distance, hence the subjective threshold will probably be chosen rather high compared to steady flow. Another aspect may be the phenomenon we have seen in an accelerating steady flow, where ψ increased as τ increased, due to the fact that the scale of the eddies is limited compared with a boundary layer with the size of the waterdepth.

When the average shear stress during a wave cycle was taken ($\tau = 1/2\tau_{max}$, see paragraph 3.3), ψ was found to be 0.03

Most research on the stability of stones on a slope was done in the field of breakwaters, which is very much related to slope protections and revetments, but it is not the same. An important difference in the stability is the porosity of the structure as a whole. Breakwaters usually have a porous core, while in dike revetments the core is made of clay or sand. This has a significant influence on the stability of the protecting armour layer as we will see in this paragraph. We will start however with simple basic principles and will discuss shortcomings and extensions later on.

With the successful results of the modified Shields curve for waves in mind, the next step would be the use of the slope correction of paragraph 9.1.2 and derive a formula for a stone on a slope. Therefore, a velocity on the slope is needed and that appears to be the first difficulty. As already stated in chapter 3, no expressions for velocities in breaking or broken waves are available. Moreover, it can be questioned whether the velocity alone is sufficient to describe the forces in such a situation; beside drag and shear forces inertia will play a role in the stability.

But, as a first guess, we will assume that the velocity in a wave on a slope is proportional to the celerity in shallow water with the wave height as a representative measure for the waterdepth:

$u \propto \sqrt{gH}$. Following the same reasoning as in paragraph 9.1, we find analogous to equation 9.2:

$$\rho_w g H d^2 \quad \propto \quad (\rho_s - \rho_w) g d^3 \quad (\tan \phi \cos \alpha \pm \sin \alpha) \quad (10.1)$$

"drag"force *resisting force* *slope correction*

Note: + and - in the slope correction are for uprush and backwash respectively, see paragraph 9.1.2. Raising all terms to the third power and working with the weight of the stone ($W \propto \rho_s g d^3$) we find:

$$W \propto \frac{\rho_s g H^3}{\Delta^3 (\tan \phi \cos \alpha \pm \sin \alpha)^3} \quad (10.2)$$

This is Irribarren's formula for stability of rock on slopes in waves, dating back to 1938. After the second world war, many tests were performed (particularly by Hudson, 1953) to find the constants of proportionality in equation (10.2). This did not lead to a practical expression and Hudson finally proposed another formula:

$$W = \frac{\rho_s g H^3}{K_D \Delta^3 \cot \alpha} \quad (\text{or: } \frac{H}{\Delta d} = \sqrt[3]{K_D \cot \alpha}) \quad (10.3)$$

Note: the use of $H/\Delta d$ as a stability parameter is convenient and is similar to flow, where $u^2/\Delta d$ is used. The slope correction in Irribarren's formula is now reduced to $\cot \alpha$. This means that the validity of Hudson's formula is limited, because $\cot \alpha$ is insufficient to describe friction and equilibrium on a slope: for $\alpha = 0$, $W = 0$ and for $\alpha > \phi$ W has still a finite value, both of which are nonsense. The range of α for which Hudson is valid is about $1.5 < \cot \alpha < 4$. The Hudson-formula is tested for waves that did not break at the toe of the slope and did not overtop it. For cases where this is not true, extra corrections for K_D are sometimes applied.

Hudson's formula is simple and is used worldwide. K_D is again a dustbin-factor in which implicitly the accepted degree of damage. K_D has different values for different kinds of elements (3-4 for natural rock to 8-10 for artificial elements like tetrapods and tribars). The Shore Protection Manual (SPM, 1984) gives values for K_D for various circumstances.

DISCUSSION ON VALIDITY

Some limitations of the presented formulae have already been mentioned. The most important are:

-Wave period

Already in the Irribarren-formula this parameter is absent. There are two ways in which the period can have influence on stability. The period is related to the wave-length, hence to the wave-steepness and hence to the breaking pattern on the slope, which will definitely play a role. The other one is the possible role of inertia-forces on a grain which depend on du/dt , hence on the wave-period. It is attractive to include the period by means of the surf-similarity parameter ξ . This has been done in Figure 10.2 in which two distinct areas can be seen: left for plunging waves and right for surging waves. $H/\Delta d$ is used as a stability parameter.

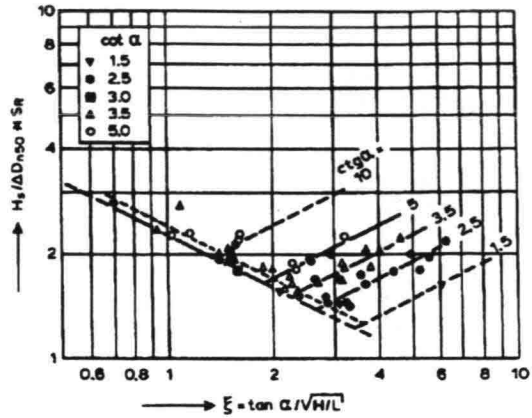


Figure 10.2 Stability as a function of ξ

-Permeability

The permeability of the structure must play an important role. In the assumptions on which Irribarren's formula is based, only a kind of drag force on the slope is included. The forces under and behind a grain will certainly be co-responsible for the equilibrium. It is easy to imagine that a homogeneous mass of stones will react different from a cover layer of stones on an impermeable core. In the first case, a lot of wave energy is dissipated in the core, while in the latter the pressure build-up under the cover-layer can be considerable. Hedar was the first to stress this influence, see Figure 10.3, in which k is some equivalent diameter, hence k/H is the reverse of $H/\Delta d$. Note that Hedar follows the same procedure as Irribarren and makes a distinction between uprush and backwash.

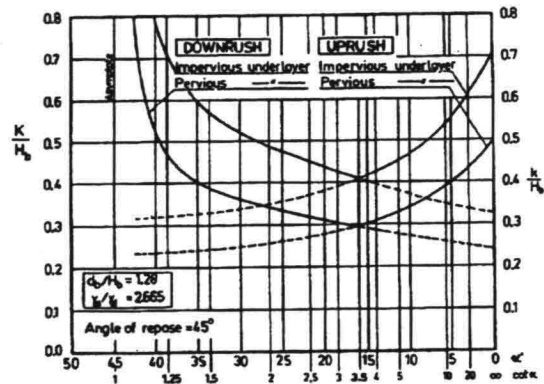


Figure 10.3 Influence of permeability (Hedar, 1986)

-Regular/irregular waves

All modeltests in the 50's and 60's were done with regular, monochromatic waves. It appeared in those tests that the equilibrium damage profile was reached in, say, one hour time. The wave height in the tests was then usually declared equivalent to H_5 . It appeared from tests with wave spectra that the number of waves is not unimportant, which is logic, since more waves mean a greater chance for a large one.

-Threshold of damage

Like stones in flow, the threshold of motion is not always clear. The K_p -values in the Hudson formula are supposed to be valid for 5% damage, but the definition of damage is not very clear.

All these objections led to new research activities, especially after some failures of breakwaters. In a period of about ten years the recommended coefficients in the Shore Protection Manual for breakwater design with the Hudson formula led to an increase in weight of about 200%.

In the Netherlands, extensive modeltests were done to overcome the limitations of and objections against the Hudson-formula. These tests were done at DHL, see van der Meer, 1988 summarized in CUR/CIRIA, 1991.

van der MEER

van der Meer's formulae are essentially the result of curve-fitting of many large-scale model-tests with irregular waves. The damage level was defined in a more manageable way, see Figure 10.4: $S_d = A_e/d^2$. This is an erosion area divided by the square of the diameter. In a strip with a width d perpendicular to the paper, S_d is more or less equal to the number of stones that is removed. The advantage of S_d is the use of an area which can be measured objectively from soundings.

For the threshold of damage, $S_d = 2-3$, can be used. When the armour-layer is locally removed completely and the filter-layer becomes exposed, the damage can be defined as failure of the structure. Depending on the slope, the matching S_d is about 10.

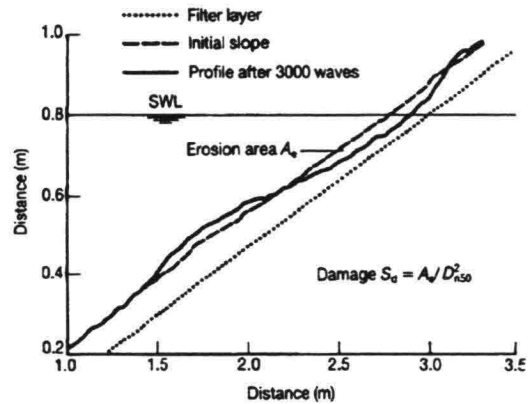


Figure 10.4 Definition of damage S_d

Three different permeabilities were tested: homogeneous rock (no core), rock armour-layer with a permeable core ($d_A/d_F \approx 3$) and an impermeable core. Unfortunately it was not yet possible to give an expression with which the influence of the permeability on the stability could be calculated. Instead, a permeability parameter P was introduced and the value for the three different structures was established by curve-fitting of the results. Figure 10.5 gives the values for the three situations (0.6, 0.5 and 0.1 respectively) with an estimated value for a fourth ($P = 0.4$). Attempts were made to derive an expression for P , based on porous flow calculations, but until now, with little or no success.

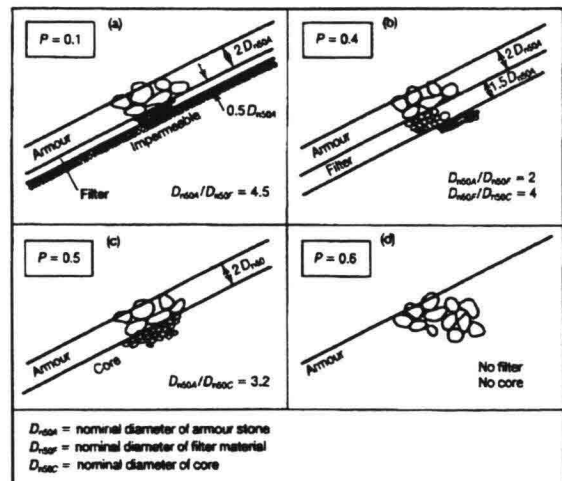


Figure 10.5 Permeability

As a stability parameter van der Meer used $H_s/\Delta d$ (to which also Irribarren and Hudson easily can be rewritten), the wave-period was thought to be included in the surf-similarity parameter, ξ_m (m means related to the average wave period), while, like Pilarczyk/de Boer, 1983, the stability curves were divided into two parts: one for plunging and one for surging waves. The formulae finally read:

$$\frac{H_s}{\Delta d} = 6.2 P^{0.18} \left(\frac{S_d}{\sqrt{N}}\right)^{0.2} \xi_m^{-0.5} \quad (\text{plunging waves})$$

$$\frac{H_s}{\Delta d} = 1.0 P^{-0.13} \left(\frac{S_d}{\sqrt{N}}\right)^{0.2} \xi_m^P \sqrt{\cot \alpha} \quad (\text{surging waves})$$
(10.4)

The transition between the two expressions is found by equating them, which gives:

$$\xi_m = [6.2 P^{0.31} \sqrt{\tan \alpha}]^{\left(\frac{1}{P+0.5}\right)} \quad (10.5)$$

In practice, for $\cot \alpha \geq 4$ surging waves do not exist and only the expression for plunging waves is recommended for use.

N is the number of waves. Figure 10.6 gives the increase of the damage with the number of waves during a test. With $N = 7500$, the damage can be considered to have reached an equilibrium. When only storms of short duration occur and intensive maintenance will be done, N can be chosen lower. 2000 waves with an average period of 7 s, represent a storm of about 4 hours.

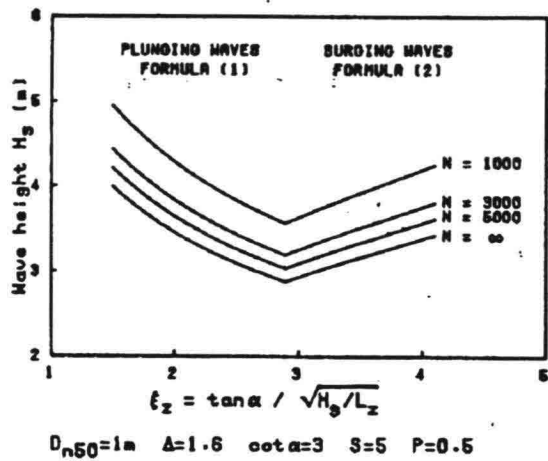


Figure 10.6 Damage vs. number of waves

Figure 10.7 shows the influence of the permeability which is considerable. $H/\Delta d$ for a revetment ($P = 0.1$), is 1.5 to 2 times smaller than for a homogeneous dam ($P = 0.6$). So the situation for a revetment is much more unfavourable. Laboratory tests in the past however, were executed either with homogeneous dams or impervious cores, while the results were often used vice versa without knowing. So, results of laboratory tests should be interpreted with care.

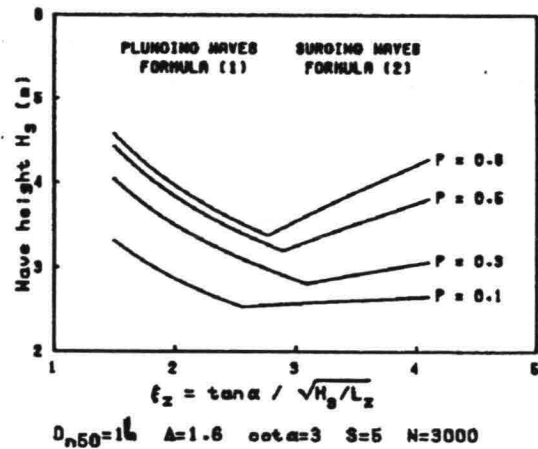


Figure 10.7 Influence of permeability

Figure 10.8 gives the influence of the slope angle. For $\cot\alpha \geq 4$ only the plunging part has been drawn. Like with the run-up of waves, see paragraph 3.4.3, the critical stability lies around $\xi = 3$. In surging waves, the stability increases with decreasing wave steepness.

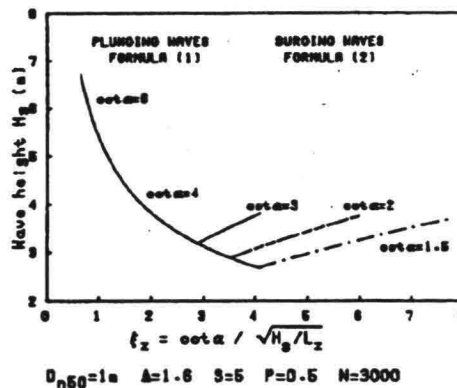


Figure 10.8 Influence Slope angle

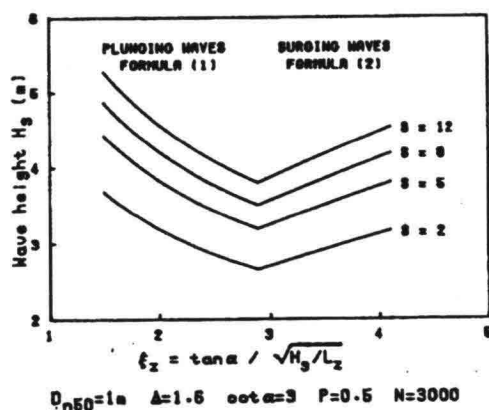


Figure 10.9 Influence of damage level

Figure 10.9 finally gives the influence of the damage level that is assumed. $S = 2$ is more or less equivalent with Hudson's "no damage". Failure (armour-layer completely removed) occurs at wave heights that are about 1.5 times as high as with $S = 2$.

DISCUSSION ON STATE OF THE ART

For practical purposes the formulae by van der Meer are clearly preferable above the classical Hudson-formula, see Figure 10.10. This is especially true for revetments, where the permeability is much less than in breakwaters, which is the origin of the Hudson-formula. Moreover, the influence of the wave period is included. From a physical point of view, the van der Meer formulae are not really a step forward, since the balance of forces like the inertia, the pore pressures etc. are not taken into account explicitly. Using the presented formulae, either by Hudson or van der Meer should be done with knowledge of the limitations.

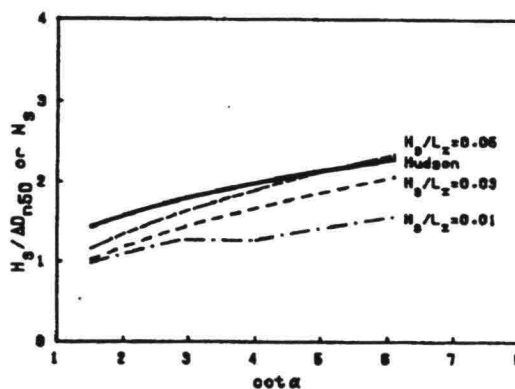


Figure 10.10 Comparison Hudson-vd Meer for impervious core and varying wave steepness

In many cases the toe of a slope or seawall is protected with stones. Dimensioning these stones with the formulae in the previous paragraph, can lead to a sub-optimal design from an economic point of view, since they are less heavily attacked then on a slope. For toes that lie deeper than half the waterdepth, Figure 10.11 gives an indication of the stability, based on experiments. For berms and toes which are situated higher than half the waterdepth, the slope formulae of the previous paragraph should be used. For deep lying toes, the experiments show a considerable increase in stability.

Note: The experiments were done for situations in which the wave height at the toe was limited by the waterdepth, meaning that $H_s/h \approx 0.5$. Therefore h_t/h can be used in the graph. For deep water no data are available; a first approximation could be done with the modified Shields from paragraph 10.1.1, in a standing wave, taking into account the slope of the toe and the reflection of the construction as a whole.

Note: For vertical walls the situation is less favourable. For shallow water, no higher values than $H_s/\Delta d = 2$, should be used. For more detail see CUR/CIRIA,1991.

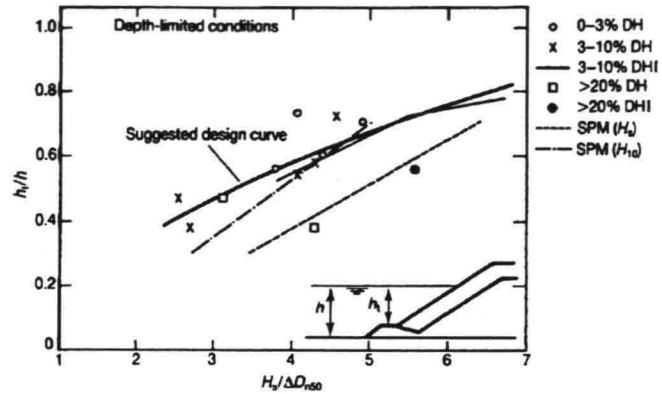


Figure 10.11 Toe stability in shallow water

The van der Meer and Hudson formulae were derived for non overtopping slopes. When this is not the case, there is a certain wave transmission, see chapter 8. That means that not all energy has to be destroyed on the slope and the stability increases (in turn the rear side should be armoured). For crests above the still water level van der Meer found a stability increase factor:

$$K_{H/\Delta d} = 1.25 - 4.8 \frac{R_c}{H_s} \sqrt{s_p/2\pi} \quad (10.6)$$

where R_c is the crest height with respect to SWL, see Figure 10.12 and s_p is the wave steepness related to the peak period; the minimum value of the increase factor is 1. For still lower crests, see e.g. Pilarczyk,1990.

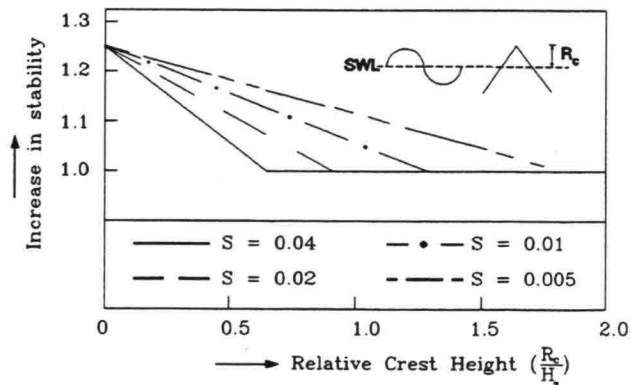


Figure 10.12 Stability increase for low crest

In contrast with the two previous examples, which were more favourable compared to a stone on a slope, stones on the head of a groyne (or breakwater, again for which the investigations were done) are attacked heavier. No systematic test results are available. The Shore Protection Manual (SPM, 1984) gives K_D -values for the head, that are about 30% lower than at the trunk, leading to a 30% higher weight or a 30% gentler slope.

In chapter 4 the wave loads due to the passage of ships were divided into primary and secondary waves. The stability of a stone protection can be estimated with the following empirical rules, derived from the investigations as described in RWS/DHL, 1988. For propeller races, see paragraph 9.1.3.

PRIMARY WAVES:

1. For a first estimate, an Izbash-type relation can be used:

$$\Delta d \geq 1.4 \frac{u_R^2}{2g} \quad (10.7)$$

where u_R is the return current. (Note: in the relation the coefficient is 1.4 instead of 0.7 for steady uniform flow).

2. For a better approximation, use the Shields approach:

$$\tau = \frac{1}{2} C_f \rho_w u_R^2 \quad (10.8)$$

with C_f according to equation (4.8).

In both cases the stability is reduced with the perpendicular slope reduction factor, equation (9.9).

3. The upper part of the bank, near the waterlevel, should be able to withstand the stern wave ($z_{\max} = 1.5z_R$) over a height of about 3 times z_{\max} under SWL:

$$\frac{z_{\max}}{\Delta d} \leq 1.5 (\cot \alpha)^{0.33} \quad (10.9)$$

SECONDARY WAVES

The following relation is recommended:

$$\frac{H(\cos \beta)^{0.5}}{\Delta d} \leq 1.8 \rightarrow \text{with } \beta = 55^\circ: \frac{H}{\Delta d} \leq 2.4 \quad (10.10)$$

Coherent, again stands for all material that does not consist of loose grains. An important material in revetments, especially in sea defences, is formed by placed elements, mostly concrete. Many research has been done in the last ten years in the Netherlands on the stability of placed blocks on a slope under wave attack. Therefore, this construction type will be discussed here in more detail. Other coherent materials are clay, asphalt and slopes with vegetation.

10.2.1

PLACED BLOCKS

Placed blocks come in many shapes where only the human phantasy is the limiting factor. The variation is in the coherence: pinched, connected with cables or geotextile or interlocked. Another variation is the shape of the upper side of the blocks which is meant to reduce the wave run-up; for this chapter this is not so important. Figure 10.13 gives some examples.

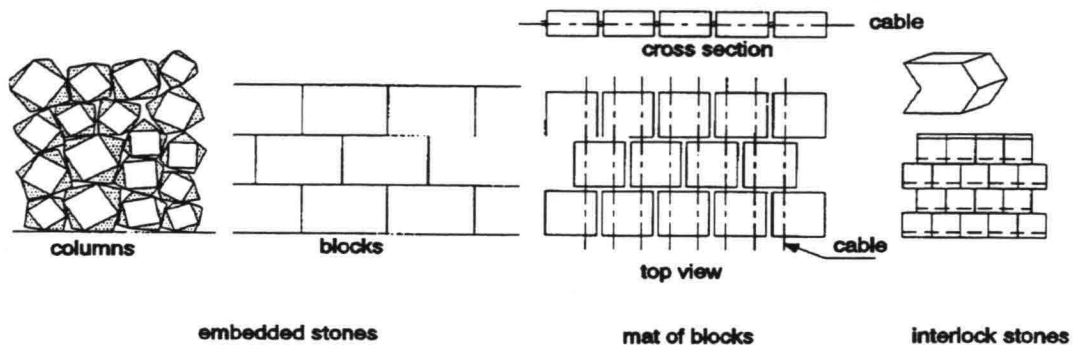


Figure 10.13 Possible block types in revetments

The transition between the blocks and the underlying soil is another variable. Figure 10.14 gives some possibilities (many other combinations are possible).

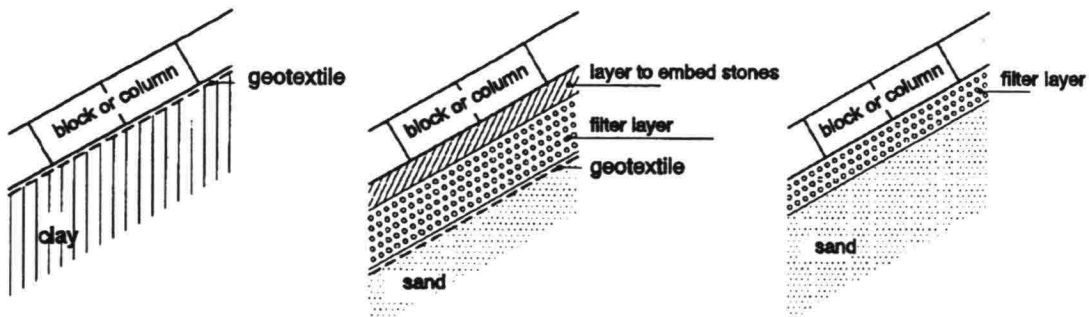


Figure 10.14 Possible transitions to underlying soil

Sometimes the blocks are placed directly on clay; this requires a high quality standard during construction. When the blocks are not exactly equal in height, a layer to embed the blocks is necessary to correct the height-differences. This is specially the case when natural material like basalt columns are used. It is sometimes combined with a filter layer. The requirements of the transition between a filter-layer and the subsoil are discussed in the next chapter.

PHENOMENA AND FORCES

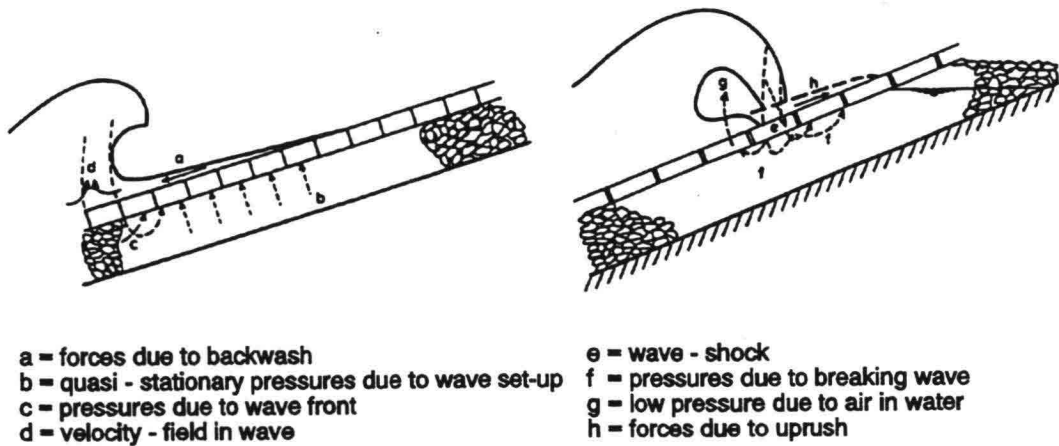


Figure 10.15 Forces on top-layer during a wave cycle

Figure 10.15 shows the phenomena that play a role in the stability of placed blocks during a wave cycle. For loose grains we already discussed in paragraph 10.1.1 that only velocity, friction and gravity were not enough to describe the stability. At least inertia and porosity should be taken into account. For placed blocks the situation is all the more complex and many energy has been put into the fathoming of the secrets of placed block stability. From tests, calculations and reasoning it was established that phenomena b and c are dominant in the process. In fact, the wave action on and under the blocks can not be separated and porous flow phenomena have to be taken into account.

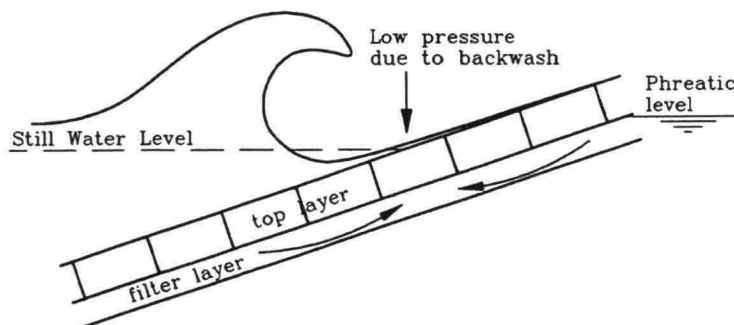


Figure 10.16 Critical situation for placed block during a wave cycle

Figure 10.16 shows the dominating situation at maximum downrush: the pressure on the blocks is low in front of the wave, while under the blocks it is high, due to the propagating wave pressure in the filter-layer and to the relatively high phreatic level in the slope. This causes an uplift-force on a block. Very important for the magnitude of this uplift-force is the relation between the permeability of the top layer and of the filter layer, usually expressed in a leakage factor, Λ . This will be discussed in more detail.

LEAKAGE AND UPLIFT

To demonstrate the relative importance of permeabilities, the porous flow in the revetment is simplified as follows: the flow through the filter layer is assumed to be parallel to the slope while the flow through the top layer is supposed to be perpendicular to it (y is the coordinate along the slope). The flow in the filter layer can be expressed as:

$$q_F = -k_F \frac{d\phi_F}{dy} \quad (10.11)$$

and through the top layer:

$$q_T = k_T \frac{(\phi_S - \phi_F)}{d} = k_T \frac{\Delta\phi}{d} \quad (10.12)$$

Based on continuity, $\Delta q_F \cdot b = q_T \cdot \Delta y$, see Figure 10.17, hence $q_T \approx b \cdot dq_F/dy$, from which follows:

$$\frac{d^2 \phi_F}{dy^2} = \frac{k_T(\phi_F - \phi_S)}{k_F b d} = \frac{\phi_F - \phi_S}{\Lambda^2} \rightarrow \Delta\phi = \Lambda^2 \frac{d^2 \phi_F}{dy^2} \quad (\Lambda = \sqrt{\frac{k_F b d}{k_T}}) \quad (10.13)$$

in which $\phi_{F,S}$ is the piezometric head ($\phi = p/\rho g + z$) in the filter and on the slope respectively, $\Delta\phi$ the head difference over the top layer and $k_{F,T}$ the permeability of the filter and top layer. b and d are the thickness of filter and toplayer. From this equation can be seen that the head difference over the top layer depends directly on Λ . A relative thick and permeable filter layer and/or a relative thick and impermeable top layer give a large Λ and hence, a large head difference over the top-layer. So, a large Λ , the leakage length, is unfavourable for the stability of the blocks.

This equation can be solved analytically for highly schematized boundary conditions and when laminar flow (or more precise: a linear relation between velocity and pressure) in the filter layer is assumed. Description is outside the scope of these notes; the reader is referred to CUR/TAW,1992 or to Bezuyen e.a,1990. A simple approach is given by Barends in CUR/CIRIA,1991 which can serve as an illustration (not as a calculation method). When the leakage is expressed as $\lambda = \Lambda \sin\alpha$ and Z_s is the height between the rundown- and the phreatic level due to wave set-up in the filter layer, the maximum difference in piezometric head over the top layer is found to be:

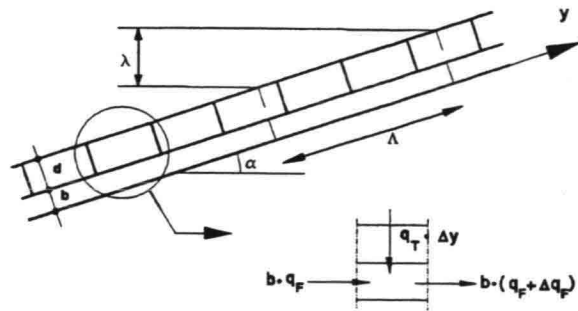


Figure 10.17 Definitions leakage

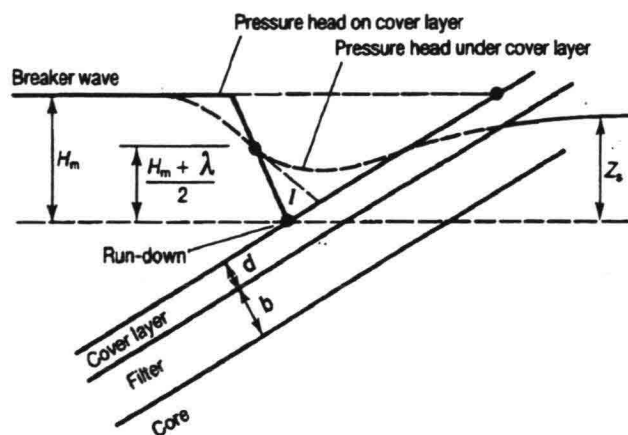


Figure 10.18 Head difference over top-layer (CUR/CIRIA,1991)

$$\Delta \phi = \frac{H_m + \lambda}{2} \text{ for } \lambda < H_m \quad \text{and} \quad \Delta \phi = Z_s \text{ for } \lambda > H_m \quad (10.14)$$

Z_s is not too easy to determine, but in revetments as a first approach $Z_s = H_m$ seems reasonable and the extremes for $\Delta\phi$ become H_m (the water level in the filterlayer can not become higher than the high water level) and $H_m/2$ for $\lambda = 0$. The idea of equation (10.14) however is not more than to demonstrate the influence of λ . Figure 10.19 shows the situation for a very high value of λ and for a very small value.

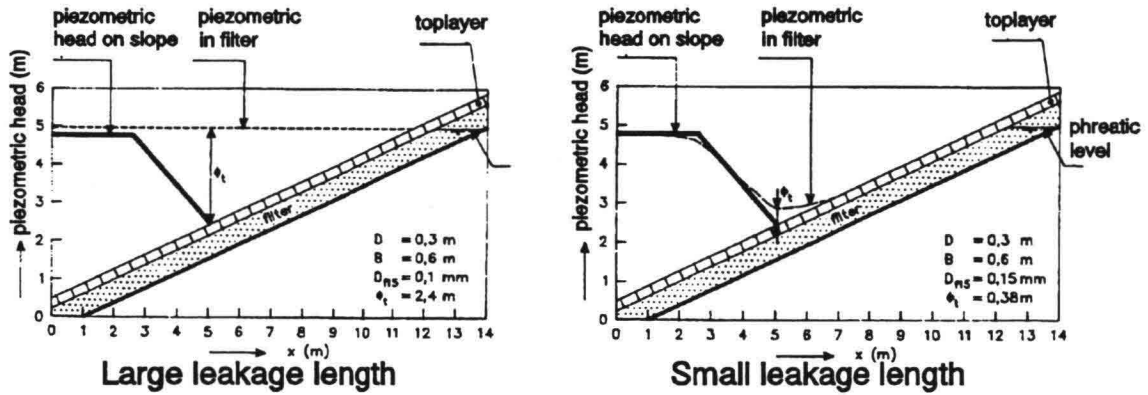


Figure 10.19 Piezometric head difference for two extreme cases of λ (Bezuyen ea, 1990)

Whether a block is pushed out or not depends further on the strength of the revetment in which two factors play an important role. In the first place of course the coherence of the blocks, which is in the case of loose blocks the friction between them. The second factor is the flow towards a stone when it is pushed out. With a relative small permeability of the filter layer, the block is sucked on the slope because only very little water can flow into the growing hole leading to a sudden decrease of the pressure under the block, see Figure 10.20.

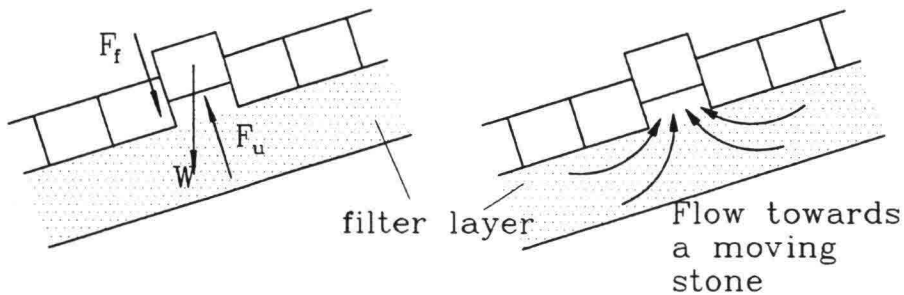


Figure 10.20 Resisting forces for a moving block

From all this it becomes clear that a permeable top layer and an "impermeable" filter layer lead to the most stable construction. This means that filter layers should be kept as thin as possible! That is why the idea of blocks directly placed on clay is a very attractive one from a theoretical point of view. Everything however depends on the quality of the construction which is difficult to assure.

It will be obvious that, with so many assumptions and so many factors, it is impossible to give more than proportionalities in the relation between all the parameters involved. It was found:

$$\frac{H_s}{\Delta d} \propto \left(\frac{d}{\Lambda \xi_p} \right)^{0.67} \quad (10.15)$$

For various construction types, experiments were done to establish the constants of proportionality, leading to graphs as presented in Figure 10.21, which serve as an indication of the stability. There is also an "analytical" method which takes more detail into account. For more information the reader is referred to CUR/TAW,1992.

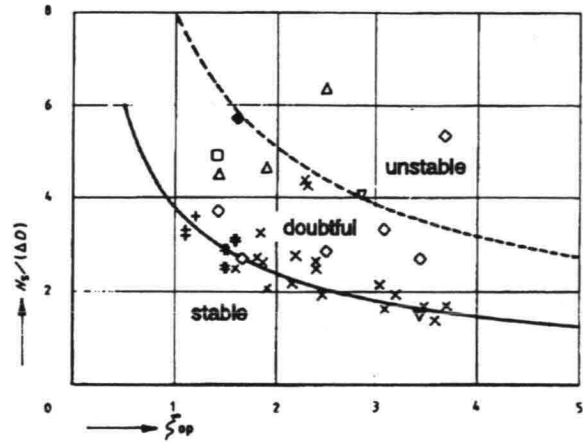


Figure 10.21 Test results for placed blocks on filter layer (CUR/TAW,1992)

Taking a closer look at equation (10.15), we see:

- a large Λ , leads to a low $H/\Delta d$, which is in line with equation (10.13) and Figure 10.19
- the same holds for ξ , which is the same as found for loose rock, see equation (10.4).a
- d plays a complicated role in this equation. It is part of Λ , indicating that a thick top layer gives a large head difference (equation (10.13), which is unfavourable. But a thick top layer also means more weight and hence more strength. With all other parameters in equation (10.15) constant, it appears: $H \propto d^2$, so a thick top layer is over-all favourable for stability.

Note: with both H and d appearing on both sides in the equation, the possibility of spurious relations should be checked thoroughly, see de Vries,1992.

In Figure 10.22 the results for placed blocks are compared with the stability of loose stones.

At this moment there is insufficient data to discriminate clearly between the possible combinations of different kind of blocks (pitched, interlocked etc.) and transitions (filter layers, geotextiles, direct on clay etc.).

It is clear that placed blocks form a superior revetment compared to rip-rap and that even better results than the line presented in Figure 10.22 are possible. Much depends however on the quality-control during construction.

Another aspect in these considerations is the permeability on the long run. A permeable top layer can become impermeable, because of dirt, vegetation, shells etc. So, practical experience remains a determining factor in the success or failure of a revetment design. See CUR/TAW,1992 or Pilarczyk,1990.

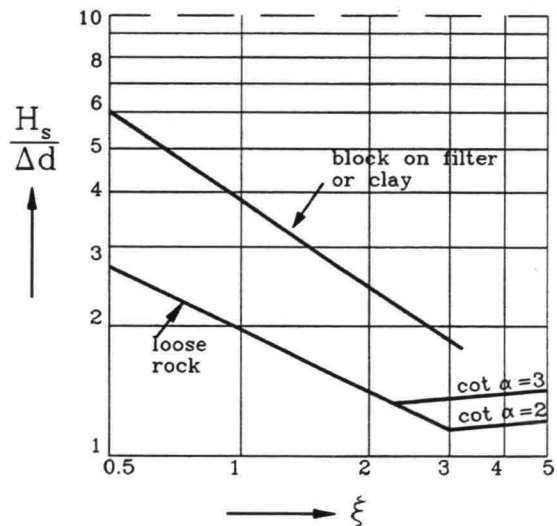


Figure 10.22 Comparison stability placed blocks and rip-rap

Impervious layers can be made from asphalt or concrete. The difference with blocks is that the protection forms a whole instead of separate elements. Usually there is no filter layer (the protection itself is sandtight) and the wave pressures can attenuate only a limited distance from the edge of the protection. In the case of a protection with a length smaller than a wave length, the maximum uplift pressure is given by, see Barends, 1979:

$$P_m = \rho_w g \frac{H}{2} \frac{1}{\cosh Lh} \tag{10.16}$$

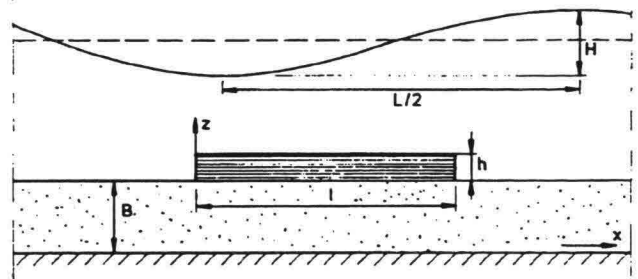


Figure 10.23 Impervious protection in waves

For stability, the weight of the protection should be equal or more than this value.

When the protection is long there are always areas where the wave pressure on top is about half the waveheight less than the pressure in the subsoil. The pore pressure then tries to lift the protection. This can only be effectuated when water flows into the hole between bottom and protection. In TAW, 1984 it is shown that this is hardly possible and that this is not an important stability factor for impervious revetments. Threats are wave impacts (and porous flow due to waterlevel differences over the protection, see next chapter).

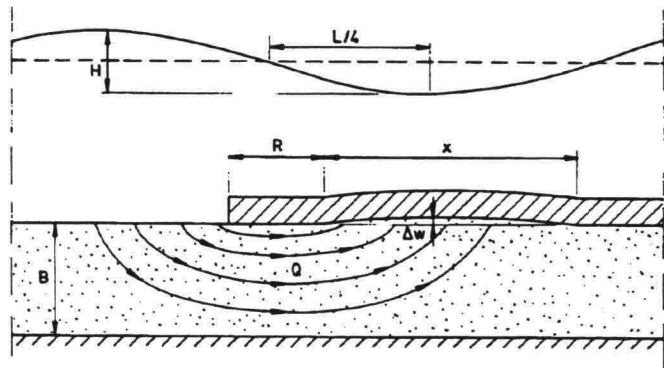


Figure 10.24 Lifting of protection by waves

WAVE IMPACTS

In paragraph 3.4.4 the special character of wave shocks compared to the cyclic quasi-static pressures was discussed. These shocks induce stresses in the material which should be lower than the failure stress. The response of the layer depends a.o. on the stiffness of layer and subsoil: a stiff layer on a soft subsoil gives the highest stresses. From elementary mechanics is known:

$$\left. \begin{aligned} \sigma &= \frac{M}{W} \\ W &= \frac{d^2}{6} \end{aligned} \right\} d^2 = \frac{6M}{\sigma_b} \quad (d = \text{layer thickness}) \tag{10.17}$$

The moment in the top layer is calculated by assuming a linear damped elastic support of the top-layer by the subsoil, see TAW,1984. In that case M is:

$$M = \frac{P}{4 \sqrt[4]{\frac{c}{4K}}} \quad (10.18)$$

with:

$$K = \frac{S d^3}{12 (1 - \nu^2)} \quad (10.19)$$

in which: ν is Poissons constant ($\approx 1/3$), S is stiffness modulus of top-layer and c is the spring constant of the subsoil. From this we find:

$$d^8 = \frac{27}{16} \frac{P^4}{\sigma_b^4} \frac{S d^3}{c (1 - \nu^2)} \rightarrow d = \sqrt[5]{\frac{27}{16} \frac{P^4}{\sigma_b^4} \frac{S}{c (1 - \nu^2)}} \quad (10.20)$$

P is the wave impact which is assumed to work over a width of $0.4 H_s$:

$$P = p.b = 12 \rho g H_s \tan \alpha (0.4 H_s) \quad (10.21)$$

This gives the necessary thickness of the layer for one impact. In reality there are many beats and asphalt or concrete have a lower σ_b after many beats, due to fatigue. Another thing is that not every wave gives an impact, say one out of every 10 waves gives an impact equal to (10.21). For a first approximation one could take H_s during a design storm and take σ_b after 1000 waves.

For more detail see TAW,1984 in which a different and complicated approach is followed to take fatigue into account.

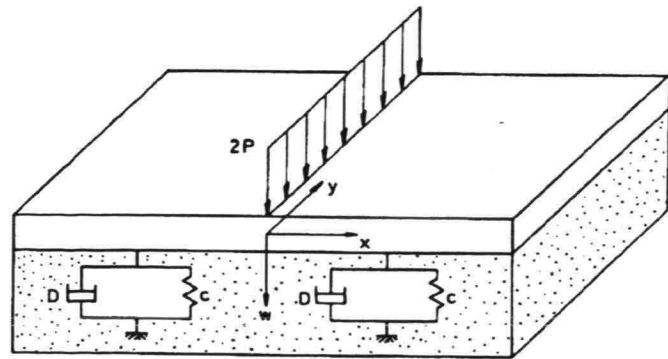


Figure 10.25 Schematization top-layer and subsoil

10.2.3

VEGETATION

Little is known of the behaviour of vegetation like grass on clay in waves, although it has been used for many years on dikes (usually well above high water). Much depends on the quality of the clay and of the roots of the grasses. Fertilization leads to "lazy" grass with very shallow roots. When the grass is in good condition it seems possible to withstand waves of 0.50 - 0.75 m.

In this chapter the focus is on porous flow. That can be either porous flow purely as a load, e.g. the pressure on an impervious revetment like asphalt; or as a load and a medium in which the stability is studied like in a granular filter. Also the influence of porous flow on the macro-stability of slopes will be discussed.

11.1**GRANULAR FILTERS****11.1.1****INTRODUCTION**

When a protection consists of large elements to resist external loads, there remains a problem to be solved, namely the transition between the protection layer and the subsoil, for which usually a filter is used. Another reason to apply a filter can be the protection against seepage flow.

Filters are especially needed in situations with large gradients on the interface of soil and water. Examples are a narrow dam with a head difference or the bottom under the slope of a breakwater where the waves are steep. In those situations gradients parallel to the interface of 10-20-30% are possible, while that gradient in open water flow is usually one or two orders of magnitude smaller. The main function of filters, consisting of one or more layers with grains of varying diameter, is to prevent the washing away of the material to be protected. That means that grains from the underlying material (the base) should not pass the pores of the upper layer (the filter). The filter has a larger diameter than the base for two reasons. The first comes from outside and is obvious: the filter layer is meant to protect base material against waves or currents which would otherwise erode. From the chapter on stability in flow we know that the larger the grain the more it can stand.

The other reason comes from inside and is meant to prevent pressure build up, see Figure 11.1. The permeability in a filter should increase from a layer with high pressure to one with low pressure. This is all the more relevant when the filter also has a drainage function.

Being closed for the base material and permeable for water are opposing demands; a solution has to be found within the margins left. The usual approach in design is to establish the necessary diameter for the stability of the top layer in waves and currents, to check the filter relations between the top layer and the original (base) material and to add as many layers in between as necessary to meet the filter demands. With more layers, every filter layer is again the base for the next layer.

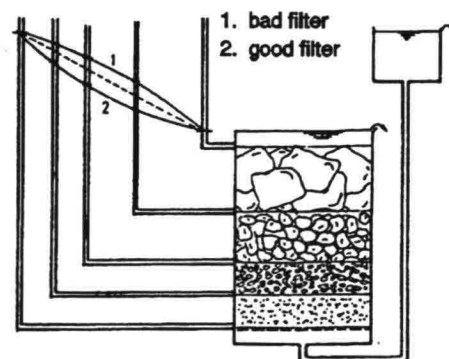


Figure 11.1 Filter lay-out

As stated above, the crux of a granular filter is to prevent washing away of grains through some upper layer without (extra) pressure build-up. The design can be based on three criteria, see Figure 11.2:

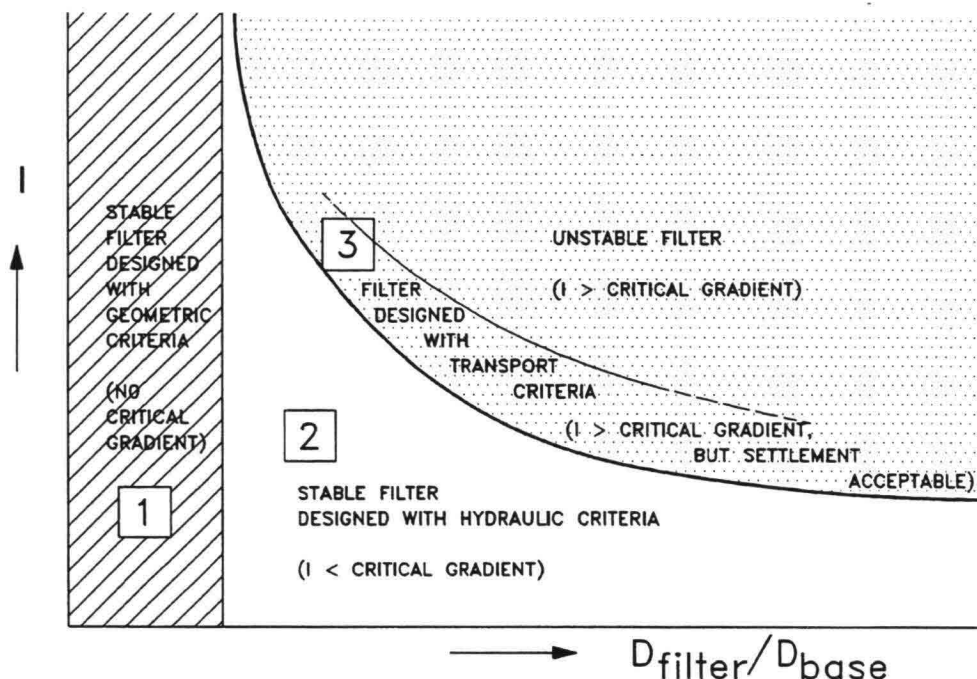


Figure 11.2 Possible design criteria for granular filters

This figure presents the critical gradient in porous flow, above which grains from the base layer are no longer stable under the filter layer, as a function of the relation between some representative diameter of the the two layers. In this figure the following areas can be discerned:

1 Geometrical: These are the classical filter rules derived by Terzghi in the 30's. The permeability and sandtightness are judged solely based on the geometrical properties of the materials, the sieve curves. They are chosen such that grains cannot move in the filter. This often leads to a conservative design, since the filter can stand any load.

(In very dynamic situations, like in breakwaters, there are even more strict geometrical rules, like $W_F/W_B < 15-25$. With $W \propto d^3$, this means $d_f/d_b < 2.5 - 3$, while the rules mentioned here show about twice that value. The practice in breakwater design also has to do with geotechnical reasons: presenting a rough surface for the armor layer.

2 Hydraulic: A critical gradient for which the base material moves through the filter is determined. The grain diameters are chosen such that the critical gradient is larger than the occurring gradients in the structure. So, now the hydraulic loads are taken into account, leading to a more economic design. Permeability is usually no problem anymore, since these filters are more open than the ones designed with the geometrical rules.

3 Transport: Some loss of material is accepted within the limits of acceptable settlements. For many situations, this would lead to an even more economic design. For flow parallel to a filter interface, calculation rules have been established. They are however rather complicated, while there is hardly any practical experience. So, for a preliminary design, the hydraulic design method should be the limit for the time being. For more information, see RWS, 1992.

A - Stability criterion

The prevention of washing out of grains from the base through the filter is based on the fact that the pores between spheres are much smaller than the spheres themselves. From geometry we can find that a sphere cannot pass the pores of spheres that are about 6 times larger, see Figure 11.3.

Translated to "real" material, an often used rule is: $d_{15F} < 5 \cdot d_{85B}$, which says that the 15% smallest particles of the filter should be less than 5 times greater than the 15% largest particles of the base, see Figure 11.3. The idea is then that the coarse particles of the base form a barrier to all other particles; to ensure that, the materials have to be internally stable, which we will discuss later. The stability criterion is sometimes called the piping criterion, since it prevents the washing away of grains like happening in the piping-phenomenon.

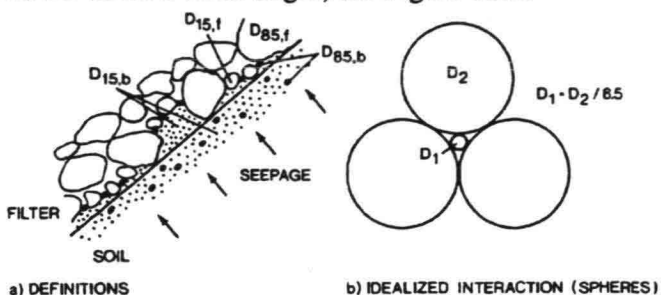


Figure 11.3 Blockage of small particles in large particles

B - Permeability criterion

When the hydraulic gradient over the filter layer is small compared to that over the base layer, the filter is permeable and no pressure is build up under the filter layer. The permeability of a material is dominated by the small particles; to judge the permeability usually the d_{15} of both filter and base is used: $d_{15F} > 5 \cdot d_{15B}$.

D - Internal stability

When a material is widely graded, it is possible that the fine particles are washed out through the pores of the big ones. When $d_{60} < 10 \cdot d_{10}$ this can be prevented. Another possibility for extreme graded materials, is to divide the material into two sieve curves and treat it with the filter rules above.

Equation (11.1) summarizes the criteria and Figure 11.4 shows the first two geometrical rules in relation to possible sieve curves.

$$\begin{aligned}
 \text{Stability:} \quad & \frac{d_{15F}}{d_{85B}} < 5 \\
 \text{Permeability:} \quad & \frac{d_{15F}}{d_{15B}} > 5 \\
 \text{Internal stability:} \quad & \frac{d_{60}}{d_{10}} < 10
 \end{aligned}
 \tag{11.1}$$

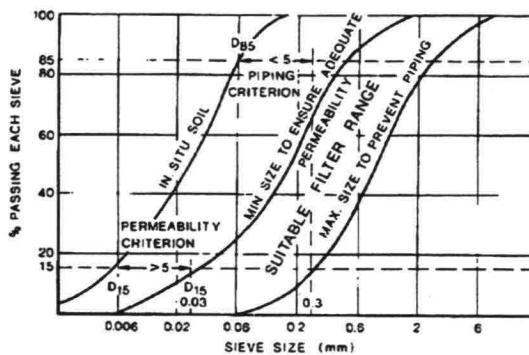


Figure 11.4 Sieve curves, stability and permeability

According to the stability rule d_F should be smaller than $5d_B$ and to the permeability rule larger than $5d_B$. However, the use of two different diameters for the base material in the denominator (the 15% largest and the 15% smallest respectively) gives the margin to design a filter.

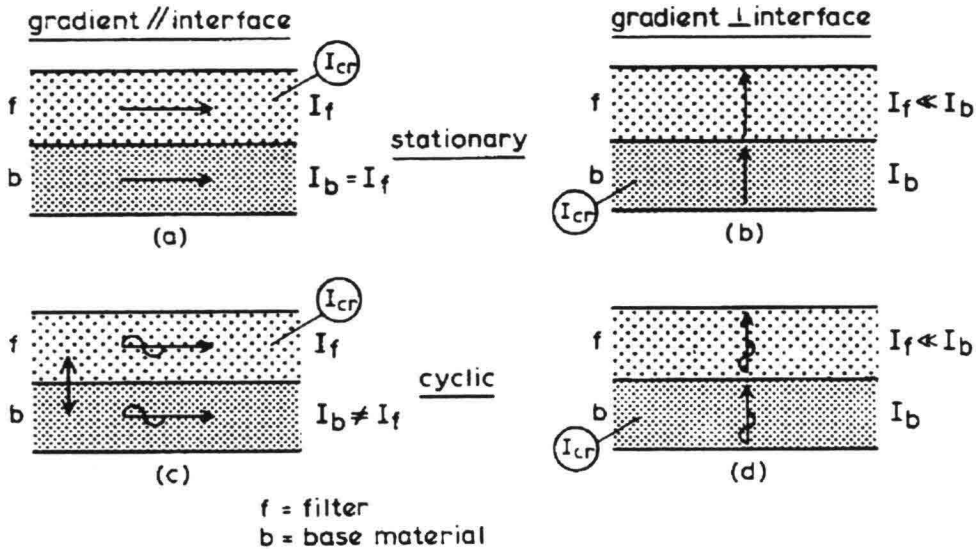


Figure 11.5 Investigated cases and definition of hydraulic gradients

Investigations were done for various loading situations, see Figure 11.5: stationary and cyclic gradients parallel and perpendicular to the interface between filter and base. The gradient parallel to the interface is defined in the filter layer and the gradient perpendicular in the base layer which follows from the nature of the flow. The results of the tests will be discussed briefly.

A - Steady flow parallel to interface

The stability of base material in a flow parallel to the interface of a filter could be seen as the stability of a grain on the bottom of a very small channel. It is an attractive idea to link the formula for porous flow, e.g. the one by Cohen de Lara see chapter 5, with some formula for the threshold of movement, like Izbash or Shields in order to establish a relation for the critical gradient in porous flow. This was tried and partially successful, see de Graauw, 1983, resulting in an empirical relation. The most important parameters appeared to be a diameter of the base material (important for the stability, like in the Shields formula), a diameter of the filter material (important for the flow through the filter) and the porosity of the filter (also important for the flow through the filter as we know from chapter 5). The experimental results finally yielded:

$$I_c = \left[\frac{0.06}{n_F^3 d_{15F}^{4/3}} + \frac{n_F^{5/3} d_{15F}^{1/3}}{1000 d_{50B}^{5/3}} \right] u_{*c}^2 \quad (11.2)$$

in which u_{*c} is the critical shear velocity according to Shields. The two terms in (11.2) come from the idea of a laminar and turbulent part like in the Forchheimer equation, see chapter 5. Figure 11.6 gives a comparison between some computed lines and the experiments. It is seen that for a given ratio of $n_F d_{15F} / d_{50B}$, the critical gradient is greater for fine base than for coarse base material. This could be explained by the lower filter velocities in fine pores.

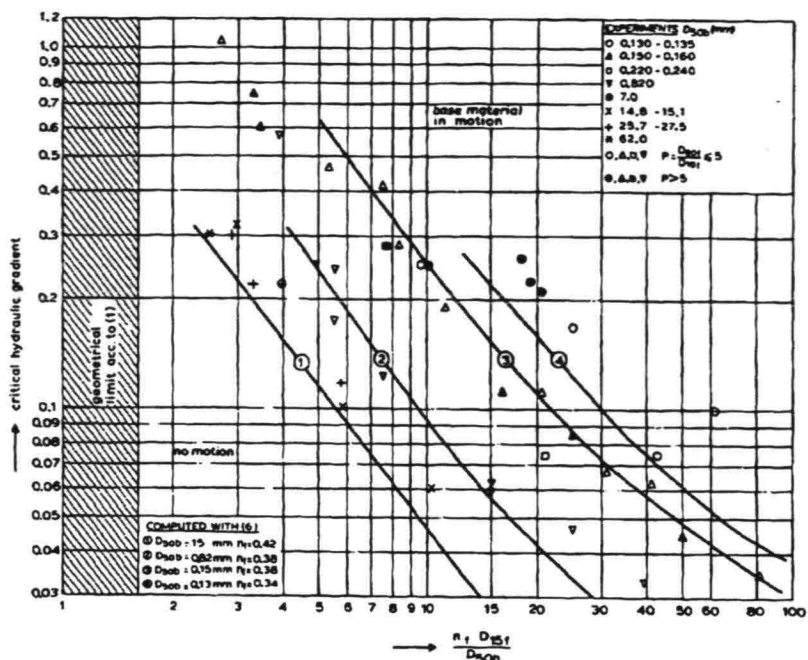


Figure 11.6 Steady parallel flow - critical gradient

B - Cyclic flow parallel to interface

In a pulsating watertunnel, tests were performed to study the critical gradient for cyclic loading. The results, see Figure 11.7, show a larger critical gradient than for steady flow (indicated as $T = \infty$). This is caused by compaction of the filter layer by the cyclic loading, leading to a lower porosity, hence to a more stable filter. This effect is greater for small wave periods, but when the tests are repeated, after being loaded for some time, there is no longer any influence of the period. What remains is a higher critical gradient than in steady flow, due to the same degree of compaction. A smaller period only causes a faster compaction.

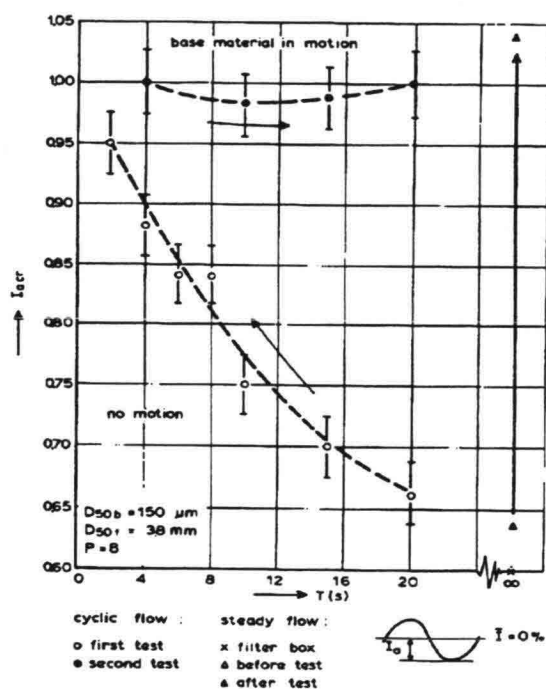


Figure 11.7 Cyclic flow parallel to interface - critical gradient

The final conclusion is that for a cyclic loading parallel to the interface, the same relation as for stationary loading can be applied, while a favourable effect on n_f can be expected.

C - Steady and cyclic flow perpendicular to interface

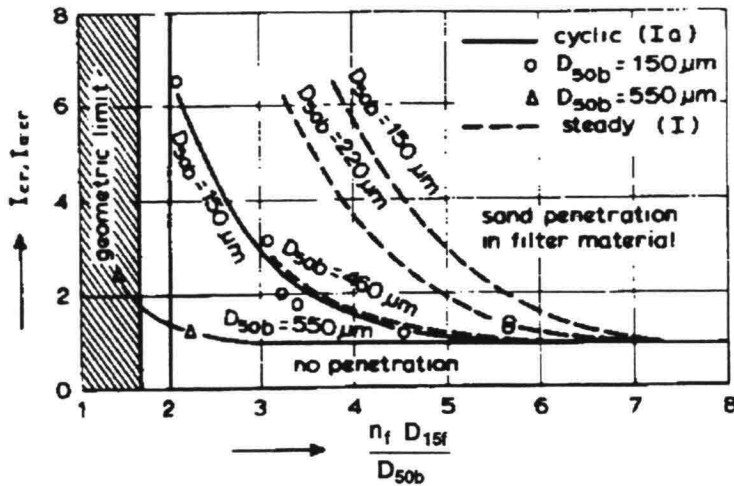


Figure 11.8 Steady and cyclic flow perpendicular to interface - critical gradient

Figure 11.8 shows the results of some tests. The lower limit is always formed by fluidization when the filter grains become so large that the base acts like there was no filter (right hand side in the figure). There is a considerable difference between steady and cyclic loading. The critical gradient for cyclic flow is now much lower than for steady flow and even the geometrical limits are no longer sacred. This can be explained as follows, see Figure 11.9, where $N_f = n_f d_{15f}/d_{50b}$. Even when individual grains are small enough to pass the filter, arching can prevent this (situation in the middle of Figure 11.9). Those arches however, are not stable in reversed flow and in cyclic conditions they can never be formed. For still smaller base particles, arches can not exist even in stationary flow and the material between the filter grains is fluidized as if there was no filter, giving a critical gradient ≈ 1 , like in unprotected soil (situation on the right in Figure 11.9).

This hypothesis was tested by superimposing extra weight on the filter and loading the filter with cyclic pressures on cases 2 and 3. Indeed, a superimposed load gave a very high critical gradient in case 2, indicating that the arches were prestressed and could hold in cyclic loading, while for case 3 there was no influence of extra weight on the critical gradient, see de Graauw e.a.,1983.

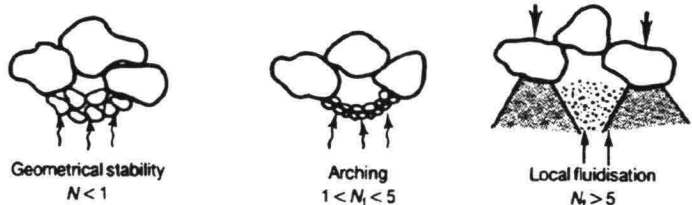


Figure 11.9 Mechanisms in filter action (de Graauw e.a.,1983)

As said, even the geometrical criteria of equation (11.1) did not prevent loss of base material in all cases, see Figure 11.8. As a safe limit for stability in heavy cyclic loading de Graauw,1983 gives $n_f d_{15f}/d_{50b} < 1$ which is about 3 times stricter than equation (11.1). It should be stressed however, that cyclic perpendicular gradients of a few hundred percent are very exceptional. In the case of the Eastern Scheldt storm surge barrier they were caused by the movement of the structure itself under wave action.

In de Graauw, 1983 some more test results are given, e.g. combinations of perpendicular and parallel flow and combinations of steady and cyclic loading. Except for steady parallel flow, no relations have been derived. The tests give some information for particular cases, but they cannot give more than insight in the relevant phenomena (which is already much more than we knew 20 years ago).

For a preliminary design, Figure 11.6 and equation (11.2) are the basis for filter design when there is a gradient parallel to the interface, both for stationary or cyclic flow.

When there is a considerable gradient perpendicular to the interface, the classical geometrical rules according to equation (11.1) can be applied. This is e.g. the case in a part of a structure that serves as a drain to prevent high pressures under a revetment, like in the toe of a dike. Also when wave action can be expected, geometrical criteria should be used in a preliminary design.

In the case of heavy dynamic loading of a filter (e.g. "rocking" of a structure on a filter foundation) and/or cases with combinations of perpendicular and parallel flow, tailored research should be done.

LAYER THICKNESS

To be effective, a filter layer should have a minimum thickness of 2 to 3 times the diameter of the larger stones. For small diameters this is not practical. For coarse sand a minimum thickness of about 10 cm is applied and for gravel about 20 cm. Another criterion could be at least half the diameter of the stones that will come on top of the layer in order to prevent that stones penetrate into the next layer when dumped. Construction of filters needs special attention, especially when built under water. In chapter 13 this will be discussed in more detail.

OPEN CHANNEL FLOW

When stones are used as a bottom protection against overflowing water, the diameter will be much larger than the original bottom. Is a filter necessary in this case? With velocities of several m/s, Chezy-values as low as 30 and a waterdepth of not more than a meter, the gradient in the filter will be hardly more than one percent. Applying filter rules, see equation (11.2), it is found that an extra filter layer will usually not be necessary. But this is uncertain for high turbulence in the flowing water, like in a vortex street over a bottom protection. In that case, turbulence can intrude from above and cause erosion, see Figure 1.10. A sometimes used empirical rule is that when the layer has a thickness of at least 3 to $5.d_{50}$, these turbulences are damped enough to do much harm to the bottom. There is no evidence of this rule being true, but the idea is probably correct that a certain thickness will help to prevent an expensive filter construction. This is applied in the so-called falling aprons, see paragraph 12.2.4 When this item really matters for the stability of a construction, experiments will be necessary. Another point to be aware of, is the question whether there is really no other gradient "active" at the interface beside the water flowing over the protection layer. In the case of a groyne, for instance, there is a head difference of about $u^2/2g$, hence a gradient parallel to the interface between groyne and original bed.

11.2.1 INTRODUCTION

Geotextiles have become more and more important in civil engineering. They are used in armouring soil in foundations and slopes, as membranes to prevent seepage or to protect the environment against pollution from a dump area and as filter in hydraulic engineering. The latter is the subject in this paragraph. Geotextiles come in many shapes, depending on the production technique. The two main types are woven and non-woven. See annex A. A possible disadvantage of geotextiles can be the weathering e.g. by ultra-violet light, wear and tear by chemical, biological or mechanical processes. These aspects are outside the scope of these lecture notes. For an extensive treatment of geotextiles the reader is referred to Veldhuijzen van Zanten,1986.

Like in granular filters, the two hot items are again sandtightness and permeability. Another similarity is the existence of geometric filter rules and hydraulic criteria. But, since geotextiles are relatively new compared to granular filters, at this moment there are not yet reliable hydraulic criteria and geometric criteria still have to be applied. But even then, geotextiles have given a breakthrough in filter design, both in cost effectiveness for large projects and in possibilities to design a sandtight filter with a limited height, see Figure 11.10. This is especially useful in cases where there is no space for a granular filter of many layers or where it is difficult to construct such a filter.

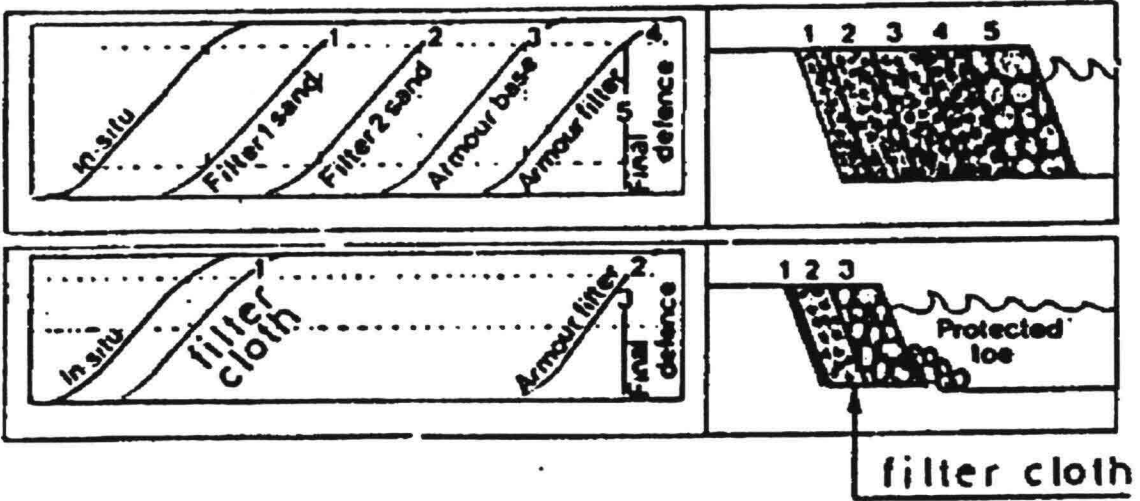


Figure 11.10 Possible effectiveness of geotextile in filter

The geotextile in this figure is completely responsible for the filter function. The main functions of the layer between the top layer and the geotextile is to prevent damaging the geotextile by individual large stones and to prevent flapping of the cloth, possibly causing losses of the base material.

Like in granular filters, the relation between the magnitude of the base material and the holes in the filtertextile is the dominating factor for sandtightness. To characterize the openings on the textile, a kind of reversed sieve test is executed with very uniform grains of different and known diameter. The textile is used as a sieve in a standardized procedure (which can be done in many ways, see Veldhuijzen van Zanten,1986; here the Dutch procedure as developed by DHL is presented). When X % of the grains with a certain diameter remains on the textile, that diameter is taken as O_x . 100 - X % passes the "sieve", this is the reversed definition of a normal sieve procedure! Figure 11.11 gives the result of such a test. Important numbers in sandtightness are O_{90} and O_{98} , sometimes named O_{max} , a measure for the largest holes in the textile.

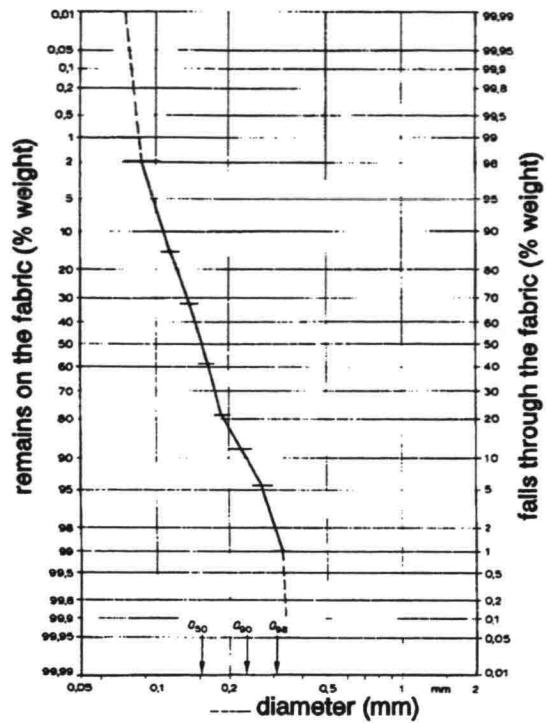


Figure 11.11 Definitions openings geotextile

The filter rules for geotextiles are:

FLOW SITUATION	BASE MATERIAL	FILTER RULE
Stationary	--	$O_{90} < 2 \cdot d_{90}$
Non-stationary	Internal stable ($d_{60}/10 < 10$)	$O_{98} < 2 \cdot d_{85}$
Non-stationary	Internal not stable	$O_{98} < 1 \cdot d_{15}$

The most strict geometrical filter rule is that the smallest particles cannot pass the largest opening in the textile. This should be applied when the filter is cyclically loaded and no loss of material is accepted. In many situations, some loss of fine material is not detrimental to the functioning since a small layer under the textile can act as part of the total filter system, see Figure 11.12. The finer parts are washed through the textile the coarser particles act as a filter for the remaining soil, provided the subsoil is internally stable, see granular filters.

1. original soil structure
2. filterzone
3. washed out filterzone
4. geotextile
5. cover layer

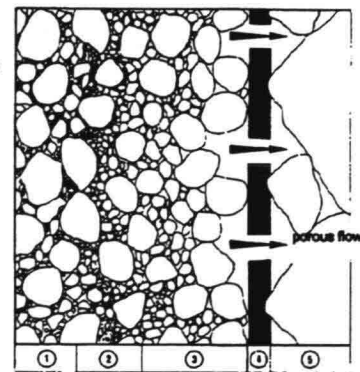


Figure 11.12 Geotextile with internal stable base

This mechanism can also work under cyclic conditions, provided the subsoil is not loosely packed and the textile is pressed on the subsoil by the first coverlayer.

These criteria are geometrical with the loading situation taken into account, but not the magnitude of the gradients. For cases with low gradients, say less than 100 %, these demands seem too strict. DHL has been testing geotextiles with a stationary gradient parallel to the interface, analogous to the tests that lead to equation (11.2). No reliable relation has been established yet, see vdKnaap, 1986.

11.2.3 PERMEABILITY

The permeability of a geotextile can be measured in the same way as for soils, using Darcy type relations. A parameter often used to characterize the permeability of geotextiles is the permittivity:

$$\psi = \frac{u_f}{\Delta h} = \frac{k}{e} \tag{11.3}$$

in which Δh is the head difference, e is the thickness of the geotextile and k the "normal" permeability coefficient. ψ can be seen as the permeability per m thickness of geotextile.

Usually, a geotextile is more permeable than the subsoil, but two factors can decrease the permeability: blocking and clogging.

Properties 209



Figure 6.84. Blocking mechanism.

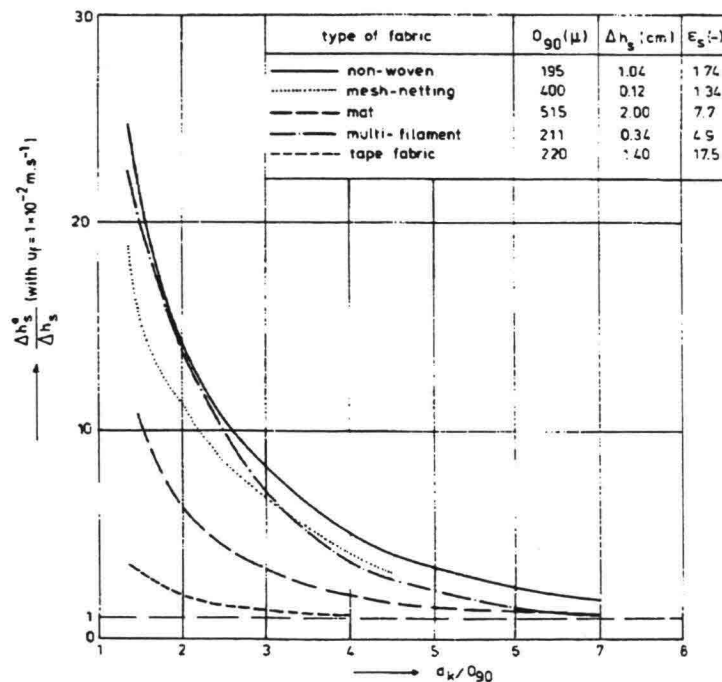


Figure 11.13 Blocking of geotextile (Veldhuijzen van Zanten, 1986)

Blocking is the phenomenon that large particles seal the openings in the textile. In that case, the permeability can decrease dramatically as is shown in Figure 11.13 where a very uniform base material is used in permeability tests (all grains have about the size d^k). When the diameter of the base material has the same order of magnitude as the O_{90} , the head difference over the textile can increase a factor 10-20. Note that not every type of textile is equally sensitive to this phenomenon. Since a relation of $d_k/O_{90} \approx 1$ comes in the range of the demands for sandtightness, this is something to examine more critically.

More important than the relative increase of head difference over the textile, is the absolute value. This determines whether a protection is pushed away from the interface or not. Since geotextiles are usually rather thin, the total pressure drop can remain limited. For a gradient of 200 % perpendicular to the interface, this is presented in Figure 11.14:

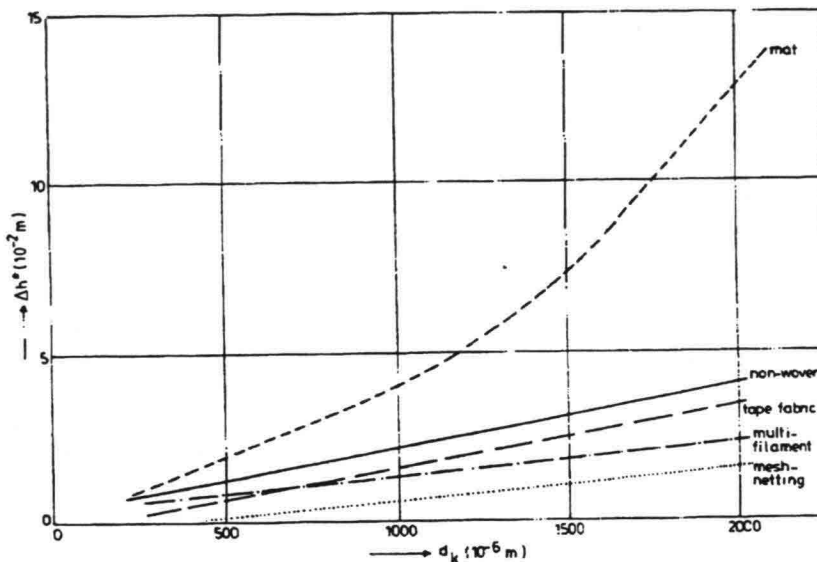


Figure 11.14 Pressure drop over blocked fabrics on uniform sand filters, $I = 200 \%$

The pressure drop has a magnitude of less than a decimeter. This means that the superimposed load of a normal cover layer on a geotextile is much greater than this pressure drop. Moreover, it should be mentioned that in practice the grains of the base are not so uniform as in these tests, making the chance of blocking of all openings very small.

Clogging is the trapping of (very) fine particles in the openings of the textile, leading also to a decrease of permeability. This can happen in water contaminated with chemicals, e.g. iron. In contrast with blocking, clogging is a time dependent process. The idea is that it stabilizes at a certain level after a certain time, but not much experimental evidence is available to support this thesis. It should be realized that clogging is not special for geotextiles; it also occurs in granular filters.

A general rule is that when the permeability of the textile is 10 times greater than that of the subsoil, there is no problem, not even with blocking or clogging. However, when used in very contaminated groundwater, one should examine the possibility of severe clogging. When the danger of blocking or clogging can be excluded, a permeability factor of 2 or 3, is sufficient.

11.3

STABILITY OF SLOPES

11.3.1

MACRO-STABILITY

The stability of a slope as a whole is usually indicated as the macro-stability, in contrast with the micro-stability, dealing with the outermost grains on a slope. Within the framework of these lectures, this kind of stability plays a role at banks, dikes and scour holes.

In general, the stability is a matter of equilibrium between the weight of the soil including pore water (the loading) and the shear stresses. The shear strength is given by, see Figure 11.15:

$$\tau = c + \sigma \tan \phi \quad (11.4)$$

The effective grain-stresses (σ) are influenced by the pore water pressures, so pore water influences both the loading and the strength.

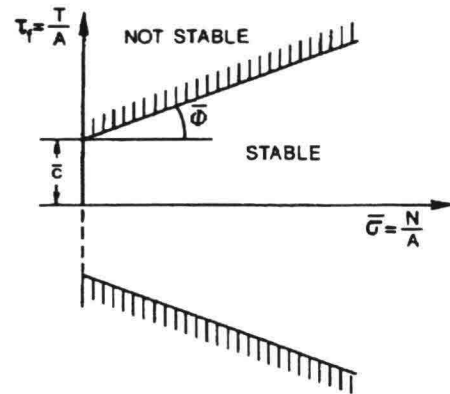


Figure 11.15 Normal vs shear stress

Figure 11.16 gives a picture of the stability of the slope of a dike. The shear strength along a possible sliding-circle should withstand the weight of the soil-mass above the circle, expressed as the equilibrium of moments around the center of the sliding circle. A critical situation occurs after high sea levels when the waterlevel suddenly drops and the slope is filled with water and heavy, increasing the load while the outflow of water decreases the strength.

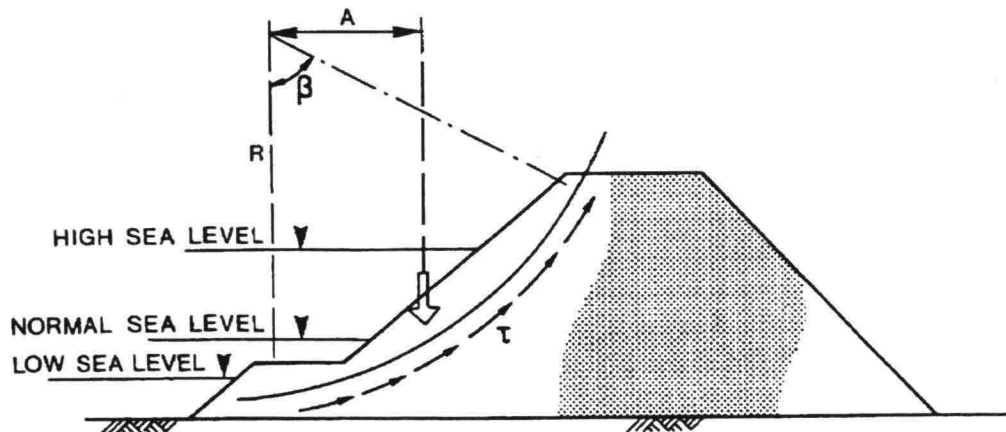


Figure 11.16 Stability of dike slope

There are methods that calculate the stability of the sliding-circle as a whole, assuming a constant τ along the circle. Since τ is directly related to σ , it will be clear that the shear along the slope is not constant.

In a homogeneous soil mass, the assumption of a sliding-circle is reasonable, but when there is a considerable inhomogeneity in the soil, the sliding will take place along the weakest layers, where c and/or $\tan\phi$ are low, hence the shear strength is low, see Figure 11.17. The same can occur when σ is low due to high pore pressures.



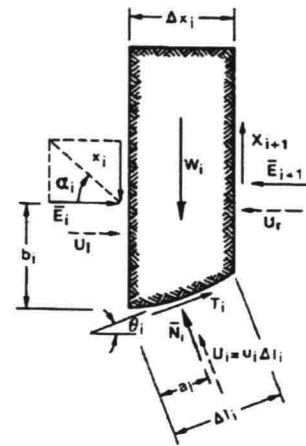
There are many calculation models for simple and complex situations, the latter mostly based on finite element methods. A relatively simple method will be shortly described here: the Bishop method of slices.



Figure 11.17 Sliding zones

BISHOP'S METHOD

In this method the slope above the sliding-circle is divided into vertical slices and the equilibrium of each slice is considered, see Figure 11.18. On the sides of each slice, normal and shear stresses are acting. The basic assumptions of Bishop's method are that the forces on the vertical sides have no vertical resultant force and that the forces on the sliding-surface can be found by considering the vertical equilibrium of forces, see Figure 11.19.



So, R and L (being the total forces acting on the right and left hand side of the slice) need not to be known. The pore pressure u_i has to be known, e.g. from a flow net.

Figure 11.18 Forces acting on a slice

The method is done for various sliding-circles and the results are usually presented as safety coefficients, F , defined in terms of moments about the center of the sliding-circle:

$$F = \frac{M_s}{M_w} = \frac{\text{Moment of shear-resistance}}{\text{Moment of weight}} \quad (11.5)$$

$$M_s = R \sum_{i=1}^{i=N} (\sigma_i \tan \phi + c) \Delta l_i = R (\tan \phi \sum_{i=1}^{i=N} N_i + cL) \quad (11.6)$$

$$M_w = R \sum_{i=1}^{i=N} W_i \sin \theta_i \quad (11.7)$$

F finally becomes:

$$F = \frac{\tan \phi \sum_{i=1}^{i=N} N_i + cL}{\sum_{i=1}^{i=N} W_i \sin \theta_i} \quad (11.8)$$

The vertical equilibrium is then calculated, see Figure 11.19, assuming that the total F is also valid for a slice ($F = 1$ in Figure 11.19):

$$W_i = N_i \cos \theta_i + U_i \cos \theta_i + \frac{T_i}{F} \sin \theta_i \quad (11.9)$$

with:

$$\begin{aligned} \Delta l_i &= \frac{\Delta x_i}{\cos \theta_i} \\ U_i &= u_i \Delta l_i \\ T_i &= \tau_i \Delta l_i \\ N_i &= \sigma_i \Delta l_i \end{aligned} \quad (11.10)$$

With equation (11.4), N_i is the only unknown in equation (11.9). N_i becomes after elaboration:

$$N_i = \frac{W_i - u_i \Delta x_i - \frac{c \Delta x_i}{F} \tan \theta_i}{\cos \theta_i \left[1 + \frac{\tan \theta_i \tan \phi}{F} \right]} \quad (11.11)$$

Note that a larger u_i leads to a smaller N_i and hence to a smaller τ . So, a high pore pressure has an unfavourable influence on macro-stability.

With equation (11.11) and (11.8), F can be computed iteratively. As said before, this is done for several sliding-circles, searching the minimum value for F. Figure 11.20 gives the result of such computations leading to a minimum $F = 1.43$ for this case. (Note: every point represents several concentric sliding-circles; only the minimum value is presented.)

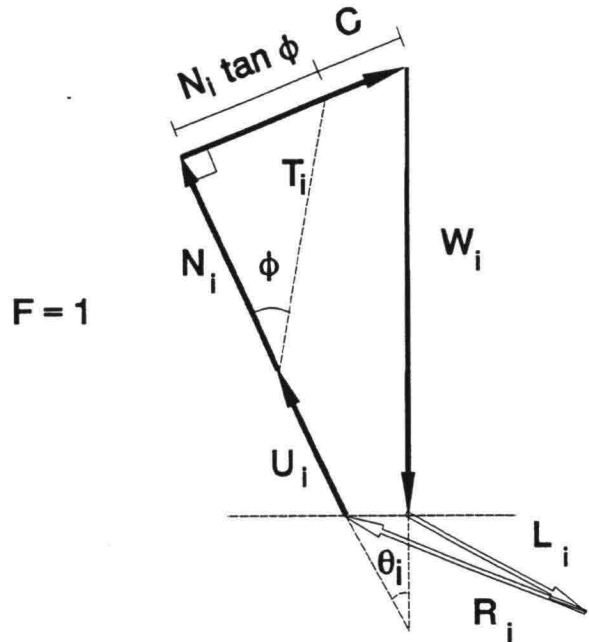


Figure 11.19 Vertical equilibrium of forces

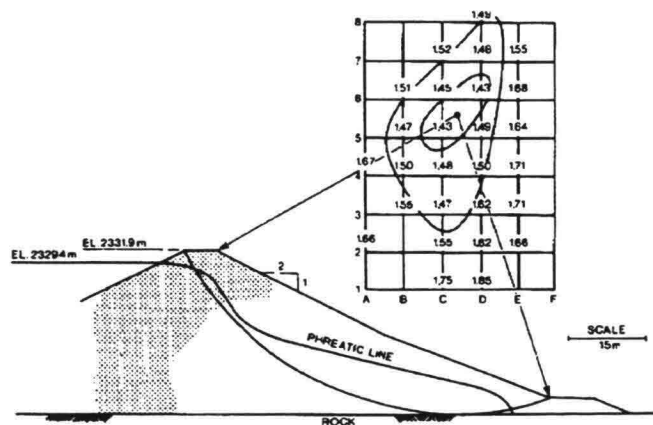


Figure 11.20 Contourlines of safety factor

The equilibrium of grains on a slope in flow or waves has been discussed before, but the attack now comes from the inside of the slope. Here we cannot consider the stability of a single grain, since we have averaged the flow over all pores by means of u_f , see paragraph 5.1. By doing so, we have given up all information on velocities in the pores and instead, we consider a volume of soil. From chapter 5 we know that the porous flow force on a unit volume F_w is equal to $\rho_w g I$. When θ is the angle between the porous flow direction and the horizontal, see Figure 11.21, the flow force along the slope is $F_w \cos(\alpha - \theta)$ and $F_w \sin(\alpha - \theta)$ perpendicular to the slope. The gravity forces on the soil are $(\rho_{SAT} - \rho_w)g \sin \alpha$ along the slope and $(\rho_{SAT} - \rho_w)g \cos \alpha$ perpendicular to the slope, where ρ_{SAT} is the specific mass of saturated soil. The equilibrium then becomes:

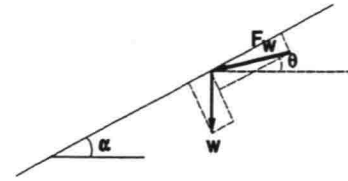


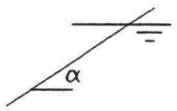
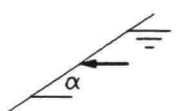
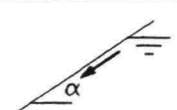
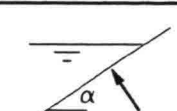
Figure 11.21 Porous flow and equilibrium on slope

$$[(\rho_{SAT} - \rho_w)g \cos \alpha - I \rho_w g \sin(\alpha - \theta)] \tan \phi \geq (\rho_{SAT} - \rho_w)g \sin \alpha + I \rho_w g \cos(\alpha - \theta) \quad (11.12)$$

from which follows, with $\rho_{SAT} \approx 2000 \text{ kg/m}^3$:

$$\tan \phi \geq \frac{\sin \alpha + I \cos(\alpha - \theta)}{\cos \alpha - I \sin(\alpha - \theta)} \quad (11.13)$$

For some special cases the equilibrium condition leads to:

Situation	I	θ	Stability
a - No porous flow; dry or wet slope 	0	-	$\alpha \leq \phi$
b - Horizontal seepage 	$\tan \alpha$	0	$\alpha \leq \phi/2$
c - Seepage parallel to slope 	$\sin \alpha$	α	$\tan \alpha \leq (\tan \phi)/2$ (For small α equal to case b)
d - Seepage perpendicular to slope 	I	$\alpha - 90^\circ$	$\sin \alpha / (\cos \alpha - I) \leq \tan \phi$ (For $\alpha = 0$: $I = 1$; Fluidization)

In paragraph 5.2.1 it was mentioned that there is always a seepage surface on a slope where water flows out. Then, with $\phi = 30^\circ$, this leads to $\alpha \approx 15-16^\circ$ or a slope of 1:3.5 (case b or c)

In chapter 10 on stability in waves, it was mentioned that pressures under an impervious revetment due to waves, usually can be neglected. The phenomenon goes too fast for a considerable deformation of the layer. When there are considerable waterlevel fluctuations, pressures from inside become very important (in contrast with relative open revetments like placed blocks; for these protections, waterlevel fluctuations are too slow, the phreatic level can follow the drop in waterlevel outside, see also chapter 12 for a review of revetment types and loads).

The pressure under an impervious revetment can be derived from one of the methods as discussed in chapter 5. There are two mechanisms that can influence the stability of the revetment:

Shear - the friction between protection and subsoil becomes smaller than the component of the weight parallel to the slope due to overpressure

Float - the component of the weight perpendicular to the slope becomes smaller than the pressure under the protection

It is clear that both mechanisms are branches of the same tree; the first occurring at a lower pressure than the second.

Figure 11.22 shows the forces on a part of a layer. The weight per unit area is: $W = d \cdot \rho_M \cdot g$
The component parallel to the slope: $W \sin \alpha$ and perpendicular: $W \cos \alpha$. The effective pressure on the slope is: $W \cos \alpha - P$.

The layer is stable against shear when:

$W \sin \alpha < f \cdot (W \cos \alpha - P)$, giving:

$$d \geq \frac{fP}{\rho_M g (f \cos \alpha - \sin \alpha)} \quad (11.14)$$

The layer is stable against floating when:

$W \cos \alpha > P$, giving:

$$d \geq \frac{P}{\rho_M g \cos \alpha} \quad (11.15)$$

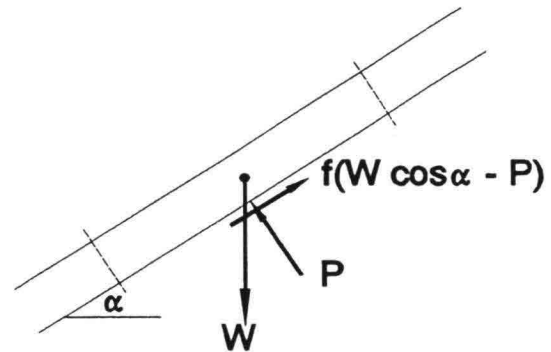


Figure 11.22 Equilibrium of layer

When the first criterion is violated, part of the layer is going to hang on the upper part of the protection or is going to lean on the lower part. This can lead to fatigue and should not happen too often. Dependent on the strength of the layer, this should not happen in situations with a frequency of occurrence in the order of magnitude e.g. of weeks.

The second situation is worse, sand can move under the protection when it is lifted and the layer can deform. Instability however, occurs at greater P (since $f/(f \cos \alpha - \sin \alpha)$ is usually larger than $1/\cos \alpha$, check for yourself). This criterion should be met in design circumstances, e.g. a fast drop of waterlevel after a storm.

Note: When $\alpha = 0$, both equations lead to the same (floating) criterion. This situation occurs with an impervious bottom protection downstream of a structure, see also section 8.4. In that case the protection should be heavy enough to withstand a chosen design head difference.

Up to now we have been talking about loads and strength of protection materials, but that has not learned us yet how a protection looks like. How long, how high, what shape, how to begin and to end them are questions that will be discussed in this chapter.

12.1

SHORE PROTECTIONS

Figure 12.1 shows some ways to defend an erodible coast. Artificial sand supply (example A) is an interesting and sometimes cheap solution, where the "natural" look of a coast can be preserved. It is outside the scope of these lectures; see the lectures on coastal morphology.

Detached breakwaters and groynes (B and C) are both meant to influence the coastal sediment transport. Groynes are only effective in longshore transport, while detached breakwaters ("tombolo") can be effective both along and perpendicular to the coast. When they are stretched along the whole coast, they act mainly as a wave reductor (see chapter 8). The constructional aspects will be mentioned in this paragraph, while the morphological effects are again part of coastal morphology. For construction details, see also the lectures on breakwaters in ports.

Dikes and seawalls are really artificial coasts. They are much alike, but a seawall is usually made when there is little space, e.g. in an urban environment. The construction of a seawall itself (made of concrete or brick) will not be elaborated here. In front of the seawall, a bottom protection is usually necessary, see paragraph 12.3

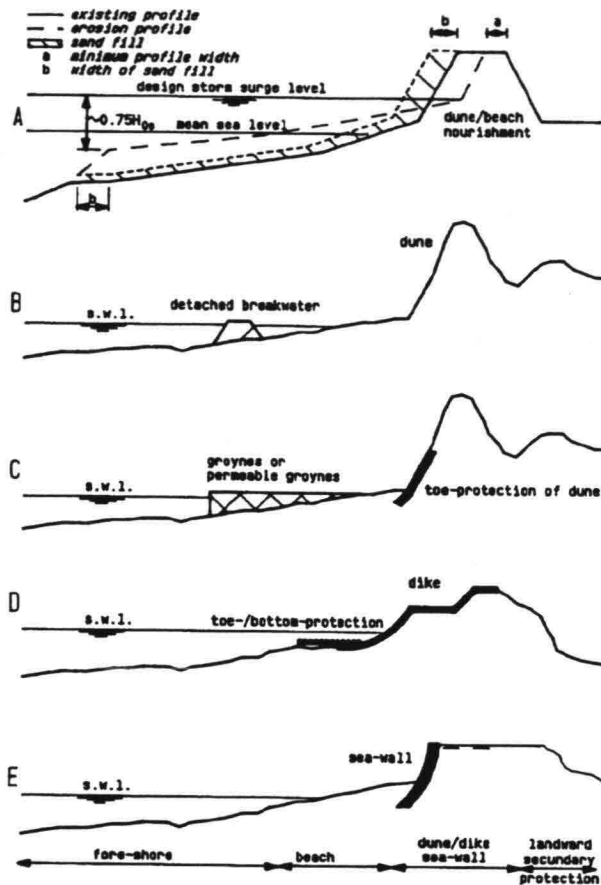


Figure 12.1 Examples of shore protection (Pilarczyk, 1990)

The focus will be now on the more or less flexible constructions, like dike revetments. First we will discuss some general aspects of the shape of the protection and the problems related to the various revetment types. Next, attention will be given to transitions in protections, which are only too often neglected in the design. Finally, groynes and the like will be reviewed shortly.

LIMITS

The upper and lower limits of a protection on a slope are determined by the loads. Figure 12.2 gives an example of an upper limit which was clearly not well-considered. The cover layer as such seems alright and also the filter design has been given attention. But the run-up of the waves is such that they attack the area on top where there is no cover and where the filter layers cannot stand the wave forces. Even the original unprotected soil is eroded by the waves and a total collapse is the result. The protection should either be made higher or strong enough behind the top to withstand the loads.

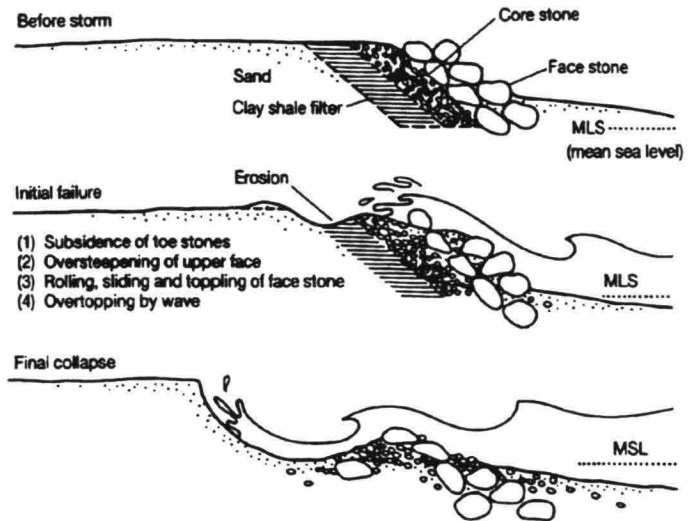


Figure 12.2 Ill-designed upper limit

Usually the lower limit of a protection on a slope is taken $1.5 H_s$ to $2 H_s$ below SWL, see Figure 12.3. In a tidal area, SWL of course can vary considerably, which has to be taken into account. Below the lowest waterlevel, the protection can be dimensioned for possible currents. In relatively shallow water, which is often the case, the protection extends to the toe of the slope. The upper limit can be taken as the $R_{2\%}$, although the protection in the uppermost half is not necessarily as heavy as around SWL.

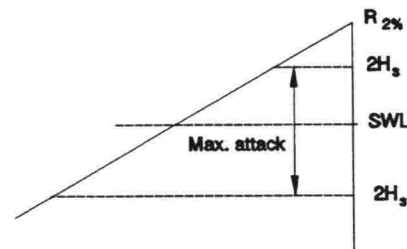


Figure 12.3 Limits of protection

BERMS

A berm in a slope can be constructed to reduce wave run-up or for very practical reasons like a road for maintenance. When the macro stability of a slope gives problems, a berm can act as a support. From an overall view of stability, a berm makes a slope look like an S-profile, which is the equilibrium profile under wave attack, see Figure 12.4. So, a berm is sometimes advocated as the natural, strong design. But a berm also introduces transitions, being weak spots in a revetment. So, unless there is any other urgent reason, it seems good practice to avoid them.

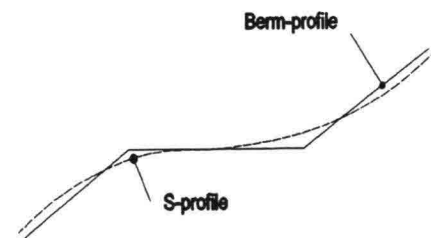


Figure 12.4 Berm and S-profile

In chapter 9 through 11 we have seen how the strength of various materials relate to the various loads. The following reviews the importance of the loads for each type of revetment.

Revetment type	Waterlevel fluctuation (hours)	Waves (seconds)	Wave impacts (s/100)
Stones, rip-rap etc.	0	XXX (velocity field)	0 (except subsoil)
Placed blocks	0	XXX (pressures)	0 (except subsoil)
Impervious layers	XXX	0	XX
Grass on clay	X	XXX (velocity field)	X

0 means hardly or not important, while the number of crosses is a measure for the relative importance. Loose stones are too permeable for slowly varying waterlevel fluctuations, while wave impacts will do no harm to the stones (they are already broken); the subsoil can liquefy (see paragraph 7.4.2) when it is not compacted. For placed blocks the situation is more or less the same, only the mechanism of failure in wave attack is completely different. Impervious layers are very sensitive to waterlevel fluctuations; the phreatic level can not follow a sudden drop. This would be true all the more for waves, but these are again too fast to lift the layer, because there can be only a very limited flow to where the layer is lifted. The very fast wave impacts now can damage the layer due to stresses in the material. Grass is sensitive to all wave action on the slope and is not used in the zone with maximum wave-attack, while a clay layer may be relatively impervious, so waterlevel fluctuations can cause some problems.

These differences depend on the local load situation and result in a comparative design resulting in costs. Beside costs there are other reasons to choose or to reject a revetment type. Some of them are summarized in the following; for more information, see TAW, 1987 where for 28 materials in various applications, a checklist for the choice is given. Criteria to use can be:

A - Strength: Every construction can be designed strong enough, but a material with a steep damage-load curve is less favourable because of the possibility of progressive failure. See also chapter 14.

B - Flexibility: When settlements or scour plays an important role, a construction that preserves its strength while it follows the changes can determine the choice.

C - Construction: Easy and fast construction can mean lower costs; sensitivity for tolerances can play an important role here.

D - Maintenance: How easy is it to inspect or to repair a (part of a) construction?

E - Sustainability: How does the material react to physical, chemical or biological processes; it should not age too easily.

F - Environment: How well does the protection fit in its environment, what other functions have to be fulfilled?

G - Recreation: A concrete slab is not the ideal place for a pick-nick.

Special attention should be given to transitions because they often form the Achilles heel of the protection; most damage starts at transitions. When we compare a protection to a roof of a house, the leakage is almost never in the roof itself, but in the transitions between roof, chimney, wall, ridge etc. Transitions can have both a reduced strength and an increased load (see Figure 12.5): due to the strip, the pressure gradient in the filter layer can increase while due to a difference in settlement between strip and blocks there can be a hole. Therefore they should be avoided as much as possible, at least in the area of maximum attack.

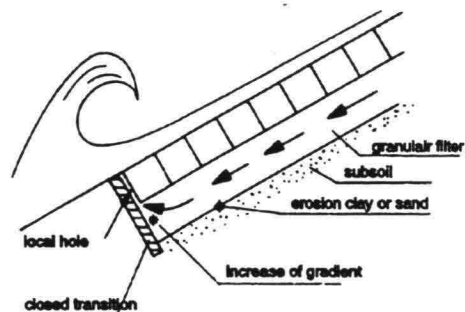


Figure 12.5 Increased load and reduced strength

It is however impossible to avoid them completely, because it is very expensive to use the same protection (designed for the maximum attack) along the whole slope. Also in the case where an existing protection has to be extended, a transition can not be avoided. Sometimes, transitions are advocated because they can limit damage to certain areas. This is possibly true, but the damage is an indication that the revetment as such is not good enough.

The ideal transition is equally strong, flexible and sustainable as the adjoining layers. Since this ideal is never reached completely, at least the following should be given attention:

1 - relation permeability-overpressure. If it is impossible to maintain the same permeability and the transition induces extra pressure, the transition should be dimensioned to withstand it.

2 - sandtightness a. Never allow a seam that goes through the whole protection, always make some overlap, avoiding loss of material through seams, see Figure 12.6.

3 - sandtightness b. Transitions are not only important in the toplayer, but in the filter as well. Figure 12.6 gives an example of an incorrect transition where clay can penetrate in the filterlayer under the blocks.

4 - care. Probably the most important. Give extra attention during construction, inspection and maintenance to transitions.

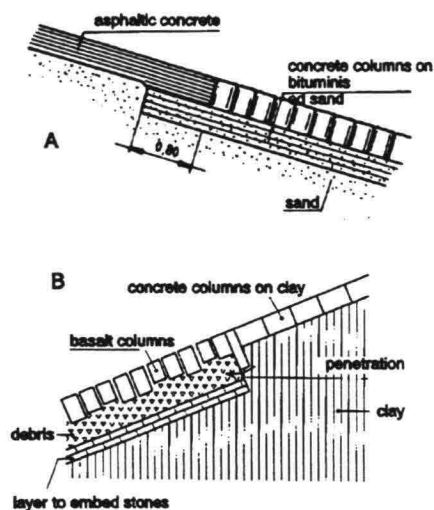


Figure 12.6 Sandtightness in transitions

It is impossible to give rules for all situations; much depends on the local situation with regard to loads, available materials, experience etc. Some general cases are presented here; for more information, see CUR/TAW,1992.

OPEN - OPEN

As said before, it is important to prevent a seam through the whole protection by continuing the filter layer, see Figure 12.6. This however, can cause a new problem. When there is a considerable difference in permeability (or leakage length), the pressure under the least permeable revetment can lead to uplifting. In the figure this is the case for the lower placed blocks, which get much more pressure via the rip-rap layer. The solution can be the penetration of the upper meter of the rip-rap, hindering the wave penetration.

When the transition is at the point of a changing slope-angle, e.g. at a berm, provisions should be made to assure a proper placing of rectangular blocks. This can be done by placing a concrete beam with an adapted shape, see Figure 12.7.

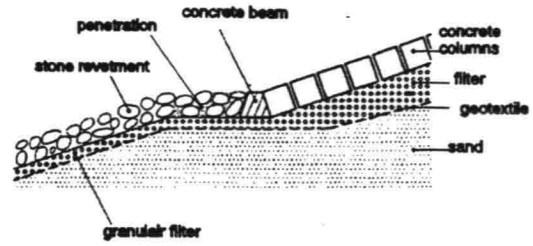


Figure 12.7 Transition open-open

OPEN - CLOSED

When the filter layer is continued under the closed layer in order to avoid a seam, the closed layer has to be made thicker to withstand the extra (wave) pressure, penetrating through the filter layer under the closed layer.

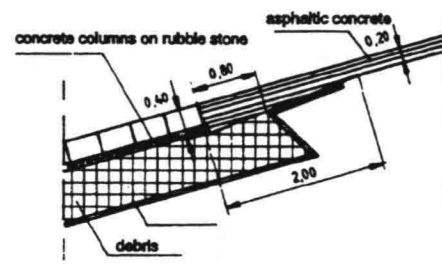


Figure 12.8 Transition open-closed

CLOSED - CLOSED

A filter is usually not necessary here. The most important is to avoid a leak at the transition. With overpressure this would lead to loss of soil material. Figure 12.9 gives an example of a transition from asphalt to clay.

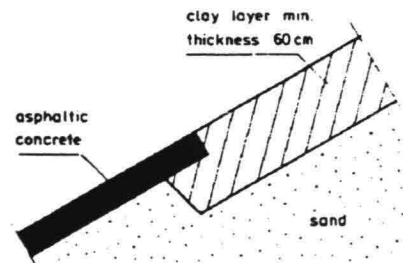


Figure 12.9 Transition closed-closed

PROTECTION - VEGETATION

This transition is often necessary for the upper limit of a protection. An abrupt transition can give a seam, aggravated by grazing cattle and the fact that the roughness is different, giving an extra load in wave run-up. Therefore a gradual transition is preferable, possibly with open blocks through which grass can grow, see Figure 12.10.

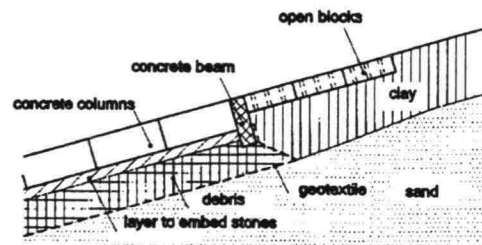


Figure 12.10 Transition protection-vegetation

Toes are a special kind of transition, i.e. from a slope to a horizontal part. The primary function is the support of the revetment. When the friction along the slope becomes too little, either due to a drop in the waterlevel or to waves, the toe has to deliver the resisting force. So, it should be able to withstand a horizontal force. In rock bottom this is very easy and very much like the connection of two wooden roof beams, see Figure 12.11.

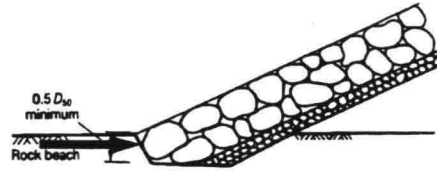


Figure 12.11 Toe in hard bottom

In soft(er) bottoms, toes are often made of piles, sheet piles, strips or combinations. It should be remembered that those can only give a reaction force by means of passive soil pressure for which some displacement is necessary, leading to deformation of the revetment, leading to seams etc. Therefore when considerable sliding forces can be expected, a layer of stone in front of the toe might help, see Figure 12.13.

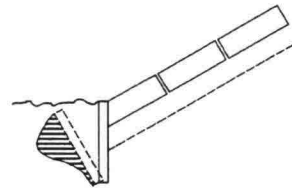


Figure 12.12 Toe in soft bottom

When the toe is threatened by scour, some bed protection is needed, like a mattress covered with stones, which can be also useful for the above mentioned horizontal forces.

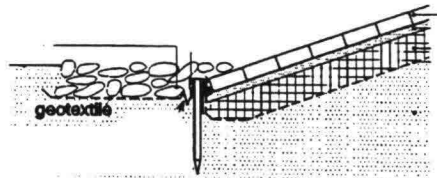


Figure 12.13 Scour protection at toe

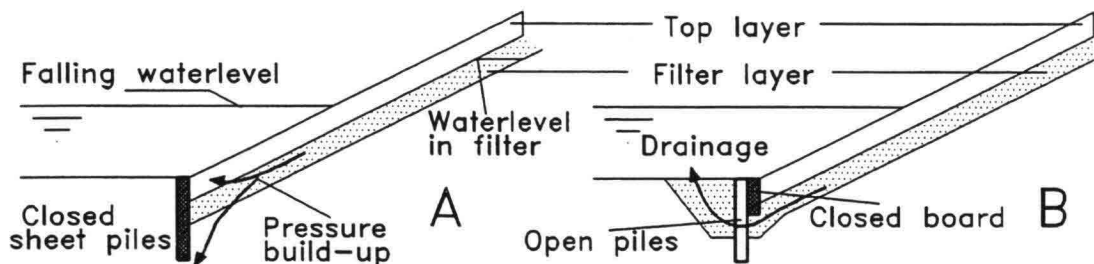


Figure 12.14 Overpressure at toe

When the toe consists of a closed layer or is constructed with sheet-piles, the pore pressure under it can form a threat to the soil directly beside the toe, see Figure 12.14 a. The solution can be a combination of piles, a strip and some granular filter with enough space between the piles to let the pressure escape, see Figure 12.14 b.

As said in the introduction of this paragraph, groynes are only effective when a coast erodes due to longshore sediment transport. With transport perpendicular to the coast, groynes do not have any positive contribution at all. This again shows that knowledge of the morphological process is of utmost importance. When applied, groynes stretch from the upper part of the beach (preventing outflanking which can lead as far as to the toe of the dunes) till the necessary depth, which depends on the sediment transport and the width of the beach that is wanted. Lengths of 25 to 100 m outside the low water line are normal. To be effective, the distance between them should be 1 to 3 times the length.

In general the groyne should not be made too high, in order to prevent unnecessary blocking of currents (scour!) and wave attack. To give an idea: 0.5 to 1 m above the wanted beach level. In that case the zone of attack goes up and down with the waterlevel, see Figure 12.15 type 1. When the groynes are necessary to keep the current from the shore at high waterlevels, the crest will be about horizontal; in that case the attack is concentrated at the head and provisions against scour at the head should be taken (Figure 12.15 type 2)

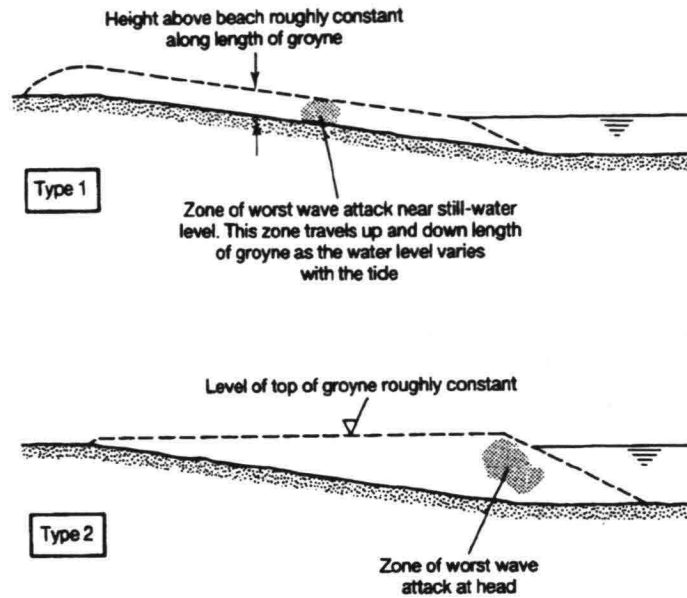


Figure 12.15 Longitudinal profiles of rock groynes

A simple type 1 groyne is given in Figure 12.16. On a mattress (either made of natural material or geotextile), penetrated stone is used. Penetration is beneficial here: the stability of the stones is increased tremendously, while large overpressures due to head differences are not to be expected (of course a check on stability of the whole layer in waves is necessary, see paragraph 10.2).

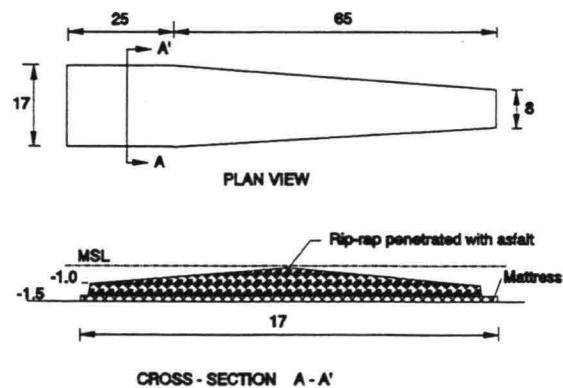


Figure 12.16 Example type 1 groyne

A type 2 groyne is very much like a breakwater, see Figure 12.17 for a typical example. The geometrical filter rules should be followed here because of the severe dynamic loading, see paragraph 11.2.

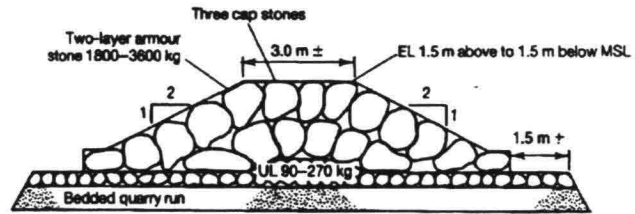


Figure 12.17 Example type 2 groyne

Sometimes, pile rows are used for type 2 groynes. They can be relatively cheap when there is a large tidal difference, since a lot of material is needed when the groyne is build completely with rock. Playing with the configuration of the piles can give some relief for the scour at the head when a gradual change in spacing between the piles is applied. To be effective however, the piles should be very close and a scour protection at the head is indispensable. Figure 12.18 gives an example.

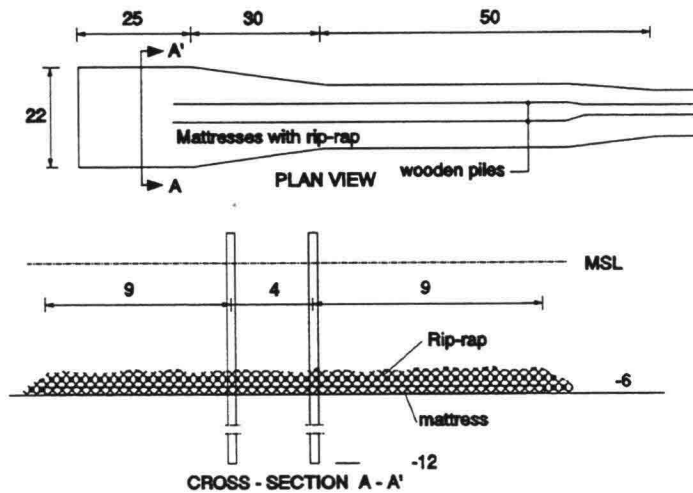


Figure 12.18 Alternative type 2: pile row

12.1.6

BREAKWATERS

Breakwaters will be mentioned here only briefly, for more detail see the lectures on this subject. Figure 12.19 gives an example of an offshore breakwater to protect a local spot. The sea-side slope is gentle (1:6), to reduce wave reflection to reduce scour in front of the breakwater. The round head has a diameter equal to about the wave length and a slope of 1:8 to increase stability of the coverlayer, but particularly to prevent eddies with a vertical axis, again to reduce scour. Even then, an apron is necessary. The height of the breakwater is usually chosen at HW level or 1-2 m above that.

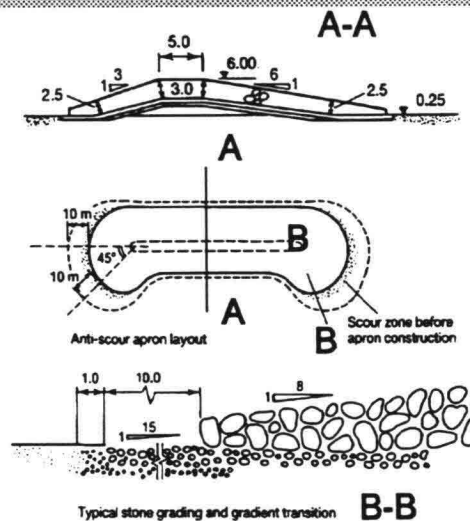


Figure 12.19 Example of detached breakwater

12.2

BANK PROTECTIONS

Bank protections are very much like shore protections. They will only be discussed here, in as far they are different. An important difference is the loading situation: ship waves and currents are usually dominating instead of wind waves. That influences the possible types of protections, therefore some types deviating from shore protections will be mentioned here. Of course all the revetment types which were discussed in the paragraph on shore protection, can also be applied (rip-rap, placed blocks, asphalt, grass etc.)

12.2.1

BANK PROTECTION TYPES

SHEET PILES

Sheet piles are seldom used in shore protections, but in banks they can have advantages, like the minimal use of space. Disadvantages are the considerable wave reflection, which hinders shipping, especially when both banks are vertical. In that case, with intensive traffic, the waterway is a dashing, turbulent pool. When the sheet piles are constructed as a cantilevered wall, the top should have a beam that can cover a possible seam due to the movement that goes with the passive soil resistance at bed level. When an anchor is used, it should be outside the potential failure circle, see Figure 12.20

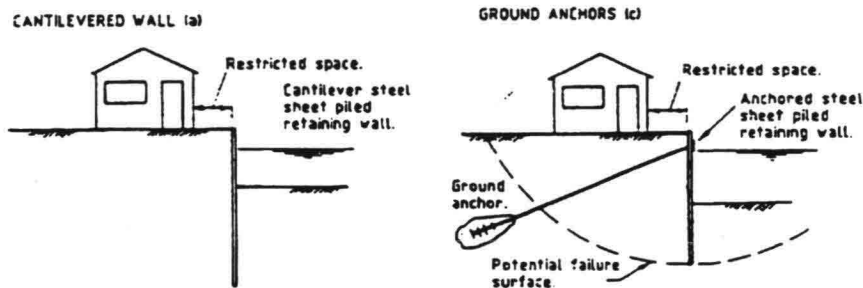


Figure 12.20 Sheet-piles as bank protection

GABIONS

Sometimes, a simple construction can be made with gabions, which can be constructed from locally available stones which on their own would be too light for protection. An advantage above penetration with asphalt or concrete (which also means to increase the effective weight of individual stones) is the fact that gabions are just as permeable as the original material.

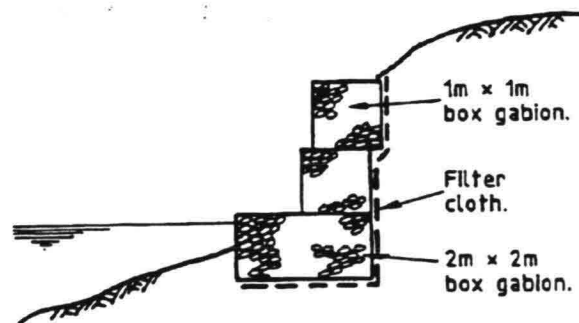


Figure 12.21 Gabion wall

This can be particularly important in cases where there is a considerable head difference between the groundwater level in the bank and the level in the waterway. Figure 12.22 gives some cases from which can be seen that a permeable protection does not hinder the outflow from the banks.

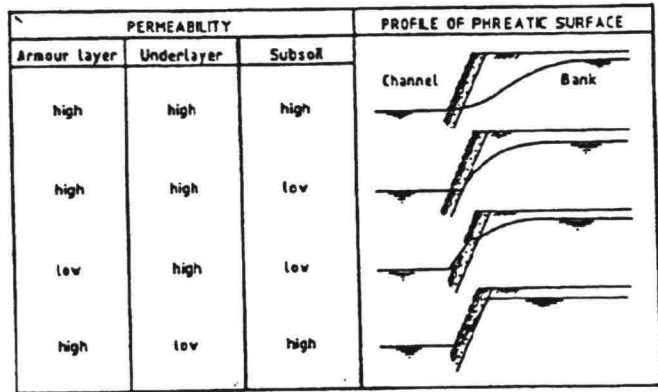


Figure 12.22 Effect of permeability of revetment on seepage pressure

REED

Dependent on the loads, a bank with reed could be an option. Figure 12.23 gives an idea of the possibilities.

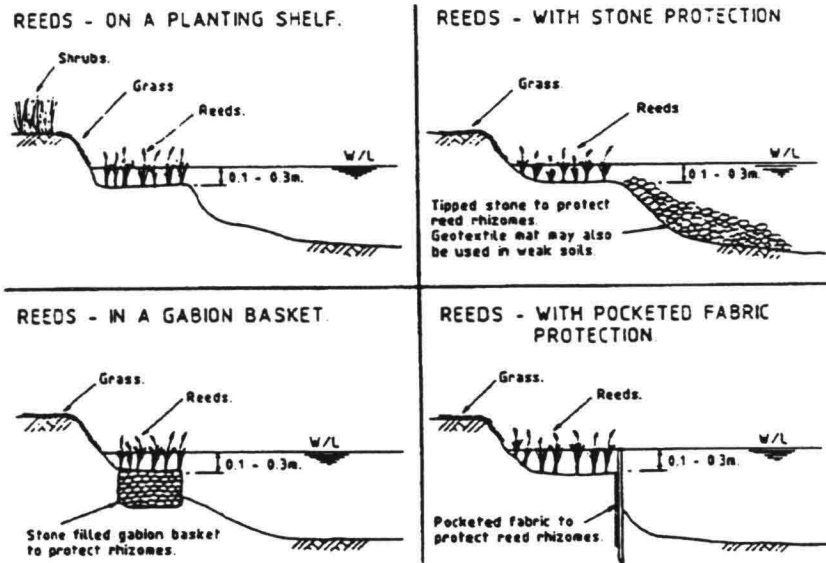


Figure 12.23 Examples of reed banks

12.2.2

LIMITS OF PROTECTION

Figure 12.24 gives the loading zones of a bank, which indicate the upper and lower limits for a protection as well as the type of load to use in the dimensioning of the bank protection. See also paragraph 10.1.6

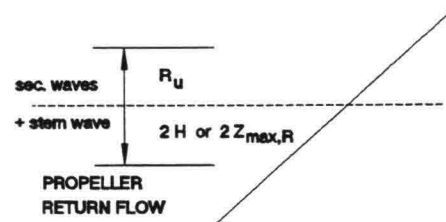


Figure 12.24 Limits of protection against ship waves and currents

Groynes are often used in rivers to control the river bed and to guarantee a navigable channel in the river bed. As a bank protection they are only economic for relatively shallow rivers; in deep rivers it costs more material than a revetment. Mostly they are constructed with rocks with sometimes pitched blocks on top. The length depends on the wanted width of the navigation channel; the relation between length and distance was discussed in paragraph 8.1. Figure 12.25 gives an example of a river groyne.

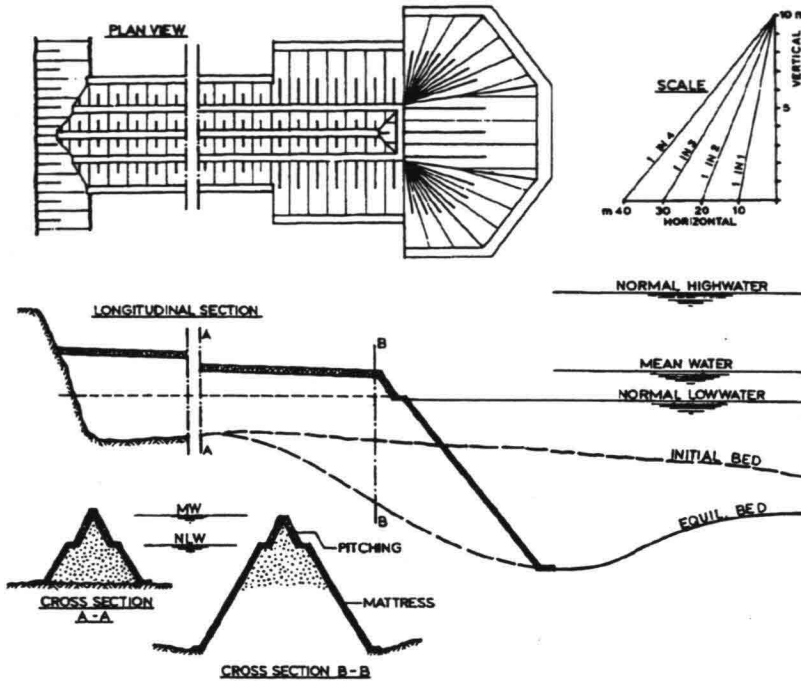


Figure 12.25 Example of a groyne

Figure 12.26 gives an alternative with a pile screen which can be cheaper. But it should be remembered that in a river there is a big chance of floating debris getting stuck to such a groyne, leading to a decreased permeability, leading to greater load on the groyne, more erosion at the head etc. So, without any local experience in the river where these constructions have to be built, application should be done with great care.

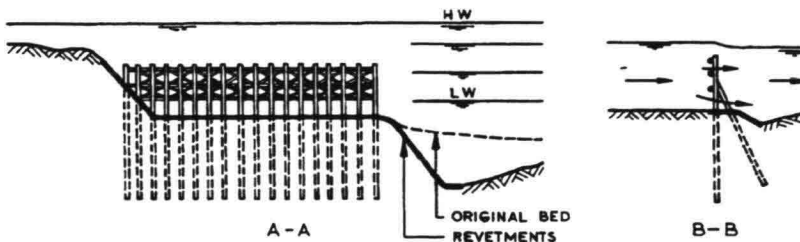


Figure 12.26 Open pile screen (spur-dike)

When a revetment is applied as a bank protection in a bend of a meandering or braiding river, it can be expected that scour will go on, or even increase, after construction of the revetment. That scour can be due to general degradation of the river bed, meandering, seasonal variations or constriction. The prediction of that scour is part of morphological calculations and is outside the scope of these lectures, see de Vries, 1992. When considerable scour is expected (say more than a few meters) there are several possibilities.

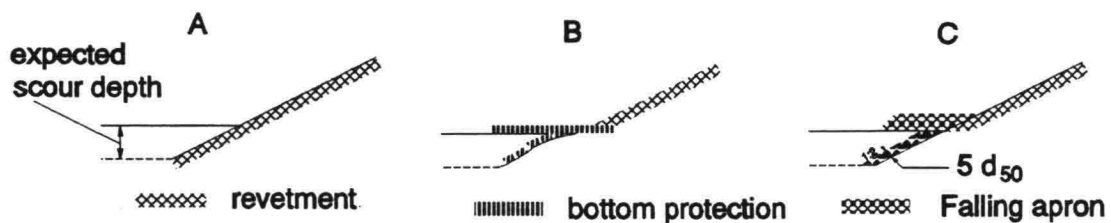


Figure 12.27 Revetment with scour

The first possibility is to dig in the protection till the expected scour depth and to cover it again with the original bottom material, see Figure 12.27a. This is a good, but usually an expensive solution.

An alternative may be the application of a fascine mattress or a geotextile with concrete blocks attached to it. This protection is constructed as a bottom protection. When the scouring process goes on, the flexible protection is lowered and follows the contours of the scour hole, see Figure 12.27b. However, when there is a large difference in scour in the flow direction, e.g. due to different soil properties, the protection will possibly hang between two resistant spots. In that case, erosion in between can go on uncontrolled, possibly leading to a local slide.

Another possible solution is the so-called falling apron, which is often applied in Indian rivers. The idea is to store an amount of stones at the toe of the revetment during construction. Scour will cause the stones to roll down, preventing an erosion with a slope that is too steep, see Figure 12.27c. The amount of stones is calculated as follows. The net volume per m in flow direction, is the expected length of the scour slope times the wanted thickness. The length can be computed from the predicted scour depth, with an assumption of the slope of stones after they rolled down, e.g. 1:2.

The thickness should be more than the normal thickness of $2-3d_{50}$, since there is no filterlayer. When the stones are well graded, the fine parts will be washed out from the top. Possibly, at the bottom the finer parts remain, acting more or less as a filter. In the paragraph on granular filters, it was said for open channel flow that a thick layer can damp turbulent fluctuations, making a filterlayer less necessary. All this leads to a layer thickness of about $5.d_{50}$. For uneven distribution during the process of falling, an extra quantity of 25% is recommended.

Bed protections can be part of a shore or bank protection or can be situated behind outlet structures. In all cases their primary function is to prevent scour at unwanted locations. The latter is essential, since it is mostly impossible to prevent all scour. The function of the bed protection is then to reduce the scour and to keep it at a place where it can do less harm. This determines the extensiveness of the protection, the main criterion being the geotechnical stability of the soil, see also paragraph 7.4. Bed protections can be made of granular material, geotextiles with concrete blocks, asphalt etc. In fact the same materials as used in revetments. An old fashioned type of bed protection often used in the Netherlands, are willow mattresses covered with stones. They formed a good combination of filter and top layer long before the invention of geotextiles. Labour cost is the primary factor that made them extinct, but they can be very useful in areas where there is little geotextile, cheap natural material (like reed or bamboo) and many hands to help. Figure 12.28 gives a cross section of such a mattress covered with stone, used at the toe of a bank protection and a modern bed protection made of geotextile with concrete blocks attached to it. Those mats are usually covered with stones after positioning to give more weight (while during construction the weight is kept as low as possible) and to prevent sand loss through the geotextile due to vibrations of the textile between the blocks in turbulence.

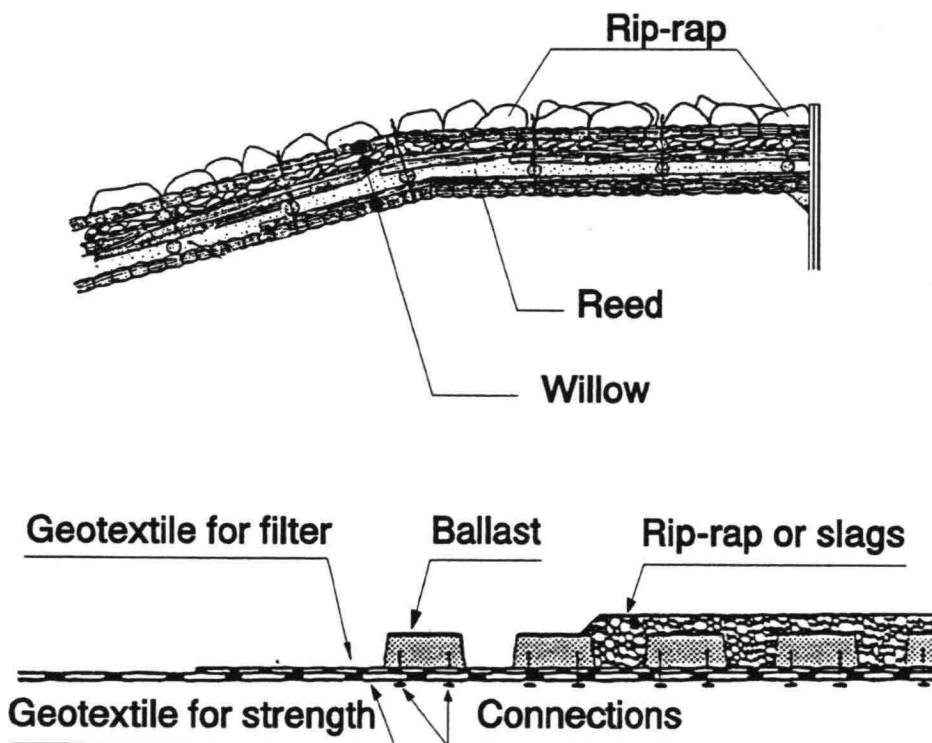


Figure 12.28 Examples of bed protections

In the following some features of bed protections will be discussed. A division is made between the various purposes of bed protections: aprons behind outlet structures, around structures like bridge piers and adjacent to toes of dikes and seawalls. With the latter we close the circle of protections where this chapter started.

The term outlet structures is used here for all kind of structures, through which water flows that can cause scour. So, not only culverts or discharge sluices, but also closure dams of estuaries can be involved. Questions arise about the limits of the apron, the vertical cross-section and the transitions.

APRON SHAPE

The length of a bed protection is determined by hydraulic and geotechnical conditions. The depth of a possible scour hole can be calculated with the techniques mentioned in chapter 6. Also a rough idea of the slope of this hole can be obtained. Since the length of the protection has to be known before calculating or investigating the scour, this is a process of iteration. Once the scour hole and its development in time is known, the stability has to be checked. This should be done with a method like Bishop's as presented in paragraph 11.3. As a rough indication it can be said that scour holes not deeper than 5m give little sorrow. A slope with a steepest part of 1:2 over 5 m height is dangerous, the same can be said of a slope with an average of 1:4 over 10 m height. Exceeding these values can induce the erosion process as described in paragraph 7.4. Taking the values mentioned in that paragraph, the bottom protection should have a length of 6 times the predicted scour depth in case of densely packed soil and 15 times in case of loosely packed soil (normal slide or flow slide), see Figure 12.29. It is assumed that the protection remains largely intact after sliding, otherwise the process will be progressive and the situation is much more dangerous. Of course these are rough indications and for important structures a thorough geotechnical survey should be done.

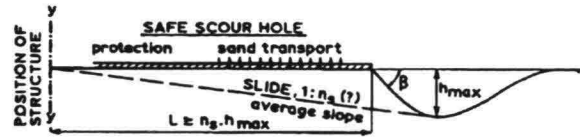


Figure 12.29 Length of bed protection

The width of the protection is mainly governed by the geometry of the water in which the structure discharges, e.g. the banks of the channel. In cases where there is complete freedom for the flow to find its way, the rules for jets as given in paragraph 2.5 can help to determine the shape. Figure 12.30 shows the situation of an outflow in a wide body of water.

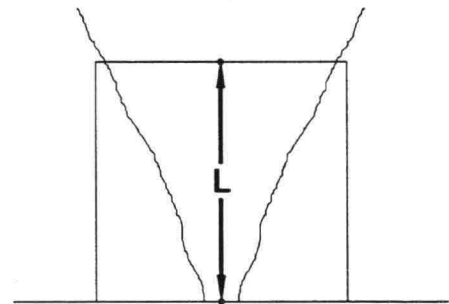


Figure 12.30 Plan of bed protection

VERTICAL CROSS-SECTION

The top layer is determined by the flow or wave attack for which chapter 9 or 10 gives the way to calculate. For a large bottom protection it can be economic to vary the top layer with the load. Downstream from a structure the flow is less; the same jet relations as mentioned for the width can serve as an indication for the flow attack. For a small protection it can be the opposite; use of different top layer material can cost more than it saves. Filter layers can be necessary when there is a considerable gradient at the interface of the protection and the subsoil. Usually this is only the case very near the structure where there is possibly a gradient in the groundwater due to the head difference along the construction. For the need of a filter see chapter 11.

TRANSITIONS

The most important transition is the edge of the bed protection at the scour hole. It is often the most vulnerable and at the same time the most crucial part for the stability of the bed protection and the structure as a whole. Here the scour starts, the slope of the scour hole is steepest and any instability starts here. To keep the situation at the edge manageable, is one of the primary tasks in designing and maintaining a bed protection.

When scour gets too deep and steep to prevent sliding, special measures can be taken at the edge, see Figure 12.31. The slope of the scour hole can be covered with material to prevent further steepening; this could even be done before the structure is used, especially when the bed protection is constructed in a dry pit. Also the (loose) sand at the edge can be compacted to prevent flow-slides.

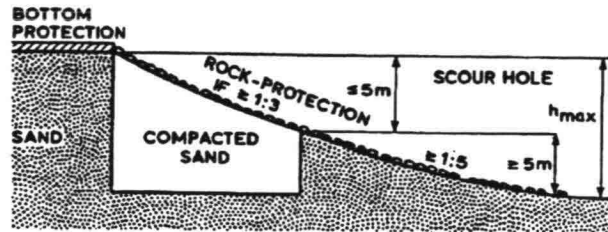


Figure 12.31 Extra measures at edge of bed protection

With regard to the stability of the edge of a bottom protection, in a tidal area where the flow changes direction, the flow situation is less favourable than in the middle. The same is true for an overlap which is also a kind of edge. Due to the curved streamlines above the edge, there will be a relatively low pressure at the upper side. In the case of a mattress or some mat with blocks, the result can be the lifting of the edge, making the difference in pressure even greater (part of the protection stands as a vertical wall in the stream, giving a considerable drag). When writing the stability in an Izbash-type of formula, the following values for β have been found:

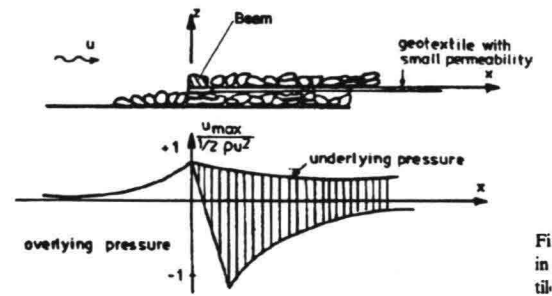


Figure 12.32 Flow situation at edges

Type of protection	$u_c \sqrt{(\Delta g d)}$ overlap	$u_c \sqrt{(\Delta g d)}$ edge scour hole
Permeable	2	1.4
Impermeable	1.4	1.1

The reversed flow in a scour hole is the most unfavourable situation, while with a permeable mattress, (like the gabion type) at an overlap, the β -value is even higher than the Izbash value for a stone on a bed (= 1.7, see paragraph 9.1). To prevent uplifting, bed protections often have a heavy beam, see Figure 12.32, which has also a function in the positioning of the mat (the sinking). Moreover, it can have a favourable influence on the stability of the protection when there is a small slide at the edge; the beam can limit the slide by its weight together with the textile of the protection.

Finally, the transition from the protection to the (concrete) structure is not to be neglected. A joint is almost inevitable. Provisions can be made, either in the building pit or with prefab connections.

"Bridge piers" stands for any obstruction in a flow or waves. When scour is unwanted or too deep, a protective apron is applied. It should stretch about 3-4 times the diameter around the pier, see Figure 12.33. It is advised to include some filter; usually a geotextile under a rip-rap layer is sufficient.

It is stressed that morphological changes influence the whole picture. When the seasonal variation of the bed level is known, it is advised to construct the apron at the lowest level. If not, the apron with the scour at all sides, will act as a bridge pier which is much wider, leading to much more erosion and probable damage to the pier. In a very dynamic morphological situation, an extensive protection is needed and one can question if there is no better place for the bridge to be found.

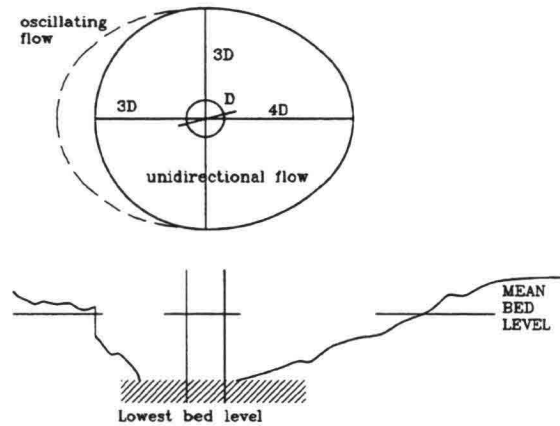


Figure 12.33 Apron around bridge pier

"Seawalls" stands for all types of constructions which are attacked by and reflect waves: dikes, breakwaters, (partly) protected dunes etc. In front of these constructions, an apron against scour is usually needed. The length can be about $3/8$ of the significant wave length, covering the node at $L/4$, see paragraph 7.1

Sometimes the toe of a dune is protected, but actually, this is a somewhat schizophrenic concept. Protecting a part will gradually lead to extensive protections. One should either choose for a dune (with occasional nourishment) or a revetment. If a dune is not completely trusted because the profile is minimal, a so-called hidden protection can be a solution. This is a last defence-line which is only active in very severe circumstances, see Figure 12.34.

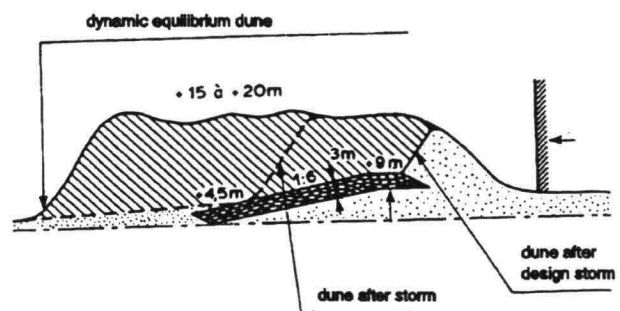


Figure 12.34 Hidden toe protection

Feasibility is an important factor in designing protections, so, after having an idea of how a protection looks like, it is useful to see how it is constructed and how it can be maintained. Construction and maintenance are not independent, see Figure 13.1. Low construction costs can lead to high maintenance costs and vice versa. An optimum has to be found. This is not necessarily governed by the economics of Figure 13.1. In the case of a sea defence, yearly necessary maintenance or at least inspection, can be preferable to a construction which ostensibly does not need attention for 20 years. In the second case unexpected things will only be discovered when it is too late.

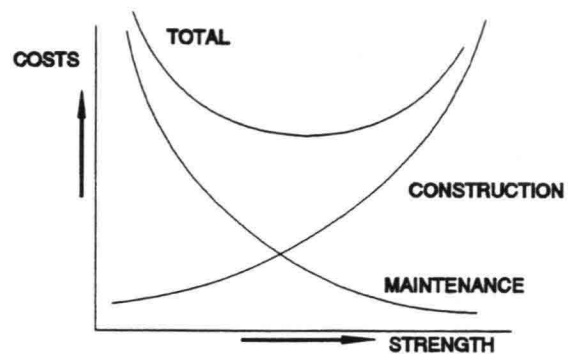


Figure 13.1 Optimum costs construction and maintenance

Even in our super-specialized society, it is necessary for a designer to have some idea of construction and maintenance practice, because they influence and sometimes dominate the design of a construction. Some examples:

Availability of material, equipment and personnel: when there is no quarry which can deliver stones of 2 tons or no equipment to handle it, it has no use to prescribe these in a design. The same goes for some types of placed block revetments that require trained personnel.

Feasibility: a placed block revetment needs at least some manual labour which cannot be done under water. This means that such a revetment cannot prolong below, say 0.5 m above Low Water level.

Quality: a filter construction in deep water has to be constructed from a floating plant. It is not possible to make thin layers accurately in deep water. So, a filter construction of loose grains in thin layers should not be applied in that case.

All engineers deal with construction practice, but hydraulic engineers, like farmers and fishermen, heavily depend on nature. Working in moving water and in changing weather conditions make things more complicated. In tidal waters, the work is dominated by the rhythm of the tides, particularly in the zone between HW and LW. Waterborne operations are sensitive for wave conditions influencing productivity, construction method or even design. Some parts are loaded during construction or repair in a completely different way than in the final stage: a filter layer will be unprotected for some time, being vulnerable for wave attack or high velocity during springtide.

All this makes it necessary to have statistical data on the conditions at the construction site. Frequencies of waterlevels, currents, waves and wind should be available or estimated before starting. During construction or maintenance, a good weather forecast is indispensable. Some activities are rather not planned during the relatively rough season. In the Netherlands, for example, execution of works in sea defences is forbidden by law between october and april.

Quality assurance is quite common for industrial activities, like the construction of cars, but not widespread in hydraulic engineering. This is sometimes explained by what was said above about farmers and fishermen and the variety of conditions. But one can also say that working under these varying and sometimes difficult conditions, require some quality control all the more. A better explanation is probably that the customer, in contrast with the car factory, was always present when his job was done. Protection of banks and shores are usually a public affair and the work is done for some authority who had his personnel at the site all the time. Moreover, the type of work was rather traditional and quality assurance was incorporated implicitly in the craftsmanship of the personnel. Two factors are changing, increasing the necessity of a quality assurance system. First, traditional methods and manual labour are replaced by new mechanical methods for which much less experience is available. Secondly, there is a shift in the relation between client and contractor. More and more "turn-key" or "design and build" contracts or whatever name they have, are coming up worldwide.

In those cases, the contractor has more responsibility for the quality of the product. Since it is impossible to rely only on a check of the final product (which is usually under water and covered with a lot of material), a good quality control system for the whole process is essential. Figure 13.2 shows a simplified picture of the various costs that are involved in quality control. Vertical is a measure for the percentage of the quality costs compared to the products total costs. Horizontal is a measure for the quality, where the right limit stands for "perfect". Prevention costs are spend to improve the quality control while failure costs are spend to repair what went wrong (either after or before completion).

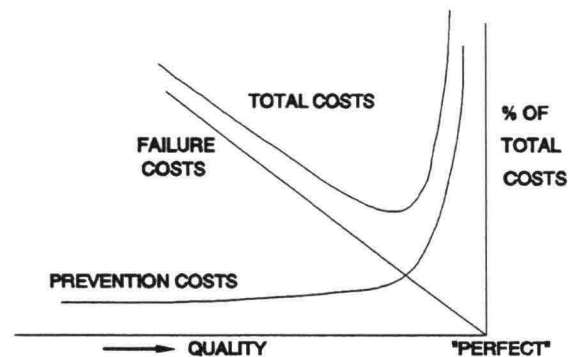


Figure 13.2 Quality costs

Quality control is a feed-back loop in a process, where measuring, comparing with pre-set standards and correction are basic elements, see Figure 13.3. The whole process, including registration and evaluation is the quality system. This should not only be done for the construction or maintenance, but also for the design and the purchase of materials, all determining the quality of the product.

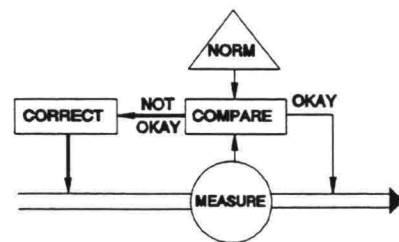


Figure 13.3 Quality control loop

As an example we take a placed block revetment. In chapter 10 we have seen that these revetments are potentially superior to a rip-rap construction but that it is not advisable to rely on the limits of this superiority in a preliminary design. This has to do with the uncertainties in the construction. A good pinch between the blocks can increase the strength considerably, but this does not come automatically. Usually a contract does not demand a certain degree of pinching, but only says that the blocks have to be washed-in with some prescribed granular material. But the toe and the transition at the upper limit of the revetment, also determine the pinching. So, only when the quality control covers the whole range from design to execution and when there is a clear translation from the design purposes to the construction process, an increase in quality can be proved.

One would possibly expect a division in the construction of bed, bank and shore protections. But many of the activities in the construction of these protection types are much alike. Here a division will be made in activities above and under the waterlevel. In the tidal zone this difference can also lead to confusion, therefore a more precise division is between land based and waterborne operations. For many activities the choice is clear: blocks on a dike are not placed from a ship and for a bottom protection in the middle of a channel, a truck is of little use. For waterborne activities at least a few meters of waterdepth are necessary, while for land based activities the limits are dominated by the accessibility and the working range of the equipment. The availability of land equipment is more widespread in the world than floating plants, which can determine the choice. Another factor can be the fact that the material which is used is already in a truck or in a barge, thus avoiding extra handling. When both are possible, other advantages and disadvantages have to be compared, see also CUR/CIRIA, 1991. The logistics for waterborne equipment can be easier when the construction site is only accessible via a narrow road on a crest. This also makes it easier to work on more than one front from the water. On the other hand, landbased activities are less vulnerable for waves. Often both methods are combined to work supplementary. Since these lectures are devoted completely to the interface of land and water, this seems logic and one would expect all kinds of amphibian devices, but their use is very limited.

13.2.1

WATERBORNE - LOOSE MATERIAL

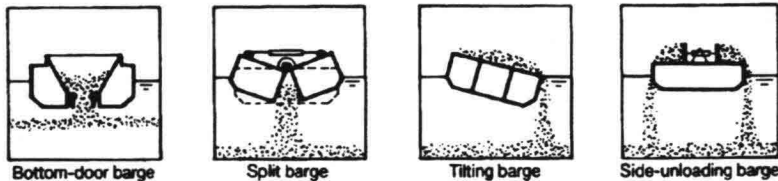


Figure 13.4 Self-unloading barges

There are many ways to get stones from a barge to the bottom. Figure 13.4 gives some possibilities, where the side-unloading barge has the best controlled process. Loading capacities of barges range from 500 to 4000 tons. The result of the dumping depends on many factors; some of them will be discussed here shortly. For accurate dumping of material, a good positioning system for the barge is essential. This is done either by anchors, usually 6, or by dynamic positioning system using a computerised thruster propulsion system. Given the position of the barge, the rest depends on the behaviour of the stones in the water in which the fall velocity plays an important role. The equilibrium velocity of a stone falling in water is: $W_s = \sqrt{4/3g\Delta d}$, which velocity is reached almost immediately. To get an idea of the impact of a stone on the bottom, it can be compared with the impact in air when falling from a height equal to its own diameter ($v = \sqrt{2gh}$). The given fall velocity is valid for a single stone. Stones dumped from a split-barge fall as a cloud having a two or three times greater fall velocity than a single stone.

The accuracy of the thickness of a layer under water can be $d/2$ with a minimum of about 0.2 m

DISPLACEMENT

Stones dumped from a barge do not all go to the position where you want to have them (compare trying to aim a coin in a bucket of water). This is something to reckon with when designing a granular protection under water. The displacement consists of a convective and a diffusive part, see Figure 13.5. The convective part again consists of the displacement due to the momentum of a stone being pushed away or rolling from a heap and a displacement due to currents. The displacement due to current can be calculated with:

$$\tan \phi = \frac{u_w}{w_s} \quad (13.1)$$

The displacement due to the momentum only occurs for side-unloading barges and is limited to 1m for moderate depths (10-20m) with a maximum of about 2m for greater depths, see RWS,1991. The diffusive displacement is caused by the eddies around the stones and the collisions between the stones, which results in a random process. For side-unloading barges, which sprinkle more than dump, the spreading has been investigated for the Eastern Scheldt storm surge barrier. It appeared that it was almost independent of the stone diameter and the discharge process, while the shape had some influence. The waterdepth is the most important factor, which is logic for a diffusive process. Figure 13.6 gives the result:

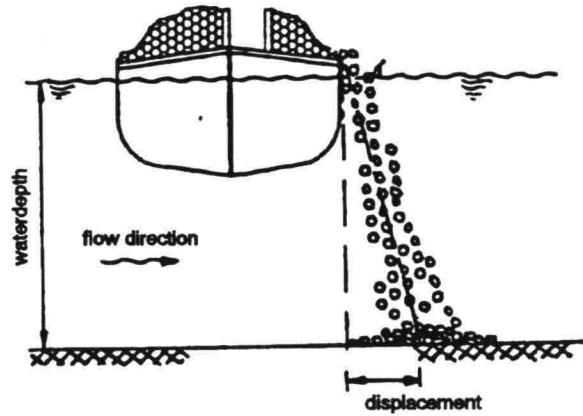


Figure 13.5 Displacement of dumped stones

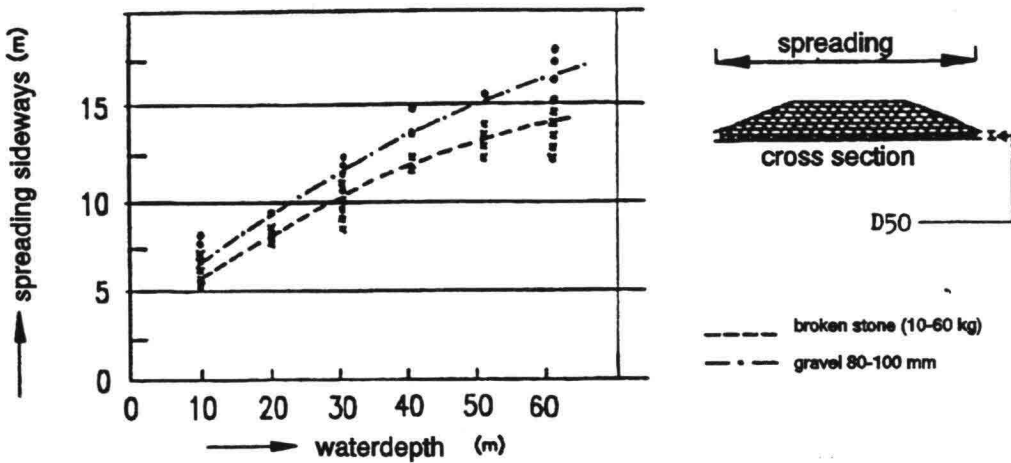


Figure 13.6 Spreading as function of waterdepth and shape

The spreading in the direction of the barges length appeared to be rather independent of anything and was about 2m at each side. When dumping from a split barge, the result is a flat and not very well predictable heap. It should be noted that dumping or sprinkling on a slope will of course lead to additional displacements; the same goes for stones being not stable in the occurring flow velocity.

SEGREGATION

Small particles have a smaller fall velocity than large ones. The consequence can be that, with side-unloading barges, the finer parts of a graded material will lie on top of the layer, which can be unfavourable for flow stability and filter action. In a cross flow there will be also a difference in $\tan\phi$, hence in the place where the various stones end, see Figure 13.7. To reduce segregation, the material should be not too graded: $d_{90}/d_{10} < 5$ to 10.

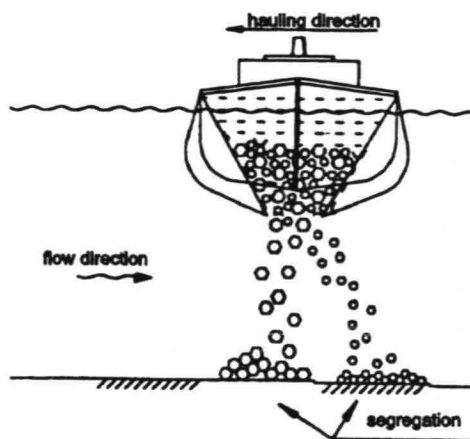


Figure 13.7 Segregation in flow

CRATERS

When stones are dumped at once from a split-barge, the result can be a hole instead of a heap, due to the impact of the mass having a fall velocity two or three times the value for the individual stones. The result is somewhat like the scour by a vertical jet, see Breusers/Raudkivi, 1991. No reliable relations with mass or water depth can be given. It can only be repeated what has been said before, that with a side-unloading barge, the dumping process can better be controlled.

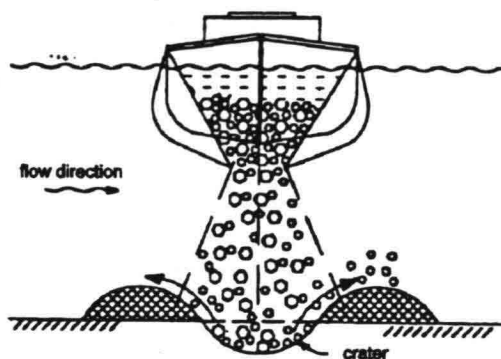


Figure 13.8 Crater

In cases where both methods are not accurate enough, a fall-pipe vessel can help. The pipe guides the stones till just above the bottom, see Figure 13.9. This is done e.g. when applied for a protection of a pipeline in deep water or in other cases where a high accuracy is wanted. The figure gives a good picture of all three methods with their characteristics. It will be clear that split-barges are only useful for dumping large quantities of the same material when accuracy is not the hottest item. This can be the case for the core of a dam or a large foundation layer.

It can be remarked finally, that small quantities of large stones and a high accuracy required, can be placed with a crane on a pontoon.

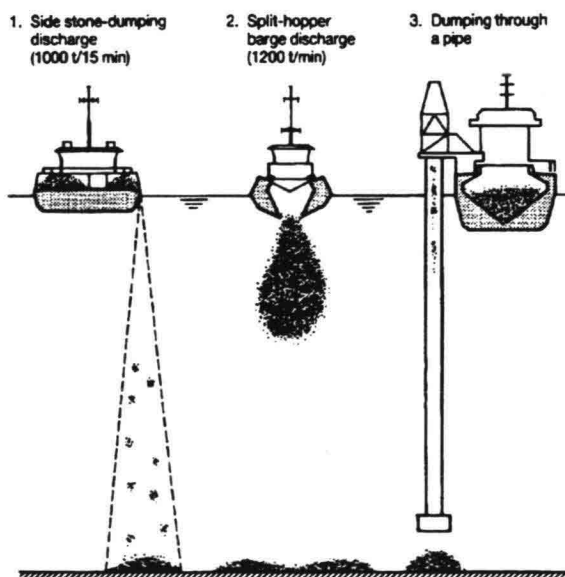


Figure 13.9 Dumping in deep water

Here the focus will be on the various types of mattresses and geotextiles, used in bed and bank protection. Traditionally, these are produced on a slope between LW and HW. The mattress can be longer than the site when the completed part is towed into the water while still working on another part, see Figure 13.10. They can also be produced in a special factory and rolled around a floating cylinder.

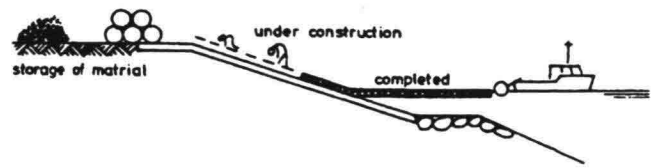


Figure 13.10 Construction site

From the construction site it is transported to the place where it is needed, either floating by itself or with the help of a pontoon or the mentioned cylinder, see Figure 13.11.



Figure 13.11 Transportation of mattress

The sinking is usually done with the help of pontoons and a stone dumper, see Figure 13.12. The dumper starts at the upstream end and warps in the direction of the current covering the whole mattress with stones.

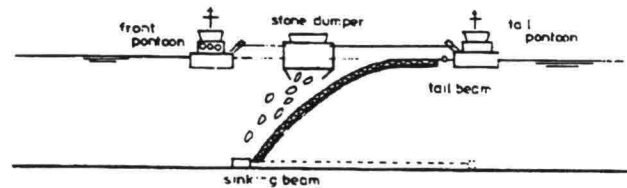


Figure 13.12 Sinking of mattress

In the case of a prefabricated mat, the ballasting is already on the mat and the dumping of stones is not necessary. It can be sunk by unrolling the cylinder in the direction of the current, see Figure 13.13. In the Eastern Scheldt lengths of 275 m were applied with this method.

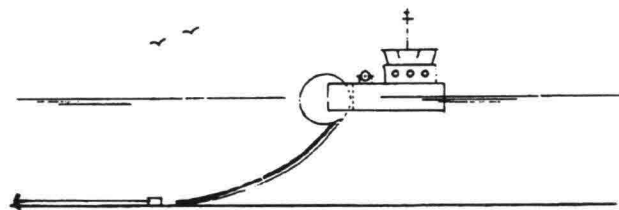


Figure 13.13 Sinking of prefabricated mat

When a mattress is used as a bank protection in a tidal area, it can be floated to its location during HW. Now it has to be anchored at the top which can be done by dumping stones, see Figure 13.14, or by using "real" anchors like piles.

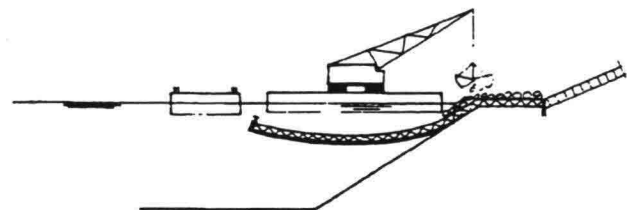


Figure 13.14 Anchoring top of bank protection

Land based equipment for hydraulic engineering is much the same as used in other construction branches: dump trucks, cranes (sometimes adapted to lift big stones or geotextiles) and bulldozers. Therefore they are more easy to obtain in areas where hydraulic engineering is no common practice. Material is transported from the quarry to the working site with dump trucks. At the site they are placed into position with cranes or bulldozers, see Figure 13.15 with additional hand barring.

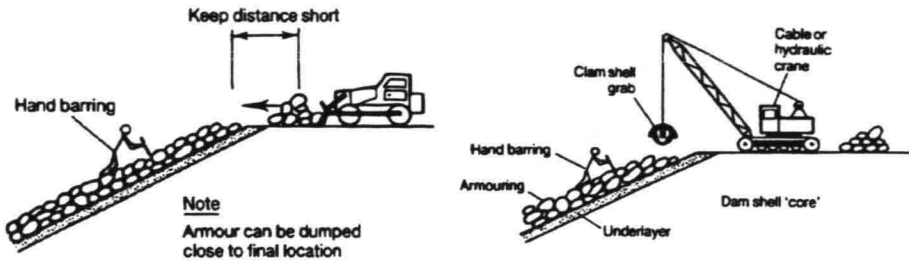


Figure 13.15 Placing armour stones

The distance on the slope that can be reached by a crane is dependent on the weight that has to be placed, see Figure 13.16. Outside the possible range, floating equipment has to be used. Although placed blocks were treated in chapter 10 as a coherent material, they are placed very much the same way as loose material. With one big difference though, the placing is often still done by hand, since that determines the quality of the revetment.

For a rockfill dam, the stones could go directly from the truck into the dam, see Figure 13.17. But it is clear that this can only be done for a homogeneous body of stones and not for a build-up of filter layers.

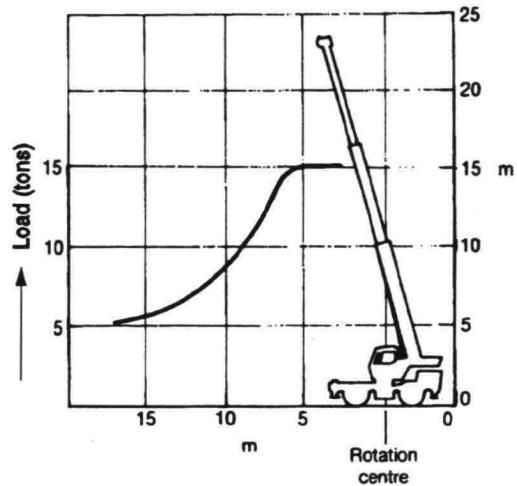


Figure 13.16 Lifting capacity of typical crane

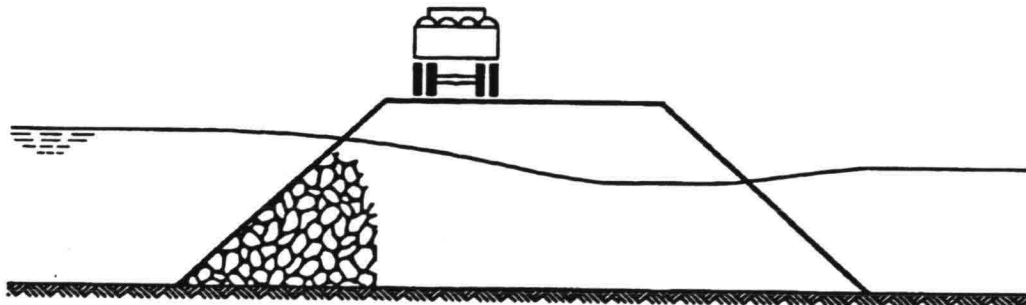


Figure 13.17 Direct dumping from truck

Here again the various types of mats are the most important constructions. In geotextiles there is the division between prefabricated and on-the-site constructions. The latter are used in a filter construction which is placed later. Prefabricated mats can have concrete blocks attached to it, mostly with plastic pins, or some mixture of asphalt and stones.

Plain filter cloth is usually carried to the site and rolled down, see Figure 13.18. The seams between the various rolls can be sewn or just covered with stones. In the latter case, the overlap should have a length of at least:

$$L > 10^3 \sqrt[3]{d/\rho_s} \quad (13.2)$$



Figure 13.18 Rolling out geotextile

The cloth has to be anchored on top or be filled from below to prevent sliding, see Figure 13.19:

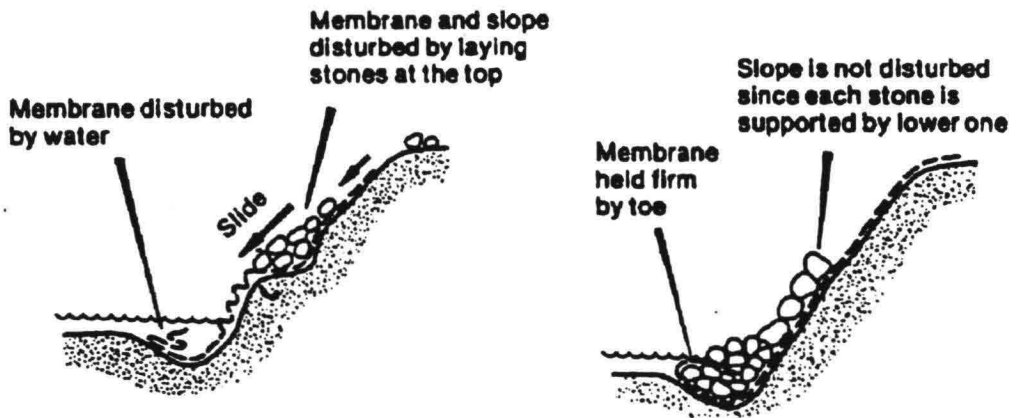


Figure 13.19 Sliding down of cloth

When a prefabricated mat is placed, a special frame is needed in order to prevent intolerable deformation, see Figure 13.20. Usually, the dominant loading situation for the mat strength is the phase of placing!

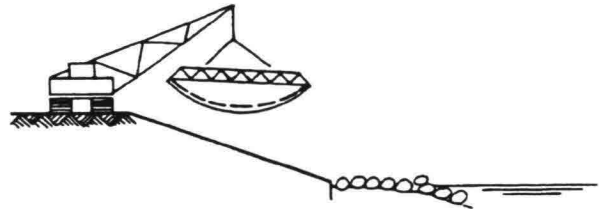


Figure 13.20 Frame for mat transportation

No need to say that slopes should be smooth and clean to prevent damage of the mat and to avoid holes under the geotextile.

It is impossible to give costs for all construction types in all circumstances. Only some comparisons will be given here.

For the situation in Figure 13.21, the costs have been calculated for four construction types:

- 1 - Classical placed stones on the slope with classical fascine mattresses at the toe
- 2 - Placed concrete blocks on the slope and fascine mattresses with geotextile at the toe
- 3 - Filter construction with gravel and rock layers
- 4 - Prefabricated mats

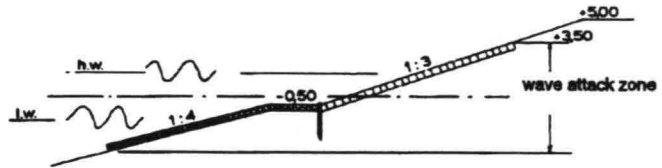


Figure 13.21 Cross-section for comparison costs

In Figure 13.22 the result is given (in guilders of 1975 per m bank) for the four constructions divided into material, equipment and labour. It appears that the classical type is the most expensive due to labour and material costs.

To make 30 m of these banks per day, the first type needs 40 people, the second 20 and the other two 4. For all construction types, the material costs (including transport) make about 75% of the total costs. For large scale projects, prefabrication will appear to be the most economic, since the production is the most industrial. The final choice often depends on other factors like the boundary conditions to be expected, availability of labour etc.

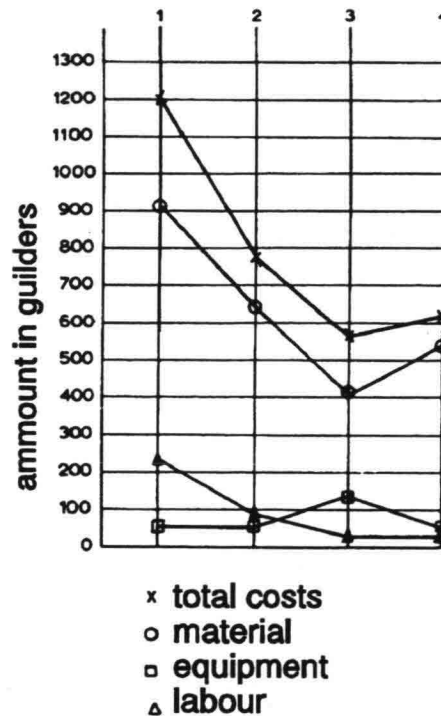


Figure 13.22 Cost comparison

Maintenance comprises all activities to be carried out (on a periodic basis) after construction, to ensure that a structure can fulfil its functions. Inspection and repair play an important role in this process, which we will discuss in the coming paragraphs. But first we will dwell for a while with the words "fulfil its functions". Of course this includes the functions from the viewpoint of hydraulic engineering like protecting against flooding or prevent the sliding of a bank in a navigation channel. There are however hardly or no hydraulic structures which have only technical functions. The interface of land and water is a public domain and more than the playground of technicians. In all cases the interface has a function in the ecosystem while in populated areas it is used for recreation, farming etc. More and more, hydraulic engineers are not only responsible for the technical functioning of the structure they manage and/or design, but also for a proper integration in all its social and public functions. It is the task of the hydraulic engineer to incorporate the maintenance strategy into an overall management plan. Such a plan serves as a basis for decisions to be made by the responsible authorities. It can be a very simple plan when it concerns the bank of a canal or a comprehensive policy analysis for a coastal zone. It should contain:

- description of all relevant functions like e.g.:
 - flood defence
 - traffic (roads, railroads, shipping)
 - habitats for animals and plants
 - recreation (landbased like bathing or waterbased like boating)
 - land use for agriculture, living, industry etc.
- description of possible conflicting functions and possible developments
- description of possible choices and consequences
- costs

One could ask what this has to do with hydraulic engineering. Although it is sometimes advocated that politics and technics should be separated as much as possible, this cannot be maintained in the society of today, because of the above mentioned public functions of the interface. This does not minimize the role of a hydraulic engineer, but its character changes. It is not longer enough to perform the management of banks and shores on a purely technical basis. Proper maintenance costs a lot of money and this money has to come from taxpayers who know that well-functioning waterways and sea defences are important, but who have also many other wishes like hospitals, education or just lower taxes. Since the responsible politicians are elected by these taxpayers, money for maintenance does not come as automatically as engineers think or want. Maintenance is never high priority for politicians. "I don't get reelected by painting a bridge every year" one of them once said. This means that expenses for maintenance have to compete with other public expenses and they should be reasoned and well-founded. The role of the hydraulic engineer is therefore crucial: he/she should present all possible conflicts and solutions and indicate the consequences when funds are cut. A politician will also understand that his reelection is in danger when the bridge collapses. It is the task of the hydraulic engineer to indicate when that will happen. This is the subject of the next paragraphs.

The strength of a construction decreases in time (we neglect the increase in strength of e.g. a newly built concrete structure within the first few weeks) because of ageing and wear and tear. The loading usually fluctuates. So, also for a well designed construction there comes a day, when the strength is smaller than the loading and its life ends, see Figure 13.23. Maintenance has everything to do with the relation between ageing, strength and loads. There are several thinkable maintenance policies, e.g. preventive and corrective. The choice depends mainly on the risk that goes with failure of a construction

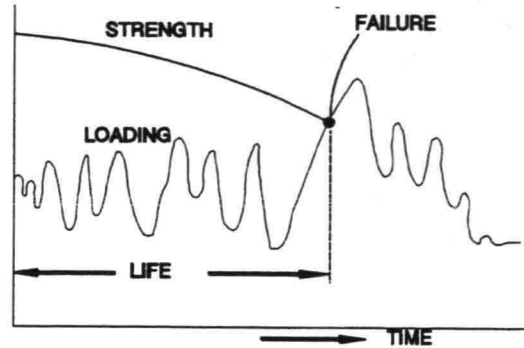


Figure 13.23 Life of a construction

(risk being defined as chance times the consequence of occurrence). Note: in this theoretical introduction we talk about constructions, not indicating what is meant; it is possible of course to make a distinction between various parts of a construction for which the approach can be completely different: the engines in a lock should be treated in another way than the concrete walls.

An important issue in this theoretical approach of maintenance is cost minimization (we assume here that the optimization as sketched in Figure 13.1 has already been done; here the question is how to optimize the maintenance itself). Figure 13.24 shows the idea behind it. The maintenance costs decrease and the risk increases when the maintenance interval increases (all costs compared on a cash base at a certain moment). The curve in Figure 13.24 is probably representative for many hydraulic structures: very frequent maintenance is expensive, while the curve at the right hand side is rather flat. Hence, a somewhat longer interval does not immediately lead to much higher costs. In all cases it is very hard to determine the optimum accurately, but in a case that the curve has indeed a shape like the one in Figure 13.24, a somewhat too large interval does not lead to extra costs. And that is what our politician probably intuitively knew when he expressed his feelings about bridge-painting. (Note: the maintenance interval is not the inspection interval; that will be much shorter). In fact the picture is more complicated than in Figure 13.24. The decreasing maintenance costs can increase again when the bridge is not painted for 10 years and many extra work has to be done to remove the rust. With all this in mind, we return to the preventive and corrective maintenance policies.

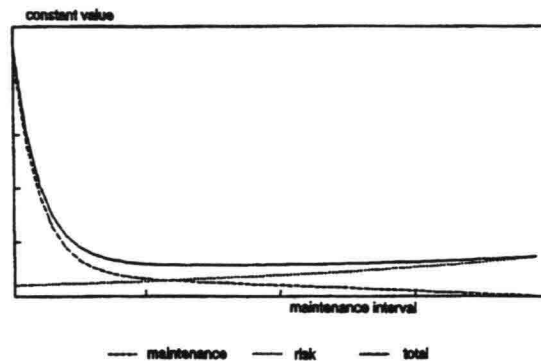


Figure 13.24 Maintenance costs as function of maintenance interval

A light bulb in a living room is replaced only after failure. With many other lights in the same room, the risk at failure is zero and this approach of maintenance is the cheapest since the life of the bulb is completely used. Lamps above an operation table however, will be replaced preventively since the risk of failure is usually too high. Preventive maintenance can be done at regular intervals, depending on the loading history or depending on the condition of the construction.

The light above the operating table will probably be replaced in a regular schedule, based on the life-expectance. Safety belts in a car are replaced after having been loaded in a crash (load dependent maintenance). These kinds of preventive maintenance are possible when the process of ageing is well described. In hydraulic engineering we are still far from that and preventive maintenance is mainly done based on the condition of the construction.

That means that inspection, to determine the condition, plays an important role in the maintenance. The comparison of the findings of the inspection and repair, if necessary, are other elements in this preventive maintenance approach. The process shows a great similarity to the feed-back loop in quality assurance, compare Figure 13.25 with Figure 13.3.

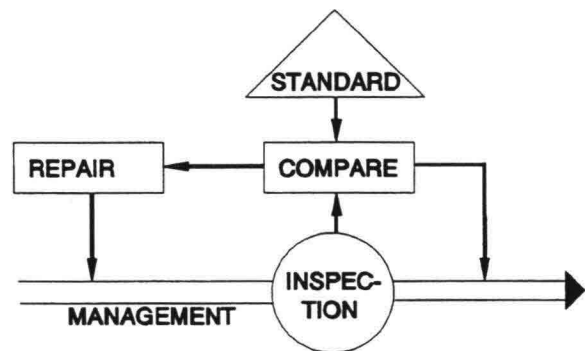


Figure 13.25 Inspection and repair in maintenance

Figure 13.26 shows the theoretical strength curve for a construction (or part of it) and three limits, see van Hijum/de Quelery, 1991:

Warning limit: a more intensive or more frequent inspection is needed

Action limit: start of preparation of repair works

Failure limit: the structure is not considered safe anymore, repair works should be done before this limit is reached

The margin between the action limit and the failure limit will depend on the inspection frequency and the mobilisation time for repair works.

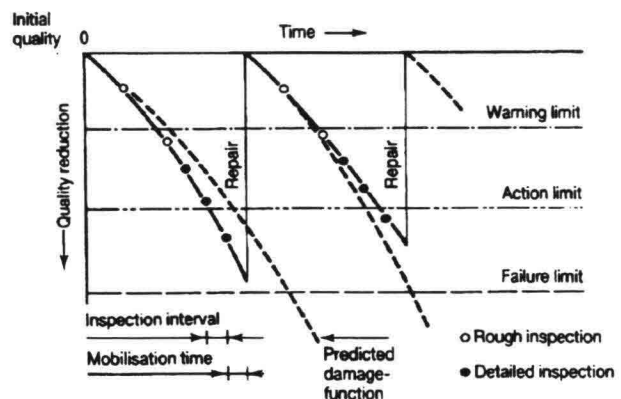


Figure 13.26 Preventive condition-based maintenance

Many energy has been put, with varying success, in rationalizing the maintenance of hydraulic structures, based on the theoretical concepts as described in the previous paragraph, see also RONIS,1990 or Kuijper,1992. Up to now, the prediction of the strength reduction, ageing or damage function as presented in Figure 13.23 and Figure 13.26 is not feasible. That means that inspection becomes all the more important. The following table gives an example of practical instructions for the inspection and repair of a placed block revetment to be given to the personnel being charged with the every day inspection of a revetment.

DAMAGE	REPAIR	REMARKS
One block removed	Repair before stormy season	
More blocks removed	Immediate repair	Top layer is too weak
Settled blocks	Replace when settlement is more than 10 cm; find cause	Probably filterconstruction is not okay
Pinching material between blocks washed away	Fill when fissure is empty over more than 10 cm	Is toe still functioning or do blocks have too large fissures
Loose block at transition	Penetrate or add pinching material	Same as above
Water remains in fissures	Hardly any repair possible	Check permeability in design

In fact, the Dutch Rijkswaterstaat has, for the time being, left the track of predicting the strength reduction and has gone back to a very empirical extrapolation of damage description based on inspection. The approach is now:

- multi-functional: description of all functions, see paragraph 13.3.1
- making an inventory of all banks, shores and bed protections, since an adequate description is often not present (in the Netherlands: 3000 km protected banks and shore, 4000 groynes). This inventory is made for segments of about 1 km
- per segment, a description is given of:
 - bank type
 - parts (toe, berm etc.)
 - state (good, moderate, bad)
 - expected development
- compare risk with public interest, particularly consequences of failure

It is repeated here what was said in paragraph 13.3.1: the hydraulic engineer should carefully indicate how the situation is and what will happen if there comes no more money or when the budget is cut. The technical point of view is very important in the reports about the condition, but not beatific. The failure of a river bank as such is no problem when no public interests are threatened. On the other hand, without proper technical knowledge, it is impossible to perform this task.

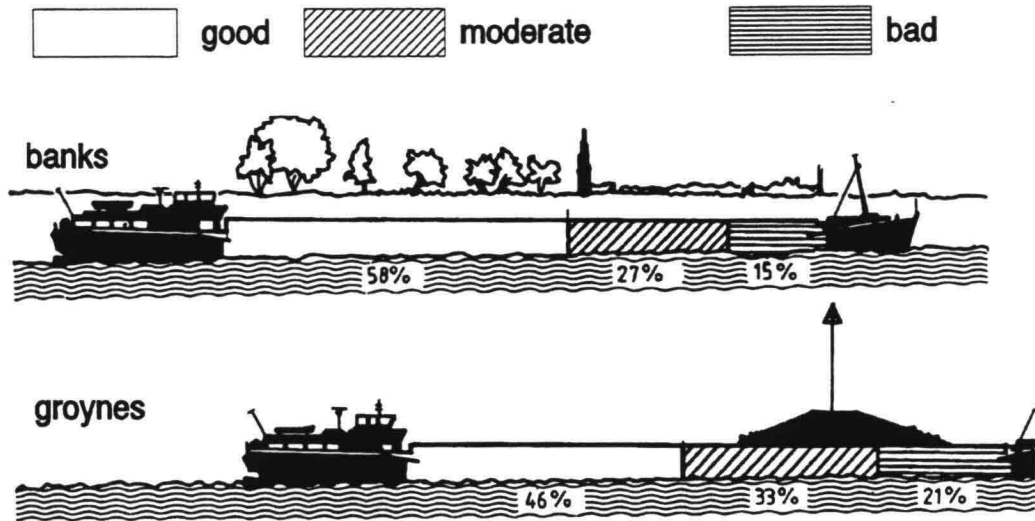


Figure 13.27 Overall picture maintenance banks and groynes Dutch waterways 1987

Figure 13.27 is a presentation of a rough inventory of the condition of all national waterways in the Netherlands, executed in 1987, see RWS,1987. A simple presentation in a graphic form and some financial numbers together with Figure 13.28 was enough to prevent further cutting of the budget.

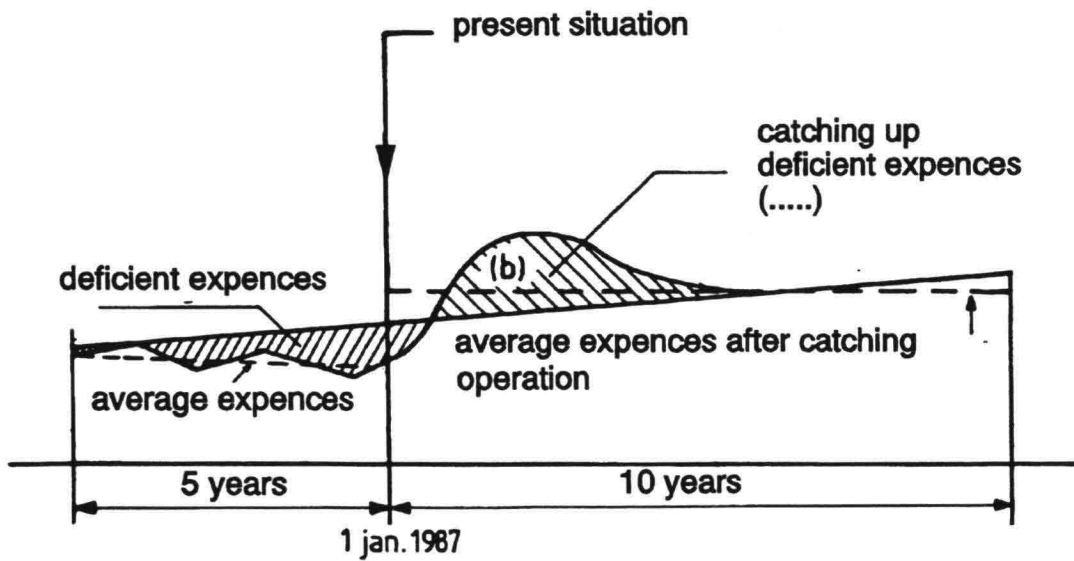


Figure 13.28 Graphical presentation of financial situation maintenance Dutch waterways

The last chapter of these lecture notes is devoted to design. This is done because design is seen as the culmination of all aspects of protections and the designer has to cover them all: the theoretical basis and the construction and maintenance practice. At least he should be able to communicate with people who do the more theoretical or more practical work. Moreover, the designer has to translate public needs into structures. In fact, the designer is an interpreter between society, technical theory and practice and he should speak all the matching languages.

Figure 14.1 gives an idea of the position of the designer in the society as a whole and in the field of hydraulic engineering.

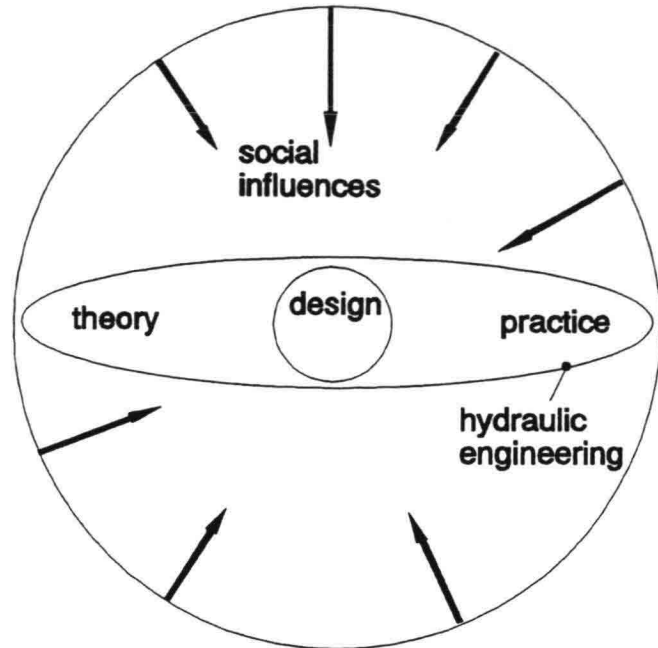


Figure 14.1 Position designer in society and hydraulic engineering

The design process can be described in many ways, the variety being an indication that there is no chrysalized recipe. Probably there never will be one single recipe, because situations, problems, possibilities and materials are different at different locations and evolve in time.

It will be attempted therefore to describe the basis of the design process, which is more or less generally applicable and less sensitive to time and fashion. A disadvantage of this approach could be the rather abstract way of description.

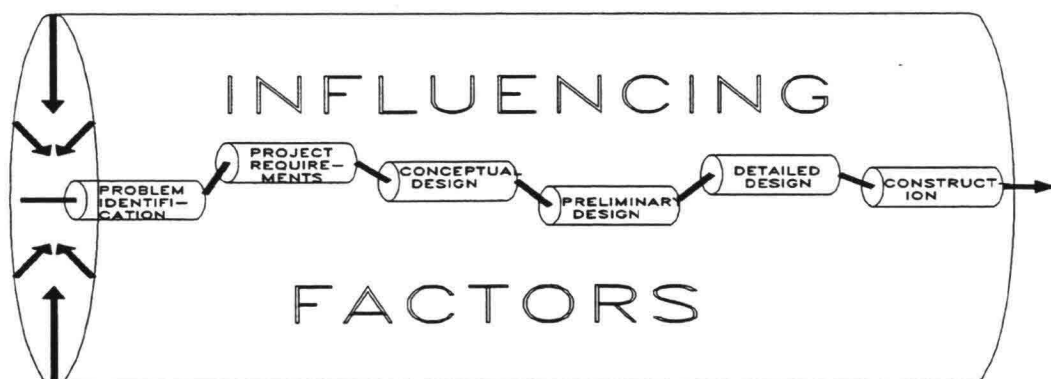


Figure 14.2 Design process in time and surroundings

The design process can possibly best be described in two dimensions: time and influencing factors, see Figure 14.2. The time dimension (the various phases of the design) will be discussed in paragraph 14.1.3 and the surroundings (the influencing factors) in paragraph 14.1.2. During the design process, the relative importance of the influencing factors will vary, so the course of the process in Figure 14.2 will certainly not be a straight line but will be pushed and pulled by forces in society.

Design of an interface-protection is usually part of a more comprehensive construction like a dam, a canal or an outlet-sluice. This again can be part of a larger plan: the development of an irrigation project, a town renewal etc. These larger frameworks will certainly influence the choices to be made in the design process.

With many factors involved, the design process has an iterative nature, which can even go on after construction. This may seem strange, since only one alternative will be actually executed, but the experiences gathered from a construction can be a guideline for future designs or other parts of the same project e.g. the revetment of a long dike which is constructed over a long period. In fact, this forms the basis of many hydraulic engineering practice, where experience plays an important role. Science made its entrance in this field only the last few decades and experience will remain crucial. The Deltaworks in the Netherlands were designed with the best available research techniques, but the planning was such that the experience gathered with one dam, could be used in the next, going from small to large.

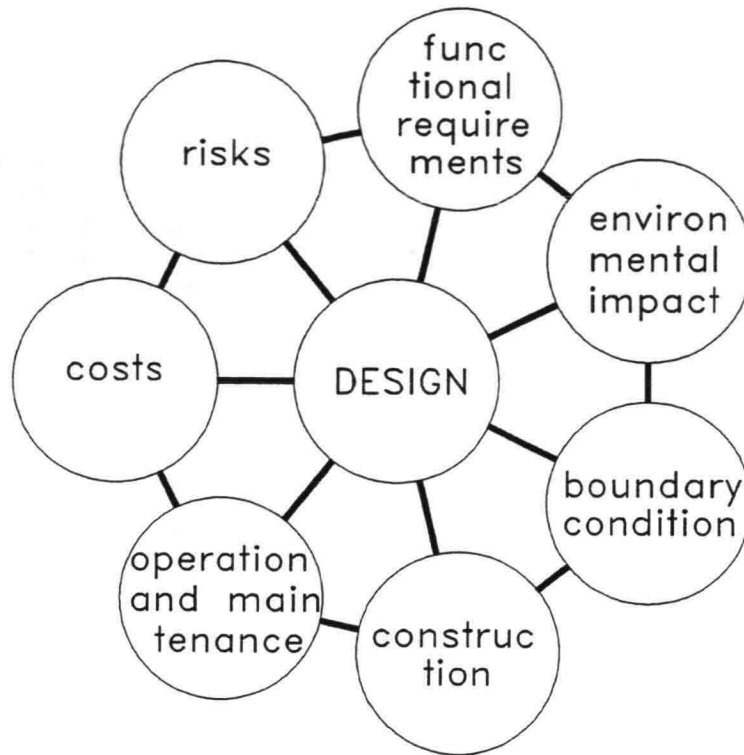


Figure 14.3 Design influencing factors

The main factors are, see Figure 14.3:

Functional requirements

These are the reasons why the structure is made e.g. flood defence or shipping guidance but possibly also other social functions which have to be taken into account, like road traffic along a canal or recreation on a shore. All these functions can already be mutual conflicting and compromises have to be made or various designs are made meeting the demands to a different degree, between which later has to be chosen, see paragraph 14.2.

Environmental Impact

An Environmental Impact Assessment (EIA) is now common practice for major hydraulic engineering projects. The various environmental impacts for all alternatives are described and compared with the zero-option (doing nothing or some inevitable variant on which everybody should agree that it is inevitable; if not, this is again part of the discussion) and possibly a most favourable option from an environmental point of view. An EIA can also comprise factors like liveability in a region, for more information, see annex B.

Boundary conditions

These include waterlevels, currents, wave conditions, sediment characteristics, soil shear stress, cohesion etc. Usually there is not very much to choose here and the data are just collected by surveying.

Construction

As already stated in the previous chapter, the construction can have a large influence on the design. The availability of materials, equipment and (skilled) personnel can be of crucial importance. For large scale projects it is not unusual to design special equipment for the construction. In that case it can open the way to other options in the design. Construction time can also play a role, either in relation to boundary conditions (e.g. stormy season) or to the need of the project being executed.

Operation and maintenance

Here the same holds as for construction. Already in the design, the possibilities for maintenance should be taken into account. Factors like the accessibility of the structure for inspection and repair, the reparability and the maintenance costs should be considered.

Costs

This factor needs no clarification.

Risks

Although all options will be designed with a same risk in the final stage, there can be differences. This can be because of unknown long-term behaviour of some new material or construction type. For the construction period there can be differences in risks, either resulting in delay, accidents or damage due to temporary lack of protection.

Not all factors will have the same importance; sometimes other factors are important as well. Their relative importance varies during the design process. In the conceptual phase, the functional requirements and the boundary conditions will probably be dominant above the possibilities of maintenance, which gets more important in the details of the structural phase. Neglecting however any one of them in any stage of the design process, will lead to extra iterations or worse, to an unsatisfying product. At least in every phase of the design process the designer should ask himself the question for every relevant factor: how does this influence my design and if I neglect it now or make an assumption, can I solve possible problems in the next phase?

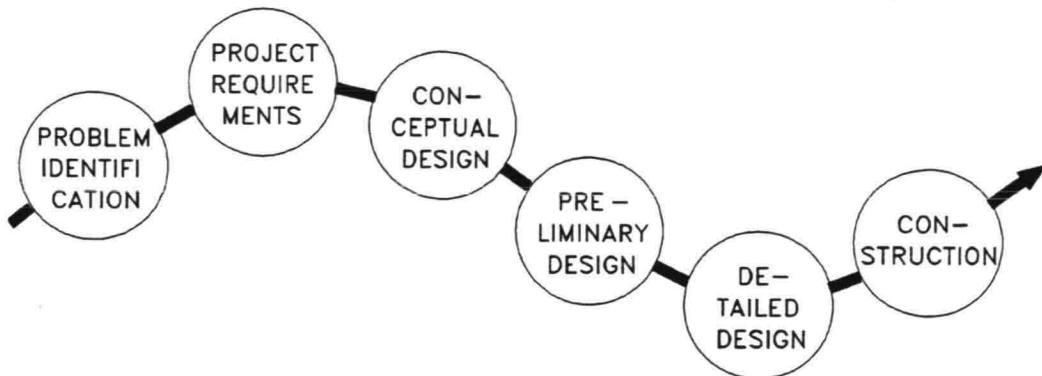


Figure 14.4 Steps in the design process

Figure 14.4 shows the most important steps in the design process:

Problem identification

An essential step is the problem identification, because it happens that different people working on the same project, have a different idea about the problem they are working at. Or the designing team as a whole has a different idea than the responsible authorities or the community. The most tragic mistake a designer can make is coming with the right answer to the wrong question.

Project requirements

The first step to the solution of the identified problem is to formulate the requirements. There is always the danger to jump into existing solutions, based on experience, while the problem may possibly ask for completely different solutions. This may show that experience is not only essential, but can also be a handicap! In fact the designer should have some "meta-experience" which tells him that he should not only use his "historical" experience.

Conceptual design

Again an essential step. With the project requirements and some basic boundary conditions, different alternatives are generated. Brainstorm sessions can be useful and alternatives should not be rejected too soon. Here the designer combines phantasy and experience, looking for opportunities and favourable solutions, fit for local circumstances.

Preliminary design

With some variants from the conceptual phase, the design is elaborated further before a final choice is made. In this phase designs are detailed to a degree that a comparison can be made in costs, feasibility and functionality.

Detailed design

The chosen alternative is detailed to a level that specifications can be made for contracts. The total concept should not change anymore in this stage, but construction details still can undergo major alterations.

Construction

The final building stage. Although formally not part of the design process, there is still a role for the designer. Alterations made during the construction period (which are not unusual in large and difficult projects) should be done with knowledge of the design background.

FINAL REMARKS

Figure 14.5 gives a picture of the relation between knowledge and the number of alternatives during the design process. From many alternatives to one with increasing detail of knowledge. Every step in the process should be finished with a clear and well documented decision, particularly when the project requires a long time and many people.

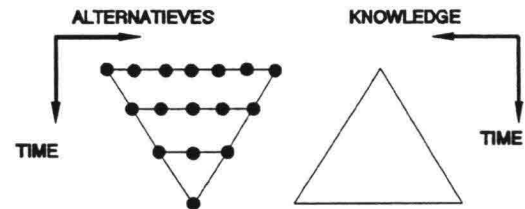


Figure 14.5 Number of alternatives vs. knowledge

Another important factor in the process of convergence to a final choice is the equivalence of detail with which variants are investigated. When a choice is made to go on with one or more alternatives and to skip others, it sometimes happens that the favourite alternative is the one that is least investigated. All the others showed one or more disadvantages in the investigations, while the disadvantages of the favourite will come up in the next phase. From this it will be also clear that iteration is usually inevitable in the design process.

As said before, here phantasy and experience are both important. Brainstorming is an appropriate way to generate alternatives, because phantasy and experience are seldom both well-developed within one person. It is important to conduct the brainstorm in such a way that premature killing of alternatives is prevented. "Postpone judgment" is the keyword in this phase of the process. Only after the generation process has dried up, the chaff and wheat are separated. A clear distinction between generation and sorting, with some time in between, is necessary because they differ essentially in nature and both have a different function.

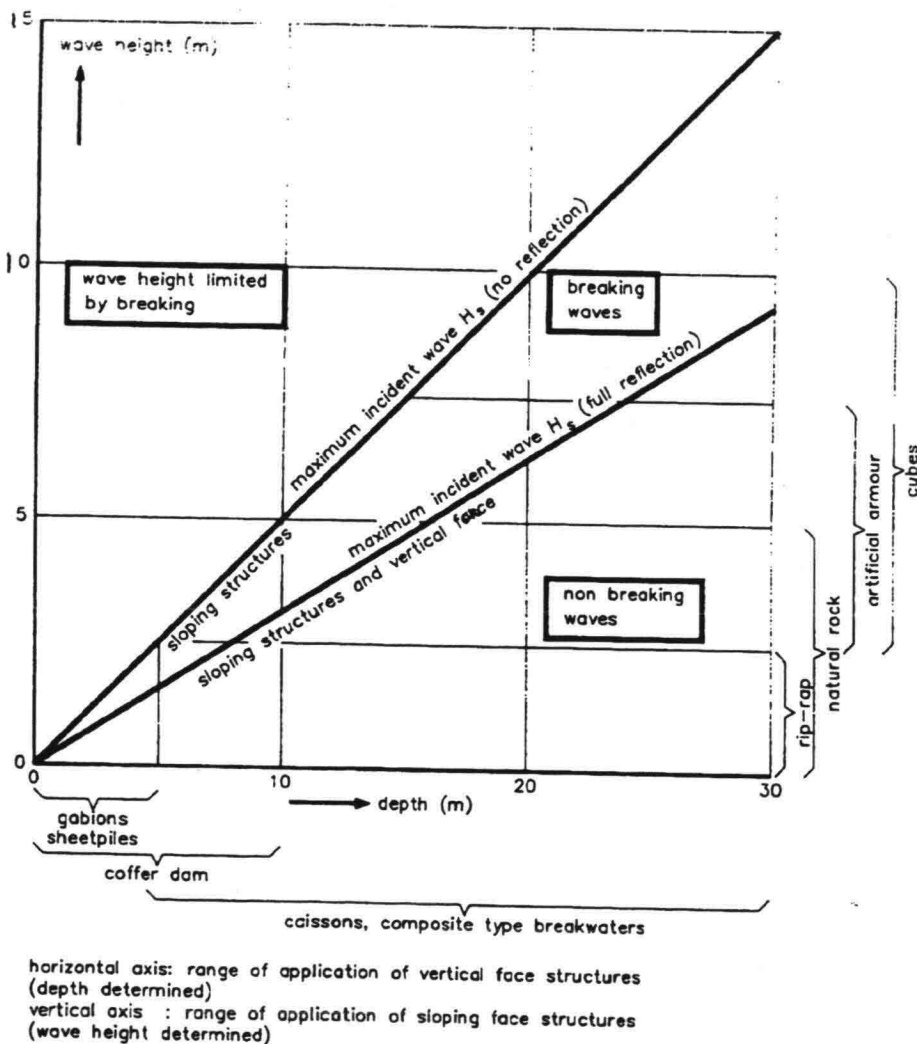


Figure 14.6 Coastal structure application (vd Weide, 1989)

Phantasy is more difficult to learn than experience. The first is less important in situations which lie within the range of earlier applications. Figure 14.6 gives an example of applicability of bank and

shore protection as a function of waterdepth and wave height. The various vertical face solutions are mainly governed by the waterdepth, while slopes can be applied in almost any waterdepth, with the type of revetment being a function of the wave height.

Important in the first selection of generated alternatives are calculations with the formulae given in these lecture notes or elsewhere in the literature. As said in the introduction, a sheet of white paper and a pencil are indispensable tools for a hydraulic engineer. This statement is specially valid for the conceptual phase. The same can be said of a pocket calculator for the first dimensioning and selection. Velocities leading to stones on a bottom protection of 50 tons are an indication that stones are not the right concept in this case and that a concrete plate might be more appropriate. Of course, nowadays a computer plays an important role also in the conceptual phase, but the above mentioned tools remain the core of a hydraulic engineers first-aid kit.

14.2.2

SELECTION OF ALTERNATIVES

The conceptual phase is concluded with the choice of 2 or 3 promising alternatives. The choice can be made in various ways, but the most convenient is the Multi Criteria Analysis (MCA). Although there are advanced techniques to perform an MCA, in this stage of the process it can be done relatively simple. A matrix is filled with the alternatives in one direction and the influence factors in the other.

The matrix can be filled in various ways:

- per criterion a sequence is determined between the alternatives, the more favourable for the criterion the higher the number. So, each alternative gets a different number from 1 to N, N being the total numbers of alternatives.
- each alternative gets a number between 1 and 10, like in the example above. So, alternatives can have the same number.
- each alternative gets + or - per criterion

Not all criteria are equally important. This can be expressed by giving each criterion a weight factor. This could be done in a team or, when public interest is at stake with a choice, with the responsible authorities. A somewhat more objective way is to place all criteria in both directions of a matrix and to compare them in pairs. More important gets 2, equally important 1 and less important 0. Adding all numbers gives the weight factor.

Some people pretend to make "objective" choices this way. There is however always subjectivity in the choice of weighting factors, or even already in the choice of the criteria. The advantage of this way of choosing is not in the objectivity, but in the visibility of how the choice is made. Even then manipulation is not completely prevented. In political important decisions, the quality of the choice is determined by the quality of the process and transparency is an important factor in that quality.

It will be clear that the same kind of choice has to be made at the end of the preliminary design phase. It depends on the importance of the problem when and whether the choice is lifted to a public level. Usually for important projects the conceptual choice is made by technicians and the final choice is made by politicians. But when outsiders come with a solution that was rejected or forgotten in the conceptual phase, it is thinkable that it should be included in the next phase.

Structural design comes after the conceptual phase and consists of the preliminary and the detailed design. The same factors, see paragraph 14.1.2, influence the design but the elaboration goes more into detail. Instead of simple calculations, computer models or scale models are used to obtain more insight in the behaviour of the structure, the boundary conditions and the strength. New alternatives may come up, but they are variations on the options from the conceptual phase. More detail is added in the design and the chosen construction will be optimized to achieve minimal costs, construction time or any other factor that dominates the design.

14.3.1

FAILURE

Failure is the exceedance of a limit state which occurs when the loading exceeds the strength. The limit state is a loading condition defined in relation to the functional requirements of the structure, (the performance) and to a failure mechanism. Two limit states are distinguished, the ultimate limit state (ULS) and the serviceability limit state (SLS). The ultimate limit state occurs under extreme conditions when a structure fails and collapses, e.g. a dike breaks during a storm and the land is flooded. The serviceability limit state occurs under "normal" conditions, leading to failure without collapse, e.g. a dike settles due to its own weight and the crest becomes lower than the design level. Sometimes a third limit state is distinguished: the accidental limit state. This is however a dangerous expression, because the designer is responsible to take these "accidents" into account if their probability of occurrence has the same order of magnitude as other boundary conditions. A ship that sails into the dike can be considered as an accident for which the designer can not be held responsible, but in a sharp river bend with much traffic, the chance of this event can be greater than the exceedance of the design level. At least the consequences should be considered e.g.

the reparability or the succeeding events after the dike is damaged. It is therefore important to have an idea of all possible threats to a construction. It is not exaggerated to say that most structures collapse due to a mechanism that was not recognized instead of a loading that is greater than expected. Figure 14.7 gives an overview for a dike.

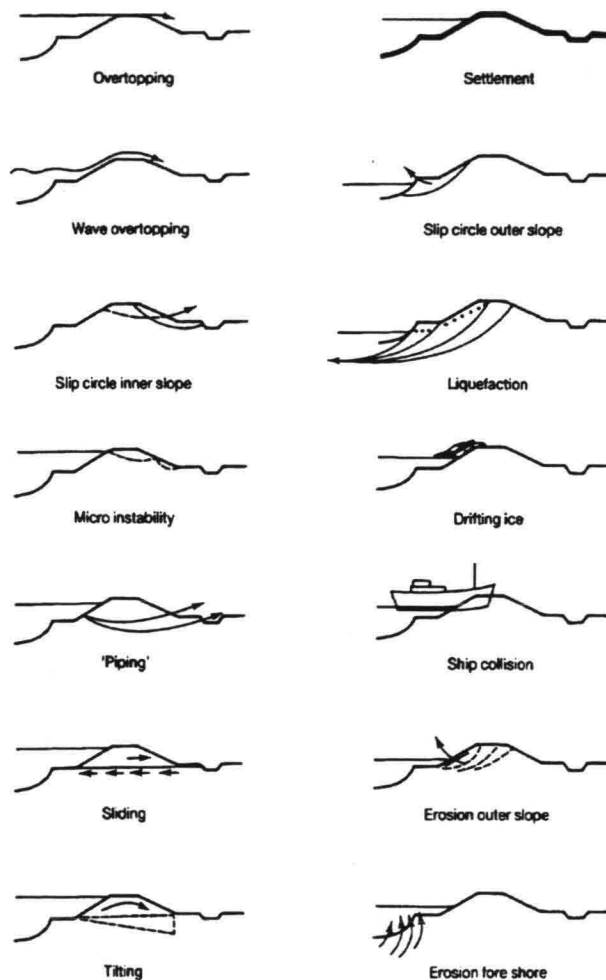


Figure 14.7 Failure mechanisms of a dike

DAMAGE

Damage is a certain change in the state of a structure due to any kind of loading. Damage is a gradual loss of function of the structure, while failure is an ultimate degree of damage with an unacceptable loss of functions. Or in other words: failure is a large increase in response due to a minor increase in loading; compare the transition from elastic to plastic deformation of a material. For the design of a structure, it is important to have insight in the relation between loading, damage and failure, particularly in the progress when a certain loading (wave height, flow velocity) is exceeded or when the duration of a certain loading is exceeded.

Figure 14.8 shows the damage of a rock revetment as a function of the parameter $H_s/\Delta d$. It can be seen that there is a strong increase in damage with increasing wave height. Failure can be defined as the situation where the top layer is locally removed and the filter layer becomes exposed (after that, the damage will increase much quicker).

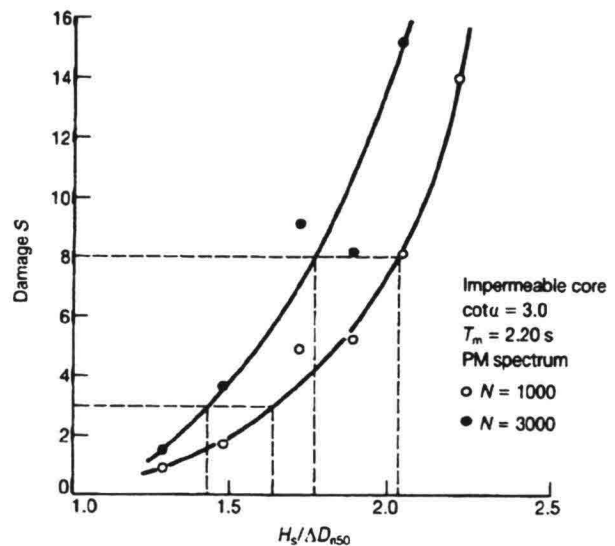


Figure 14.8 Damage curve for rock armour (vdMeer)

Damage as a function of time gives another picture. Figure 14.9 shows the relative increase in damage for a rock protection as function of the number of waves (line 2 and 3). Line 1 is a possible curve for a placed block revetment (with a wave height higher than a design wave). When such a structure relies heavily on the interlocking of the elements, progressive failure occurs when a certain level is exceeded and the duration is long enough. This is of course important for the reliability of a structure.

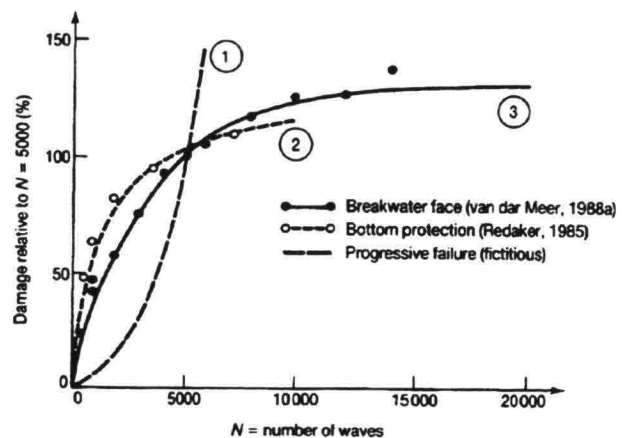


Figure 14.9 Damage as function of time

FAULT TREES

A fault tree or a failure tree can be a useful tool in the structural design phase. It gives an overview of possible events and their effects, ultimately resulting in some failure mechanism, the so-called top event. It can serve to establish the total probability of failure and/or the relative importance of various failure mechanisms. Often it is difficult or impossible to quantify the probabilities of all events and their consequences. But even then, a fault tree can contribute in the insight in possible failure modes of a structure.

Figure 14.10 gives a simplified example of a part of a fault tree for a seawall. Such a structure can be schematized as a system consisting of subsystems and components that can fail. The top event in this case is defined as excessive wave overtopping due to lowering of the crest. This lowering can be caused either by displacement of stones or by settlements. This is expressed in the fault tree by a so-called OR-gate, equivalent to a series subsystem, between these two events and the next. The displacement of stones can occur when there is scour and instability at the toe, hence an AND-gate in the fault tree, equivalent to a parallel subsystem. (Displacement due to wave action is here neglected, it is only part of a fault tree)

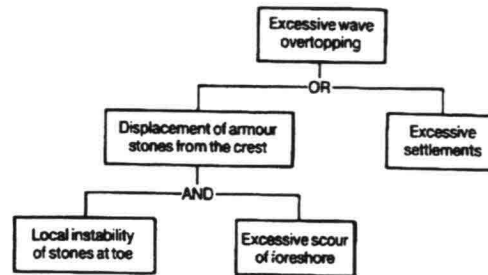


Figure 14.10 Part of fault tree

(Displacement due to wave action is here neglected, it is only part of a fault tree)

The probability of failure has to be determined either from available models, from experience with similar structures or from expert judgment. When the subsystems in Figure 14.10 are assumed to be uncorrelated, the probabilities are multiplied for a parallel system and added for a series system. Figure 14.11 gives the result.

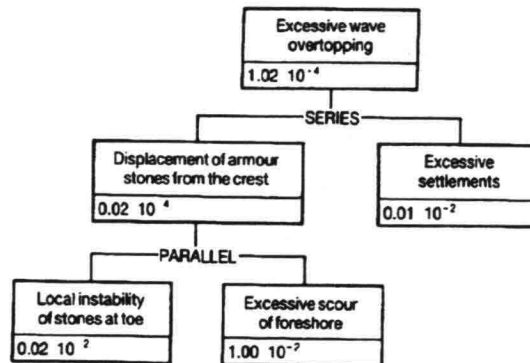


Figure 14.11 Failure probabilities

When there is some correlation between two components in a subsystem, the probability of failure, P_F , lies between:

$$\begin{aligned} \max(p_{f1}, p_{f2}) &\leq P_F \leq p_{f1} + p_{f2} && \text{(series system)} \\ p_{f1} \cdot p_{f2} &\leq P_F \leq \max(p_{f1}, p_{f2}) && \text{(parallel system)} \end{aligned} \quad (14.1)$$

where p_{fi} is the probability of failure of a component.

For a system with n components and all p_{fi} equal, Figure 14.12 gives P_F related to p_{fi} and to the degree of correlation, ρ_c ($\rho_c = 0$: no correlation, $\rho_c = 1$: full correlation) It can be seen that for a series system it is favourable when there is full correlation. A chain is as strong as its weakest link (which is what Figure 14.12 shows), with $\rho_c = 1$ all links are equally strong. For a parallel system, P_F is minimal when $\rho_c = 0$. Note that for $\rho_c = 1$, there is no difference between a parallel or a series system.

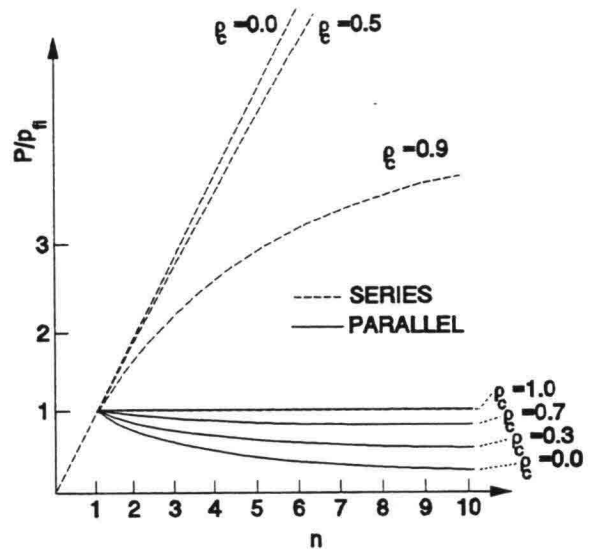


Figure 14.13 finally gives an example of a fault tree with risk-levels included (risk $r = p.c$, p is probability of failure and c is cost consequence). For more detail, see CUR/CIRIA,1991.

Figure 14.12 P_F/p_{fi} as function of correlation and number of components (all p_{fi} equal)

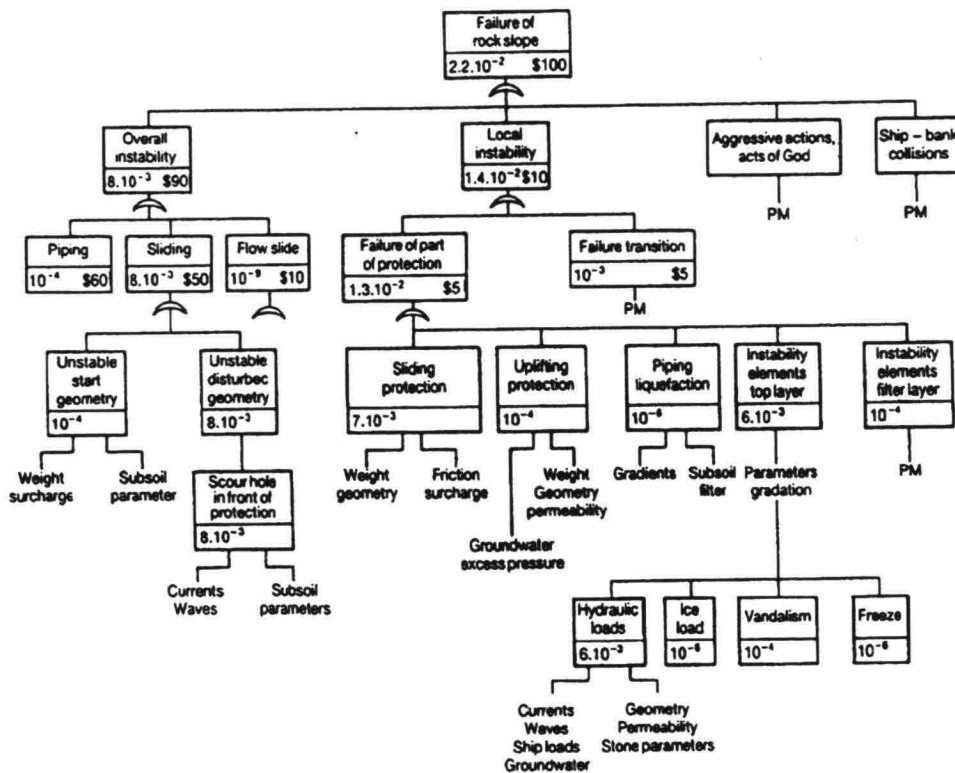


Figure 14.13 Example of fault tree for seawall with risk-level assessment

Every structure is designed with some safety, which means that the probability of failure is tried to keep below some accepted level. There are several ways of dealing with safety, usually distinguished as deterministic or probabilistic approach. In the latter, the probability of failure is explicitly calculated, while in the first there is a safety factor between a chosen design load and a characteristic strength, leaving the total probability of failure in the dark.

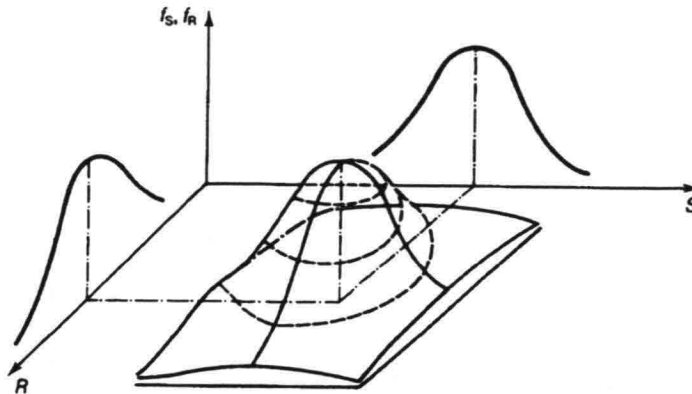


Figure 14.14 Distribution of loading and strength

Figure 14.14 shows the probability distribution of loading (S) and strength (R). The reliability (Z) can be defined as $Z = R - S$ and $Z = 0$ indicates the state of failure. There are several ways to treat this problem more or less completely. The usual division in completeness is:

- Level III:** $Z = 0$ is determined taking the completely known probability distribution of R and S into account
- Level II :** simplifications are made, like the linearization of Z , which again can be done in several ways
- Level I :** a quasi-probabilistic approach where the distance between characteristic values for loading and strength is formed by partial safety factors
- Level 0 :** deterministic approach with one overall safety factor between R and S

A probabilistic approach is superior to the classical deterministic because it gives

- a - a better appreciation of strength and loading statistics
- b - prevention of unnecessary conservatism, often leading to cost saving.

ad a: in a deterministic approach, only one loading level is considered. Lower loading levels can give cumulated damage, while higher levels can contribute considerably to the total failure probability, see Figure 14.8

ad b: strongly related to a. In a level 0 or I approach, partial safety factors are often accumulated, which is avoided when the real probability density function is taken into account.

For a conceptual design, a deterministic approach is usually sufficient, while for the structural design more and more use is made of level II or at least level I methods. This is in line with what was said about calculations and modelling, which go more into detail when the design evolves.

DETERMINISTIC APPROACH

Figure 14.15 gives an example of a deterministic approach where the strength R is expressed as a chosen stone diameter and the loading S as a certain wave height. This wave height is based on a long term distribution of wave heights e.g. a Weibull-distribution, see chapter 3.

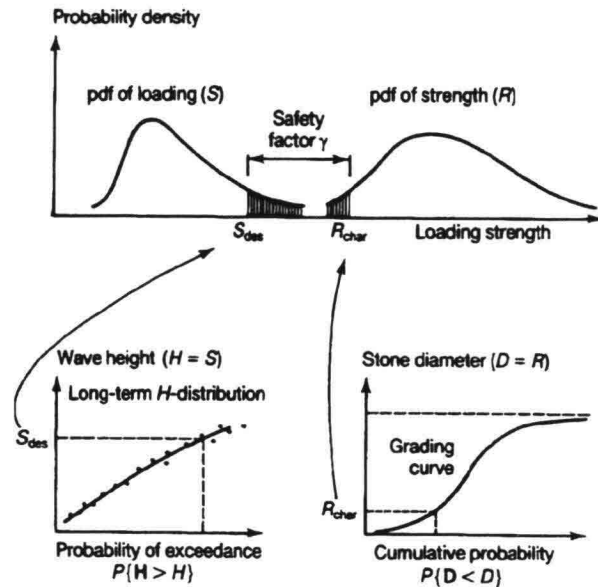


Figure 14.15 Deterministic approach

The choice of the frequency of the design load depends, among other things, on the chosen period e.g. the life of a structure or the duration of a construction period. The chance that an event occurs one or more times in a period T , can be derived from the Poisson-distribution:

$$P = 1 - e^{-m} \quad (14.2)$$

in which m is the average number of occurrences in the period T . For small m , $P \approx m$: a waterlevel that is exceeded once every hundred years, has a probability of exceedance in one year:

$$1 - e^{-0.01} = 0.00995 \approx 0.01 = m.$$

Note that a waterlevel that is exceeded once every year as an average, has a probability of exceedance in one year: $1 - e^{-1} = 0.63$. That means that there is 63% chance that such a level is exceeded, so usually for a construction period of a year a much less frequent situation will be chosen. For a construction that has to "last forever", like a dike, this approach does not lead to useful numbers. In that case one can take for example a man's life. A probability of exceedance of e.g. 1% in an average life of 75 year, leads to a loading with an average occurrence of once every 7500 years.

For a conceptual design this is an acceptable way of establishing a design load. For a structural design the probabilistic approach is recommended. Since these lectures are only an introduction, the reader is referred for more information to CUR/CIRIA,1991 or to the lecture notes on probabilistic design.

ANNEX

A	MATERIALS
----------	------------------

It is impossible, within the framework of these lecture-notes, to describe all properties of all materials that can be used in hydraulic engineering. In this appendix some reprints of relevant texts from the reference list are presented for the most important materials:

STONE:

Dimensions, weights, gradations. Source: CUR/CIRIA, 1991

CONCRETE BLOCKS:

Examples of shape. Source: Pilarczyk, 1990

ASPHALT:

Types and use of mixtures. Source: RWS, 1985

GEOTEXTILES:

Types and properties. Source: CUR/CIRIA, 1991

Other references:

COMPOSITE MATERIALS:

Principle and examples. Source: CUR/CIRIA, 1991

CLAY AND VEGETATION:

Gradations, properties and fitness of soil-types for vegetation. Source: CIRIA, 1990

Source: Manual on the use of rock in coastal and shoreline engineering, CUR/CIRIA, 1991

3.2.2.3 Block weight and size

The relationships between size and weight of individual blocks may be defined in terms of the equivalent-volume cube (side D_n) or the equivalent volume sphere (diameter D_s) which, with weight density γ_a and block weight W , give the following relationships:

$$D_n = 1.0(W/\gamma_a)^{1/3}$$

$$D_s = 1.24(W/\gamma_a)^{1/3}$$

with $D_n = 0.806 D_s$,

As indicated in the previous section, where graded rock materials are used, size and weight relations refer to medians or averages.

Where the particles are small enough (less than 200 mm) the statistical values are most conveniently derived from sieve analyses. The median sieve size (square openings) (D_{50}) on the percentage passing cumulative curve can be related to the median weight (W_{50}) on the percentage lighter by weight cumulative curve by a simple conversion factor and γ_a or ρ_a . (This dimension D_{50} is the same as the median value of the gross shape dimension z .)

The 50% passing nominal diameter D_{n50} is the size of the cube with equivalent volume to the block with median weight, and is given by

$$D_{n50} = (W_{50}/\gamma_a)^{1/3}$$

The conversion factors relating D_{50} to D_{n50} or W_{50} have been determined experimentally by various workers. The most extensive study is that by Laan (1981), for which the following summary value was obtained and recommended for future use:

$$D_{n50}/D_{50} = 0.84 \text{ or } F_s = W_{50}/(\gamma_a D_{50}^3) = 0.60$$

where F_s is the shape factor. As a cautionary note, Laan's study used several different rock types and sizes of stones and found that the value of F_s varied from 0.34 to 0.72, while in the study using different shape classes of limestone fragments (Latham *et al.*, 1988), F_s for all five classes fell between 0.66 and 0.70.

Samples containing blocks larger than 100 mm are difficult to analyse by sieving techniques and direct measurement becomes a more appropriate means of determining size distribution. The relationship between size and weight distributions have been noted above. With large block sizes (i.e. larger than sieve sizes of 250 mm) measurement of weight may prove more practicable than measurement of dimensions, and the size-weight conversion factor such as F_s can be used to determine the median sieve size and other geometric design parameters that may be expressed in terms of sieve sizes.

W_{50} (or M_{50}) is the most important structural parameter in the rock armour design being related to the design parameter D_{n50} , as described above. The controls on block weights were discussed under 'Discontinuities' (Section 3.2.1.4) and the changes in W_{50} from quarry to site were discussed under 'Block integrity' in Section 3.2.2.1. Gradings of rock fulfilling the class limit specification described in the following section may be expected to have standard deviations in D_{n50} , varying from 1% for heavy gradings to 7% for wide light gradings.

3.2.2.4 Grading

In a sample of natural quarry blocks there will be a range of block weights, and in this sense, all rock materials is, to some extent, graded. The particle weight distribution is most conveniently presented in a percentage lighter by weight cumulative curve, where W_{50} expresses the block weight for which 50% of the total sample weight is of lighter blocks (i.e. the median weight) and W_{85} and W_{15} are similarly defined. The overall steepness of the curve indicates the grading width, and a popular quantitative indication of grading width is the W_{85}/W_{15} ratio or its cube root, which is equivalent to the D_{85}/D_{15} ratio determined from the cumulative curve of the equivalent cube or sieve diameters of the sample. The following ranges are recommended for describing the grading widths:

	D_{85}/D_{15} or	$(W_{85}/W_{15})^{1/3}$	W_{85}/W_{15}
Narrow or 'single-sized' gradation	Less than 1.5	1.7-2.7	
Wide gradation	1.5-2.5	2.7-16.0	
Very wide or 'quarry run' gradation	2.5-5.0+	16.0-125+	

The term 'rip-rap' usually applies to armouring stones of wide gradation which are generally bulk placed and used in revetments. The phrase 'well graded' should generally be avoided when describing grading width. It merely implies that there are no significant 'gaps' in material sizes over the total width of the grading.

Standardisation of gradings

There are many advantages in introducing standard grading classes. These mostly concern the economics of production, selection, stockpiling and quality control from the producer's viewpoint. With only a few specified grading classes, the producer is encouraged to produce and stock the graded products, knowing that designers are more likely to provide them the market by referring to these standards wherever possible. The proposed standard gradings for armour are relatively narrow. This can result in increased selection costs, but these will often be completely offset by the possibility of using thinner layers to achieve the same design function. Standard gradings are not needed for temporary dedicated quarries supplying single projects where maximised utilisation of the blasted rock is required.

It is convenient to divide graded rock into:

'Heavy gradings' for larger sizes appropriate to armour layers and which are normally handled individually;

'Light gradings' appropriate to sheltered cover applications, underlayers and filterlayers that are produced in bulk, usually by crusher opening and grid bar separation adjustments;

'Fine gradings' that are of such a size that all pieces can be processed by production screens with square openings (i.e. less than 200mm). For fine gradings, the sieve size ratio from the cumulative sieve curve ($D_{60}/D_{10} = U_c$, the uniformity coefficient) is often used to characterise the width of grading in a sample.

Standard gradings are more or less essential for fine and light gradings. However, for heavy gradings it is not difficult because of individual handling to define and produce gradings other than standard (see below). For example, if the 1-3 t grading is (just) too small for a particular application, choice of the first safe standard grading of 3-6 t will lead to an excessive layer thickness and weight of stone, and here use of a non-standard grading may well be appropriate. Again, ceiling sizes of stones in quarries arising from geological constraints may dictate an upper limit.

Box 24 Explanation of class limit system of standard gradings

Rather than using envelopes drawn on a cumulative plot to define the limits of a standard grading, the proposed system refers to either:

1. A series of weights of stones and their corresponding ranges of the cumulative percentage by weight lighter than values which are acceptable; or
2. A series of 'sieve' size of stones and their corresponding ranges of cumulative percentage by weight passing values, together with the average weight of stones in the grading.

Each weight-standardised grading class is designated by referring to the weights of its lower class limit (LCL) and its upper class limit (UCL). In order to further define the grading requirements realistically and to ensure that there are not too many undersized or oversized blocks in a given grading class, it is necessary to set two further limits, the extreme lower class limit (ELCL) and the extreme upper class limit (EUCL). The standard grading scheme then uses percentage by weight lighter than values, y (equivalent to percentage by weight passing for aggregated), 0, 2, 10, 70, 97 and 100 to set the maximum and minimum percentiles corresponding with each of the four weight values given by ELCL, LCL, UCL, and EUCL (see below and Figure 51, Table 19). Note that although straight-line segments have been drawn in Figure 51 to indicate an envelope, grading curves can go outside these straight-section envelopes and still fulfil the requirements given by the four class limits. However, the further requirement specifying that the effective mean weight, W_{em} , should fall within a set range will help to reassure the designer that there is an appropriate range of W_{50} values.

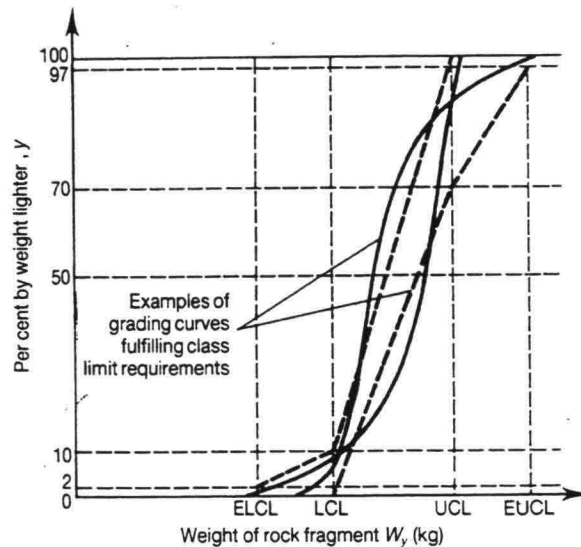
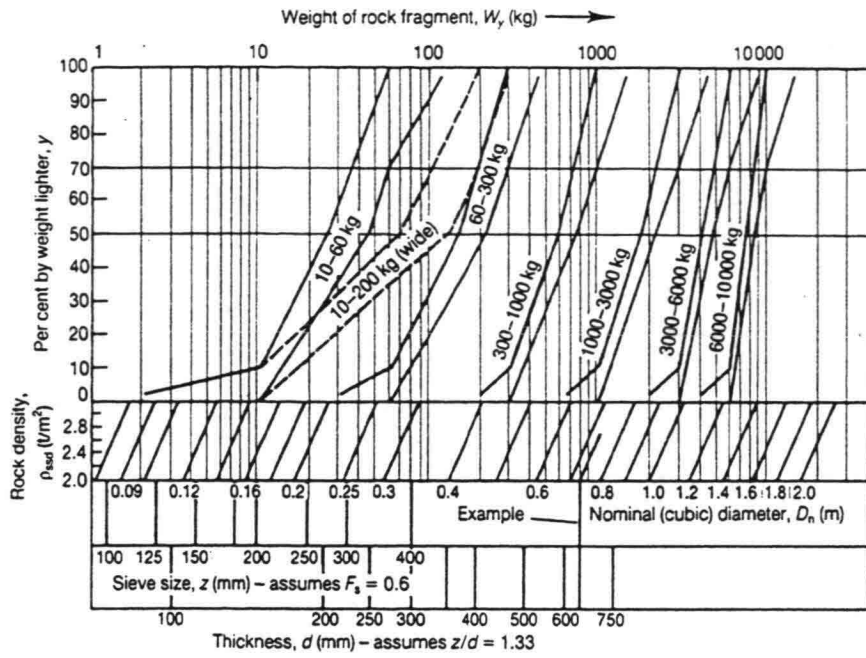


Figure 55 Explanation of the grading class limits of a standard grading

Size and average weight standardised gradings

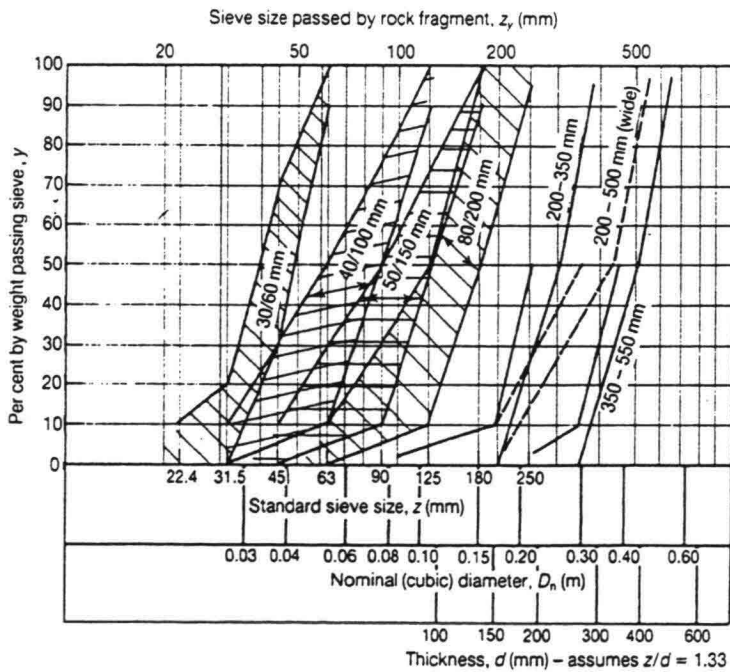
Each size-standardized grading class is defined with reference to the 'sieve' sizes of its ELCL, LCL and EUCL as explained above (no UCL specified) together with the average weight, \bar{W}_L , of all rocks not passing the LCL hole. However, for consistency they are designated i.e. named using the LCL and UCL hole sizes. Apart from bulk weighing to determine \bar{W}_L , the test verification of size is limited to gauging of blocks using three square gauge holes of sizes as defined in Table 19 and imposing the requirement consistent with the weight-grading scheme that:

1. Less than 2% by weight shall pass the ELCL hole, known as the EL hole;
2. Less than 10% by weight shall pass the LCL hole, known as the L hole;
3. At least 97% by weight shall pass the EUCL hole, known as the EU hole.



Note: W_{50} values given for grading envelopes reflect estimates of W_{em} range and are not obligatory (cf. Fig 55)

Figure 56 Weight gradings and size relationships for the standard light and heavy grading classes



Note: z_{50} values given for envelopes of light gradings reflect estimates of W_{em} range and are not obligatory (cf. Fig 55)

Figure 57 Size gradings and relationships for the standard fine and light grading classes

The weight envelopes for the standard light and heavy gradings are shown in Figure 56 with appropriate size-weight conversion. In this figure, rocks of any density and weight can be related to the corresponding nominal diameter, D_n , sieve size, z , and minimum rock thickness, d , using the alternative horizontal scales on this chart. The 'sieve' size, z , enveloped for the standard fine and light gradings are shown in Figure 57, again with conversions to D_n and d .

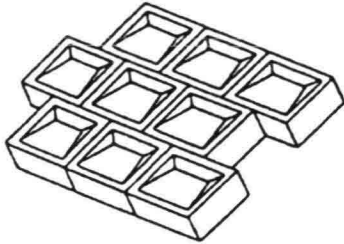
The standard fine and light gradings are produced by screens and grids and sometimes with eye selection to remove oversize material in the 60–300 kg and 10–200 kg classes. The poor screening efficiency that occurs in practice means that a correction factor would be needed in addition to the given theoretical relationships for sieve size, z , and minimum stone thicknesses, d , should a producer wish to use Figures 56 and 57 to indicate the combination of screens and grids that would yield the standard gradings. For the 10–200 kg more widely graded class, experience in the UK quarries using simple grizzlies to remove undersize material and eye selection to remove oversize material suggests that for rock of average (2.7 t/m^3) density, setting the grizzly clear spacing at 225 mm and using eye selection of material above 450 mm will be a good starting point. This advice must be tempered, however, by individual quarry managers' own experience at their particular quarry.

The grading envelopes become progressively narrower in the 'heavy grading' classes, consistent with design requirements and the geological constraints on producing large sizes of blocks. However, projects requiring blocks larger than 10 t should not make the (non-standard) grading class excessively narrow because of the producer's extreme difficulty in selecting accurately and the wastage from oversize block production. For example at $\rho_r = 2.7 \text{ t/m}^3$, D_n for a 15 t block = 1.7 m, and D_n for a 20 t block = 1.95 m, a difference of about 10%, which is very difficult to select precisely except by individual weighing.

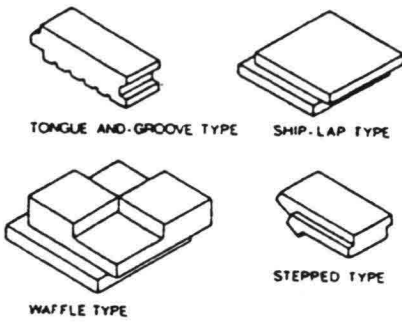
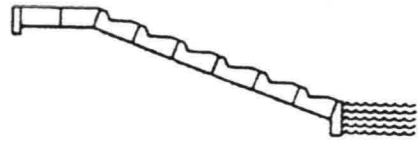
Box 25 Median and effective mean weight

A number of parameters in addition to the designated class limits may be required for design and specification purpose. An acceptance range for the important design parameter, W_{50} (median weight), is also useful for each grading class. However, in some circumstances an effective mean weight W_{em} for a particular consignment may be more easily obtained simply by bulk weighing and counting. In order to avoid including fragments and splinters in the distribution, W_{em} is defined as the arithmetic average weight of all blocks in the consignment or sample, excluding those which fall below the ELCL weight for the grading class. An empirical conversion factor relating W_{em} to W_{50} allows an estimate of W_{50} without the necessity of weighing each piece to obtain a weight-distribution curve. As the grading becomes wider, so will W_{50} depart more from W_{em} . Approximate relations are as follows:

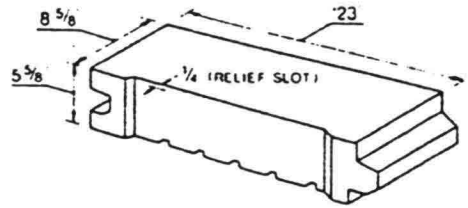
10–60 kg	$W_{50}/W_{em} = 1.3$
60–300 kg	$W_{50}/W_{em} = 1.15$
300–1000 kg	$W_{50}/W_{em} = 1.10$
1000–3000 kg	$W_{50}/W_{em} = 1.05$
3000–6000 kg and 6000–10 000 kg	$W_{50}/W_{em} = 1.00$



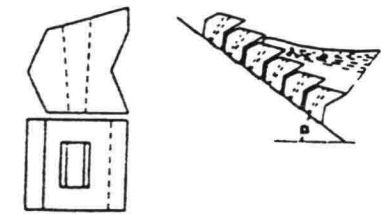
A. FREE RECTANGULAR-BLOCKS



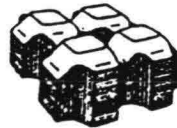
B. INTERLOCKING - BLOCKS



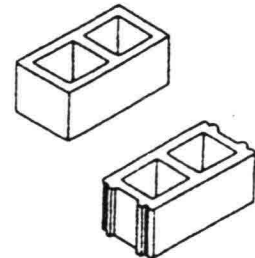
MODIFIED TONGUE AND GROOVE BLOCK



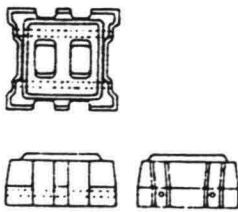
C. VEE-BLOCKS



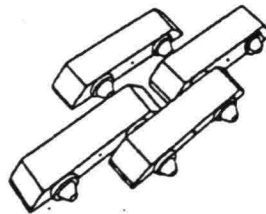
D. GOBI-BLOCK



E. BUILDING - BLOCKS



F. ARMORFLEX - BLOCK



G. TERRAFIX - BLOCKS

Source: The use of asphalt in hydraulic engineering, RWS, 1985

1.1 Mix components

Asphalt is a mix of various components:

- bitumen;
- mineral aggregate;
- additives, if required.

The mineral aggregate is composed of crushed stone, gravel, sand or filler or a combination.

The choice of the most suitable composition for a particular application depends mainly on the requirements which the material has to meet and the associated mix properties. see Section 6.1.

The mix properties are specified by the composition, that is, the relative proportions of the various components, the properties of the components themselves, and the properties which result from the application and compaction method.

1.2 The degree of filling of the mix

The mineral aggregate mix contains voids. Initially, the bitumen coats and binds the various aggregate components together. If more bitumen is applied than is necessary for coating and binding then the pores will gradually be filled.

Mixes, in which the bitumen only serves as a binder, are referred to as 'underfilled' mixes, see Figure 1.1a. The properties of such a mix are directly related to the properties of the stone skeleton (4). If the proportion of bitumen is increased the voids in the mineral become filled and the influence of the bitumen on the properties of the mix is increased while that of the stone skeleton is reduced. With mixes in which the pores are almost filled with bitumen, see Figure 1.1b, both the stone skeleton and the bitumen contribute to the mix properties. This type of mix must be compacted, either mechanically or under its own weight.

'Overfilled' mixtures are those in which the volume of bitumen is greater than that of the voids in the mineral aggregate. In such a mix the properties of the bitumen predominate, the mineral providing only a certain amount of stiffening, see Figure 1.1c. This type of mix is impermeable and requires no compaction.

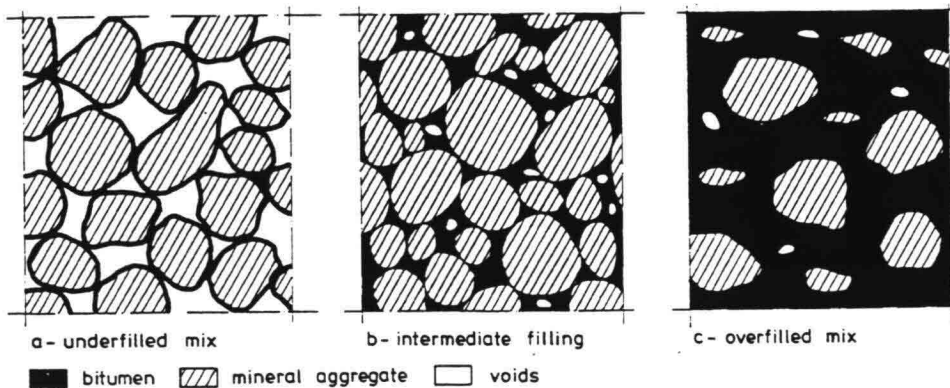


Figure 1.1 The degree of bitumen filling in the mineral aggregate.

1.3 Voids in asphalt mixtures

The term 'voids' refers to the volume of pores in the compacted asphalt (5). The voids ratio, VIM (voids in mix), is given by:

$$\text{VIM} = 100 \left(\frac{d_m - d_a}{d_m} \right) \text{ vol } \%$$

d_m = density of the mix without voids (kg/m^3)

d_m = density of the mix with voids (kg/m^3)

In general, the smaller the voids ratio (HR) the more resistant is the mix to erosion and the greater its durability. A mix with a small voids ratio is better 'sealed' against external influences such as oxygen, light and water. If water penetrates between the bitumen and the mineral (through the material) there is a loss of adhesion which is referred to as 'stripping'.

Exposure to the atmosphere and light ages the bitumen. In this respect, the size of individual pores and degree of interconnection between voids are also important.

The voids ratio and the distribution of voids also determine whether or not the mix is sand and watertight. Although water impermeability is not always a functional requirement it gives a good indication of the durability of a mix.

To illustrate:

- A mix containing sand with 5%, by mass, of bitumen and a voids ratio of 25% is sand-tight. A mix, however, of open stone asphalt with 80%, by mass, of stone and 20%, by mass, of mastic with the same voids ratio is not.
- An asphaltic concrete with a voids ratio of 3% can be considered as absolutely watertight. In this case the voids are not interconnected. For the same reasons a mastic with the relatively large voids ratio of 10% is also watertight.

7 Use of asphalt products in hydraulic structures

The most important mix types applied in hydraulic structures are:

1. Asphaltic concrete
2. Asphalt mastic
3. Grouting mortars
4. Dense stone asphalt
5. Open stone asphalt
6. Lean sand asphalt
7. Asphalt membranes

Mixes are defined by the constituents, the nature of asphalt mix and the binder material.

7.1 Asphaltic concrete

Asphaltic concrete is probably the best known mix type. It is a mixture of crushed stones or gravel, sand and filler in which the pores are practically completely filled with bitumen. The voids ratio is 3 to 6%.

In general the material must be compacted and is unsuitable for application under water or in the tidal zone. In view of the small voids ratio required, see Section 9.2.1., asphaltic concrete can be considered to be impermeable.

Asphaltic concrete is applied as a watertight dike revetment above the mean high water level, and as a lining for canals, reservoirs etc.

7.2 Mastic

Mastic is a mixture of sand, filler and bitumen. There is more bitumen available than necessary for filling the voids in the sand filler mixture. The mix, therefore, is naturally dense and need not be compacted. Mastic can be poured at working temperatures and is used, for asphalt slabs above and under water for lining or as bed and toe protection. When cold, mastic forms a viscous quasi-static mass.

7.3 Grouting mortars

Grouting mortars are hot-type mixes of sand, filler and bitumen of which there is more than required to fill the voids in the mineral; stone and gravel can be added if necessary. These mortars are used for grouting stone revetments above and below water-level, and also for slab construction.

7.4 Dense stone asphalt

Dense stone asphalt is a gap-graded mixture of stone, sand, filler and bitumen. The amount of bitumen slightly overfills the mixture. The material is, therefore, water impermeable.

It is used as bottom and slope protection and also in toe construction.

7.5 Open stone asphalt

Open stone asphalt is a gap-graded mixture of mastic and stone — a stone frequently used is limestone 20/40 mm. Mixing is carried out in two stages. First mastic is prepared and secondly it is mixed with limestone. The mastic binder only coats and connects the limestone particles together.

It is an 'underfilled' mix and, because of its open structure, should not be placed under water except in the form of prefabricated mattresses.

7.6 Lean sand asphalt

Lean sand asphalt is a mixture of sand, often locally obtained, with 3 to 5% bitumen. It is a greatly 'underfilled' mix and the function of the bitumen is simply to coat the sand grains and bind them together. After some time the permeability is very similar to the sand from which it is made.

It is used as a core material for reclamation bunds, filter layers and as permanent or temporary cover layer above and below water-level.

7.7 Membranes

Membranes are thin impermeable watertight layers of bitumen which are prepared in-situ or prefabricated. Membranes are used as impermeable linings for canals, banks and water courses.

Source: Manual on the use of rock in coastal and shoreline engineering, CUR/CIRIA, 1991

Geotextiles are permeable textiles made from artificial fibres used in conjunction with soil or rocks as an integral part of a man-made project and were first used in the Netherlands. They are frequently employed as filter membranes and as the interface between differently graded layers. Geotextiles are also used as bottom protection and can be loaded with concrete blocks (block mattress), bituminous bound crushed stone and sand (fixtone mattress) and geotextile tubes filled with gravel (gravel-sausage mattress). Gravel bags have also been used for special filter requirements.

The basic functions of geotextiles may be listed as follows:

1. *Separation*: the geotextile separates layers of different grain size;
2. *Filtration*: the geotextile retains the soil particles while allowing water to pass through;
3. *Reinforcement*: the geotextile increases the stability of the soil body;
4. *Fluid transmission*: the geotextile functions as a drain because it has a higher water-transporting capacity than the surrounding materials.

3.5.4.1 Geotextile manufacture

Geotextiles are manufactured from a variety of artificial polymers:

1. Polyamide (PA);
2. Polyester (PETP);
3. Polyethylene (low-density LDPE and high-density HDPE);
4. Polypropylene (PP);
5. Polyvinylchloride (PVC);
6. Chlorinated polyethylene (CPE).

The first four are the most widely used although many variations are possible. Additives are also employed in geotextile manufacture to minimise ageing, to introduce colour and as anti-oxidants and UV stabilisers.

Comparisons of properties of the four main polymer families are shown in Figure 90. These are very broad, because there are many variants within each group. Some properties (such as strength) are also greatly influenced by the different processes of manufacture. A classification of geotextiles based on the type of production and the form of the basic elements is given in Figure 91.

The basic elements used in geotextiles are monofilaments, multifilaments, tapes, weaving film and staple fibres. Monofilaments are single, thick, generally circular cross-sectioned threads with a diameter ranging from 0.1 mm up to a few millimetres. Multifilaments (yarns) are composed of a bundle of very thin threads. Yarns are also obtained from strips and from wide films. Tapes are flat, very long plastic strips between 1 and 15 mm wide with a thickness of 20–80 μm . A weaving film is sometimes used for the warp 'threads' in a fabric.

The basic fibre is a fibre of length and fineness suitable for conversion into yarns or non-woven geotextiles. For non-woven fabrics the length is usually about 60 mm.

COMPARATIVE PROPERTIES		POLYMER GROUP			
		Polyester	Polyamide	Polypropylene	Polyethylene
Strength		●	●	•	•
Elastic modulus		●	●	•	•
Strain at failure		•	●	●	●
Creep		•	●	●	●
Unit weight		●	●	•	•
Cost		●	●	•	•
RESISTANCE TO:					
UV light	Stabilized	●	•	●	●
	Unstabilized	●	●	•	•
Alkalis		•	●	●	●
Fungus, vermin, insects		•	●	•	●
Fuel		•	●	•	•
Detergents		●	●	●	●

● high
• low

Figure 90 Comparative properties of general polymer families

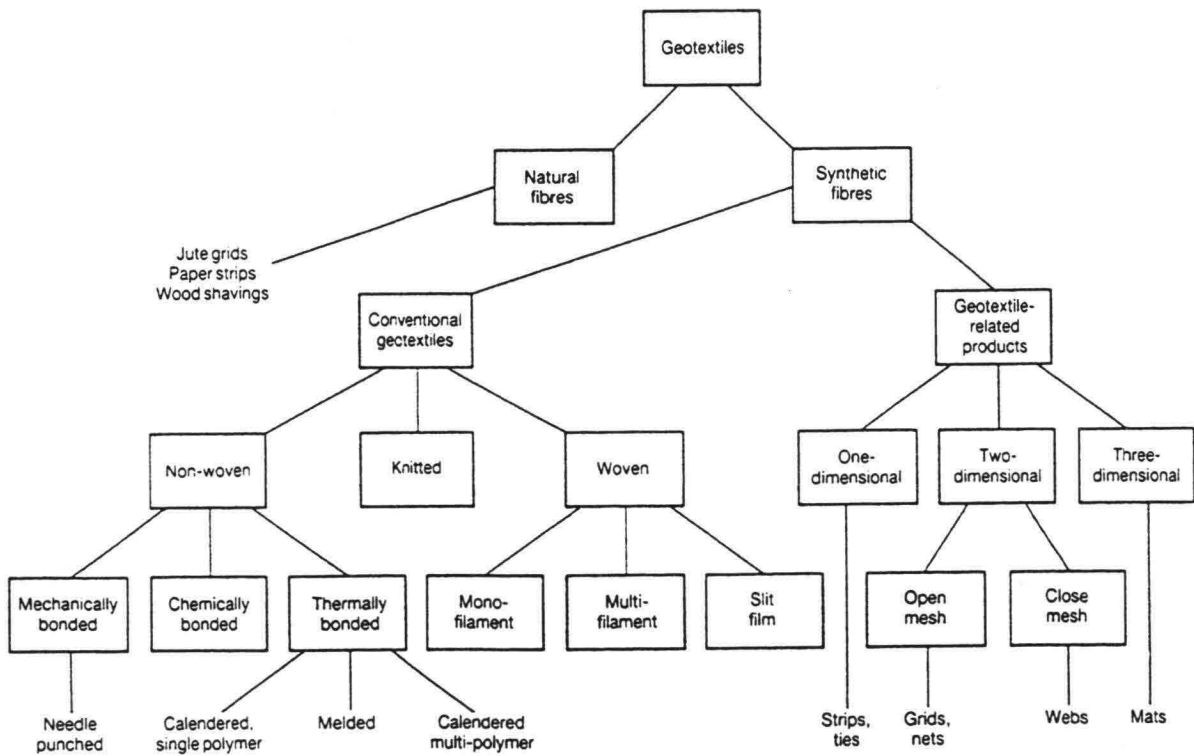


Figure 91 Geotextile classification groups

Woven geotextiles

A woven fabric is a flat structure of at least two sets of threads. The sets are woven together, one referred to as the warp, running in a lengthwise direction, and the other, the weft, running across. Woven geotextiles can be categorized by the type of thread from which the fabric is manufactured.

Monofilament fabrics are used for gauzes of meshes which offer relatively small resistance to through-flow. The mesh size must obviously be adapted to the grain size of the material to be retained. Monofilament fabrics are made principally from HDPE and PP.

Tape fabrics are made from very long strips of usually stretched HDPE or PP film, which are laid untwisted and flat in the fabric. They are laid closely together, and as a result there are only limited openings in the fabric (Figure 92).

Split-film fabrics are made from mostly fibrillated yarns of PP or HDPE (Figure 93). The size of the openings in the fabric depends on the thickness and form of the cross-section of the yarns and on the fabric construction. These split-film fabrics are generally heavy. Tape and split-film fabrics are often called slit-films.

Multifilament fabrics are often described as cloth, because they tend to have a textile appearance and are twisted or untwisted multifilament yarns. The fabrics are usually made from PA 6, PA 6.6 or from PETP.

Besides the above-mentioned monofilament fabrics, special *mesh-type constructions* are produced such as those with a monofilament warp and a multifilament weft which have outstanding water-permeability and sand-retention properties. Other examples include open meshes in which the woven or unwoven warp and weft threads are attached at crossing points by chemical or thermal bonding and other meshes constructed by using knitting techniques.

Non-woven geotextiles

A non-woven geotextile is a textile structure produced by bonding or interlocking of staple fibres, either monofilaments or multifilaments arranged at random, accomplished by mechanical, chemical, thermal or solvent means. Non-woven gauzes are structures with large meshes which are formed by placing threads or tapes at predetermined distances on top of one another and bonding them at the intersections by a chemical, thermal or mechanical process.

Geotextile-related products

These products are distinguished in one-dimensional (strips, ties), two-dimensional (gids, nets, webs) and three-dimensional (mats) products. Grids are lattices made from perforated and then stretched polymer sheets. Three-dimensional mats are produced by extruding monofilaments into a rotating profile roller, followed by coating so that the threads adhere to each other at crossings which are spatially arranged. The matting material itself occupies less than 10% of the mat volume. The mats are 5–25 mm thick and about 1–6 m wide.

3.5.4.2 Characteristics and properties

The geotextile properties stem primarily from their functional requirements. Since the geotextile can have a variety of functions, requirements are diverse. For reinforcement the emphasis is on mechanical properties such as *E*-modulus and strength, for filters it is on properties such as water permeability and soil tightness. The durability required will depend on the specific application and lifetime required. Geotextiles must also fulfil secondary functional requirements related to the execution of the work (e.g. a certain amount of UV resistance is needed) or it must have resistance to mechanical wear and tear if construction equipment is to be driven over the fabric. The suitability of a geotextile should be checked against these functional requirements during the design phase of the project.

Although specification requirement tests need only be carried out once, the following quality control tests may be required during production: tearing strength, grab test strength, tensile strength, strain at breaking load, moduli and mass distribution. These tests should be made in both the length and width directions. The thickness, the mass per unit area and the bursting strength may also need to be checked, and in some applications water permeability and sand-retaining properties will be important. A large number of national and a few international standard test methods are available covering these requirements.

Dimensions

The maximum standard width available for both woven and non-woven fabrics is 5–5.5 m. The length is limited by the available transport facilities and ease of handling on-site. Depending on the mass per unit area, the length generally lies in the range 50–200 m.

Jointing is necessary to obtain greater dimensions. In practice, large areas can be covered by overlapping sheets. Where physical continuity is required without overlap then heat welding (some non-wovens) or stitching may be used. The seam forms the weakest link in the geotextile construction and should therefore be checked thoroughly against the specifications. The thickness of most geotextiles lies between 0.2 and 10 mm when unloaded, although this may sometimes reduce under pressure.

In general, the mass of non-woven geotextiles lies in the range 100–1000 g/m², 100–300 g/m² being the most commonly used. Woven fabrics can be heavier and masses between 100 and 2000 g/m² are possible. The greater demand is for the lighter grades in the range 100–200 g/m². Generally, the lighter types of geotextiles are used as separators, the heavier woven fabrics for reinforcement and the heavier non-wovens for fluid transmission.

Chemical properties

One of the characteristic features of synthetic polymers is their relative insensitivity to the action of a great number of chemicals and environmental effects. Nonetheless, each plastic has a number of weaknesses which must be taken into account in the design and application. Specifically, the life of geotextiles can be affected by oxidation and by some types of soil/water/air pollution. Many synthetic polymers are sensitive to oxidation. The end result of oxidation is that mechanical properties such as strength, elasticity and strain absorption capacity deteriorate and the geotextile eventually becomes brittle and cracks.

Source: Manual on the use of rock in coastal and shoreline engineering, CUR/CIRIA, 1991

3.5.5 COMPOSITE MATERIALS

Composite systems are normally adopted where improved stability of the rock materials being used is sought (see Section 5.1.3.9) or where ease of placing the protection system is important.

3.5.5.1 Gabions

A gabion is a box or mattress-shaped container made out of hexagonal (or sometimes square) steel wire mesh strengthened by selvedges of heavier wire, and in some cases by mesh diaphragms which divide it into compartments (Figure 94). Assembled gabions are wired together in position and filled with quarried stone or coarse shingle to form a retaining or anti-erosion structure. The wire diameter varies but is typically 2–3 mm. The wire is usually galvanised or PVC-coated. PVC-coated wire should be used for marine applications and for polluted conditions.

The durability of gabions depends on the chemical quality of the water and the presence of waterborne attrition agents. The influence of the pH on the loss of the galvanic zinc protection is small for pH values in the range 6–12 and there are examples of gabions with negligible loss over 15 years. Grouting of the stone-filled gabions or mattresses can give some protection to the wire mesh against abrasion and corrosion, but this depends on the type of grout and the amount used.

The dimensions of gabions vary; but typically range in length from 2 to 4 m (mattress, 6 m), with widths about 1 m (mattress, 2 m), and height 0.3–1.0 m (mattress, max. 0.3 m). The mesh size is typically 50–100 mm.

The units are flexible and conform to changes in the ground surface due to settlement. Prefabricated gabions can be placed under water. Gabions can thus be used in a wide variety of marine works: groynes, dune and cliff protection, protection of pipelines and cables, and as toe protection. Mattress-shaped gabions are flexible and are therefore able to follow bed profiles both initially and after any scouring which may take place. Gabions can also be piled up to the form retaining walls or revetments (see Section 6.2, Box 80). In order to prevent migration of solid through the structure they may be used in conjunction with geotextile filter layers.

In certain applications the gabion structure needs impermeability or weight to counter uplift. To give these characteristics, the stone is grouted with mastic or a cement-bound grouting. The weight of the structure can also be influenced by the choice of the density of the stone blocks with which the gabion or gabion-mattress is filled.

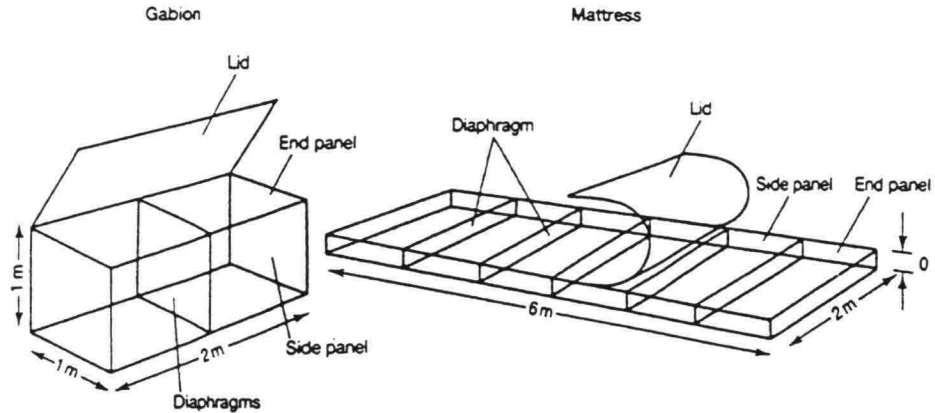


Figure 94

3.5.5.2 Mattresses

Prefabricated mats for hydraulic constructions have been used extensively as a medium for combating bottom and embankment erosion. The range of mat types have increased considerably during the last decade. Formerly, use was made of handmade mats of natural materials such as reed, twigs/branches (willow), rope, quarry stone and rubble. Today, geotextiles, bituminous and cement-bonded materials, steel cables and wire gauze are used as well as the more traditional materials.

Functions and principles

A distinction must be made between mattresses used for the protection of continually submerged beds and foreshores and mats employed for slope or front face protection of embankments. Bottom protection mats are concerned with:

- The mitigation of groundwater flow in the underlying seabed to prevent horizontal transport and erosion;
- Prevention of piping of soil particles;
- Assisting in the overall geotechnical stability of a larger structure;
- Offering resistance to loads imposed by anchors, trawler boards, etc. and thereby protecting pipes and cable lines;
- Providing a protection system with the flexibility to allow for anticipated settlements.

Mattresses for embankment retention have similar functions, i.e:

- Prevention of soil transport;
- Resistance to wave action;
- Provision of flexibility to allow for settlement.

Additionally, they may be required to:

Not trap refuse; and

- Support vegetative growth.

Mats are manufactured from the following elements:

1. *The carrier*: Fabric, gauze, cables and bundlings by which the necessary strength is obtained for its manufacture, transport and installation.
2. *The filter*: A geotextile which satisfies the conditions with respect to permeability, soil density, strength, etc. In some embankment-mat constructions the geotextile is applied separately.
3. *The ballast*: Concrete blocks, packaged sand, gravel, stone or asphalt necessary for the stability of the protection. Quarry stone can be used to serve as a material to sink the mat.
4. *The connections*: Pegs, wires, etc. by which the ballast material is fixed to the filter and the carrier materials.

In addition to the mat proper, a further deposit of gravel, aggregates, quarry stone, slag, etc. may be necessary when the ballast material stability in itself is insufficient or when extra protection is demanded.

The carrier and the filter can often be combined in the form of a single geotextile with the necessary mechanical and hydraulic properties. Sometimes the filter is combined with the ballast, which is then dimensioned as a granular filter.

Manufacture and placing

Fascine mats are typically up to 100m long and 16–20m wide. Historically, these mats were manufactured from osiers which were clamped between the so-called 'raster' of bundles of twigs/branches bound together to a circumference of 0.3m.

'Plugs' were driven into the crossing-points of the bundles to serve as anchor points for towing and sinking the mats (for bottom protection) or collar-pieces (for foreshore protection). Because of the destruction of the osiers by pile-worm attack, a reed layer was incorporated into the mats. These fascine mats were made on embankments in tidal areas or on special slipways.

The finished mat or collar-piece was then towed to its destination and sunk using quarry stones which were placed in position by hand, with the uppermost rasterwork of bundles serving to maintain the stone in place during sinking. After sinking, more and heavier stones were discharged onto the mat if this was found to be necessary.

Modern mats are made in accordance with the same principles. The twigs/branches and reed are replaced by a geotextile into which loops are woven and to which the rasterwork of bundles are affixed. A reed mat may be affixed onto the geotextile in order to prevent damage to the cloth during the discharge of stones onto the mat. The geotextile extends out beyond the rasterwork with the aid of lath outriggers so that, on sinking, the mats overlap. Sometimes a double rasterwork is applied to give the mats a greater rigidity and more edge support to the quarry stone load. The mat construction can serve as a protection for the bottom, a foreshore and even as an embankment protector. In the last case the mat is hauled up against the embankment itself.

Modern alternatives to fascine mats include mats where the quarried stone is replaced by open-stone asphalt reinforced with steel mesh, or by 'sausages' of cloth or gauze filled with a ballast material such as sand, gravel, bituminous or cement-bound mixtures.

Source: Use of vegetation in civil engineering, CIRIA, 1990

Box 2.3 summarises the important physical parameters of the soil. The soil characteristics which affect vegetation establishment and growth, their principal determinants and the ways in which they can be modified are given in Box 2.4. Soil contains water, air, fine earth, stones and organic matter.

Box 2.3 Soil physical parameters (definitions relating to plant growth)

Parameter	Definition	Assessment
Soil texture	Description based on proportions by weight of sand, silt and clay as percentages of fine earth fraction <2 mm in size	Field estimations or laboratory measurement
Stoniness, % vol	Proportion of large particles, >2 mm	Direct measurement, or field estimation
Dry bulk density* (ρ_d) Mg/m ³	Apparent density of soil <i>in situ</i> (on a dry basis)	Field measurement, either removal of undisturbed core or replacement method (sand or water)
Particle density* (ρ_s) Mg/m ³	Density of the soil particles	Laboratory measurement by displacement. Most soils are consistent with a value about 2.65 Mg/m ³
Void ratio (e)	Ratio: volume of soil voids to volume of solids	$e = \rho_s / (\rho_b - \rho_s)$
Porosity (ϵ) %* (total pore space, η)	Volume of soil voids expressed as a percentage of total <i>in situ</i> soil volume <i>note</i> – voids occupied by air and water.	$\epsilon = (1 - \rho_b / \rho_s) \times 100$
Soil erodibility factor	The risk of erosion by air or water due to the nature of the soil itself	Direct measurement or estimation based on soil texture, see Sections 6.3.2 and 6.5.2
Packing density (L_d)* (rooting potential)	A more reliable indicator of the effects of compaction than bulk density alone: allows for clay content	$L_d = \rho_b + (0.009 \times \% \text{ clay})$

* see Hall *et al.*, (1977), Jarvis and Mackney (1979).

Box 2.4 Soil physical characteristics

Important soil characteristics	Principal determinants				Modifiers					
	Particle size	Packing density	Porosity	Organic matter	Vegetation cover	Topography	Cultivation	Compaction	Additions	Time
Texture	●									
Soil structure	●		●	●			○	○		○
Rooting potential	●	●	●	●			○	○		
Soil water capacity	●		●	●				○	○	
Permeability and water acceptance			●		○	○	○	○		○
Ion exchange capacity	●			●	○				○	
Erodibility	●		●	●	○	○	○	○		
Ease of cultivation	●	●	●			○		○	○	

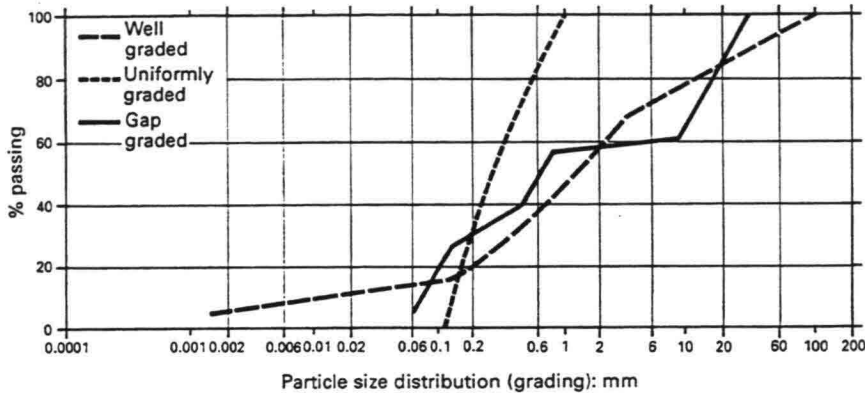
Rooting potential indicates the resistance of the soil to root penetration, which depends mainly on the soil's bulk density and on mechanical strength. Roots have great difficulty penetrating soil with strengths greater than 2.0 to 2.5 MN/m², though higher limiting values have been suggested for coarse-textured soils. Generally, root growth is enhanced by greater moisture content and voids, and is retarded by higher bulk density and clay content. Critical dry bulk densities for soils, above which root growth is severely restricted, are about 1.4 Mg/m³ for clay soils and 1.7 Mg/m³ for sandy soils. As clay content is so important in determining the rooting potential, a term *packing density* (L_d) is often used to determine the maximum density to which a soil can be compacted and still permit root growth (see Box 2.3).

Soil texture describes the particle size distribution and gives an indication of the likely behaviour of a soil in respect of handling, root growth or drainage. Descriptions such as sandy loam or clay are based on measured proportions and mixtures of clay, silt and sand in the fine earth (<2 mm) fraction, as shown in Box 2.5.

Soil structure is a characteristic which describes the arrangement and size of particle aggregates or 'peds'. Structure develops over time, as fine soil particles aggregate into crumbs and blocks. This increases the number of large pore spaces and thus the permeability and rooting potential of the soil. The presence of organic matter and plant roots plays a major role in developing and maintaining soil structure. Structure is easily damaged by handling or cultivation during wet conditions, when the soil is weaker.

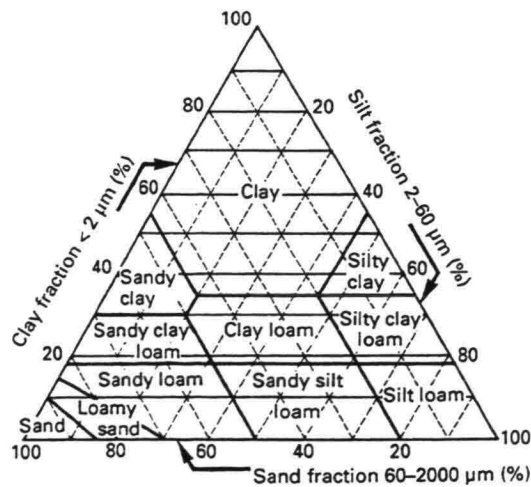
Box 2.5 Soil texture

The usual particle grading curves prepared to BS 5930:1981 are familiar to most engineers. Soils are described according to the British Soil Classification System for Engineering Purposes.



Clay fraction	Fine	Medium	Coarse	Fine	Medium	Coarse	Fine	Medium	Coarse	Cobbles
	Silt fraction			Sand fraction			Gravel fraction			
Fine earth							Stones			

For soil survey work, texture descriptions are based on the fine earth fractions, that is <2 mm size. The overall proportion of gravel and cobbles defines the *stoniness*. The proportions of sand, silt and clay in the fine earth soil matrix define the texture classes as given in the triangular diagram.



The proportions of sand, silt and clay can be obtained from the particle grading curve, calculating the quantity of each size fraction as a percentage of the <2 mm fraction.

2.4.5 Soil potential

The physical, water and chemical characteristics of the soil can be combined into an overall assessment of soil potential for plant growth. A scheme for this is given in Box 2.10.

Box 2.10 Assessment of soil potential

Class A is the highest quality and suitable for situations where good quality fertile topsoil is necessary. However, class C, whilst of poorer quality, would still be suitable for many situations (see Section 4.2.1). In many cases it would be possible to modify or manage a class B or C soil to improve its quality.

Parameter	Unit	Suitability class			Unsuitable
		A	B	C	
<i>Soil type</i>					
Texture	description ¹ and clay%	fLS,SL SZL,ZL	SCL,CL, ZCL,LS	C<45% SC,ZC,S	C>45%
Stoniness	% vol	<5	5–10	10–15	>15
Available water capacity (at packing density 1.4–1.75)	% vol	>20	15–20	10–15	<10
pH		5.7–7.0	5.2–5.5	4.7–5.5	<4.7
			7.0–7.3	7.3–7.8	>7.8
Conductivity	mmho/cm	<4	4–8	8–10	>10
Pyrite	% weight	–	<0.2	0.2–3.0	>3.0
<i>Soil fertility</i>					
Total nitrogen	% weight	>0.2	0.05–0.2	<0.05	
Total phosphorus	mg/kg	>37	27–37	<27	
Total potash	mg/kg	>360	180–360	<180	
Available phosphorus	mg/kg	>20	14–20	<14	
Available potassium	mg/kg	>185	90–185	<90	

Notes: 1. f = fine, S = sand, C = clay, L = loam, Z = silt

4.2.1 Selection of soil materials

The simple system for assessing soil potential described in Box 2.10 can be used as a general guide to classify all material which the engineer intends to use as soil, regardless of origin, according to its potential for plant growth. Classes are allocated as follows.

Soil type

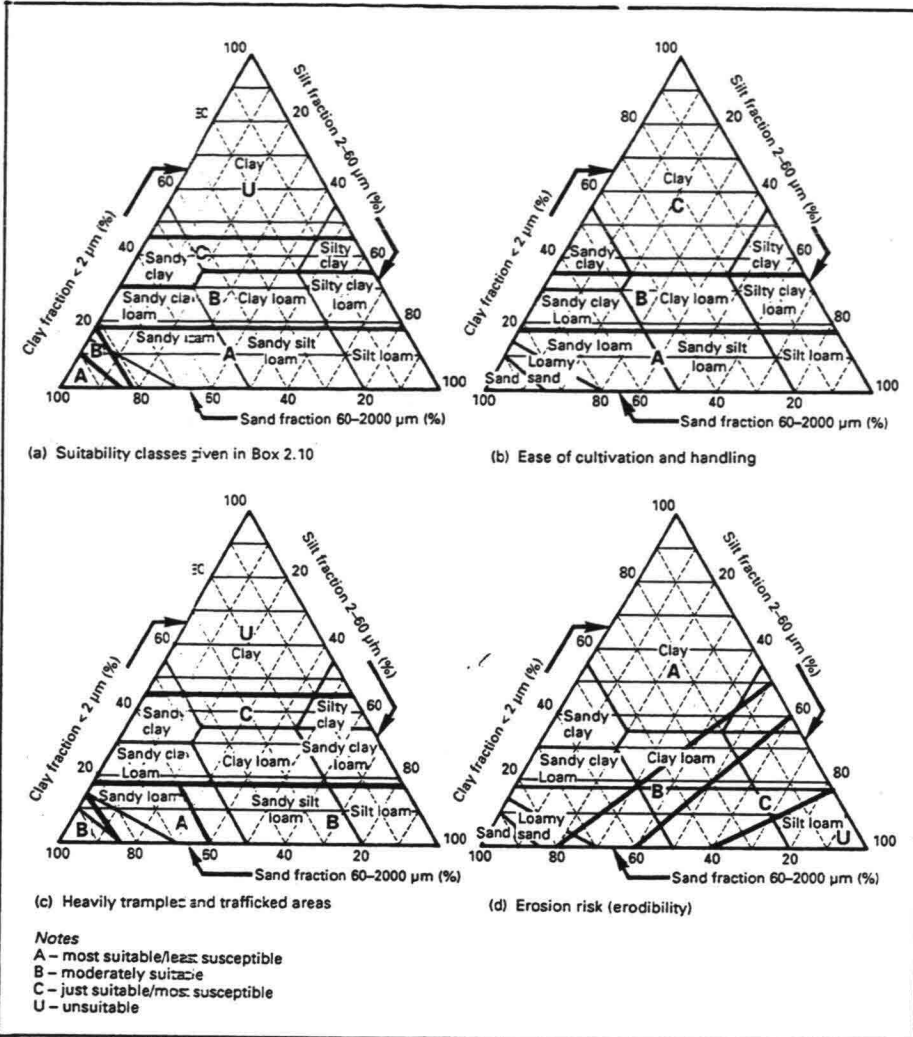
Class A Highest growth potential, important when it is necessary for soil to have minimal restrictions on plant growth. Suitable for final soil covering or topsoil.

Class B Where growth potential is not critical, but reasonable growth is still required. Also suitable for subsoil layers beneath Class A.

Class C Will still support good growth if managed properly, but susceptible to handling problems which may restrict growth. Can also be used as subsoil layers.

Suitability cannot be based on soil texture alone and the classes proposed in Box 2.10 have only general application. For some uses special soil characteristics may be required; examples are given in Box 4.3.

Box 4.3 Soil suitability for specific purposes based on texture



Soil fertility

Class A Highly fertile, will produce dense vigorous growth, requiring higher maintenance and leading more quickly to successional changes. This is not always necessary nor desirable, however, and the group is best used for intensively managed areas and for grazing.

Class B Moderate fertility; fertilisers may be required to support very productive growth.

Class C Minimal fertility, suitable for low-maintenance vegetation but fertilisers will be necessary. Swards should have good legume component.

Soil physical properties and fertility are defined separately so that different classes can be selected for each, depending on the situation.

APPENDIX

B

ENVIRONMENTAL ASPECTS

The relation between the protection of the interface of land and water and the environment is manifold. Three aspects are selected:

- 1 - The influence that a construction can have on the environment. A reprint is presented, dealing with Environmental Assessment.
- 2 - The incorporation of environmental aspects in the design itself. Both the demands from an ecological point of view, as well as examples of designs that are "friendly to the environment" are presented.
- 3 - The environmental demands in the use of different materials, like slags or other waste material, with emphasis on leaching in water.

Source: Manual on the use of rock in coastal and shoreline engineering, CUR/CIRIA, 1991

Environmental assessment (EA) is a procedure more commonly referred to outside the European Community as Environmental Impact Assessment (EIA), whereby the likely effects of a proposed development on the wider environment are considered as part of the planning and design of the project. The objectives of environmental assessment are:

- To make projects environmentally sensitive and less environmentally damaging;
- To provide suitable information to assist those organisations responsible for development control to make environmentally informed decisions.

2.4.1 REASONS FOR CARRYING OUT EA

Shoreline engineering works may affect (or be affected by) the natural and social environment in which they are situated. Typical aspects of the environment on which this type of project may impinge either during construction or in the long term are listed below and illustrated in Figure 37:

- Geomorphology, landscape and exciting physical processes (sediment transport, drainage, erosion, climate, etc.)
- Ecology (flora and fauna)
- Social and socio-economic aspects
- Human sensory aspects (visual intrusion, noise, odour, etc.)
- Palaeontological, archaeological, historical and cultural aspects
- Air, water and soil quantity (pollution, contamination, etc.)

The developer may perceive environmental assessment as an additional financial burden. However, the cost of the environmental assessment will be a small proportion (usually less than 0.5–1.0%) of overall project value and the procedure has a number of advantages from the developer's point of view:

- Identification of environmental impacts during the planning and design stage will enable the most cost-effective inclusion of measures to mitigate adverse impacts.
- The liaison and consultation exercise, which is normally an integral part of the assessment, will reduce the risk of an unexpected refusal of development consent at a late stage.
- EA should identify probable areas of objection to a project at an early stage to enable sensitive matters to be addressed and project delays minimised.
- EA provides an opportunity for public consultation and resulting greater acceptance of a project in the affected community.
- Unforeseen adverse environmental impacts may incur considerable future financial liabilities.

Environmental assessment may be voluntary or a specific legal requirement, depending on the state or other authority within whose jurisdiction the project falls. Advice should be sought from the relevant planning or other authority in this regard. Regulations affecting environmental assessment within the European Community are discussed in Box 13 (page 58). However, for the reasons just discussed, even where an EA is not formally required, some form of environmental study will prove valuable in project planning.

Box 13 European Community (EC) environmental assessment regulations

Legal requirements

In mid-1988 the requirements for environmental assessment in the European Community became formalised with the implementation of EC Directive 85/337 (Council Directive of 27 June 1985 'on the assessment of the effects of certain public and private projects on the environment' refers). Relevant statutory instruments, regulations and guidelines are listed in Appendix 7. The EA regulations, recommendations and publications are continually being updated. If in doubt, reference should be made to the appropriate authorities before undertaking a formal assessment.

EC Directive 85/337 states that environmental assessment shall be a mandatory part of the planning process for project types listed in Annex I of the directive. For projects listed in Annex II, which covers most typical shoreline engineering works using rock; the requirement for environmental assessment is at the discretion of the planning authority or other body responsible for granting consent for the development to proceed. (If an environmental assessment is required as part of an application for planning consent an increased period may be allowed for the planning authority to determine the consent.)

Scoping; aspects to be addressed

Article 3 of EC Directive 85/337 gives a particular description of the aspects to be covered in any EA:

1. Human beings, fauna and flora;
2. Soil, water, air, climate and the landscape;
3. Interaction between the factors mentioned in (1) and (2) above;
4. Material assets and the cultural heritage.

Requirements for the Environmental Statement

There is no precise definition with EC Directive 85/337 as to the form of the Environmental Statement. The only requirement is that it contains the information specified in Articles 3 and 5 and Annex III of the Directive and includes a 'non-technical summary'. More detailed formats for the ES may be specified in national regulations.

Statutory consultees

In addition to the issuance of public notices as required by regulations, the proponent of the scheme may be under a statutory obligation to notify or consult certain authorities and organisations specified in EA or planning regulations as part of the formal environmental assessment process.

(Continued opposite)

		Human beings	Fauna	Flora	Soil	Water	Air	Climate	Landscape
Human beings	(cd)		(b)	(b)	(cf)	(cf)	(cf)	(ca)	(da)
Fauna	(b)	(b)		(b)	(bf)	(bf)	(bf)	(ba)	(ba)
Flora	(b)	(b)	(b)		(bf)	(bf)	(bf)	(ba)	(ba)
Soil	(f)	(fc)	(fb)	(fb)		(f)	(f)	(fa)	(fa)
Water	(f)	(fc)	(fb)	(fb)	(f)		(f)	(fa)	(fa)
Air	(f)	(fc)	(fb)	(fb)	(f)	(f)		(fa)	(fa)
Climate	(a)	(ac)	(ab)	(ab)	(af)	(af)	(af)		(a)
Landscape	(a)	(ad)	(ab)	(ab)	(af)	(af)	(af)	(a)	
Material assets	(ce)								
Cultural heritage	(e)								

Note: Letters in the above matrix refer to the discipline-based environmental aspects discussed in Section 2.4.1

Figure 38 EC Directive 85/337 aspect and aspect interaction scoping chart

Box 13 (Continued)

Consent from other bodies may be required whether or not a development is outside the jurisdiction of the local planning authority. For example, shoreline works may require a licence for placing material on the seabed or approval for navigation. These bodies may also require an environmental assessment as part of the application for their consent, licence or approval. Statutory consultees for the UK are listed in Appendix 7.

Sensitive locations

Projects which impinge on particular sensitive locations (such as those listed in Appendix 7) will require special attention. Development directly or indirectly affecting such sites is likely to make the requirement for environmental assessment mandatory.

This categorisation of environmental aspects is peculiar to the EC directive, but it is compatible with a more conventional discipline-based aspect listing such as that given in Section 2.4.1. Figure 40 indicates in each of the matrix boxes by letter (referring to the list in Section 2.4.1) the discipline-based aspects which are relevant to each of the EC environmental categories.

2.4.3 METHOD OF ASSESSMENT

Phases of an assessment

An environmental assessment will normally comprise three phases:

1. The baseline survey, to define the existing environment;
2. The projection of the proposed project onto the existing environment and the assessment of the probable impacts (beneficial and adverse);
3. Where impacts are found to be adverse, the investigation of measures to mitigate those impacts and the possible incorporation of those measures into the design.

Scoping

The aspects of the environment on which rock coastal and shoreline engineering works may have significant effects will include those listed in Section 2.4.1 and the various interactions between them. For an EA to be cost-effective, the distribution of time and effort must match the relative needs of the different aspects. At the start of an assessment it will be necessary to decide on the probable scope of the investigations and the appropriate level of detail required from the results.

Where the assessment is to be carried out under European Community Directive 85/337 or its derivative national regulations, a particular presentation of the aspects is required. This is compatible with the aspects as listed in Section 2.4.1 and is detailed in the scoping diagram in Box 13.

Source: Translation of parts of "Milieuvriendelijke Oevers" (Environment-friendly banks), RWS, 1988

Policy on the design of banks

Policy on the design and management of banks has been revised. The new approach is set forth in several policy documents, not only in the above-mentioned Policy Document on "Living with Water", but also in the Third Policy Document on Water Management drawn up by the Ministry of Transport and Public Works, the National Environmental Policy Plan drawn up by the Ministry of Housing, Physical Planning and the Environment, and the National Nature Policy Plan drawn up by the Ministry of Agriculture and Fisheries, all of which appeared in 1989. The Environmentally Friendly Banks Project deals with the development, acceptance and application of this policy from a pragmatic angle.

The management of a watercourse should be related to the management of connected waters and the functions of the adjacent land. What is required is integrated management of a water basin. This approach demands that a thorough analysis be made of the functions, management and general situation in the whole of the area concerned. Such analysis is of prime importance in the case of the design and management of banks, which form the boundary between water and land and therefore themselves consist of both elements. A functional analysis based solely on criteria deriving from hydraulic engineering is no longer adequate; other requirements and related criteria must also be taken into account.

In functional terms a watercourse bank may be variously described as:

- at once a dividing-line and a transition between water and land, each having its own functions;
- a means of protecting the land against the water: it affords protection against high water levels, waves and currents;
- a means of protecting the water against the land: it affords protection against cave-ins and the formation of shallows;
- a habitat for specific aquatic plants and animals. In this sense banks play an ecological role, one that is related to the general ecological function of the aquatic environment as expounded in the Indicative Multi-Year Programme for Water;
- an environment through which specific bank-related plants may spread, and animals move, across the land, thus forming part of the ecological infrastructure;
- a scenic element affecting the overall recreational enjoyment of the landscape;
- an element in water-related activities, such as shipping, fishing and recreation.

There are many types of banks, which differ in respect of functions, morphology, soil composition, hydrological conditions and vegetation. In actual fact, no two banks are alike. But even on one long bank considerable variations can occur, or even be introduced, greatly enhancing the diversity of the scenery and its wildlife.

It is therefore futile, or ill-advised, to seek one uniform type of environmentally friendly bank. It would be wrong to try to eradicate the diversity which has arisen, which is in many cases of great value. The term "environmentally friendly" was opted for in the new policy to emphasise the contrast with the usual civil engineering approach to bank protection. The qualification "multipurpose" would, perhaps, have been more to the point.

Source: Delft Hydraulics, publication nr. 464, 1991

ENVIRONMENT-FRIENDLY BANK PROTECTIONS

R.E.A.M. Boeters, H.J. Verheij* and M. van der Wal*

Rijkswaterstaat, Road and Hydraulics Engineering Division,
Delft, The Netherlands

* Delft Hydraulics, Emmeloord, The Netherlands

ABSTRACT: Embankments along navigation canals and rivers usually require a protection against the erosive forces of currents and waves. Up to now, in most cases riprap, concrete blocks or sheet-pilings have been applied. However, the increased public awareness about more environment-friendly solutions has been leading to greater attention for design criteria for protective structures allowing the presence of vegetation. After surveying several types of environment-friendly protections the recently-developed design rules for two particular structures will be presented. In addition, we will also present a summary of the expected outcome of research projects being carried out presently.

1. INTRODUCTION

In the Netherlands much attention is focussed on building environment-friendly protections along embankments of navigation canals, levees and summer dikes along rivers [1]. These protections are designed in such a way that plants and animals can grow and reproduce, whereas the protection itself blends nicely into the surrounding environment. Thus, they do not only provide a habitat for plants and animals, but they are also attractive for recreational purposes. The environment-friendly structure should resist the occurring hydraulic forces induced by currents, wind-waves and ship-induced water motions. In some situations the vegetation will have a protective function. In that case the stems and leaves are expected to reduce the hydraulic loads (active role of the vegetation), while the roots are expected to improve the stability of the subsoil against erosion (passive role of the vegetation). However, in other situations the vegetation will only play an aesthetical role. In this paper results will be presented of physical model tests and other studies dealing with the current environmental bank protection research in the Netherlands.

2. TYPES OF ENVIRONMENT-FRIENDLY PROTECTIONS

Several types of environment-friendly protections can be distinguished. The difference between the various types is determined by the function of the vegetation in relation to the hydraulic loads (aesthetical or protective role). In Fig. 1 the following environment-friendly types of bank protection are shown schematically:

- A) Embankments without any protection, resulting in the most natural environment for animals and plants. This type can only be applied in the case of low hydraulic loads and/or a very large available construction width.
- B) Partially protected embankments, i.e. the lower part of the embankment is protected against (ship-induced) currents, the upper part is protected by the vegetation. This type is suitable for smaller canals and rivers in which relatively low hydraulic loads occur. The vegetation then has to be temporarily protected against incoming ship or wind waves during the first stage after construction.
- C) Structures with a shallow pool behind a fixed protection. In the pool plants and animals find their habitat. The water in the pool is refreshed through gaps in the fixed protection. The fixed protection absorbs all the hydraulic loads. This type may be applied in the case of medium to heavy hydraulic loads and sufficient construction width.

D) Protections through which plants can grow and develop. For these structures block mattresses can be used, but also gabions and specially designed protections consisting of open riprap layers. This type of structure is suitable in the case of little available width and medium hydraulic loads.

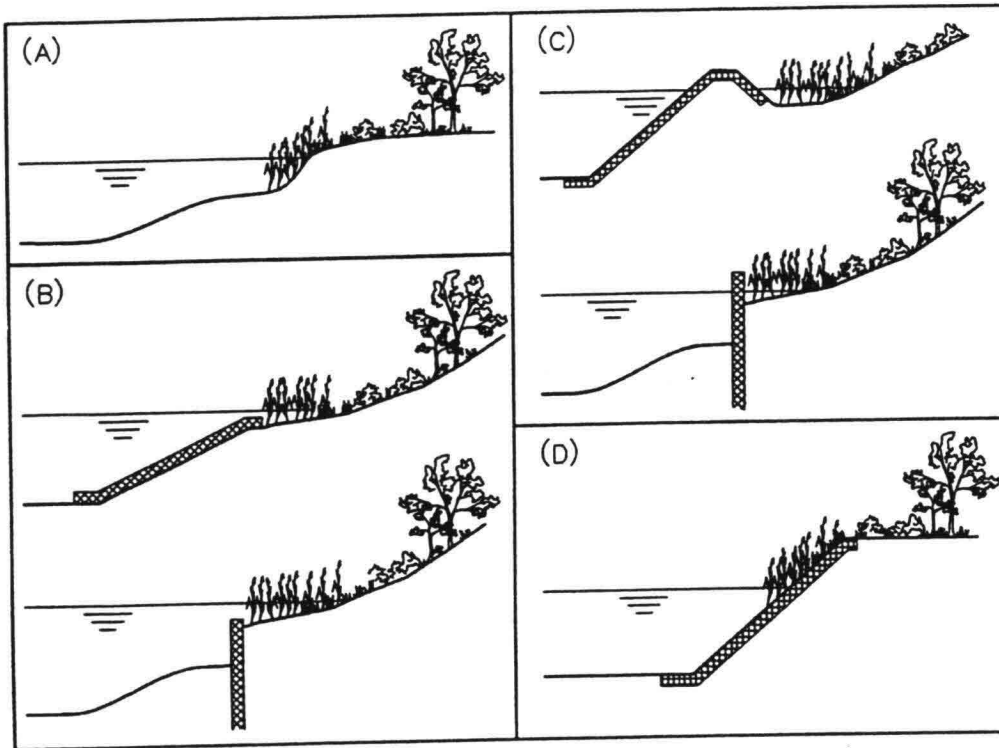


Fig. 1 Types of environment-friendly bank protections

In the Netherlands various research projects are carried out yet with respect to environment-friendly bank protections. Among these protections, one of them concerns a combined system, such as cellular concrete revetment blocks allowing vegetation. Another project deals with the water exchange between a navigable fairway and a shallow pool with vegetation behind a fixed protection along the fairway. In the next sections design criteria for both structures will be presented.

3. EROSION OF SEDIMENT THROUGH CELLULAR BLOCKS

A promising structure with respect to providing a natural habitat for plants and animals living along the water, blending into the surrounding landscape is the application of cellular concrete revetment blocks, particularly in the case of limited available space for constructing a bank protection (Fig.2). The cells in this type of structure allow vegetation to grow through or between hard elements. The blocks are permeable enough to prevent the occurrence of high uplift pressures while, on the other hand the individual blocks support each other against severe wave attack. The erosion of the cell fillings is decisive for the stability of the slope protection and the growth of the vegetation in the first stage.

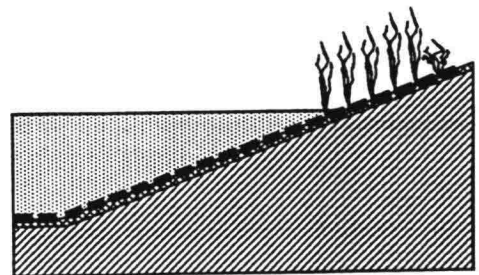


Fig. 2 Cellular concrete block revetment

As soon as vegetation has established itself, erosion will be prevented by the roots and leaves of the plants.

In order to establish design criteria studies have been carried out at Delft Hydraulics in a small-scale model [2]. The objective of the project was to assess the rate of erosion of soil material out of the cells. Fig. 3 shows the cellular concrete block revetment schematically.

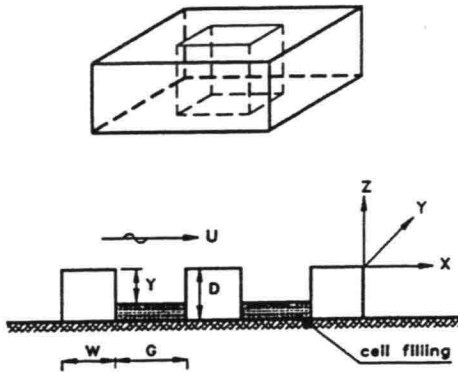


Fig. 3 Schematized cellular block

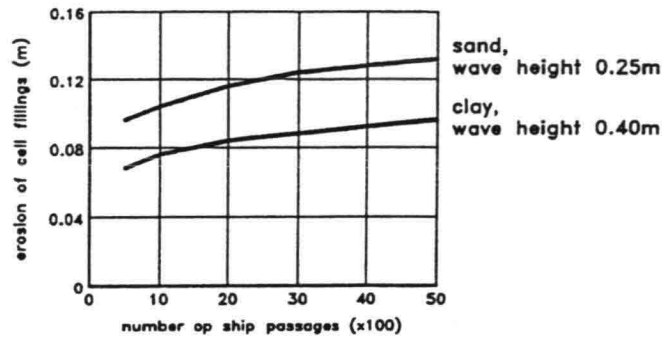


Fig. 4 Typical test results of erosion of cell fillings

For wave loads attacking around the undisturbed water level, the following design equation was found after the tests:

$$Y/G = c \cdot H^{0.5} \cdot \log(N + 1) \quad (1)$$

in which: c = coefficient ($m^{0.5}$), G = cell width (m), Y = maximum erosion (m), H = wave height (m), N = number of waves or ship passages (-). The coefficient c has a value of 0.7 for non-cohesive cell fillings and $0.25 \cdot p^{-0.2}$ for cohesive fillings with a very low compaction (p = soil fraction with particles smaller than 0.002 mm). A specific result is presented in Fig. 4.

The main conclusion after having carried out the research project is that cellular blocks can be applied along inland waterways. A safe design approach is to apply blocks with a cell width G less than half the block thickness D for cohesive and non-cohesive cell fillings and to allow maximum wave heights not larger than 0.4 m. In the case of a cohesive cell filling values for the wave height up to 1.0 m are allowed, whereas the cell width G may be less or equal to D . The erosion of cohesive material predicted by equation (1) can be reduced considerably by increasing the compaction of this material in the cell.

Meanwhile, a prototype inventarization is carried out to the establishment of vegetation on cellular block revetments. For that purpose real test embankments are examined. The results of this inventarization will become available soon.

4. WATER EXCHANGE BETWEEN POOL AND WATERWAY

An environment-friendly bank protection along inland waterways that is often applied consists of a fixed protection, bordering a shallow pool with varying depth. This shallow pool provides a habitat for all kinds of plants and animals improving the appearance of the bank protection while befitting the surrounding environment. Fig. 5 shows several varieties of the structure mentioned above.

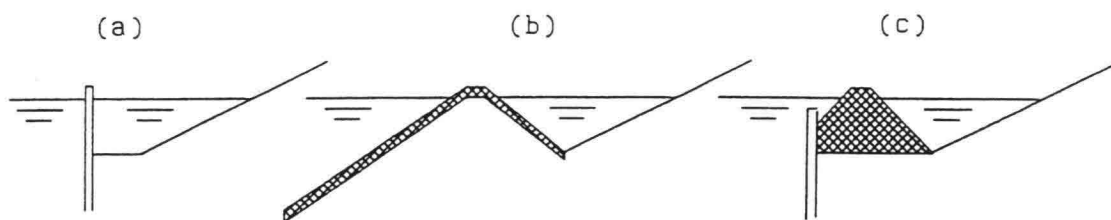


Fig. 5 Protective structures with a shallow pool

The fixed protection may consist of a sheet-piling (a), a riprap or block mattress protection (b) or a combination of the structures mentioned before (c). A very important aspect of this type of structure is the exchange of water between waterway and pool in order to keep the quality of the water in the pool on a sufficient level. This exchange is possible by wave-overtopping, but more importantly, it can be realized by gaps in the fixed protection. Another advantage of the application of gaps is that fish and other animals use these gaps to get in and out of the pool.

The distance between these apertures as well as the effective area largely govern the rate of water exchange, and, consequently, fluctuations of the waterlevel in the pool. In order to make a proper design, in terms of the dimensions of the gaps and their distance, a numerical model has been developed.

The model is based on the following assumptions:

- * Water exchange is possible by the water level depression caused by a passing ship.
- * During the passage time of a ship, the water level in the waterway is lowered and due to the head difference between pool and waterway, water flows out of the pool.
- * After the ship's passage, the original water level in the waterway is restored, resulting in an inverse flow, since the water level in the pool has decreased during the stage of outflow.
- * The process can be described using the one-dimensional partial differential equations, that describe non-stationary flow in open channels, combined with suitable discharge-head relations for the applied gaps.

In Fig. 6 the system of waterway, permeable protection and shallow pool has been schematized. Each gap is defined as some kind of weir or spillway, and the distance

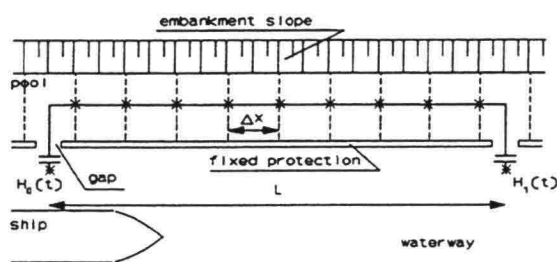


Fig. 6 Schematization of the waterway, permeable protection and shallow pool

L between two gaps is divided into sections of equal length Δx . The water level depression caused by the passing ship starts at $t = 0$ s at the first aperture, and at $t = L/V_{ship}$ s at the next (V_{ship} is the speed of the ship in m/s). For each section the water movement is governed by the equations for conservation of mass and conservation of momentum. By applying discharge-head relations at the boundaries (both gaps), the set of equations can be solved.

The outcome of the model is governed by a selected volume of water that will be exchanged during the passage of a characteristic vessel. This volume is expressed relative to the original volume of water in the shallow pool. This criterion is dependent on the number of characteristic ships that pass the structure daily. For a waterway with a relatively low intensity of shipping traffic, about ten per cent of the original volume is regarded to be sufficient.

In the graphs below, some results of the model are shown. They apply to the

depicted situation. In this case, the relation between discharge and head for a sharp-crested weir has been applied at the gaps [3]:

$$Q(t) = \frac{2}{3} c_s \sqrt{2g} m b H(t)^{1.5} \quad (2)$$

in which: c_s = coefficient for submerged flow (-), m = discharge coefficient (-), b = gap width (m), g = acceleration due to gravity (m^2/s), $Q(t)$ = discharge (m^3/s), $H(t)$ = water level (m).

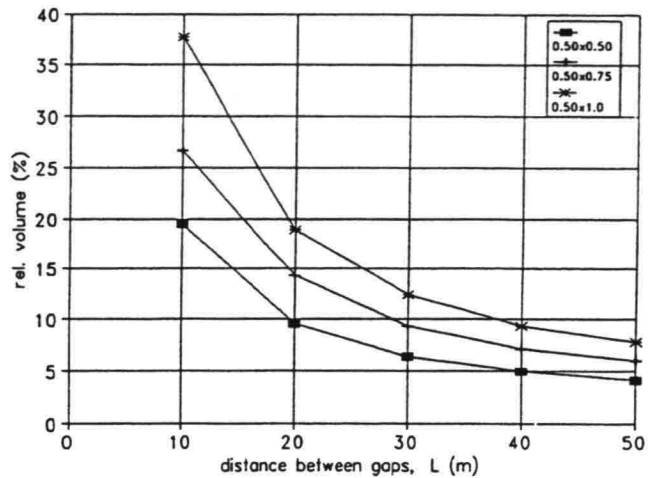
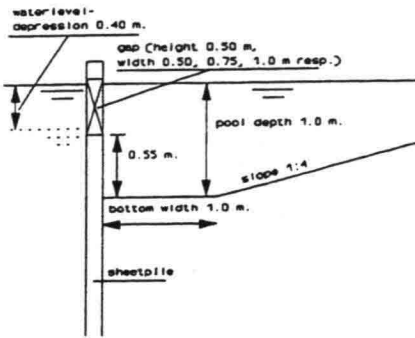


Fig. 7 An example of the use of the derived mathematical model

The example shows that in order to exchange a relative volume of about ten per cent per passage, for the smallest gap a distance of 20 meters is necessary, while for the largest gap a distance of 40 metres suffices.

By using the model, the proper distance between the gaps and their geometry can be assessed, related to a selected level of water movement in the shallow pool. Besides structures using all sorts of sheet-piling, the model can handle riprap or block mattress protections with lowered crests (Figure 5 (b)) or pipes (culverts) as aperture, simply by adapting the discharge-head relations. Also the water exchange via a riprap protection without any gap can be calculated. In this situation water flows through the pores between the stones, which can be described using Forchheimer's equation for combined turbulent and laminar flow through stones [4].

The establishment and development of vegetation in the pool, and the use of the pool as habitat or breeding place by fish or other animals depends largely on the quality of the water and the intensity of water movements inside the pool. With the model described above, a proper design of the structure and the pool can be realized.

5. RECENT AND FUTURE DEVELOPMENTS

The trend to environment-friendly solutions for protective structures has resulted in many other research projects in the Netherlands. For example, at this moment research is carried out in order to develop conceptual models for the behaviour of non or less protected banks. The influence on a non-protected embankment of the hydraulic loads under normal daily conditions will be a gradual erosion of the original profile (Fig. 8) eventually resulting in an equilibrium profile. Small-scale model tests together with theoretical considerations

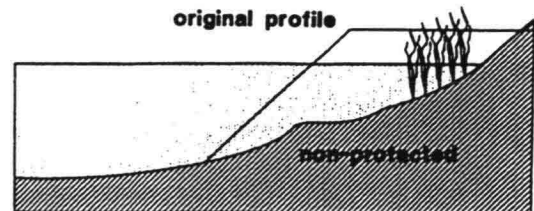


Fig. 8 Schematized gradual erosion of a non-protected embankment

should allow to develop a mathematical model describing the time-dependent erosion of the embankment profile. The results of the studies will also be important for determining maintenance strategies.

Another research project deals with the properties of geotextiles as a filter layer in which the question is: does geotextile allow vegetation? If the openings in a particular geotextile do not allow the vegetation to grow through the geotextile vegetation will not develop in the way it was expected. Obviously, a compromise has to be found between the traditional requirements, viz. water permeability and soil tightness, and the properties of the geotextile. Ten geotextiles are investigated of which one is made of the natural fibre jute.

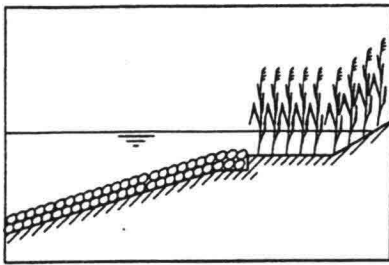


Fig. 9 Vegetated berm as bank protection

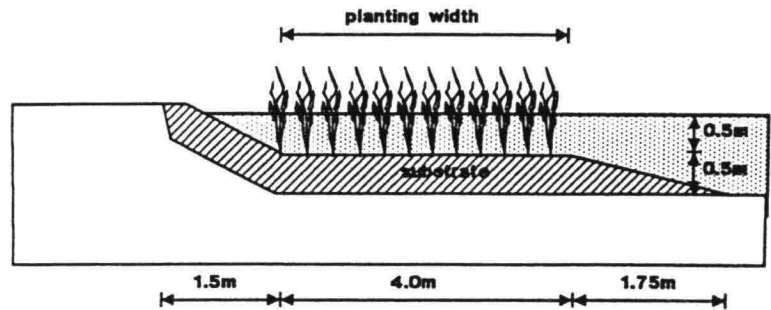


Fig. 10 Cross-section of a test section with reed for wave damping tests

A third project deals with the damping of waves by plants like reed or bulrush on a horizontal berm at the embankment (Fig. 9). For this purpose a special facility was built at Delft Hydraulics next to a wave basin, in which in fourteen test sections reed and bulrush on a substrate of sand or clayey sand are growing in the open air (Fig. 10). During the growing season and in wintertime waves will be generated

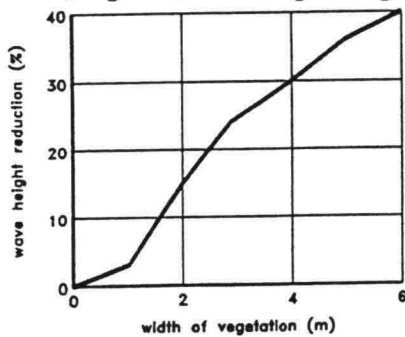


Fig. 11 Previous results of wave damping characteristics of reed

in the basin and the wave damping caused by vegetation will be studied. In addition, the influence of the roots of the plants on the prevention or retardation of the substrate will be studied as well. Results of earlier tests are presented in Fig 11.

The results of all the research projects described above will be included in the mathematical design program DIPRO (DIMensioning PROtections) [5]. This program yet contains the design formulas for traditional bank protections. In the near future it will also allow the determination of stable environment-friendly protections. DIPRO will then be of particular interest for consultants, contractors and management and maintenance authorities of waterway systems.

REFERENCES:

- [1] Pilarczyk, K.W., Havinga, H., Klaassen, G.J., Verheij, H.J., Mosselman, E. and Leemans, J.A.A.M. (1989). "Control of bank erosion in The Netherlands. State-of-the-art", 3rd Nat. Conf. on Hydr. Eng. of ASCE, New Orleans.
- [2] Klein Breteler, M., Laboyrie, J.H. and Verheij, H.J. (1988). "Erosion of sediment through cellular blocks applied as slope protection along coasts and inland waterways", Proc. Symp. on Modelling Soil-Water-Structure Interactions, Delft, The Netherlands.
- [3] Chow, Ven te (1959). "Open Channel Hydraulics", McGraw-Hill.
- [4] Forchheimer, P. (1930) "Hydraulik", Teubner Verlag, Leipzig.
- [5] Delft Hydraulics (1991). "DIPRO, a computer aided design system for bank protections along navigation fairways", Delft, The Netherlands.

2.4.2 Eisen met betrekking tot het milieu

Waterbouwkundige werken vormen in het algemeen een ingreep in het milieu. Het effect dat deze ingreep heeft, wordt ten dele veroorzaakt door de materiaalkeuze bij de uitvoering van de werken.

Vanuit milieuhygiënisch oogpunt kunnen eisen worden geformuleerd waaraan bepaalde bouwmaterialen en hun alternatieven moeten voldoen. Deze eisen worden enerzijds bepaald door het feit dat met de materialen een verontreiniging in het milieu kan worden gebracht en anderzijds dat deze materialen een verandering van de natuurlijke omgeving teweegbrengen.

Het milieu-effect bij een bepaalde materiaalkeuze wordt beoordeeld aan de hand van:

- chemische samenstelling van de materialen;
- emissie van ongewenste stoffen die een bepaalde toepassing van de materialen tot gevolg heeft;
- geschiktheid van een materiaal als drager van flora, fauna of menselijke activiteiten.

Deze beoordeling moet worden gebaseerd op van overheidswege gestelde richtwaarden of normen. Deze zijn (nog) niet opgesteld voor waterbouwkundige werken. Wel is er een aantal milieuwetten, uitvoeringsvoorstellen en beleidsbeslissingen die van toepassing kunnen zijn. In het geval van hergebruik van afvalstoffen is er echter een tegenstrijdigheid aanwezig tussen enerzijds het beperken van de hoeveelheid afval door stimulering van hergebruik, en anderzijds bescherming van het milieu. Deze problematiek wordt waarschijnlijk van materiaal tot materiaal verschillend benaderd en opgelost. Vooral voor wat betreft alternatieve bulkmaterialen moet een keuze gemaakt worden tussen het zoeken naar toepassingen binnen de huidige regelgeving of aanpassing van de regelgeving aan een bepaalde toepassing.

De toepassing van richtwaarden of normen moet steeds worden gerelateerd aan de waarde en de kwetsbaarheid van het systeem waarin de ingreep plaatsvindt. In het Indicatief Meerjarenprogramma (IMP) Water 1985-1989 worden de ecologische kwaliteitsdoelstellingen voor Nederlandse oppervlaktewateren geformuleerd, gebaseerd op de rapportage van de CUWVO (Commissie Uitvoering Wet Verontreiniging Oppervlaktewater), werkgroep V (1984) [2.20].

Chemische samenstelling

De samenstelling van materialen geeft informatie over het potentieel nadelige effect dat een materiaal op het milieu kan hebben.

Een beoordeling kan geschieden aan de hand van :

- Zwarte en grijze stoffenlijsten. Deze lijsten (officieel lijsten I en II) zijn onder andere opgesteld in het kader van het Rijnchemieverdrag, een EG-richtlijn en het Verdrag van Parijs. De zwarte-lijst-stoffen zijn voornamelijk geselecteerd op basis van hun toxiciteit, persistentie en bio-accumulatie.
- Toetsingskader van de interimwet bodemsanering. In dit toetsingskader zijn voor een groot aantal verontreinigingen concentratiewaarden vermeld die als beoordelingscriteria gelden voor de mate van verontreiniging in zowel de "droge" grond als het grondwater.
- Wet chemische afvalstoffen. Bij algemene maatregel van bestuur, het stoffen- en processenbesluit, wordt aangegeven wat wordt verstaan onder chemisch afval.
- Toetsingscriteria baggerslib. Rijkswaterstaat, Directie Benedenrivieren heeft een toetsingssysteem ontworpen voor vergelijking van onderwaterbodems, rekening houdend met onderlinge verschillen in samenstelling en textuur, specifiek voor het benedenrivierengebied (en dus niet direct vertaalbaar voor andere materialen).

Het in het milieu brengen van milieuvreemde stoffen in grote hoeveelheden wordt door de wet slechts toegestaan indien deze toepassing geïsoleerd, beheersbaar en controleerbaar is (IBC-criteria). Dit betekent in de praktijk dat aan toepassing van materialen, die een potentieel nadelig effect hebben op het milieu, de eis kan worden gesteld dat ze "herneembaar" moeten worden toegepast en niet mogen worden gemengd met niet-verontreinigd materiaal. Indien het materiaal wordt hernomen, ontstaan mogelijk extra kosten indien een verwerkingsmogelijkheid voor het afval met potentieel verontreinigende stoffen moet worden gevonden. Ook dient een systeem te worden opgezet om de milieueffecten te beheersen.

Het uitlooggedrag van een stof kan worden getoetst aan verschillend richtwaarden, afhankelijk van de vraag naar welk milieucompartiment de emissie is gericht:

- interimwet bodemsanering, bijvoorbeeld in het geval van kwel door het materiaal naar het grondwater en de bodem;
- waterkwaliteitsdoelstellingen, zoals opgenomen in het "IMP-Water 1985 1989";
- toetsingscriteria voor baggerslib in het geval van emissie naar de onderwaterbodem.

Bij deze beoordeling moeten zowel de totale belasting van het milieu als specifieke concentratie-eisen worden betrokken.

Een beoordeling van de totale emissie is afhankelijk van zowel de tijdsduur waarover deze plaatsvindt als het systeem waarop de emissie effect heeft. Chloride-emissie naar zeewater is onschadelijk, maar een korte doch hoge emissie (bijvoorbeeld na hoge waterstanden) van koper naar het oppervlaktewater kan dodelijk zijn voor vissen.

Emissie als gevolg van mechanische verwerking treedt alleen op indien het materiaal als toplaag of filterlaag wordt toegepast. Duurzaamheidseisen gesteld en acceptabel geacht vanuit civieltechnische hoek, kunnen te milieuhygiënisch onaanvaardbare emissies van fijn verdeeld verontreinigend materiaal leiden.

Milieuwetgeving

Een aantal milieuwetten is van toepassing op het gebruik van afvalstoffen reststoffen in en onder water, te weten;

- Wet verontreiniging oppervlaktewater (WVO) voor onder andere het in het oppervlaktewater brengen van stoffen.
- Wet chemische afvalstoffen voor de verwijdering van chemisch afval.
- Afvalstoffenwet voor de verwerking van afval via vergunningen.
- Wet bodembescherming voor de bescherming van de bodem via richtlijnen algemene maatregelen van bestuur.

TOETSINGSTABEL voor de beoordeling van de concentratieniveaus van diverse verontreinigingen in de bodem.
 Indikatieve richtwaarden: A-referentiewaarde, B-toetsingswaarde t.b.v. (nader)onderzoek, C-toetsingswaarde t.b.v. sanering.

Voorkomen in	grond (mg/kg droge stof)			grondwater (µg/l)		
	A	B	C	A	B	C
1. Metalen						
Cr	①	250	800	1	50	200
Co	20	50	300	20	50	200
Ni	①	100	500	15	50	200
Cu	①	100	500	15	50	200
Zn	①	500	3000	150	200	800
As	①	30	50	10	30	100
Mo	10	40	200	5	20	100
Cd	①	5	20	1,5	2,5	10
Sn	20	50	300	10	30	150
Ba	200	400	2000	50	100	500
Hg	①	2	10	0,05	0,5	2
Pb	①	150	600	15	50	200
2. Anorganische verbindingen						
NH ₄ (als N)	-	-	-	②	1000	3000
F (totaal)	①	400	2000	②	1200	4000
CN (totaal-vrij)	1	10	100	5	30	100
CN (totaal-complex)	5	50	500	10	50	200
S (totaal-sulfiden)	2	20	200	10	100	300
Br (totaal)	20	50	300	②	500	2000
PO ₄ (als P)	-	-	-	②	200	700
3. Aromatische verbindingen						
Benzeen	0,05(d)	0,5	5	0,2(d)	1	5
Ethylbenzeen	0,05(d)	5	50	0,2(d)	20	60
Toluene	0,05(d)	3	30	0,2(d)	15	50
Xylenen	0,05(d)	5	50	0,2(d)	20	60
Fenolen	0,05(d)	1	10	0,2(d)	15	50
Aromaten (totaal)	-	7	70	-	30	100
4. Polycyclische aromatische koolwaterstoffen						
Naftaleen	③	5	50	0,2(d)	7	30
Fenantreen	③	10	100	0,005(d)	2	10
Antraceen	③	10	100	0,005(d)	2	10
Fluoranteen	③	10	100	0,005(d)	1	5
Chryseen	③	5	50	0,005(d)	0,5	2
Benzo(a)antraceen	③	5	50	0,005(d)	0,5	2
Benzo(a)pyreen	③	1	10	0,005(d)	0,2	1
Benzo(k)fluoranteen	③	5	50	0,005(d)	0,5	2
Indeno(1,2,3cd)pyreen	③	5	50	0,005(d)	0,5	2
Benzo(ghi)perylene	③	10	100	0,005(d)	1	5
PAK (totaal)	1	20	200	-	10	40
5. Gechloroerde koolwaterstoffen						
Alifatische chloorkwst (Indiv.)	③	5	50	0,01(d)	10	50
Alifatische chloorkwst (totaal)	-	7	70	-	15	70
Chloorbenzenen (Indiv.)	③	1	10	0,01(d)	0,5	2
Chloorbenzenen (totaal)	-	2	20	-	1	5
Chloorfenolen (Indiv.)	③	0,5	5	0,01(d)	0,3	1,5
Chloorfenolen (totaal)	-	1	10	-	0,5	2
Chloorpck's (totaal)	③	1	10	-	0,2	1
PCB's (totaal)	③	1	10	0,01(d)	0,2	1
EOCl (totaal)	0,1	8	80	1	15	70
6. Bestrijdingsmiddelen						
Organisch chloor (Indiv.)	③	0,5	5	1/0,01(d)	0,2	1
Organisch chloor (totaal)	-	1	10	-	0,5	2
Niet chloor (Indiv.)	③	1	10	1/0,01(d)	0,5	2
Niet chloor (totaal)	-	2	20	-	1	5
7. Overige verontreinigingen						
Tetrahydrofuran	0,1	4	40	0,5	20	60
Pyridine	0,1	2	20	0,5	10	30
Tetrahydrothiofeen	0,1	5	50	0,5	20	60
Cyclohexanon	0,1	6	60	0,5	15	50
Styreen	0,1	5	50	0,5	20	60
Ftalaten (totaal)	0,1	50	500	0,5	10	50
Geoxydeerde PAK (totaal)	1	200	2000	0,2	100	400
Minerale olie	③	1000	5000	50(d)	200	600

d = detectielimiet

①②③ = zie tabel 1,2 en 3

Uit: Leidraad Bodemsanering (afl. 4, november 1988)

B.16

Tabel 1: Referentiewaarden voor zware metalen, arseen en fluor

Grond (mg / kg droge stof)		Referentiewaarden voor zware metalen, arseen en fluor kunnen voor alle grondsoorten worden berekend met de voor elk element gegeven formule. In deze formule wordt de referentiewaarde afhankelijk gesteld van het lutumgehalte (L) en/of het organische stofgehalte (H). Onder het lutumgehalte wordt verstaan het gewichtpercentage minerale bestanddelen met een doorsnede kleiner dan 2 µm, betrokken op het totale drooggewicht van de grond. Onder het organische stofgehalte wordt verstaan het gewichtpercentage gloeiverlies, betrokken op het totale drooggewicht van de grond.
Stof	Berekeningswijze	
Cr (chroom)	50 + 2L	
Ni (nikkel)	10 + L	
Cu (koper)	15 + 0,6 (L + H)	
Zn (zink)	50 + 1,5 (2L + H)	
As (arsen)	15 + 0,4 (L + H)	
Cd (cadmium)	0,4 + 0,007 (L + 3H)	
Hg (kwik)	0,2 + 0,0017 (2L + H)	
Pb (lood)	50 + L + H	
F (fluor)	175 + 13L	

Uit: Leidraad Bodemsanering (afl. 4, november 1988)

Tabel 2: Referentiewaarden overige anorganische verbindingen

Stof	Grondwater	Opmerkingen
- nitraat - fosfaat (totaal fosfaat)	5,6 mg N/l 0,4 mg P/l zandgebieden 3,0 mg P/l klei- en veengebieden	ter bescherming van voedselarme gebieden kunnen lagere waarden vereist zijn
- sulfaat - bromiden - chloriden - fluoriden - ammonium- verbindingen	150 mg/l 0,3 mg/l 100 mg/l 0,5 mg/l 2 mg N/l zandgebieden 10 mg N/l klei- en veengebieden	In gebieden met mariene beïnvloeding komen van nature hogere waarden voor (zout en brak grondwater)

Uit: Leidraad Bodemsanering (afl. 4, november 1988)

Tabel 3: Referentiewaarden voor organische verbindingen in grond

Stof	Referentiewaarde per stof bij		
	H = 0 - 2	H = 2 - 30	H = 30 - 100
a) Gehalogeneerde koolwaterstoffen en cholinesterase remmers.			
hexachloorcyclohexaan; endrin (µg/kg)	0,2 *	0,1 x H *	3 *
tetrachloorethaan; tetrachloormethaan; trichloorethaan; trichlooretheen; trichloormethaan (µg/kg)	0,2 *	0,1 x H *	3 *
PCB (IUPAC nummers 28 en 52) (µg/kg)	0,2 *	0,1 x H *	3 *
chloropropen; tetrachlooretheen; hexachloorethaan; hexachloorbutadien; heptachloorepoxide (µg/kg)	2	1 x H	30
dichloorbenzeen; trichloorbenzeen; tetrachloorbenzeen; hexachloorbenzeen; monochloornitrobenzeen; dichloornitrobenzeen (µg/kg)	2	1 x H	30
aldrin; dieldrin; chloordaan, endosulfan; trifluralin; azinfos-methyl; azinfos-ethyl; disulfoton; fenitrothion; parathion en -methyl; triazofos (µg/kg)	2	1 x H	30
PCB (IUPAC nummers 101, 118, 138, 153 en 180) (µg/kg)	2	1 x H	30
DDD, DDE, pentachloorfenol (µg/kg)	20	10 x H	300
b) Polycyclische aromatische koolwaterstoffen			
naftaleen; chryseen (µg/kg)	2	1 x H	30
fenantreen, antraceen, fluorantreen benzo(a)pyreen (µg/kg)	20	10 x H	300
benz(a)antraceen (mg/kg)	0,2	0,1 x H	3
benzo(k)fluorantreen; indeno(1,2,3,cd)pyreen benzo(ghi)peryleen (mg/kg)	2	1 x H	30
c) Minerale olie			
totaal (mg/kg)	10	5 x H	150
octaan, heptaan (mg/kg)	0,2	0,1 x H	3

Uit: Leidraad Bodemsanering (afl. 4, november 1988)

Voor de bodems met meer dan 30 % resp. minder dan 2 % organische stof zijn referentiewaarden in de tabel gegeven. Voor de bodems met 2 - 30 % organische stof zijn de referentie waarden afhankelijk van het % organische stof (H in %).

* of detectiegrens indien hoger dan aangegeven waarde

